ROLE OF LIPID METABOLIC PATHWAYS IN THE PROGRESSION OF HEPATIC LIPOTOXICITY

By

Alexandra Kathlene Leamy

Dissertation

Submitted to the Faculty of the

Graduate School of Vanderbilt University

In partial fulfillment of the requirements

For the degree of

DOCTOR OF PHILOSOPHY

in

Chemical Engineering

May 2015

Nashville, Tennessee

Approved:

Professor Jamey Young

Professor Scott A. Guelcher

Professor Doug LeVan

Professor David Wasserman

DEDICATION

"It was the best of times, it was the worst of times, it was the age of wisdom, it was the age of foolishness, it was the epoch of belief, it was the epoch of incredulity, it was the season of Light, it was the season of Darkness, it was the spring of hope, it was the winter of despair"

-Charles Dickens, *Tale of Two Cities*

To light at the end of the tunnel.

ACKNOWLEDGEMENT

Almost five long years later, it is still almost surprising that this time is finally upon me. I came to Vanderbilt fresh out of college without a single minute of non-classroom lab experience so as expected, the first month was overwhelming. Despite a few trip-ups and a lab presentation that will forever be burned into my mind as everything to avoid when giving a presentation, I managed to make my way through the last four and half years and now find myself defending the work I've labored over for so long. And I could not have made it here without the advice, support and guidance of those around me. I am grateful that my advisor, Dr. Jamey Young, took the chance on inviting a novice laboratory scientist such as myself into his lab and has supported me all along the way. His guidance and constant questioning pushed me outside of my "risk adverse" comfort zone, toward new challenges to understand and conquer. He only rolled his eyes a couple of times when I asked to take *yet another* class beyond the requirements of the degree as I tried to more fully understand the biology that was within my project but outside of my realm of knowledge. I am thankful for all of his advice, supervision and patience as I traveled along the long and turbulent journey that is graduate school.

I also would like to thank the other members of my thesis committee, Dr. Scott Guelcher, Dr. Doug LeVan and Dr. David Wasserman, for their continued support throughout the years of my project. Their differing perspectives and insights provided much food for thought and consideration as I steered my project along its various course changes. I am also thankful for all of the collaborators I have worked with on Vanderbilt's campus throughout my time here, including the Wasserman lab, specifically Curtis Hughey, Alex Brown's lab, including Pavlina Ivanova and David Myers, Carla Harris from Vanderbilt's DRTC/MMPC hormone assay core and a host of others who provided expertise and guidance that helped propel my project forward. I would like to most especially thank Dr. Masakazu Shiota, without whom much of this project would have never come to fruition. His experience and knowledge in all things surgical and technical are unrivaled and he was never too busy for any question or problem I had, no matter how inconvenient I'm sure it was for him.

The fellow graduate students and lab members I have grown to know and love also made such a difference in my graduate studies. The conversations I've had over the years with Taylor Murphy, Adeola Adebiyi, Ali McAtee, Martha Wall, Irina Trenary, Young Mi Whang and Neil Templeton have driven my work forward. I am forever grateful for all of the patience and help Lara Jazmin has given me, having to even suffer through two years of living with me both in the lab and at home. And most importantly, I would like to thank Dr. Robert Egnatchik, my wonderful lab mate and forever friend. He had to deal with me when I didn't even know how to count cells and I was pestering him with questions every minute of the day, but he truly helped make me into the scientist I am today. Without him and his unshakeable support, I don't know how I would have made it through graduate school, much less such a thorough investigation into the mechanisms of lipotoxicity.

And last, but definitely not least, I am eternally grateful for my family and all of the undiminishing support they have provided throughout my tenure at Vanderbilt. My parents instilled in me from an early age a thirst for knowledge, a spirit of relentless questioning, a desire to reach for the stars, a tenacious work ethic and the idea that I can accomplish whatever it is I set my mind to do – all of which served me well as a graduate student. Without their words of wisdom and patient listening, I might not have made it past my first disastrous presentation. My sister, Shannon, wishes to have a separate and specific acknowledgement, and rightfully so. She has also been on the receiving end of many a panicked and/or distraught phone calls, having to listen to all of my "science talk" while I try to figure out whatever was wrong while going though it with her over the phone. And I can't leave out my brother, Spencer, who certainly makes life interesting. My family has been there for me though everything, even having gone so far as to pray for the well-being of my cells when I went through a particularly terrible time of contamination, and without them, none of this would have been possible. Thank you is not even close to adequate.

TABLE OF CONTENTS

LIST OF TABLES

LIST OF FIGURES

ABBREVIATIONS

ATF3, activating transcription factor 3; *BSA*, bovine serum albumin; *CHOP***,** CCAAT/enhancer-binding protein homologous protein; *CPT1*, carnitine palmitoyltransferase 1; *DAG*, diacylglycerol; *DGAT*, diacylglycerol acyltransferase; *ER*, endoplasmic reticulum; *FAO*, fatty acid oxidation; *FFA*, free fatty acid; *iPLA*$_2$, calcium-independent phospholipase A_2; *LC-MS*, liquid chromatography mass spectroscopy; *LPA*, lysophosphatidic acid; *MUFA*, monounsaturated fatty acid; *NALFD*, non-alcoholic fatty liver disease; NASH, non-alcoholic steatohepatitis; *OA*, oleic acid; *PA*, palmitic acid; *PACOCF*$_3$, palmityl trifluoromethyl ketone; *PC*, phosphatidylcholine; *Pcyt1a*, phosphate cytidylyltransferase 1, choline, alpha; *PI*, propidium idodide; *PL*, phospholipid; *PS*, phosphatidylserine; *PtdOH*, phosphatidic acid; *ROS*, reactive oxygen species; *SFA*, saturated fatty acid; *TEM*, transmission electron microscopy; *TAG/TG*, triacylglycerol; *UPR*, unfolded protein response

CHAPTER 1

INTRODUCTION

The steady rise in Western obesity rates has been closely linked to significant increases in a multitude of accompanying health problems including type II diabetes and non-alcoholic fatty liver disease (NAFLD). NAFLD severity ranges from simple steatosis to acute steatohepatitis, but the molecular mechanisms controlling progression of this disease are poorly understood (1). The liver plays a central role in whole-body lipid, amino acid and glucose metabolism and therefore impairments in hepatic function are detrimental to a variety of biological processes including lipoprotein export, lactate and nitrogen recycling, gluconeogenesis and overall physiological homeostasis. Hepatic dysfunction associated with NAFLD is thought to be triggered by elevated free fatty acid flux from either adipose tissue or diet that results in ectopic deposition of fat in the liver (2). It is known to be accompanied by increased signaling though cellular stress pathways, oxidative stress and hepatocyte apoptosis. This phenotype is collectively termed hepatic lipotoxicity (3, 4).

Recent literature suggests that elevated free fatty acids (FFAs), especially saturated FFAs, play a central role in lipotoxic mechanisms, both in experimental models and in NAFLD patients (5). Relevant cellular processes that have been causally linked to lipid-induced apoptosis, known as lipoapoptosis, include endoplasmic reticulum (ER) stress, oxidative stress, mitochondrial dysfunction, and Jun N-terminal kinase (JNK) signaling (6-10). In contrast, increased triglyceride synthesis has been shown to have a protective effect against lipotoxicity (5, 6, 8, 11), despite being one of the hallmark traits of NAFLD. The overarching theme of this dissertation is to examine how the degree of intrahepatic lipid saturation controls cell fate in response to an elevated FFA load and to identify the mechanisms though which these fatty acids promote hepatocyte dysfunction. Developing a more nuanced understanding of the molecular mechanisms underlying NAFLD progression will lead to more targeted and effective therapeutics for this increasingly prevalent disease, which to date has no proven pharmacologic treatment to prevent or reverse its course.

Chapter 2 provides a summary review of pertinent background information that is important for understanding the motivation behind this dissertation. The review covers general metabolic syndrome and its hepatic manifestation of NAFLD and NASH, as well as experimental methods, both *in vitro* and *in vivo*, that have been used previously to gain insight into the molecular mechanisms involved in these diseases.

Chapter 3 investigates differences between the effects that saturated fatty acids (e.g., palmitate) and unsaturated fatty acids (e.g., oleate) have on hepatic cells *in vitro* (Fig 1-1 A and B). We found that palmitate treatment resulted in lipotoxic cell death that was characterized by increased membrane phospholipid saturation, ER stress and eventual apoptosis. Oleate, however, increased

lipid accumulation but did not induce cell death. Furthermore, co-supplementation of oleate with palmitate protected cells from palmitate-associated lipotoxic phenotypes. Interestingly, in palmitate-supplemented cells we observed accumulation of lipid intermediates that are indicative of increased Kennedy pathway activity and phospholipid synthesis. Our data reveal that palmitate-supplemented cells exhibit increased abundance of saturated phospholipids and reduced triglyceride accumulation, a phenotype that is reversed by palmitate and oleate co-treatment.

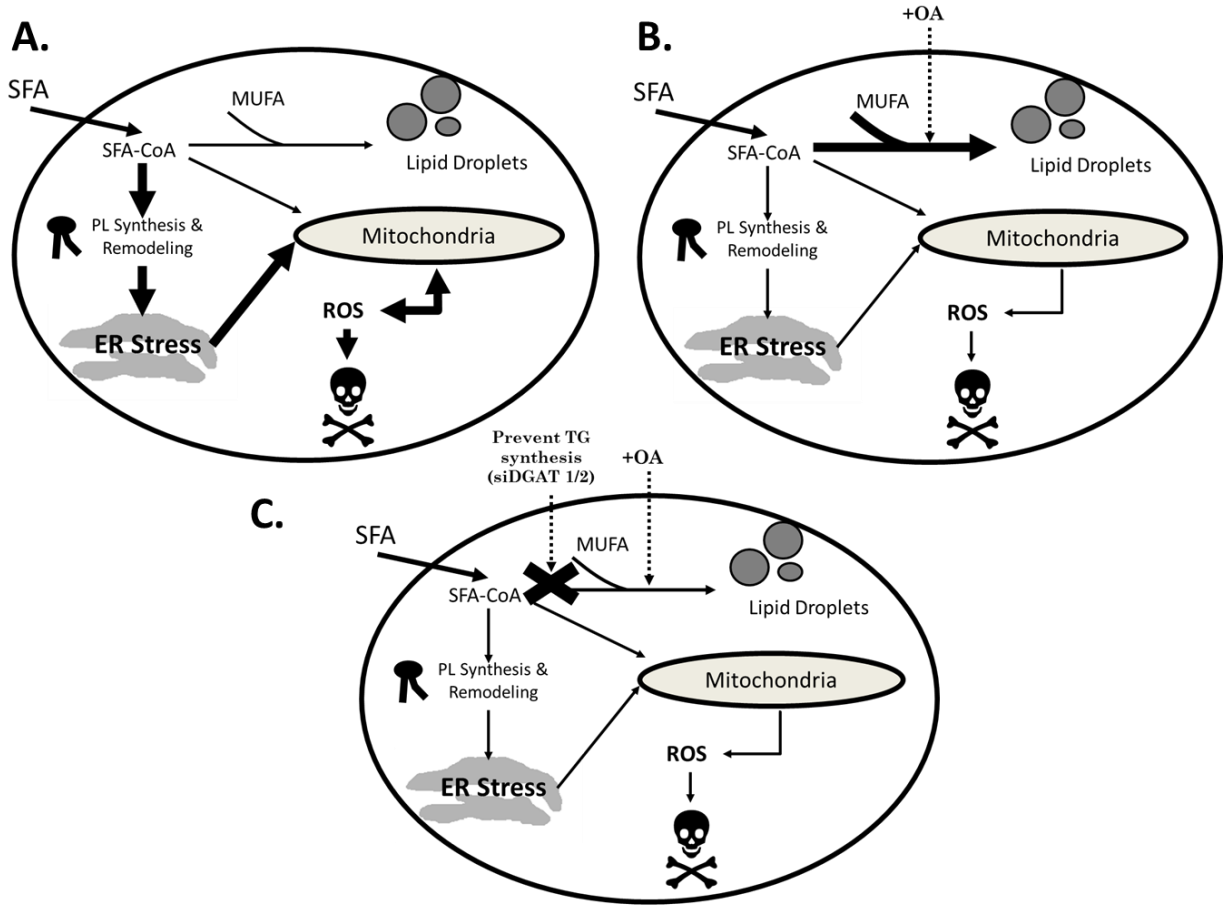

Figure 1-1. Summary of proposed mechanisms investigated in Chapters 3 and 4. In Chapter 3, we investigated the mechanism by which the saturated fatty acid palmitate (PA) initiates ER stress and culminates in apoptosis (A) and how this changes with addition of the monounsaturated fatty acid oleate (OA) (B). In Chapter 5, we examined the effect that inhibiting triglyceride (TG) synthesis would have on PA-treated hepatic cells (C).

These findings led to the work described in **Chapter 4,** where we investigated whether it was oleate's stimulatory effect on triglyceride synthesis that led to reversal of ER stress and cell death in palmitate-treated cells or if it was the desaturating effect it had on membrane phospholipids that led to the rescue. In these studies, we used siRNA targeted knockdown of DGAT1 and DGAT2, the rate limiting enzymes in triglyceride synthesis, to prevent oleate-mediated increases in lipid droplet accumulation (Fig 1-1C). Interestingly, even with significant reductions in triglyceride synthesis, oleate co-supplementation still provided an equally strong rescue effect in palmitate-treated cells. Our data indicate that oleate supplementation enables hepatocytes to counteract palmitate's saturating effect on membrane phospholipids and to renormalize fluidity in the lipid bilayer, thus rescuing palmitate-induced ER stress and lipoapoptosis.

In **Chapter 5**, our aim was to examine whether channeling palmitate away from phospholipid incorporation and into alternative pathways of cellular utilization, such as β-oxidation, would reduce its toxic effect. A small molecule agonist (AICAR) and/or specific inhibitor (etomoxir) of β-oxidation was applied to our *in vitro* hepatic system to determine the effect that modulating this route of fatty acid disposal had on lipotoxic phenotypes (Fig. 1-2A). We determined that inhibiting β-oxidation provided no positive benefits in terms of the lipotoxic phenotype in palmitate-treated cells. Conversely, increasing oxidation of palmitate did provide some beneficial effects to normalize phospholipid saturation, ER stress and cell survival, although this might have been partially due to the pleiotropic effects of AICAR.

We also sought to test whether direct intervention in phospholipid synthesis and remodeling to prevent palmitate-induced saturation would reduce lipotoxicity in the studies described in **Chapter 6**. Our method was to use a pharmacologic inhibitor of $iPLA_2$ ($PACOCF_3$) to prevent breakdown and remodeling of phospholipids via the Lands' cycle as well as siRNA targeted knockdown of the rate limiting step (*Pcty1α)* in phosphatidylcholine synthesis to accomplish this task (Fig. 1-2B). Our hypothesis was that preventing incorporation of palmitate into phospholipids in either of these two pathways would reduce the membrane oversaturation that is characteristic of palmitate-treated cells and thereby relieve ER stress. While both methods did lead to some improvements in lipotoxic phenotypes in hepatic cells, neither was completely effective. This is likely due to the fact that we were targeting only specific routes of palmitate incorporation into the phospholipid pool and, therefore, were unable to fully normalize membrane saturation due to redundancy in these lipid biosynthetic pathways.

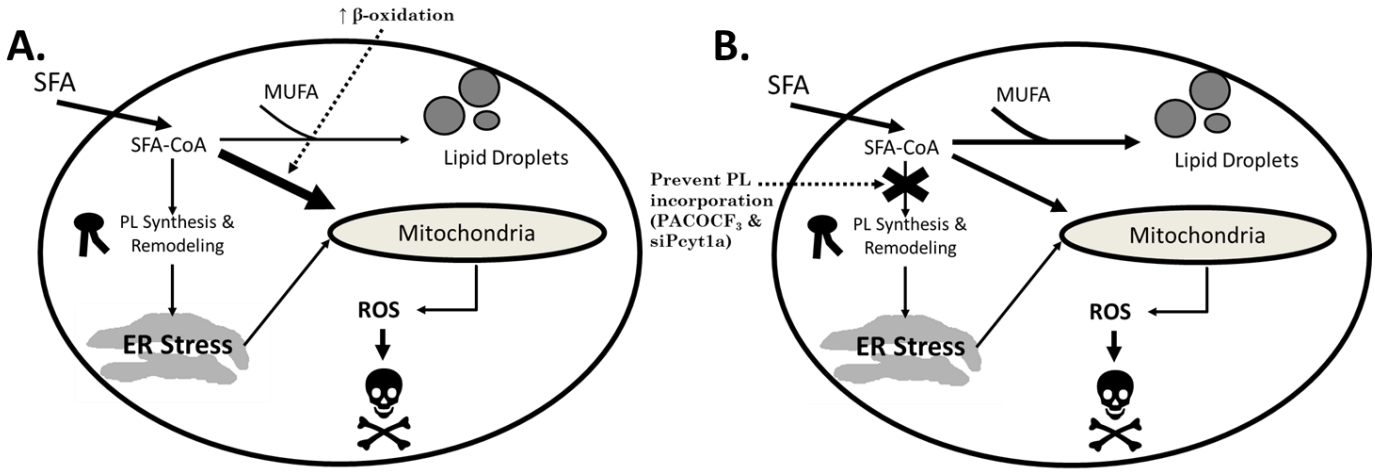

Figure 1-2. Summary of proposed mechanisms investigated in Chapters 5 and 6. In Chapter 5, we asked whether modifying ß-oxidation rates would impact PA-induced lipotoxicity using pharmacological modulators (A). In Chapter 6, we sought to determine the effects that blocking PA incorporation into phospholipids (PL) by inhibiting $iPLA_2$ or Pcyt1α would have in PA-treated hepatic cells (B).

Finally, we were interested in developing an *in vivo* model system that would enable us to test specific hypotheses generated from our *in vitro* studies. We performed a pilot study that involved feeding rats a Western-style diet rich in saturated fats and cholesterol for up to 12 weeks. Unfortunately, this strategy did not prove to be effective at inducing a NASH-like phenotype with traits characteristic of human disease within the time-frame of our study. However, direct infusion of ethyl palmitate into the jugular vein of mice has yielded interesting initial results that appear to parallel the mechanisms we have previously identified in our *in vitro* hepatic models. The results of these pilot studies are described in **Chapter 7**, with an eye toward continued development of *in vivo* model systems for the study of NAFLD and NASH.

Chapter 8 summarizes the overall findings of this dissertation and presents suggestions for future experimental work to further this research.

References

1. Leamy, A. K., R. A. Egnatchik, and J. D. Young. 2013. Molecular mechanisms and the role of saturated fatty acids in the progression of non-alcoholic fatty liver disease. *Prog. Lipid Res.* **52**: 165-174.

2. Brookheart, R. T., C. I. Michel, and J. E. Schaffer. 2009. As a Matter of Fat. *Cell Metabolism* **10**: 9-12.

3. Schaffer, J. E. 2003. Lipotoxicity: when tissues overeat. *Current Opinion in Lipidology* **14**: 281-287.

4. Malhi, H., and G. J. Gores. 2008. Molecular Mechanisms of Lipotoxicity in Nonalcoholic Fatty Liver Disease. *Semin. Liver Dis.* **28**: 360-369.

5. Listenberger, L. L., X. L. Han, S. E. Lewis, S. Cases, R. V. Farese, D. S. Ory, and J. E. Schaffer. 2003. Triglyceride accumulation protects against fatty acid-induced lipotoxicity. *Proceedings of the National Academy of Sciences of the United States of America* **100**: 3077-3082.

6. Hardy, S., W. El-Assaad, E. Przybytkowski, E. Joly, M. Prentki, and Y. Langelier. 2003. Saturated fatty acid-induced apoptosis in MDA-MB-231 breast cancer cells - A role for cardiolipin. *Journal of Biological Chemistry* **278**: 31861-31870.

7. Turpin, S., G. Lancaster, I. Darby, M. Febbraio, and M. Watt. 2006. Apoptosis in skeletal muscle myotubes is induced by ceramides and is positively related to insulin resistance. *American Journal of Physiology-Endocrinology and Metabolism* **291**: E1341-E1350.

8. Okere, I., M. Chandler, T. McElfresh, J. Rennison, V. Sharov, H. Sabbah, K. Tserng, B. Hoit, P. Ernsberger, M. Young, and W. Stanley. 2006. Differential effects of saturated and unsaturated fatty acid diets on cardiomyocyte apoptosis, adipose distribution, and serum leptin. *American Journal of Physiology-Heart and Circulatory Physiology* **291**: H38-H44.

9. Srivastava, S., and C. Chan. 2008. Application of metabolic flux analysis to identify the mechanisms of free fatty acid toxicity to human hepatoma cell line. *Biotechnology and Bioengineering* **99**: 399-410.

10. Pagliassotti, M., Y. Wei, and D. Wang. 2005. Saturated fatty acids induce cytotoxicity in hepatocytes via effects on the endoplasmic reticulum. *Obesity Research* **13**: A31-A31.

11. Leamy, A. K., R. A. Egnatchik, M. Shiota, P. T. Ivanova, D. S. Myers, H. A. Brown, and J. D. Young. 2014. Enhanced synthesis of saturated phospholipids is associated with ER stress and lipotoxicity in palmitate-treated hepatic cells. *J. Lipid Res.* **55**: 1478-1488.

CHAPTER 2

BACKGROUND AND SIGNIFICANCE

Introduction

As the global waistline continues to expand, the incidences of obesity and type II diabetes are reaching epidemic proportions. Insulin resistance and obesity are often associated with a cluster of other metabolic abnormalities including hypertension, dyslipidemia, and hyperinsulinemia, collectively termed the "metabolic syndrome." The pathogenesis of this disease state is hypothesized to begin with abnormal accumulation of lipids in non-adipose tissues (steatosis) due to increased export of free fatty acids from adipose tissue. The hepatic manifestation of metabolic syndrome is known as non-alcoholic fatty liver disease (NAFLD), a chonic condition affecting approximately one-third of the US population (1). Because of its growing prevalence in Western society, NAFLD is currently the leading cause of referrals to hepatology clinics in the US. An estimated 10% of NAFLD patients will progress to a more severe condition known as nonalcoholic steatohepatitis (NASH), which involves liver inflammation and apoptotic cell death and can eventually result in cirrhosis and/or liver failure (2). Despite its prevalence and potential serious complications, the underlying molecular mechanisms that regulate NAFLD progression remain poorly understood, and further investigation is needed to identify targeted therapeutic approaches for prevention and treatment of this disease. Lack of such knowledge represents an important problem, because it limits the ability of biomedical researchers to develop novel nutritional and/or pharmacologic interventions to combat the effects of NAFLD and to prevent its progression toward NASH (3).

Models of NASH and the role of free fatty acids

Identifying and diagnosing individuals with pathological NASH relies on biopsies and blood plasma samples to determine disease severity. NAFLD/NASH progression identification is based on the NAFLD Activity Score (NAS) and indicators of liver fibrosis. NAS was created by the Pathology Committee of the NASH Clinical Research Network (4) as method to use 14 histological features of NASH, including lobular inflammation, lipid accumulation (steatosis) and hepatocellular ballooning, to score the degree of liver disease and differentiate the severity of NAFLD progression in liver biopsies (NAS $\geq$5 indicates a diagnosis of NASH, NAS $\leq$3 diagnosis "not NASH"). Plasma markers of liver disease have historically included elevated levels of alanine aminotransferase (ALT) and aspartate aminotransferase (AST). While these plasma makers are commonly accepted as indicators of general liver disease, they are not reliable biomarkers of nor specific to NASH. In fact, there appears to be only a weak correlation between elevated AST/ALT levels and diagnosis of NASH, and is a poor metric for the independent diagnosis of NASH (5, 6).

Animal models are an important research tool for investigating pathological mechanisms of NASH development as diagnosis of human NASH in the medical setting is invasive and not always definitive and the scope of experimental interventions that can be applied clinical studies is limited. Larter *et al* provide an excellent review of a multitude of animal experimental models of NASH, including those that are induced though diet, genetics or pharmacological intervention (7). Each of these models, however, has its advantages, disadvantages and discrepancies that must be taken into consideration when making correlation to manifestations and mechanisms of human NASH.

Common animals models used in obesity and diabetes research, such as leptin receptor deficient *db/db* and leptin deficient *ob/ob* mice, do not spontaneously develop NASH without further intervention, despite significant accumulations of hepatic lipids (8, 9). Rodent models often employ secondary assaults, such lipopolysaccharide (10) or a methionine and choline deficient (MCD) diet (11), in order to induce clinical symptoms of NASH. The MCD diet has been particularly popular in the past because even wild-type animals on this diet will rapidly develop hepatic steatosis, inflammation and fibrosis (12-14), providing a model free of the confounding effects of insulin resistance (15). However, the etiological difference between MCD-induced rodent models of NASH and clinical human NASH raises questions about whether this model is ideal or relevant for determining mechanisms of the human disease (16). More recently developed rodent models of NASH, whereby genetically unaltered rodents are fed a "western" like diet of high calorie, saturated fat, cholesterol and/or fructose diet, appear to more closely mimic development and histological features of human NASH. These models include "cafeteria-diet rats" (17), fed actual human "junk" food found in cafeterias, and the "fast-food mouse" (18), fed a specially formulated rodent feed designed to imitate a typical westernized diet. These animals develop features and symptoms of NASH gradually over a longer period of time making them less idea for the fast past laboratory environment, but appear to make more ideal models as they represent a more human-like manifestation of NASH.

In vitro models offer an alternative to human and animal studies. Hepatic cell lines and primary hepatocytes provide a platform for exploring the detailed molecular mechanisms that regulate transition and severity of hepatic disease *in vivo*. Progressive liver and metabolic diseases have been associated with elevated plasma levels of free fatty acids and triglycerides (19). *In vitro* experiments have used free fatty acids supplemented to the media to mimic this environment and found that saturated fatty acid (SFA) overexposure promotes expression of pro-inflammatory cytokines, impairs inulin signaling and increases apoptotic signaling characterized by ER dysfunction and oxidative stress (20-24). On the other hand, monounsaturated fatty acids (MUFAs) increase steatotic accumulations of triglycerides but do not initiate the lipotoxic cascade culminating in apoptotic cell death (19, 20, 22, 25). Several putative mechanisms have been proposed to explain this phenomenon and how SFA overexposure may promote progression of NAFLD to NASH, including reactive oxygen species accumulation, increased endoplasmic

reticulum (ER) stress and elevated ceramide synthesis, but no definitive mechanism had been conclusively determined (26, 27). Ceramide formation and signaling would seem to be an easy and attractive explanation for the initiation of hepatic lipoapoptosis by SFAs because ceramides are synthesized *de novo* from palmitate and serine and have shown pro-apoptotic effects in myocytes (28). However, numerous pharmacologic and genetic intervention studies have demonstrated that SFA induced lipoapoptosis can occur independently of ceramide synthesis in a variety of cell types including CHO (19, 29), breast cancer cells (20) and hepatoma liver cells (30). This suggests that other mechanisms of SFA induced lipotoxicity, such as ER stress and ROS accumulation, present more important targets promotion of apoptosis.

SFAs promote cellular dysfunction by activating ER stress pathways

The ER is a specialized organelle that is integral in many cellular functions, particularly disulfide bond formation, proper protein folding, and synthesis and secretion of several critical biomolecules including steroids, cholesterol, and lipids (31). The ER also is the most important regulator of intracellular calcium (Ca^{2+}) as a result of its large Ca^{2+} stores and Ca^{2+} ATPases, which are necessary for proper functioning of Ca^{2+}-dependent chaperones that stabilize protein folding. Very small changes in cellular redox state (32) or abnormal accumulation of unfolded proteins and/or toxic lipid species (33) can result in activation of compensatory response pathways, which comprise the unfolded protein response (UPR) (31, 34, 35). The UPR stress signaling pathway is initiated by thee main ER transmembrane proteins, protein kinase RNA-like endoplasmic reticulum kinase (PERK), inositol-requiring 1 (IRE-1), and activating transcription factor 6 (ATF6), which together promote transcription of genes designed to increase protein folding and degradation. Markers that are often assessed in order to demonstrate cellular ER stress include phosphorylation of the thee aforementioned transmembrane proteins as well as the splicing of X-box binding protein, initiated by IRE1 signaling, and CHOP, a pro-apoptotic protein downstream of PERK activation. The UPR initially serves a protective role to increase protein folding capacity and degrade any misfolded proteins already synthesized. However, excessive and/or prolonged stress can trigger apoptosis via JNK signaling and release of ER Ca^{2+} stores (36) (see (35) for a comprehensive review of general ER stress pathways). The released Ca^{2+} is readily taken up by the mitochondria adjacent to ER Ca^{2+}-release channels (37). Acute Ca^{2+} overload results in changes in mitochondrial potential and opening of the permeability transition pore (PTP) (38), invoking a potent cellular death signal (32).

Increasing empirical evidence points towards endoplasmic reticulum (ER) stress as an upstream signal in SFA-induced cellular dysfunction and apoptosis (Table 1). Clinical studies of patients suffering from metabolic syndrome disorders, such as NAFLD, have increased levels of ER stress markers in the liver and other tissues (39-41). *In vivo* data from male Wistar rats indicate that diets high in saturated, but not unsaturated, fat results in induction of hepatic ER stress and liver damage (42). SFAs have also demonstrated a potent ability to induce ER stress in a

multitude of cell types *in vitro*, including hepatocytes (42-44), pancreatic β-cells (45, 46), adipocytes (47) and CHO cells (48). Therefore, prior studies have sought to define the role of ER stress in mediating SFA-induced lipotoxicity. Pfaffenbach et al. (49) investigated the role of ER stress in palmitate (PA)-treated H4IIEC3 cells and found that although CHOP expression was increased in PA-treated cells, siRNA knockdown of CHOP did not attenuate apoptosis, demonstrating that CHOP was not critical for lipoapoptosis to occur. Additionally they showed that $CHOP^{-/-}$ mice and their wild-type counterparts displayed comparable levels of liver injury when both were fed a MCD diet, as assessed by alanine and aspartate aminotransferase levels. Similarly, another study found that CHOP inhibition via siRNA in PA-treated HepG2 cells had no effect on apoptosis (50). These results confirm that palmitate alters ER function, but does not fully define how ER stress contributes to apoptosis, implying that alternate downstream targets of ER stress could mediate lipotoxicity.

Type	Model	Key Findings	Reference
In vitro/ in vivo	H4IIEC3 rat hepatomas/ CHOP -/- mice	Palmitate induced significant ER stress as assessed by CHOP expression, but CHOP knockdown did not attenuate apoptosis *in vitro*. Knockout of CHOP in C57BL/6J mice (CHOP -/-) did not reduce liver injury compared to wild-type mice when fed a MCD diet.	Pfaffenbach, *et al* 2010
In vivo	Male Wistar rats	Hepatic steatosis was associated with elevated SFAs, but not unsaturated fatty acids, and was characterized by increased liver injury and markers of ER stress.	Wang, *et al* 2006
In vitro	CHO-K1	In lipotoxic conditions, palmitate was rapidly incorporated into microsomal membrane lipid components resulting in compromised ER membrane integrity and subsequent UPR stress signaling.	Borradaile, *et al* 2006
In vitro	HeLa	Knockdown of SCD-1 resulted in increased SFA content in phospholipids and expression of ER stress signaling chaperones. Synergistic knockdown of SCD-1 and lysophosphatidyl acyltransferase 3, an enzyme associated with preferential incorporation of polyunsaturated fatty acids into phospholipids, further exacerbated UPR.	Ariyama, *et al* 2010
In vitro	NIH-3T3 fibroblasts	UPR-mediated splicing generates an active form of X-box binding protein-1. Activation of this transcription factor significantly increased the synthesis of phospholipids, particularly PC.	Sriburi, *et al* 2004
In vivo	*S. cervisiae*	SFA incorporation into phospholipids increased the order of membranes due to the characteristic suboptimal shape they create within the bilayer. The detrimental effects can be relieved by incorporation of unsaturated fatty acids with a more optimized shape that restores membrane disorder.	Deguil, *et al* 2011
In vivo/ in vitro	Chang cells, ICR mice, human biopsy	LPC is the death effector in cellular apoptosis resulting from SFA overexposure. SFA toxicity can be attenuated by the addition of phospholipase A_2 inhibitors which prevent the generation of LPC species and ER stress. Direct administration of LPC *in vivo* induced significant hepatitis. LPC content was also found to be significantly increased in liver specimens from NASH patients.	Han, *et al* 2008
In vitro	Huh-7, mouse/human primary hepatocytes	LPC content increased linearly with increasing exogenous SFA concentration. Substitution of LPC for SFA in models of lipotoxicty resulted in induction of ER stress, glycogen synthase kinase-3/JNK dependent apoptosis and p53 dysregulation.	Kakisaka, *et al* 2011
In vivo	C57BL/6 genetically unaltered mice	"Fast food diet" mouse model. Used a high saturated fat, high cholesterol and high fructose diet to mimic typical westernized diet. Mice on fast food diet demonstrated histological markers of clinical steatohepatitis including hepatocyte ballooning, inflammation, ER stress, lipoapoptosis and fibrosisin comparison to mice fed a simple "high fat" diet.	Charlton, *et al* 2011
In vivo	Male Wistar rats	"Cafeteria diet" rat model. Rats were fed actual junk food (eg. Oreos, chips, etc) found in typical American dietary consumption and results were compared to simple high fat and standard chow diet. Cafeteria fed rats had significantly higher weight gain, hyperinsulinemia, hyperglycemia, glucose intolerance, inflammation, macrophage infiltration and fibrosis than either high fat or standard chow diets.	Sampey, *et al* 2011
In vivo	Male Wistar rats	Rats were infused intravenously with either soybean (enriched with unsaturated fatty acids) or lard (enriched with saturated fatty acids) oil or a control emulsion. Animals infused with either oil demonstrated elevated ER stress and activation of inflammatory pathways compared to control infusions, but was increased to a much greater extent in lard infused animals compared to soybean infusions.	Nivala, *et al* 2013

Table 2-1. The role of ER stress in SFA-induced lipotoxicity. Abbreviations: Endoplasmic reticulum (ER); Saturated fatty acid (SFA); Unfolded protein response (UPR); Steroyl-CoA desaturase-1 (SCD-1); Phosphatidylcholine (PC); Lysophosphatidylcholine (LPC); Non-alcoholic steatohepatitis (NASH);

Molecular mechanisms of SFA-induced ER stress

Although there is no definitive mechanism explaining how SFAs induce ER stress, increasing evidence points to disordered phospholipid metabolism as one initiating factor. Unsaturated fatty acids are readily incorporated into inert TGs, but excess SFAs remain largely unesterified (30). Recent literature suggests that these free SFAs are rapidly assembled into saturated phospholipid species that are subsequently integrated into ER membrane bilayers (48). The degree of saturation in membrane phospholipids plays an important role in many membrane-associated functions. Abnormal incorporation of saturated phospholipid species can result in detrimental stiffening of cellular membranes and loss of functionality (51). The composition of the ER membrane is unique and typically contains unsaturated phosphatidylcholine (PC) as its major phospholipid component (48, 52, 53). This allows the ER to maintain a high degree of fluidity in order to carry out its critical role in maintaining proper protein folding and trafficking. Relatively small changes in ER homeostasis can result in the induction of UPR (34, 52). Therefore, even limited incorporation of saturated phospholipid species could be detrimental to the ER and lead to the increased UPR signaling observed in response to SFA overexposure.

Borradaile *et al.* (48) published a comprehensive study investigating the mechanism leading to ER stress in palmitate-treated CHO cells. Following exposure to deuterated palmitate for 1 h, the cells displayed a 1.5-fold and 3.0-fold increase in the saturation of membrane-bound PC and TG, respectively, in the rough microsomal fraction. Accompanying the increased saturation were markers of ER stress including the dissociation of protein-folding chaperones protein disulfide isomerase (PDI) and GRP78 from the membrane into the cytosol and presentation of a drastically dilated rough ER morphology, indicating severely impaired ER function. Similar effects were not observed in response to H_2O_2 treatment alone, demonstrating that ER stress induced by SFA overexposure was not solely the result of increased oxidative stress. The study also reported a rapid depletion of ER calcium stores in response to palmitate treatment, pointing to impairment of calcium ATPase activity associated with the ER membrane, a phenomenon that has been previously linked to increased saturation of phospholipid fatty acyl chains (54) and palmitate induced lipotoxicity (55).

Another recent study explored the implications of increasing saturation of membrane phospholipids in HeLa cells (56). Specifically, they investigated the effects of inhibiting steroyl-CoA desaturase 1 (SCD-1), the enzyme responsible for the desaturation of saturated fatty acids for lipid biosynthesis, and lysophosphatidylcholine acyltransferase 3 (LPCAT3), an enzyme that preferentially incorporates polyunsaturated fatty acids into PC. Even without SFA supplementation, both the SCD-1 knockdown and LPCAT3 knockdown cells demonstrated a significant increase in phospholipid saturation and UPR activation indicated by increased X-box binding protein splicing and PERK phosphorylation. These results were exacerbated by the simultaneous LPCAT3 /SCD-1 knockdown and further enhanced by palmitate supplementation. Overall, these experiments indicate that proper incorporation of unsaturated fatty acids into

phospholipids is of critical importance for maintaining normal ER membrane functionality, and that SFA overexposure may disrupt this process. Further investigation into the mechanism and effects of SFAs in controlling the phospholipid composition of cellular membranes will be important in formulating a complete picture of lipotoxic cell death.

Generation of lysophospholipid species, and lysophosphotidylcholine (LPC) in particular, has also been implicated as an important mediator in the apoptotic response to SFAs. LPC is generated from phosphatidylcholine though cleavage of the fatty acid from the sn-2 position by the enzyme phospholipase A_2. In two small-scale biopsy studies, concentrations of LPC in hepatic tissue samples were determined to be greater in livers of NASH patients than healthy controls (57, 58). Direct injection of LPC into the tail vein of ICR mice significantly increased *in vivo* AST/ALT levels, lobular hepatitis, and apoptosis without any evidence of steatosis (58). Using a variety of *in vitro* models, including Huh-7, Chang, and primary mouse and human hepatocytes, SFA lipotoxicity was shown to be significantly attenuated in the presence of the phospholipase inhibitors bromoenol lactone (BEL) and palmityl trifluoromethyl ketone ($PACOCF_3$). This indicates that action of the phospholipase A_2 enzyme may play an important role in the lipotoxic phenotype (58, 59). LPC content was also shown to be linearly correlated with the concentration of exogenous SFA supplied (59). Data from these same *in vitro* models also demonstrate that addition of exogenous LPC produces a similar lipotoxic phenotype as SFA overexposure, including markers of ER stress, caspase activation and apoptosis (58, 59). Kakisaka et al. (59) demonstrated that LPC-dependent lipoapoptosis is dependent on activation of caspase and glycogen synthase kinase-3/ JNK signaling, and is associated with p53 upregulated modulator of apoptosis activation. Identifying the role of LPC accumulation in SFA-induced lipotoxicity presents an interesting new avenue of investigation, but further work is needed to define if and how the two events are directly connected.

Oxidative stress and β-oxidation

The mitochondrion is the cellular powerhouse, as it is the main supplier of energy within the cell. This organelle consumes significant portions of the oxygen supplied to the cell for metabolism in the tricarboxylic acid cycle (TCA cycle) and electron transport chain (ETC). Oxidative phosphorylation, the major process for generating ATP in mitochondria, and ETC are coupled together by the proton gradient across the inner mitochondrial matrix created by electron flow along the ETC. Due to inherent ETC inefficiencies, premature leakage of electrons occurs, mainly at complexes I and III (60). Leaked electrons combine with oxygen to form reactive oxygen species (ROS) such as H_2O_2, $\cdot O_2$- and $\cdot OH$. ROS are powerful oxidizing agents and can indiscriminately damage many cellular components including proteins, fatty acids and DNA (60) but are present only at low levels under normal physiologic conditions. However, ROS can become elevated in response to mitochondrial dysfunction, reduced antioxidant capacity or cellular stress, resulting in a state of oxidative stress. At elevated levels, ROS have been shown

to serve as triggers of pro-apoptotic pathways that initiate programmed cell death (61) though mechanisms including mitochondrial phospholipid peroxidation (62) and/or c-Jun N-terminal kinase (JNK) signaling (61, 63, 64). Evidence for oxidative stress in human patients and animal models of NASH includes the accumulation of oxidized lipids such as malodialdehyde (65). NASH-associated oxidative stress has also been attributed to a variety of mechanisms including upregulated levels of cytochome P450 2E1 (66), NADPH oxidase (67), and changes in mitochondrial function such as increased beta-oxidation (68-70).

Hepatic oxidation of free fatty acids is elevated in obese individuals (71), but the role of enhanced beta-oxidation in promoting lipotoxic ROS accumulation is unclear. In β-oxidation, long chain fatty acyl-CoAs are activated in the cytosol by coupling to carnitine though the enzymatic activity of carnitine palmitoyl transferase-1 (CPT-1), the rate limiting step in β-oxidation (72). Fatty acyl-carnitines are then shuttled across the inner mitochondrial membrane by carnitine-acylcarnitine translocase. Once inside the matrix, they are transformed back into fatty acyl-CoAs primed for oxidation (72). The fatty acids are broken down into two carbon acetyl-CoA units in successive cycles to feed into the TCA cycle for NADH and ATP production or into ketogenic pathways to generate ketone bodies (73). There has been speculation that the overexposure of hepatic cells to SFAs provides an enormous increase in substrate availability for β-oxidation and stimulation of this cycle may lead to increased downstream ROS production. Literature reports on the role of β-oxidation in lipotoxicity have been inconclusive, with some studies indicating that it is a major source of ROS (74) while others indicate that ROS overproduction is due to mitochondrial dysfunction resulting from an upstream target of SFA-induced impairment (30). A recent *in vivo* study demonstrated that increased β-oxidation may actually confer a protective effect against NASH by enhancing lipid disposal. Administration of a PPAR-α agonist to MCD mice resulted in attenuated NAS scores while simultaneously increasing peroxisomal beta-oxidation (75). *In vitro* studies in pancreatic β-cells (76) and breast cancer cells (20) agree with these results. Reducing β-oxidation using the pharmacological agent etomoxir had no positive effect on palmitate-induced apoptosis (20, 76). Overall, these studies indicate that SFAs likely play a more complex role in initiating hepatic ROS accumulation and lipoapoptosis than simply oversupplying a substrate fuel for increased oxidative metabolism. This role could involve indirect effects to dysregulate normal mitochondrial function or a signaling cascade resulting from ER stress-induced Ca^{2+} release. In contrast, β-oxidation of SFAs may actually play a protective role is SFA-mediate liptoxicity.

Triglyceride synthesis is a protective mechanism to prevent lipotoxicity

The most widely regarded theory in NAFLD progression is the so-called “two hit hypothesis” (77). The first hit is a product of imbalanced fatty acid metabolism leading to hepatic triglyceride (TG) accumulation that is characteristic of NAFLD. The second hit is thought to involve

oxidative and/or metabolic stress as the liver attempts to compensate for prolonged alterations in lipid metabolism, which culminates in hepatic inflammation and cell death (77). However, questions remain as to whether the accumulation of intrahepatic TGs is actually the initial cause of progressive liver disease or merely an early adaptive response to increased lipid load. Recent literature points to the latter, suggesting that while TG synthesis is symptomatic of hepatic lipid overload, it is actually serving a protective role by providing a route to inertly dispose of excess fatty acids and prevent the formation of more toxic lipid intermediates (78).

Data from *in vitro* experiments provide some important clues as to the role of TGs in hepatic lipotoxicity. For example, experiments with H4IIEC3 rat hepatomas demonstrate that palmitate-induced ROS production and subsequent cell death occur in the absence of excess TG formation. Conversely, treatment with oleate causes significant TG formation with little ROS production or cell death (30). Interestingly, when palmitate is co-supplemented with oleate, the lipotoxic effects of palmitate are completely abolished with a coincident increase in lipid droplet formation. These experiments suggest that the increased toxicity of SFAs may be in large part attributable to the fact that they are less efficiently esterified into TGs. When the supply of unsaturated fatty acids becomes limited or there is insufficient capacity to dispose of SFAs by either TG synthesis or beta-oxidation, the resulting accumulation of saturated phospholipids and other toxic lipid intermediates may subsequently promote cellular dysfunction and apoptosis. Several different cell types including β-cells (46, 76) , cultured rat islets (79), Chinese hamster ovary (CHO) cells (19), breast cancer cells (20) and rat liver cells (30, 80, 81) have shown similar results: acute SFA lipotoxicity is inversely correlated with triglyceride synthesis.

SCD-1 is the enzyme responsible for catalyzing the endogenous desaturation of SFAs, such as palmitate (16:0) and sterate (18:0), into their monounsaturated counterparts, palmitoleate (16:1) and oleate (18:1), respectively (82, 83). Altering the cellular capacity for fatty acid saturation can dramatically change the potential lipotoxic effects of SFA supplementation. Hepatic models with SCD-1 inhibition have previously been shown to display significant reductions in triglyceride content (84). Both primary C57BL/6 hepatocytes and HepG2 cells with pharmacological and genetic siRNA inhibition of SCD-1 showed significantly increased sensitivity to palmitate-mediated apoptosis compared to controls treated with palmitate alone (81). Alternatively, CHO cells overexpressing SCD-1 displayed significant increases in TG synthesis and labeled SFA incorporation into TG species and were almost completely resistant to SFA-induced apoptosis (19).

The beneficial effects of partitioning FFAs into TGs demonstrated by *in vitro* models also translates to *in vivo* rodent models. Mice expressing SCD-1 ($SCD\text{-}1^{+/+}$) had significantly increased levels of TG accumulation in the liver compared to both high fat diet (HFD) controls and SCD knockout mice ($SCD\text{-}1^{-/-}$), but also significantly reduced markers of hepatic apoptosis and inflammation compared to $SCD\text{-}1^{-/-}$ (81). Interestingly, *in vivo* rodent models of progressive

liver disease have demonstrated a highly suppressed expression level of SCD-1 (81, 85), suggesting a possible impairment in SFA esterification into TG, thereby implicating compromised and/or reduced TG synthesis as an instigator in the progressive pathology of NAFLD.

Methods for overexpressing or inhibiting enzymes responsible for TG synthesis have also been utilized in order to investigate the relationship between hepatic TG synthesis and progressive liver disease. Yamaguchi et al. (86) studied male *db/db* mice on a MCD diet. These animals have a genetically defective leptin receptor and provide a useful model of severe obesity and type II diabetes, and develop NASH when placed on an MCD diet (9, 87). Their study sought to investigate whether inhibiting TG synthesis with a liver-specific knockdown of diacylglycerol acyltrasferase 2 (DGAT2) would prevent hepatic steatosis and protect the liver from further progression to NAFLD. DGAT2 is responsible for catalyzing the final step in hepatic TG biosynthesis (88); therefore, the antisense oligonucleotide suppression of this enzyme was successful in preventing hepatic steatosis resulting from MCD-induced accumulation of TGs. However, contrary to the investigators' expectations, reduction of hepatic steatosis with DGAT2-ASO did not protect the MCD-diet fed mice from hepatic inflammation and fibrosis. In fact, these mice experienced increased markers of inflammation and disease associated with NASH, including increased levels of alanine aminotransferase (ALT), aspartate aminotransferase (AST), lobular inflammation, FFA levels and oxidative damage as assessed by TBAR and 4-HNE levels, compared to MCD-diet controls (86). An alternate study by Monetti et al. (89) investigated the link between hepatic steatosis and insulin resistance in mice overexpressing the DGAT2 gene in the liver (liv-DGAT2). Finding DGAT-mediated steatosis in the liver to be insufficient to cause insulin resistance in the tissue, they investigated markers of inflammation and ER stress previously shown to promote insulin resistance. Mice expressing a 2-fold increase in hepatic DGAT2 mRNA (Liv-DGAT2-low) displayed a ~5-fold increase in hepatic TG content, but interestingly had reduced levels of phosphorylated Jun-N-terminal kinase (JNK), nuclear factor kappa B (NF-κB), and PERK compared to the WT littermates when both groups were maintained on a high-fat diet (89). Together, these findings suggest that TG synthesis provides a protective mechanism to buffer against toxic accumulation of FFAs in the liver.

Overall, recent literature points to a dissociation between hepatic triglyceride formation and progression towards severe fatty liver disease. While increased hepatic triglyceride formation is most certainly an early indicator of liver metabolic stress and disease, it does not appear to be the initiating factor in NASH, but instead serves as a protective metabolic mechanism to counter FFA overload (78). Triglycerides may serve as inert storage species for diverting FFAs away from toxic pathways and thus protecting the cell from lipoapoptotic effects. The degree of FFA saturation has also been demonstrated to have a strong effect on the tendency of the cell to store FFAs as TGs, where unsaturated FFAs are more likely incorporated into TGs and their saturated counterparts are channeled towards other cellular fates. Once the ability of the cell to channel

FFAs away from other metabolic pathways leading to lipotoxicity and into neutral TGs becomes diminished and/or overwhelmed, cellular FFA levels increase, resulting in a diseased phenotype characteristic of NASH.

From bench to bedside: clinical trials in NASH patients

Investigations into the molecular etiology of NASH have provided potential therapeutic targets to both ameliorate and prevent hepatic apoptosis and inflammation. For example, vitamin E was administered to insulin-tolerant patients to investigate antioxidants as a potential treatment for NASH (90). Treatment with vitamin E resulted in reduced liver injury assessed by a reduction in serum alanine and aspartate aminotransferase levels. Although fibrosis scores were unimproved, other histologic features such as lobular inflammation and hepatocellular ballooning were improved. Similarly, pentoxifylline has been utilized successfully in mouse models (91) and human clinical trials (92) for treatment of NASH. Pentoxifylline is a non-selective phosphodiesterase inhibitor that has well known effects to suppress production of pro-inflammatory cytokines, such as TNF-alpha, as well as antioxidant properties that include reducing ROS production, scavenging free radicals (93, 94), and preventing the depletion of glutathione stores (95). In the clinical trial, 55 patients with confirmed NASH received thee daily doses of pentoxifylline or placebo over a 1-year period. After the duration of treatment, analysis showed significantly more patients on pentoxifylline than placebo had NAS decrease by $\geq$2 points. Steatosis, lobular inflammation and fibrosis also showed significant improvements although no change in hepatocellular ballooning was observed (92).The ameliorating effects of antioxidant therapy highlight the central pathogenic role oxidative stress has in NASH disease progression.

Well-known anti-diabetic drugs, such as metformin and thiazolidinedione derivatives, have also been frequently utilized as NASH treatments in diabetic and non-diabetic patients alike. Metformin is a first-line treatment for type II diabetes that inhibits hepatic gluconeogenesis (96) and alters fatty acid metabolism (97), often resulting in patient weight loss. In a clinical trial of NASH, metformin was shown to improve liver histology and ALT levels in a significant portion of patients (30%), which could not be attributed to increases in insulin sensitivity (98). The beneficial effects on NASH appeared to be mediated partly by the ability of metformin to promote weight loss, where the most weight loss correlated with the most improvement in liver histology. In fact, reduction in body mass by itself has been described as an effective intervention in NALFD progression (99). Results from clinical studies indicate that reductions in body weight of just 5% to >7% result in significant reductions in steatosis, NAS, and other laboratory abnormalities associated with progressive NAFLD in children (100) and adults with NASH (101, 102), respectively. Studies (103-105) and reviews (106, 107) on the impact of weight loss due to bariatric surgery have demonstrated similar improvements.

Pioglitazone is a derivative of the thiazolidinedione class of drugs used to treat type II diabetes mellitus due to its ability to reduce insulin resistance by activating PPAR-γ and controlling glucose and lipid metabolism in peripheral tissues (108). A placebo-controlled clinical trial of pioglitazone in patients with NASH revealed encouraging results, where patients receiving pioglitazone displayed significant improvements in ALT and AST levels as well as hepatic histological markers such as reduced steatosis, ballooning, necrosis and inflammation despite a small weight gain (109). However, fibrosis improvements were not significantly different than that of a placebo+dietary intervention group. The conclusions about the mediator of this marked NASH improvement in patients treated with pioglitazone were not attributable to a single factor, but speculation regarding several mechanisms was briefly discussed. Mechanisms postulated include the following two: (i) thiazolidinediones are known to increase insulin sensitivity and reduce peripheral lipolysis from adipose tissue (110), thus significantly decreasing the flux of free fatty acid substrates to the liver and (ii) pioglitazone has been shown to activate AMPK (110) and raise adiponectin levels in the liver (111), which may play an important role in mediating the effects of thiazolidinediones in the liver. The serum aminotransferase level and histological improvements demonstrated with some classic diabetes drugs in patients with NASH warrants further investigation into the metabolic mechanisms activated in order to develop more targeted therapies in the future.

A new drug has recently made waves in the medical community when clinical trials for obeticholic acid (OCA) for treatment of NASH were stopped early for efficacy based on interim analysis that shows recipients have already met the primary endpoint of the trial. OCA is a farnesoid X receptor (FXR) agonist that was orally administered in a double-blind, placebo-controlled clinical trial known as FXR Ligand OCA in NASH Treatment (FLINT) at a dosage of 25 mg daily in biopsy-proven adult NASH patients over 72 weeks. OCA is essentially a semi-synthesis bile acid that serves to activate FXR. FXR is a nuclear receptor that expressed at high levels in the liver and intestines and plays role in various metabolic pathways including bile acid, glucose and lipid metabolism (112). When lipophilic bile acids, such as OCA, bind to FXR it is activated and promotes decreased hepatic gluconeogenesis, circulating triglycerides, hepatic lipid synthesis and enhanced peripheral clearance of VLDL and HDL (113). Based on these metabolic attributes, pharmacological activation of FXR was targeted as therapeutic treatment for NASH. Results from the FLINT study demonstrate highly statistically significant reductions in NAS score of at least two points and no worsening of fibrosis compared to placebo treated patients (113). Of the OCA-treated patients, 45% had improved liver histology compared to 21% in the placebo group (113) which demonstrates promising results for future clinical treatment of high-risk NASH patients.

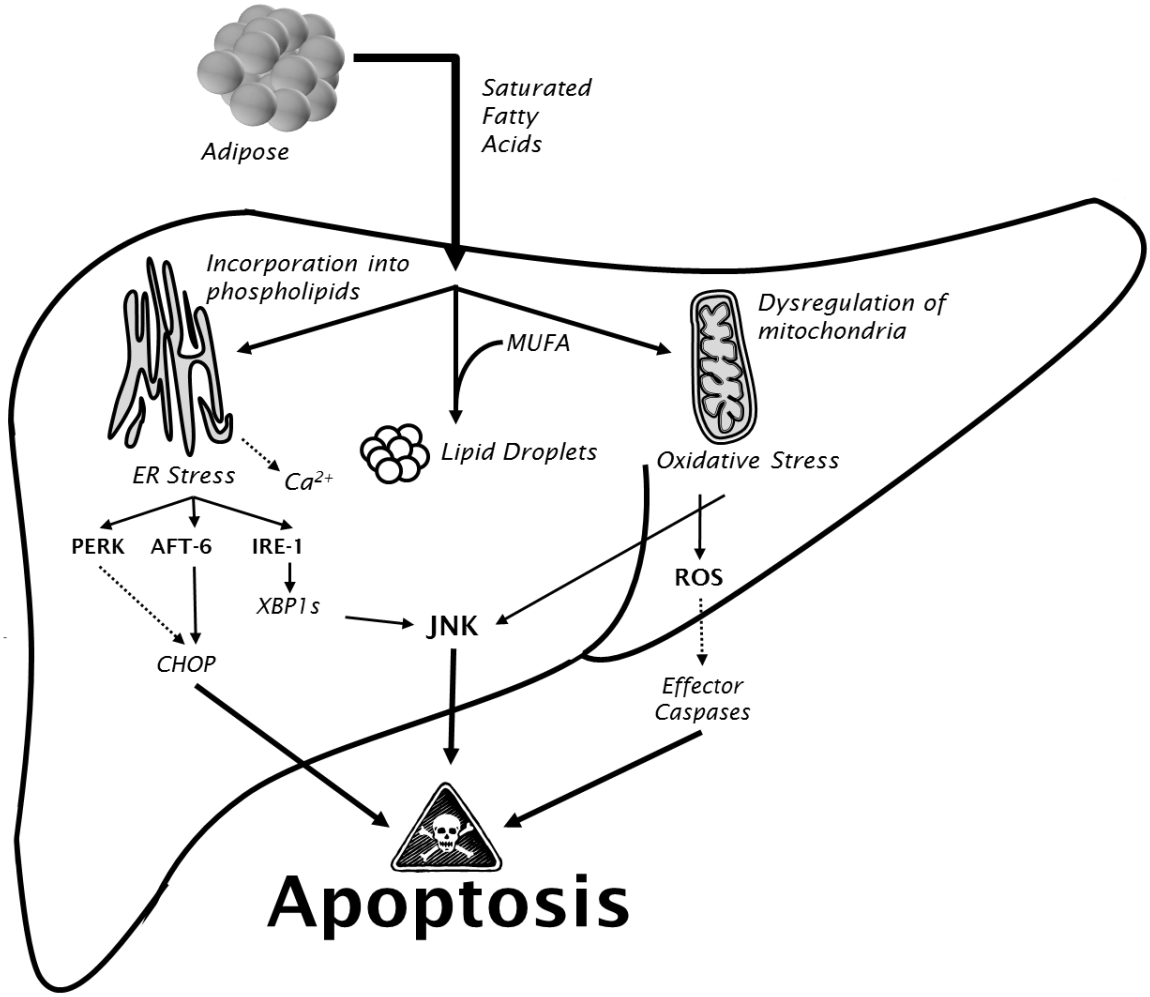

Figure 2-1. Saturated fatty acids initiate cellular dysfunction in lipotoxicity/NAFLD. Lipolysis of subcutaneous and visceral adipose tissue gives rise to higher concentrations of free fatty acids in the blood resulting in ectopic fat storage within the liver. Upon entering the liver, FFAs are partitioned toward thee main lipid disposal pathways: β-oxidation, TG synthesis, and phospholipid synthesis/remodeling. Mitochondrial β-oxidation gradually breaks down fatty acids into two-carbon acetyl-CoA units, which are subsequently used to fuel the TCA cycle. Esterification of FFAs into TG and phospholipids provides an alternate route for disposing of elevated FFAs. High concentrations of saturated fatty acids, however, avoid protective sequestration into triglyceride stores and/or β-oxidation. Instead, SFAs are channeled toward phospholipid incorporation. Increased saturation of ER phospholipids can compromise the integrity of the ER-membrane structure resulting in stimulation of UPR signaling pathways and disruption of mitochondrial function. Additionally, elevated SFAs deregulate TCA cycle metabolism leading to ROS accumulation. Both ER-stress pathways and mitochondrial dysfunction activate JNK stress signaling, thus leading to eventual apoptotic cell death. Abbreviations: Monounsaturated fatty acid (MUFA); Endoplasmic reticulum (ER); Protein kinase RNA-like endoplasmic reticulum kinase (PERK); Inositol-requiring protein–1 (IRE-1); Xbox binding protein-1 spliced (XBS-1s); Activating transcription factor 6 (ATF-6); Jun N-terminal kinase (JNK); Reactive oxygen species (ROS).

Conclusion

Nonalcoholic steatohepatitis is the liver manifestation of obesity and the metabolic syndrome and is marked by lipid deposition, inflammation and apoptosis. While triglyceride accumulation is a hallmark of NAFLD, several *in vitro* and animal models suggest triglyceride accumulation is a protective mechanism to delay the toxic effects of excess lipids. Altered composition of intrahepatic free fatty acids and phospholipid metabolites have instead been implicated as major contributors to acute liver dysfunction and apoptosis. Many studies have demonstrated that saturated fatty acids are more toxic than their unsaturated counterparts, resulting in a progressive lipotoxic cascade (Fig. 2-1). SFAs have been shown to increase the saturation of membrane phospholipids, thus initiating UPR and leading to ER stress. SFAs also affect mitochondrial metabolism and promote ROS accumulation. Furthermore, hepatocyte apoptosis has been shown to be dependent on the activation of JNK stress signaling pathways that respond to prolonged ER and oxidative stress. Despite these common molecular features of lipotoxicity, a unifying mechanism is still unclear and has prevented the development of novel treatments for NASH. However, recent literature provides strong evidence that fatty acid saturation plays a critical role in determining cell fate under lipotoxic conditions. Continued research in understanding these molecular mechanisms will provide direction for more targeted therapeutics for NAFLD and NASH patients in the future.

References

1. Barshop, N. J., C. B. Sirlin, J. B. Schwimmer, and J. E. Lavine. 2008. Review article: epidemiology, pathogenesis and potential treatments of paediatric non-alcoholic fatty liver disease. *Aliment. Pharmacol. Ther.* **28**: 13-24.

2. Reddy, J. K., and M. S. Rao. 2006. Lipid metabolism and liver inflammation. II. Fatty liver disease and fatty acid oxidation. *Am. J. Physiol.-Gastroint. Liver Physiol.* **290**: G852-G858.

3. Feldstein, A., and G. J. Gores. 2004. Steatohepatitis and apoptosis: Therapeutic implications. *American Journal of Gastroenterology* **99**: 1718-1719.

4. Kleiner, D. E., E. M. Brunt, M. Van Natta, C. Behling, M. J. Contos, O. W. Cummings, L. D. Ferrell, Y. C. Liu, M. S. Torbenson, A. Unalp-Arida, M. Yeh, A. J. McCullough, A. J. Sanyal, and C. Nonalcoholic Steatohepatitis. 2005. Design and validation of a histological scoring system for nonalcoholic fatty liver disease. *Hepatology* **41**: 1313-1321.

5. Bacon, B. R., M. J. Farahvash, C. G. Janney, and B. A. Neuschwandertetri. 1994. NONALCOHOLIC STEATOHEPATITIS - AN EXPANDED CLINICAL ENTITY. *Gastroenterology* **107**: 1103-1109.

6. Mofrad, P., M. J. Contos, M. Haque, C. Sargeant, R. A. Fisher, V. A. Luketic, R. K. Sterling, M. L. Shiffman, R. T. Stravitz, and A. J. Sanyal. 2003. Clinical and histologic spectrum of nonalcoholic fatty liver disease associated with normal ALT values. *Hepatology* **37**: 1286-1292.

7. Larter, C. Z., and M. M. Yeh. 2008. Animal models of NASH: Getting both pathology and metabolic context right. *Journal of Gastroenterology and Hepatology* **23**: 1635-1648.

8. Leclercq, I. A., G. C. Farrell, R. Schriemer, and G. R. Robertson. 2002. Leptin is essential for the hepatic fibrogenic response to chronic liver injury. *Journal of Hepatology* **37**: 206-213.

9. Sahai, A., P. Malladi, X. M. Pan, R. Paul, H. Melin-Aldana, R. M. Green, and P. F. Whitington. 2004. Obese and diabetic db/db mice develop marked liver fibrosis in a model of nonalcoholic steatohepatitis: role of short-form leptin receptors and osteopontin. *Am. J. Physiol.-Gastroint. Liver Physiol.* **287**: G1035-G1043.

10. Yang, S. Q., H. Z. Lin, M. D. Lane, M. Clemens, and A. M. Diehl. 1997. Obesity increases sensitivity to endotoxin liver injury: Implications for the pathogenesis of steatohepatitis. *Proceedings of the National Academy of Sciences of the United States of America* **94**: 2557-2562.

11. Sahai, A., P. Malladi, R. M. Green, and P. F. Whitington. 2003. Steatohepatitis and liver fibrosis associated with upregulated osteopontin expression in diabetic/insulin-resistant db/db mice fed a methionine and choline deficient diet. *Hepatology* **38**: 497A-497A.

12. Dela Pena, A., I. Leclercq, J. Field, J. George, B. Jones, and G. Farrell. 2005. NF-kappa B activation, rather than TNF, mediates hepatic inflammation in a murine dietary model of steatohepatitis. *Gastroenterology* **129**: 1663-1674.

13. Weltman, M. D., G. C. Farrell, and C. Liddle. 1996. Increased hepatocyte CYP2E1 expression in a rat nutritional model of hepatic steatosis with inflammation. *Gastroenterology* **111**: 1645-1653.

14. Koteish, A., and A. M. Diehl. 2001. Animal models of steatosis. *Semin. Liver Dis.* **21**: 89-104.

15. Rinella, M. E., and R. M. Green. 2004. The methionine-choline deficient dietary model of steatohepatitis does not exhibit insulin resistance. *Journal of Hepatology* **40**: 47-51.

16. Larter, C. Z. 2007. Not all models of fatty liver are created equal: Understanding mechanisms of steatosis development is important. *Journal of Gastroenterology and Hepatology* **22**: 1353-1354.

17. Sampey, B. P., A. M. Vanhoose, H. M. Winfield, A. J. Freemerman, M. J. Muehlbauer, P. T. Fueger, C. B. Newgard, and L. Makowski. 2011. Cafeteria Diet Is a Robust Model of Human Metabolic Syndrome With Liver and Adipose Inflammation: Comparison to High-Fat Diet. *Obesity* **19**: 1109-1117.

18. Charlton, M., A. Krishnan, K. Viker, S. Sanderson, S. Cazanave, A. McConico, H. Masuoko, and G. Gores. 2011. Fast food diet mouse: novel small animal model of NASH with ballooning, progressive fibrosis, and high physiological fidelity to the human condition. *Am. J. Physiol.-Gastroint. Liver Physiol.* **301**: G825-G834.

19. Listenberger, L. L., X. L. Han, S. E. Lewis, S. Cases, R. V. Farese, D. S. Ory, and J. E. Schaffer. 2003. Triglyceride accumulation protects against fatty acid-induced lipotoxicity. *Proceedings of the National Academy of Sciences of the United States of America* **100**: 3077-3082.

20. Hardy, S., W. El-Assaad, E. Przybytkowski, E. Joly, M. Prentki, and Y. Langelier. 2003. Saturated fatty acid-induced apoptosis in MDA-MB-231 breast cancer cells - A role for cardiolipin. *Journal of Biological Chemistry* **278**: 31861-31870.

21. Turpin, S., G. Lancaster, I. Darby, M. Febbraio, and M. Watt. 2006. Apoptosis in skeletal muscle myotubes is induced by ceramides and is positively related to insulin resistance. *American Journal of Physiology-Endocrinology and Metabolism* **291**: E1341-E1350.

22. Okere, I., M. Chandler, T. McElfresh, J. Rennison, V. Sharov, H. Sabbah, K. Tserng, B. Hoit, P. Ernsberger, M. Young, and W. Stanley. 2006. Differential effects of saturated and unsaturated fatty acid diets on cardiomyocyte apoptosis, adipose distribution, and serum leptin. *American Journal of Physiology-Heart and Circulatory Physiology* **291**: H38-H44.

23. Srivastava, S., and C. Chan. 2008. Application of metabolic flux analysis to identify the mechanisms of free fatty acid toxicity to human hepatoma cell line. *Biotechnology and Bioengineering* **99**: 399-410.

24. Pagliassotti, M., Y. Wei, and D. Wang. 2005. Saturated fatty acids induce cytotoxicity in hepatocytes via effects on the endoplasmic reticulum. *Obesity Research* **13**: A31-A31.

25. Leamy, A. K., R. A. Egnatchik, M. Shiota, P. T. Ivanova, D. S. Myers, H. A. Brown, and J. D. Young. 2014. Enhanced synthesis of saturated phospholipids is associated with ER stress and lipotoxicity in palmitate-treated hepatic cells. *J. Lipid Res.* **55**: 1478-1488.

26. Malhi, H., and G. J. Gores. 2008. Molecular Mechanisms of Lipotoxicity in Nonalcoholic Fatty Liver Disease. *Semin. Liver Dis.* **28**: 360-369.

27. Leamy, A. K., R. A. Egnatchik, and J. D. Young. 2013. Molecular mechanisms and the role of saturated fatty acids in the progression of non-alcoholic fatty liver disease. *Prog. Lipid Res.* **52**: 165-174.

28. Turpin, S. M., G. I. Lancaster, I. Darby, M. A. Febbraio, and M. J. Watt. 2006. Apoptosis in skeletal muscle myotubes is induced by ceramides and is positively related to insulin resistance. *Am. J. Physiol.-Endocrinol. Metab.* **291**: E1341-E1350.

29. Listenberger, L. L., D. S. Ory, and J. E. Schaffer. 2001. Palmitate-induced apoptosis can occur through a ceramide-independent pathway. *J. Biol. Chem.* **276**: 14890-14895.

30. Noguchi, Y., J. D. Young, J. O. Aleman, M. E. Hansen, J. K. Kelleher, and G. Stephanopoulos. 2009. Effect of Anaplerotic Fluxes and Amino Acid Availability on Hepatic Lipoapoptosis. *J. Biol. Chem.* **284**: 33425-33436.

31. Kaufman, R. J. 2002. Orchestrating the unfolded protein response in health and disease. *J. Clin. Invest.* **110**: 1389-1398.

32. Scorrano, L., S. A. Oakes, J. T. Opferman, E. H. Cheng, M. D. Sorcinelli, T. Pozzan, and S. J. Korsmeyer. 2003. BAX and BAK regulation of endoplasmic reticulum Ca2+: A control point for apoptosis. *Science* **300**: 135-139.

33. Wek, R. C., and T. G. Anthony. 2010. Obesity: stressing about unfolded proteins. *Nature Medicine* **16**: 374-376.

34. Ron, D., and P. Walter. 2007. Signal integration in the endoplasmic reticulum unfolded protein response. *Nature Reviews Molecular Cell Biology* **8**: 519-529.

35. Zhang, K. Z., and R. J. Kaufman. 2006. The unfolded protein response - A stress signaling pathway critical for health and disease. *Neurology* **66**: S102-S109.

36. Ozcan, U., Q. Cao, E. Yilmaz, A. H. Lee, N. N. Iwakoshi, E. Ozdelen, G. Tuncman, C. Gorgun, L. H. Glimcher, and G. S. Hotamisligil. 2004. Endoplasmic reticulum stress links obesity, insulin action, and type 2 diabetes. *Science* **306**: 457-461.

37. Rizzuto, R., M. Brini, M. Murgia, and T. Pozzan. 1993. Microdomains with high Ca2+ close to IP(3)-sensitive channels that are sensed by neighboring mitochondria. *Science* **262**: 744-747.

38. Bernardi, P. 1999. Mitochondrial transport of cations: Channels, exchangers, and permeability transition. *Physiological Reviews* **79**: 1127-1155.

39. Gregor, M. F., L. Yang, E. Fabbrini, B. S. Mohammed, J. C. Eagon, G. S. Hotamisligil, and S. Klein. 2009. Endoplasmic Reticulum Stress Is Reduced in Tissues of Obese Subjects After Weight Loss. *Diabetes* **58**: 693-700.

40. Puri, P., F. Mirshahi, O. Cheung, R. Natarajan, J. W. Maher, J. M. Kellum, and A. J. Sanyal. 2008. Activation and dysregulation of the unfolded protein response in nonalcoholic fatty liver disease. *Gastroenterology* **134**: 568-576.

41. Sharma, N. K., S. K. Das, A. K. Mondal, O. G. Hackney, W. S. Chu, P. A. Kern, N. Rasouli, H. J. Spencer, A. Yao-Borengasser, and S. C. Elbein. 2008. Endoplasmic Reticulum Stress Markers Are Associated with Obesity in Nondiabetic Subjects. *Journal of Clinical Endocrinology & Metabolism* **93**: 4532-4541.

42. Wang, D., Y. R. Wei, and M. J. Pagliassotti. 2006. Saturated fatty acids promote endoplasmic reticulum stress and liver injury in rats with hepatic steatosis. *Endocrinology* **147**: 943-951.

43. Wei, Y., D. Wang, F. Topczewski, and M. J. Pagliassotti. 2006. Saturated fatty acids induce endoplasmic reticulum stress and apoptosis independently of ceramide in liver cells. *Am. J. Physiol.-Endocrinol. Metab.* **291**: E275-E281.

44. Pfaffenbach, K. T., C. L. Gentile, A. M. Nivala, D. Wang, Y. R. Wei, and M. J. Pagliassotti. 2010. Linking endoplasmic reticulum stress to cell death in hepatocytes: roles of C/EBP homologous protein and chemical chaperones in palmitate-mediated cell death. *Am. J. Physiol.-Endocrinol. Metab.* **298**: E1027-E1035.

45. Diakogiannaki, E., H. J. Welters, and N. G. Morgan. 2008. Differential regulation of the endoplasmic reticulum stress response in pancreatic beta-cells exposed to long-chain saturated and monounsaturated fatty acids. *Journal of Endocrinology* **197**: 553-563.

46. Thorn, K., and P. Bergsten. 2010. Fatty Acid-Induced Oxidation and Triglyceride Formation Is Higher in Insulin-Producing MIN6 Cells Exposed to Oleate Compared to Palmitate. *Journal of Cellular Biochemistry* **111**: 497-507.

47. Guo, W., S. Wong, W. Xie, T. Lei, and Z. Luo. 2007. Palmitate modulates intracellular signaling, induces endoplasmic reticulum stress, and causes apoptosis in mouse 3T3-L1 and rat primary preadipocytes. *Am. J. Physiol.-Endocrinol. Metab.* **293**: E576-E586.

48. Borradaile, N. M., X. Han, J. D. Harp, S. E. Gale, D. S. Ory, and J. E. Schaffer. 2006. Disruption of endoplasmic reticulum structure and integrity in lipotoxic cell death. *J. Lipid Res.* **47**: 2726-2737.

49. Pfaffenbach, K., C. Gentile, A. Nivala, D. Wang, Y. Wei, and M. Pagliassotti. 2010. Linking endoplasmic reticulum stress to cell death in hepatocytes: roles of C/EBP homologous protein and chemical chaperones in palmitate-mediated cell death. *American Journal of Physiology-Endocrinology and Metabolism* **298**: E1027-E1035.

50. Gu, X., K. Li, D. R. Laybutt, M.-l. He, H.-L. Zhao, J. C. N. Chan, and G. Xu. 2010. Bip overexpression, but not CHOP inhibition, attenuates fatty-acid-induced endoplasmic reticulum stress and apoptosis in HepG2 liver cells. *Life Sciences* **87**: 724-732.

51. Spector, A. A., and M. A. Yorek. 1985. Membrane lipid-Composition and cellular function. *J. Lipid Res.* **26**: 1015-1035.

52. Deguil, J., L. Pineau, E. C. R. Snyder, S. Dupont, L. Beney, A. Gil, G. Frapper, and T. Ferreira. 2011. Modulation of Lipid-Induced ER Stress by Fatty Acid Shape. *Traffic* **12**: 349-362.

53. Van der Sanden, M. H. M., M. Houweling, L. M. G. Van Golde, and A. B. Vaandrager. 2003. Inhibition of phosphatidylcholine synthesis induces expression of the endoplasmic reticulum stress and apoptosis-related protein CCAAT/enhancer-binding protein-homologous protein (CHOP/GADD153). *Biochemical Journal* **369**: 643-650.

54. Li, Y. K., M. T. Ge, L. Ciani, G. Kuriakose, E. J. Westover, M. Dura, D. F. Covey, J. H. Freed, F. R. Maxfield, J. Lytton, and I. Tabas. 2004. Enrichment of endoplasmic reticulum with cholesterol inhibits sarcoplasmic-endoplasmic reticulum calcium ATPase-2b activity in parallel

with increased order of membrane lipids - Implications for depletion of endoplasmic reticulum calcium stores and apoptosis in cholesterol-loaded macrophages. *J. Biol. Chem.* **279**: 37030-37039.

55. Egnatchik, R., A. Leamy, D. Jacobson, M. Shiota, and J. Young. 2014. ER calcium release promotes mitochondrial dysfunction and hepatic cell lipotoxicity in response to palmitate overload. *Molecular Metabolism* **3**: 544-553.

56. Ariyama, H., N. Kono, S. Matsuda, T. Inoue, and H. Arai. 2010. Decrease in Membrane Phospholipid Unsaturation Induces Unfolded Protein Response. *J. Biol. Chem.* **285**: 22027-22035.

57. Puri, P., R. A. Baillie, M. Wiest, F. Mirshahi, and A. J. Sanyal. 2006. A lipidomic analysis of non-alcoholic fatty liver disease (NAFLD). *Journal of Hepatology* **44**: S260-S261.

58. Han, M. S., S. Y. Park, K. Shinzawa, S. Kim, K. W. Chung, J.-H. Lee, C. H. Kwon, K.-W. Lee, J.-H. Lee, C. K. Park, W. J. Chung, J. S. Hwang, J.-J. Yan, D.-K. Song, Y. Tsujimoto, and M.-S. Lee. 2008. Lysophosphatidylcholine as a death effector in the lipoapoptosis of hepatocytes. *J. Lipid Res.* **49**: 84-97.

59. Kakisaka, K., S. C. Cazanave, C. D. Fingas, M. E. Guicciardi, S. F. Bronk, N. W. Werneburg, J. L. Mott, and G. J. Gores. 2012. Mechanisms of lysophosphatidylcholine-induced hepatocyte lipoapoptosis. *Am. J. Physiol.-Gastroint. Liver Physiol.* **302**: G77-G84.

60. Koek, G. H., P. R. Liedorp, and A. Bast. 2011. The role of oxidative stress in non-alcoholic steatohepatitis. *Clinica Chimica Acta* **412**: 1297-1305.

61. Kamata, H., S. Honda, S. Maeda, L. F. Chang, H. Hirata, and M. Karin. 2005. Reactive oxygen species promote TNF alpha-induced death and sustained JNK activation by inhibiting MAP kinase phosphatases. *Cell* **120**: 649-661.

62. Petrosillo, G., F. M. Ruggiero, M. Pistolese, and G. Paradies. 2004. Ca2+-induced reactive oxygen species production promotes cytochrome c release from rat liver mitochondria via mitochondrial permeability transition (MPT)-dependent and MPT-independent mechanisms - Role of cardiolipin. *J. Biol. Chem.* **279**: 53103-53108.

63. Malhi, H., S. F. Bronk, N. W. Werneburg, and G. J. Gores. 2006. Free fatty acids induce JNK-dependent hepatocyte lipoapoptosis. *J. Biol. Chem.* **281**: 12093-12101.

64. Barreyro, F. J., S. Kobayashi, S. F. Bronk, N. W. Werneburg, H. Malhi, and G. J. Gores. 2007. Transcriptional regulation of Bim by FoxO3A mediates hepatocyte lipoapoptosis. *J. Biol. Chem.* **282**: 27141-27154.

65. Chalasani, N., M. A. Deeg, and D. W. Crabb. 2004. Systemic levels of lipid peroxidation and its metabolic and dietary correlates in patients with nonalcoholic steatohepatitis. *American Journal of Gastroenterology* **99**: 1497-1502.

66. Weltman, M. D., G. C. Farrell, P. Hall, M. Ingelman-Sundberg, and C. Liddle. 1998. Hepatic cytochrome p450 2E1 is increased in patients with nonalcoholic steatohepatitis. *Hepatology* **27**: 128-133.

67. Lambertucci, R. H., S. M. Hirabara, L. D. R. Silveira, A. C. Levada-Pires, R. Curi, and T. C. Pithon-Curi. 2008. Palmitate increases superoxide production through mitochondrial electron

transport chain and NADPH oxidase activity in skeletal muscle cells. *Journal of Cellular Physiology* **216**: 796-804.

68. Nakamura, S., T. Takamura, N. Matsuzawa-Nagata, H. Takayama, H. Misu, H. Noda, S. Nabemoto, S. Kurita, T. Ota, H. Ando, K. Miyamoto, and S. Kaneko. 2009. Palmitate Induces Insulin Resistance in H4IIEC3 Hepatocytes through Reactive Oxygen Species Produced by Mitochondria. *Journal of Biological Chemistry* **284**: 14809-14818.

69. Sanyal, A. J., C. Morowitz, J. Clore, M. L. Shiffman, V. A. Luketic, R. Sterling, and N. Ghatak. 1999. Nonalcoholic steatohepatitis (NASH) is associated with insulin resistance and mitochondrial structural abnormalities. *Gastroenterology* **116**: A1271-A1271.

70. Sanyal, A. J., C. Campbell-Sargent, F. Mirshahi, W. B. Rizzo, M. J. Contos, R. K. Sterling, V. A. Luketic, M. L. Shiffman, and J. N. Clore. 2001. Nonalcoholic steatohepatitis: Association of insulin resistance and mitochondrial abnormalities. *Gastroenterology* **120**: 1183-1192.

71. Iozzo, P., M. Bucci, A. Roivainen, K. Nagren, M. J. Jaervisalo, J. Kiss, L. Guiducci, B. Fielding, A. G. Naum, R. Borra, K. Virtanen, T. Savunen, P. A. Salvadori, E. Ferrannini, J. Knuuti, and P. Nuutila. 2010. Fatty Acid Metabolism in the Liver, Measured by Positron Emission Tomography, Is Increased in Obese Individuals. *Gastroenterology* **139**: 846-U203.

72. Cook, G. A., and M. S. Gamble. 1987. REGULATION OF CARNITINE PALMITOYLTRANSFERASE BY INSULIN RESULTS IN DECREASED ACTIVITY AND DECREASED APPARENT KI VALUES FOR MALONYL-COA. *J. Biol. Chem.* **262**: 2050-2055.

73. McGarry, J. D., and D. W. Foster. 1980. REGULATION OF HEPATIC FATTY-ACID OXIDATION AND KETONE-BODY PRODUCTION. *Annu. Rev. Biochem.* **49**: 395-420.

74. Nakamura, S., T. Takamura, N. Matsuzawa-Nagata, H. Takayama, H. Misu, H. Noda, S. Nabemoto, S. Kurita, T. Ota, H. Ando, K.-i. Miyamoto, and S. Kaneko. 2009. Palmitate Induces Insulin Resistance in H4IIEC3 Hepatocytes through Reactive Oxygen Species Produced by Mitochondria. *J. Biol. Chem.* **284**: 14809-14818.

75. Ip, E., G. C. Farrell, G. Robertson, P. Hall, R. Kirsch, and I. Leclercq. 2003. Central role of PPAR alpha-dependent hepatic lipid turnover in dietary steatohepatitis in mice. *Hepatology* **38**: 123-132.

76. Choi, S.-E., I.-R. Jung, Y.-J. Lee, S.-J. Lee, J.-H. Lee, Y. Kim, H.-S. Jun, K.-W. Lee, C. B. Park, and Y. Kang. 2011. Stimulation of Lipogenesis as Well as Fatty Acid Oxidation Protects against Palmitate-Induced INS-1 beta-Cell Death. *Endocrinology* **152**: 816-827.

77. Day, C. P., and O. F. W. James. 1998. Steatohepatitis: A tale of two "hits"? *Gastroenterology* **114**: 842-845.

78. Schaffer, J. E. 2003. Lipotoxicity: when tissues overeat. *Current Opinion in Lipidology* **14**: 281-287.

79. Cnop, M., J. C. Hannaert, A. Hoorens, D. L. Eizirik, and D. G. Pipeleers. 2001. Inverse relationship between cytotoxicity of free fatty acids in pancreatic islet cells and cellular triglyceride accumulation. *Diabetes* **50**: 1771-1777.

80. Mantzaris, M. D., E. V. Tsianos, and D. Galaris. 2011. Interruption of triacylglycerol synthesis in the endoplasmic reticulum is the initiating event for saturated fatty acid-induced lipotoxicity in liver cells. *Febs Journal* **278**: 519-530.

81. Li, Z. Z., M. Berk, T. M. McIntyre, and A. E. Feldstein. 2009. Hepatic Lipid Partitioning and Liver Damage in Nonalcoholic Fatty Liver Disease - Role of stearoyl-CoA desaturase. *J. Biol. Chem.* **284**: 5637-5644.

82. Enoch, H. G., A. Catala, and P. Strittmatter. 1976. Mechanism of rat-liver microsomal steroyl-CoA desaturase - Studies of substrate specificity, enzyme substrate interactions, and function of lipid. *J. Biol. Chem.* **251**: 5095-5103.

83. Miyazaki, M., W. C. Man, and J. M. Ntambi. 2001. Targeted disruption of stearoyl-CoA desaturase1 gene in mice causes atrophy of sebaceous and meibomian glands and depletion of wax esters in the eyelid. *Journal of Nutrition* **131**: 2260-2268.

84. Ntambi, J. M., M. Miyazaki, J. P. Stoehr, H. Lan, C. M. Kendziorski, B. S. Yandell, Y. Song, P. Cohen, J. M. Friedman, and A. D. Attie. 2002. Loss of stearoyl-CoA desaturase-1 function protects mice against adiposity. *Proceedings of the National Academy of Sciences of the United States of America* **99**: 11482-11486.

85. Rizki, G., L. Arnaboldi, B. Gabrielli, J. Yan, G. S. Lee, R. K. Ng, S. M. Turner, T. M. Badger, R. E. Pitas, and J. J. Maher. 2006. Mice fed a lipogenic methionine-choline-deficient diet develop hypermetabolism coincident with hepatic suppression of SCD-1. *J. Lipid Res.* **47**: 2280-2290.

86. Yamaguchi, K., L. Yang, S. McCall, J. W. Huang, X. X. Yu, S. K. Pandey, S. Bhanot, B. P. Monia, Y. X. Li, and A. M. Diehl. 2007. Inhibiting triglyceride synthesis improves hepatic steatosis but exacerbates liver damage and fibrosis in obese mice with nonalcoholic steatohepatitis. *Hepatology* **45**: 1366-1374.

87. Chen, H., O. Charlat, L. A. Tartaglia, E. A. Woolf, X. Weng, S. J. Ellis, N. D. Lakey, J. Culpepper, K. J. Moore, R. E. Breitbart, G. M. Duyk, R. I. Tepper, and J. P. Morgenstern. 1996. Evidence that the diabetes gene encodes the leptin receptor: Identification of a mutation in the leptin receptor gene in db/db mice. *Cell* **84**: 491-495.

88. Yen, C.-L. E., S. J. Stone, S. Koliwad, C. Harris, and R. V. Farese, Jr. 2008. DGAT enzymes and triacylglycerol biosynthesis. *J. Lipid Res.* **49**: 2283-2301.

89. Monetti, M., M. C. Levin, M. J. Watt, M. P. Sajan, S. Marmor, B. K. Hubbard, R. D. Stevens, J. R. Bain, C. B. Newgard, R. V. Farese, Sr., A. L. Hevener, and R. V. Farese, Jr. 2007. Dissociation of hepatic steatosis and insulin resistance in mice overexpressing DGAT in the liver. *Cell Metabolism* **6**: 69-78.

90. Sanyal, A. J., N. Chalasani, K. V. Kowdley, A. McCullough, A. M. Diehl, N. M. Bass, B. A. Neuschwander-Tetri, J. E. Lavine, J. Tonascia, A. Unalp, M. Van Natta, J. Clark, E. M. Brunt, D. E. Kleiner, J. H. Hoofnagle, P. R. Robuck, and C. R. N. Nash. 2010. Pioglitazone, Vitamin E, or Placebo for Nonalcoholic Steatohepatitis. *New England Journal of Medicine* **362**: 1675-1685.

91. Koppe, S. W. P., A. Sahai, P. Malladi, P. F. Whitington, and R. M. Green. 2004. Pentoxifylline attenuates steatohepatitis induced by the methionine choline deficient diet. *Journal of Hepatology* **41**: 592-598.

92. Zein, C. O., L. M. Yerian, P. Gogate, R. Lopez, J. P. Kirwan, A. E. Feldstein, and A. J. McCullough. 2011. Pentoxifylline Improves Nonalcoholic Steatohepatitis: A Randomized Placebo-Controlled Trial. *Hepatology* **54**: 1610-1619.

93. Bhat, V. B., and K. M. Madyastha. 2001. Antioxidant and radical scavenging properties of 8-oxo derivatives of xanthine drugs pentoxifylline and lisofylline. *Biochem. Biophys. Res. Commun.* **288**: 1212-1217.

94. Freitas, J. P., and P. M. Filipe. 1995. Pentoxifylline - A hydroxyl radical scavenger. *Biological Trace Element Research* **47**: 307-311.

95. Gomez-Cambronero, L., B. Camps, J. G. De la Asuncion, M. Cerda, A. Pellin, F. V. Pallardo, J. Calvete, J. H. Sweiry, G. E. Mann, J. Vina, and J. Sastre. 2000. Pentoxifylline ameliorates cerulein-induced pancreatitis in rats: Role of glutathione and nitric oxide. *Journal of Pharmacology and Experimental Therapeutics* **293**: 670-676.

96. Kim, Y. D., K.-G. Park, Y.-S. Lee, Y.-Y. Park, D.-K. Kim, B. Nedumaran, W. G. Jang, W.-J. Cho, J. Ha, I.-K. Lee, C.-H. Lee, and H.-S. Choi. 2008. Metformin inhibits hepatic gluconeogenesis through AMP-activated protein kinase-dependent regulation of the orphan nuclear receptor SHP. *Diabetes* **57**: 306-314.

97. Collier, C. A., C. R. Bruce, A. C. Smith, G. Lopaschuk, and D. J. Dyck. 2006. Metformin counters the insulin-induced suppression of fatty acid oxidation and stimulation of triacylglycerol storage in rodent skeletal muscle. *Am. J. Physiol.-Endocrinol. Metab.* **291**: E182-E189.

98. Loomba, R., G. Lutchman, D. E. Kleiner, M. Ricks, J. J. Feld, B. B. Borg, A. Modi, P. Nagabhyru, A. E. Sumner, T. J. Liang, and J. H. Hoofnagle. 2009. Clinical trial: pilot study of metformin for the treatment of non-alcoholic steatohepatitis. *Aliment. Pharmacol. Ther.* **29**: 172-182.

99. Tuyama, A. C., and C. Y. Chang. 2012. Non-alcoholic fatty liver disease. *J. Diabetes* **4**: 266-280.

100. Nobili, V., M. Manco, R. Devito, V. Di Ciomm, D. Comparcola, M. P. Sartorelh, F. Piemonte, M. Marcellini, and P. Angulo. 2008. Lifestyle intervention and antioxidant therapy in children with nonalcoholic fatty liver disease: A randomized, controlled trial. *Hepatology* **48**.

101. Promrat, K., D. E. Kleiner, H. M. Niemeier, E. Jackvony, M. Kearns, J. R. Wands, J. L. Fava, and R. R. Wing. 2010. Randomized Controlled Trial Testing the Effects of Weight Loss on Nonalcoholic Steatohepatitis. *Hepatology* **51**.

102. Harrison, S. A., W. Fecht, E. M. Brunt, and B. A. Neuschwander-Tetri. 2009. Orlistat for Overweight Subjects with Nonalcoholic Steatohepatitis: A Randomized, Prospective Trial. *Hepatology* **49**.

103. Clark, J. M., A. R. A. Alkhuraishi, S. F. Solga, P. Alli, A. M. Diehl, and T. H. Magnuson. 2005. Roux-en-Y gastric bypass improves liver histology in patients with non-alcoholic fatty liver disease. *Obesity Research* **13**.

104. Barker, K. B., N. A. Palekar, S. P. Bowers, J. E. Goldberg, J. P. Pulcini, and S. A. Harrison. 2006. Non-alcoholic steatohepatitis: Effect of Roux-en-Y gastric bypass surgery. *American Journal of Gastroenterology* **101**.

105. Weiner, R. A. 2010. Surgical Treatment of Non-Alcoholic Steatohepatitis and Non-Alcoholic Fatty Liver Disease. *Digestive Diseases* **28**.

106. Rabl, C., and G. M. Campos. 2012. The Impact of Bariatric Surgery on Nonalcoholic Steatohepatitis. *Semin. Liver Dis.* **32**.

107. Rafiq, N., and Z. M. Younossi. 2008. Effects of Weight Loss on Nonalcoholic Fatty Liver Disease. *Semin. Liver Dis.* **28**.

108. Miyazaki, Y., A. Mahankali, M. Matsuda, S. Mahankali, J. Hardies, K. Cusi, L. J. Mandarino, and R. A. DeFronzo. 2002. Effect of pioglitazone on abdominal fat distribution and insulin sensitivity in type 2 diabetic patients. *Journal of Clinical Endocrinology & Metabolism* **87**: 2784-2791.

109. Belfort, R., S. A. Harrison, K. Brown, C. Darland, J. Finch, J. Hardies, B. Balas, A. Gastaldelli, F. Tio, J. Pulcini, R. Berria, J. Z. Ma, S. Dwivedi, R. Havranek, C. Fincke, R. DeFronzo, G. A. Bannayan, S. Schenker, and K. Cusi. 2006. A placebo-controlled trial of pioglitazone in subjects with nonalcoholic steatohepatitis. *New England Journal of Medicine* **355**: 2297-2307.

110. Saha, A. K., P. R. Avilucea, J. M. Ye, M. M. Assifi, E. W. Kraegen, and N. B. Ruderman. 2004. Pioglitazone treatment activates AMP-activated protein kinase in rat liver and adipose tissue in vivo. *Biochem. Biophys. Res. Commun.* **314**: 580-585.

111. Abbasi, F., S. A. Chang, J. W. Chu, T. P. Ciaraldi, C. Lamendola, T. McLaughlin, G. M. Reaven, and P. D. Reaven. 2006. Improvements in insulin resistance with weight loss, in contrast to rosiglitazone, are not associated with changes in plasma adiponectin or adiponectin multimeric complexes. *American Journal of Physiology-Regulatory Integrative and Comparative Physiology* **290**: R139-R144.

112. Adorini, L., M. Pruzanski, and D. Shapiro. 2012. Farnesoid X receptor targeting to treat nonalcoholic steatohepatitis. *Drug Discovery Today* **17**: 988-997.

113. Neuschwander-Tetri, B. A., R. Loomba, A. J. Sanyal, J. E. Lavine, M. L. Van Natta, M. F. Abdelmalek, N. Chalasani, S. Dasarathy, A. M. Diehl, B. Hameed, K. V. Kowdley, A. McCullough, N. Terrault, J. M. Clark, J. Tonascia, E. M. Brunt, D. E. Kleiner, and E. Doo. Farnesoid X nuclear receptor ligand obeticholic acid for non-cirrhotic, non-alcoholic steatohepatitis (FLINT): a multicentre, randomised, placebo-controlled trial. *The Lancet* **385**: 956-965.

CHAPTER 3

ENHANCED SYNTHESIS OF SATURATED PHOSPHOLIPIDS IS ASSOCIATED WITH ER STRESS AND LIPOTOXICTY IN PALMITATE TREATED HEPATIC CELLS

Journal of Lipid Research (55) 2014, pp. 1478-1488

Introduction

Free fatty acids (FFAs) are involved in a diverse range of functions within hepatic cells, including esterification into triacylglycerols (TAGs), oxidation to fuel mitochondrial metabolism, synthesis and remodeling of phospholipids (PLs), and conversion to signaling molecules such as prostaglandins or leukotrienes. The effects of elevated FFAs have been previously studied in cultured hepatic cell lines as a model for recapitulating the lipotoxicity that has been observed in obese type 2 diabetes and nonalcoholic fatty liver disease (NAFLD) (1-5). In these disease states, ectopic accumulation of FFAs in non-adipose tissues such as liver, pancreas, and skeletal muscle can interfere with normal cellular function and induce apoptotic cell death. These lipotoxic effects have shown dependence on fatty acid chain length and saturation. Exposure to long-chain saturated fatty acids (SFAs), such as palmitate (PA) or stearate, leads to lipoapoptosis in many cell types including hepatocytes (2, 6, 7). In contrast, monounsaturated fatty acids (MUFAs), such as oleate (OA), are not acutely cytotoxic to hepatic cells and have been shown to exert a protective effect when combined with toxic loads of SFAs (8-10).

The mechanism by which metabolism of specific lipid species results in apoptosis has not been fully elucidated. A prior *in vivo* study demonstrated the deleterious effects of increased dietary saturated fat by feeding mice a so-called “fast food diet” that was high in saturated fat and cholesterol. These mice developed pathological symptoms of non-alcoholic steatohepatitis (NASH), in contrast to mice fed a typical high-fat diet that only developed simple steatosis without NASH symptoms (11). *In vitro* lipotoxicity experiments in a variety of cell lines, including Chinese hamster ovary (CHO) cells (10, 12, 13), pancreatic beta cells (14, 15), breast cancer cells (16), and hepatic cells (6, 9, 17-19), have shown that SFA overexposure is characterized by expression of pro-inflammatory cytokines, endoplasmic reticulum (ER) impairment, elevated reactive oxygen species (ROS), and eventual apoptosis without significant TAG formation. In contrast, MUFAs and poly-unsaturated fatty acids (PUFAs) induce substantial TAG formation but do not initiate apoptosis (6, 10). These findings suggest that lipotoxicity does not correlate with accumulation of TAGs containing unsaturated FAs, and that other lipid classes may mediate responses to SFA overload. Ceramide accumulation has been postulated as a major contributing factor in palmitate-induced lipotoxicity due to the fact that PA and serine are substrates for *de novo* ceramide biosynthesis. Although previous work has demonstrated the ability of ceramides to activate apoptotic signaling in muscle cells (20), recent

studies have shown that SFAs promote ER stress (13, 17) and ROS accumulation (10) independently of ceramide synthesis in CHO and hepatic cells. Therefore, identifying specific lipid metabolites that induce lipotoxicity in hepatic cells, as well as strategies to circumvent them by diverting SFAs into non-toxic disposal pathways, represents a potential research area for prevention and treatment of NAFLD.

Markers of ER stress, including CCAAT/enhancer-binding protein homologous protein (CHOP) and depletion of Ca^{2+} stores from the ER lumen, appear soon after exposure to SFAs but are not found in cells treated with MUFAs (21). ER Ca^{2+} depletion has been shown to occur in a range between one to four hours following SFA exposure (8, 13), indicating that the initial metabolism of SFA results in rapid perturbations to ER homeostasis and initiation of the compensatory ER stress pathway known as the unfolded protein response (UPR). Aberrant lipid metabolism has been previously linked to disruptions in ER homeostasis leading to chonic ER stress in obesity (22). Based on this recent literature, we hypothesized that dysfunctional PL metabolism and subsequent changes to fatty acid composition of membrane lipid species may play a critical role in initiating ER stress under conditions of lipotoxicity. The composition of the ER membrane typically contains unsaturated phosphatidylcholine (PC) as its major phospholipid component (23). This allows the ER to maintain a high degree of fluidity in order to carry out its critical role in preserving proper protein folding and trafficking. The degree of saturation of phospholipids plays an important role in many membrane-associated functions and homeostasis. Abnormal incorporation of saturated phospholipid species can result in detrimental stiffening of cellular membranes and loss of function (24). Relatively small changes in ER homeostasis can result in the induction of UPR and reduced capacity to transport calcium (25, 26). Therefore, even limited incorporation of SFAs into phospholipid species, particularly PC, could be detrimental to ER function and lead to the increased UPR signaling observed in response to SFA overexposure.

In the present study, we investigated the mechanisms by which upstream SFA metabolism induces hepatic cell lipotoxicity in both the H4IIEC3 rat hepatoma cell line and freshly isolated primary hepatocytes. We demonstrated that exogenous PA induces dramatic and rapid alterations in ER morphology, indicative of compromised ER integrity confirmed by high-resolution cellular imaging with transmission electron microscopy (TEM). Palmitic acid treatment resulted in dramatic increases in 16:0 lysophosphatidic acid (LPA) and dipalmitoyl phosphatidic acid (32:0 PtdOH), suggesting *de novo* lipid biosynthesis via the Kennedy pathway (27). Diacylglycerols (DAGs) also show incorporation of PA and further conversion preferentially into membrane PLs as opposed to TAGs. The resulting changes in PL acyl chain composition are associated with an increase in markers of ER stress and characteristic indicators of lipotoxicity (mitochondrial dysfunction, caspase activation, and cell death). Co-treatment with OA was found to suppress dysfunction and dilation of the ER membrane, reduce PA incorporation into PLs, and restore overall membrane saturation. Supplementing PA-treated cells with varying concentrations of OA almost completely abolished 16:0 LPA and 32:0 PtdOH accumulations and rerouted DAG species away from PL synthesis and into TAG esterification. Reduction in

markers of ER stress and lipotoxicity were observed in those cases. To our knowledge, this is the first time that changes in phospholipid synthesis, phospholipid fatty acid composition and ER membrane structure have been directly linked to lipotoxicity initiation in hepatic cells. We demonstrate that MUFA supplementation reduces PA incorporation into PL species and restores a more balanced saturated:unsaturated membrane PL composition while increasing metabolic flux toward more benign TAG synthesis.

Experimental Procedures

Materials and Reagents

Oleic and palmitic acids, bovine serum albumin (BSA), and Dulbecco's modified Eagle's medium (DMEM) were all purchased from Sigma-Aldrich (St. Louis, MO). CHOP primary (mouse) and goat anti-mouse secondary antibodies were purchased from Abcam (Cambridge, MA). β-Actin primary (goat) and donkey anti-goat secondary antibodies were procured from Santa Cruz Biotechnology. All other chemicals were purchased from standard commercial sources.

Preparation of Fatty Acid Solutions

Fatty acid treatments solutions were prepared by coupling free fatty acids to bovine serum albumin (BSA). Specifically, palmitate or oleate was fully dissolved in 200-proof ethanol for a concentration of 195 mM. This FFA stock solution was added to a pre-warmed BSA solution (10% w/w, 37°C) for a final FFA concentration of 3 mM, ensuring that the concentration of ethanol in the FFA solution did not exceed 0.5% by volume. The solution was fully dissolved by warming at 37°C for an additional 10 minutes. The final ratio of FFA:BSA was 2:1. Vehicle control treatments were prepared using stocks of 10% w/w BSA with an equivalent volume of ethanol added to match that contained in the final FFA stock. The final concentration of ethanol was less than 0.2% in all experiments.

Cell Culture

Rat hepatoma cells, H4IIEC3 (ATCC), were cultured in low-glucose Dulbecco's modified Eagle's medium (DMEM) supplemented with 10% fetal bovine serum and 1% penicillin/streptomycin/glutamine (2mM). Measurements were done at 70-80% confluency.

Primary Hepatocyte Isolation and Culture

Sprague Dawley rats were purchased from Jackson Laboratories (Bar Harbor, ME) and housed in temperature- and humidity-controlled environment with 12:12 h light-dark cycle and fed standard CHOW diet ad libitum. Following a 1-week acclimation period, rats were used for primary hepatocyte isolation. Briefly, the hepatic cells of 5-6 week old rats were isolated using

collagenase perfusion and first incubated in DMEM-based attachment media containing 20 mM glucose, 100 nM dexamethasone and 5 nM insulin on collagen IV coated plates for 4 h (attachment period). The cells were washed once with PBS and the medium was changed to a DMEM-based growth medium containing 20 mM glucose, 100 nM dexamethasone and 1 nM insulin for 16h. Experimental treatments were performed after this period using the same growth medium. All experimental protocols were approved by the Animal Care and Use Committee at Vanderbilt University.

JCI Membrane Potential Measurement

JC1 is a dye which exists in a monomeric form in non-polarized mitochondria and fluoresces in the green emission (530nm) spectrum when excited at 485 nm. The dye accumulates in the mitochondria based upon the potential which results in formation of dye aggregates. The aggregation shifts the fluorescence to the red emission (590 nm) spectrum when excited at 485 nm. Therefore, the ratio of red/green is determined and represents alterations in the mitochondrial potential between different cells and treatments.

Cell Toxicity

Toxicity was assessed using the dead cell dye propidium iodide as described previously (28). Propidium iodide is an intercalating dye that can only permeate dead cells. It becomes highly fluorescent when embedded in the double stranded DNA exposed after cell death. After culturing cells in 96-well plates with experimental treatments, the medium was removed and replaced with a solution of the dye and serum-free DMEM. Cells were incubated at 37°C for 1 h in the dark prior to the fluorescence measurement at ex/em wavelength of 530/645 nm.

Caspase Activation

The Apo-ONE Homogenous Caspase 3/7 Assay kit was used to measure apoptotic caspase activation. Cells were cultured in 96-well plates and incubated with desired treatments for 6 hours. The Apo-ONE kit uses a lysis buffer combined with a caspase 3/7 specific substrate (Z-DEVD-R110), which becomes fluorescent once these caspases remove its DEVD peptide. Fluorescence was measured at ex/em wavelength of 485/535 nm.

Western Blotting

Cells were lysed with ice-cold RIPA lysis buffer (sc-24948, Santa Cruz Biotechnology, Inc., Santa Cruz, CA) supplemented with Na-orthovanadate, protease inhibitor cocktail, and PMSF for 30 min on ice. Samples were centrifuged at 16,100 rcf and 4°C for 20 min, and the resulting supernatants constituted the total protein extracts. Protein concentrations were determined by BCA assay (Thermo Fisher Scientific, Rockford, IL). Samples were added in concentrations of 30 μg/lane for SDS-PAGE western blotting. Dilutions of the primary antibodies were anti-CHOP (1:1000) and anti-β-actin (1:1000).

Phospholipid Fatty Acid Profiles

Cells seeded in 10-cm Petri dishes at an initial density of 4×10^6 cells per plate were incubated in standard medium until reaching ~70-80% confluency, at which time experimental treatments were administered. Cells were then trypsinized for 3 min and scraped using cold PBS. Cell suspensions were pelleted by centrifugation and resuspended in fresh PBS. Fatty acyl lipid analysis was performed by the Vanderbilt Hormone Assay and Analytical Services Core using thin-layer chromatography (TLC) and gas chromatography-flame ionization detection (GC-FID) techniques. Briefly, lipids were extracted from the aforementioned cell pellets using a modified Folch separation. An internal standard (1,2-dipentadecanoyl-*sn*-glycero-3-phosphocholine) for phospholipids was added to the lipid-containing chloroform phase. Total lipids were then extracted and separated by TLC using petroleum ether/ethyl ether/acetic acid (80/20/1, v/v/v) on silica plates. Spots corresponding to PLs, TAGs, and FFAs were visualized with rhodamine 6G in 95% ethanol and scraped individually into glass tubes for transmethylation. Transmethylation was performed using a boron trifluoride-methanol 10% (w/w) solution. Derivatized lipids were then analyzed using a GC-FID, where standardized calibration curves were used to analyze fatty acid content.

^{3}H-Palmitate Lipid Class Incorporation

Cells seeded in 6-well dishes at 1.5×10^6 cells per well were incubated in standard medium until reaching ~70-80% confluency. Next, the cells were incubated for the indicated duration at 37°C in 400 μM [9,10-^{3}H] palmitic acid (1 μCi ^{3}H/μmol PA), either in the presence or absence of oleic acid. Lipids were extracted using a modified Folch procedure. Twice, 0.75 mL chilled methanol was added to each well and cells were scraped into 1:1 chloroform:water. Once vortexed and centrifuged, the lipid-containing chloroform phase was vacuum dried without heat. Lipid classes were separated by TLC, as described above. Each TLC spot was added to an individual vial and radioactivity was assessed by scintillation counting.

Electron Microscopy

Cells were seeded in 10-cm dishes at 4×10^6 cells per dish and incubated in standard medium until reaching ~70-80% confluency. Cells were then incubated with desired treatments at 37°C for the indicated time period and then washed thoroughly with 0.1M sodium cacodylate buffer (with 1% calcium chloride), pH 7.4. After washing, cells were fixed with a 2.5% glutaraldehyde solution in 0.1 M sodium cacodylate buffer for 1 h at room temperature followed by 23 h at 4°C. Samples were postfixed in 1.25% osmium tetroxide and subsequently stained with 2% aqueous uranyl acetate. Embedded cells were then thin-sectioned and viewed on a Philips/FEI T-12 high-resolution transmission electron microscope.

Quantification of Electron Micrographs

Images produced from electron microscopy were loaded into the publically available software program Image J. The straight-line measurement function of this program was used to determine the relative length of the scale bar (in nm) embedded in the image. Four randomly selected images from each treatment type were then quantitatively analyzed by measuring 10 points on the ER membranes displayed (n=10/image). The relative ER widths of these data points could then be converted to an absolute value (in nm) using the relative multiplicative factor determined by measuring the scale bar. Once converted to an absolute value, all data points from the respective treatments were pooled together to calculate the mean and standard error.

Phospholipid Analysis

H4IIEC3 cells were grown in 6-cm dishes and treated with the indicated fatty acid(s) for 12 h before they were pelleted and immediately snap frozen using liquid nitrogen. Glycerophospholipids were extracted using a modified Bligh and Dyer procedure (29, 30). Briefly, each pellet was homogenized in 800 µL of ice-cold 0.1 N HCl:CH_3OH (1:1) by vortexing for one minute at 4°C. This suspension was then vortexed with 400 µL of ice-cold $CHCl_3$ for one minute at 4°C and the extraction proceeded with centrifugation (5 min, 4°C, 18 000 × g) to separate the two phases. The lower organic layer was collected and solvent evaporated. The resulting lipid film was dissolved in 100 µL of isopropanol:hexane:100 mM NH_4COOH(aq) 58:40:2 (mobile phase A). Quantification of glycerophospholipids was achieved by the use of an LC-MS technique employing synthetic odd-carbon diacyl and lysophospholipid standards. Typically, 200 ng of each odd-carbon standard was added per sample. Glycerophospholipids were analyzed on an Applied Biosystems/MDS SCIEX 4000 Q TRAP hybrid triple quadrupole/linear ion trap mass spectrometer (Applied Biosystems, Foster City, CA, USA) and a Shimadzu high pressure liquid chromatography system with a Phenomenex Luna Silica column (2 × 250 mm, 5-µm particle size) using a gradient elution as previously described (30, 31). The identification of the individual species, achieved by LC-MS/MS, was based on their chomatographic and mass spectral characteristics. This analysis allows identification of the two fatty acid moieties but does not determine their position on the glycerol backbone (*sn-1* versus *sn-2*). Therefore, glycerophospholipids species are referred to thoughout using X:Y notation (X- total number of carbon atoms, Y – total number of double bonds in both FA, e.g. 36:1 PC).

Neutral Lipid Analysis

Neutral glycerolipids (monoacylglycerol (MAG), DAG and TAG) were extracted by homogenizing cell pellets in the presence of internal standards (300 ng each 14:0 MAG and 24:0 DAG, and 600 ng 42:0 TAG) in 2 mL 1X PBS and extracting with 2 mL ethyl acetate:trimethylpentane (25:75). After drying the extracts, the lipid film was dissolved in 1 mL hexane:isopropanol (4:1) and passed though a bed of Silica gel 60 Å to remove remaining polar phospholipids. Solvent from the collected fractions was evaporated and lipid film was redissolved in 90 µL 9:1 CH_3OH:$CHCl_3$, containing 10µL of 100mM CH_3COONa for MS

analysis essentially as described (32).

Statistical Analysis

All data are represented as mean ± standard error. Type I ANOVA (Student's t test) was used to assess statistical differences involving multiple (two) treatments. ANOVA was followed with Tukey-Kramer post-hoc testing for ^{3}H-labeled PA experiments.

Results

Treatment of hepatocytes with the saturated fatty acid PA is associated with perturbations in ER morphology and organelle stress

We hypothesized that the lipotoxic effects of PA could be mainly attributed to its ability to destabilize the structure and function of key organelles, specifically the ER. Increased saturation of PL species has been previously associated with stiffening of cellular membranes (24, 33) and organelle dysfunction (13, 34). Therefore, we sought to examine the effect that fatty acid treatments have on the structure and morphology of hepatic cellular organelles. We were particularly interested in its impacts on the ER membrane, since the ER constitutes more than half of total membrane content in hepatocytes and smooth ER is the major site of cellular PL biosynthesis (35, 36). Furthermore, ER stress has been implicated as a critical mediator in the PA-induced lipoapoptotic cascade (8, 13, 21) and is involved in diseased states such as obesity (22, 37) and progressive liver disease (38, 39). The morphology of this organelle appears normal in TEM images of vehicle-treated cells, with tubular cisternae studded by the electron-dense dots characteristic of attached ribosomes (Fig. 3-1A and 3-2A). In contrast, both primary hepatocytes and H4IIEC3 cells treated with 400 μM PA for 12h and 4h, respectively, exhibited distended ER structures that were dramatically increased in size relative to those of vehicle-treated cells (Fig. 3-1B and 3-2B). Quantification of ER expansion revealed that its average thickness increased significantly in cells treated with PA compared to vehicle-treated cells (Primary hepatocytes: 40.22 ± 2.93 nm vs. 24.59 ± 1.00 nm, $p<0.01$, Fig. 3-1E; H4IIEC3: 64.08 ± 2.39 nm vs. 25.79 ± 0.90 nm, $p<0.01$, Fig. 3-2E;). The drastic dilation in ER morphology is indicative of ER stress and dysfunction in PA-treated cells (40). There does not appear to be any indication of significant changes in mitochondrial structure between treatments at this time point.

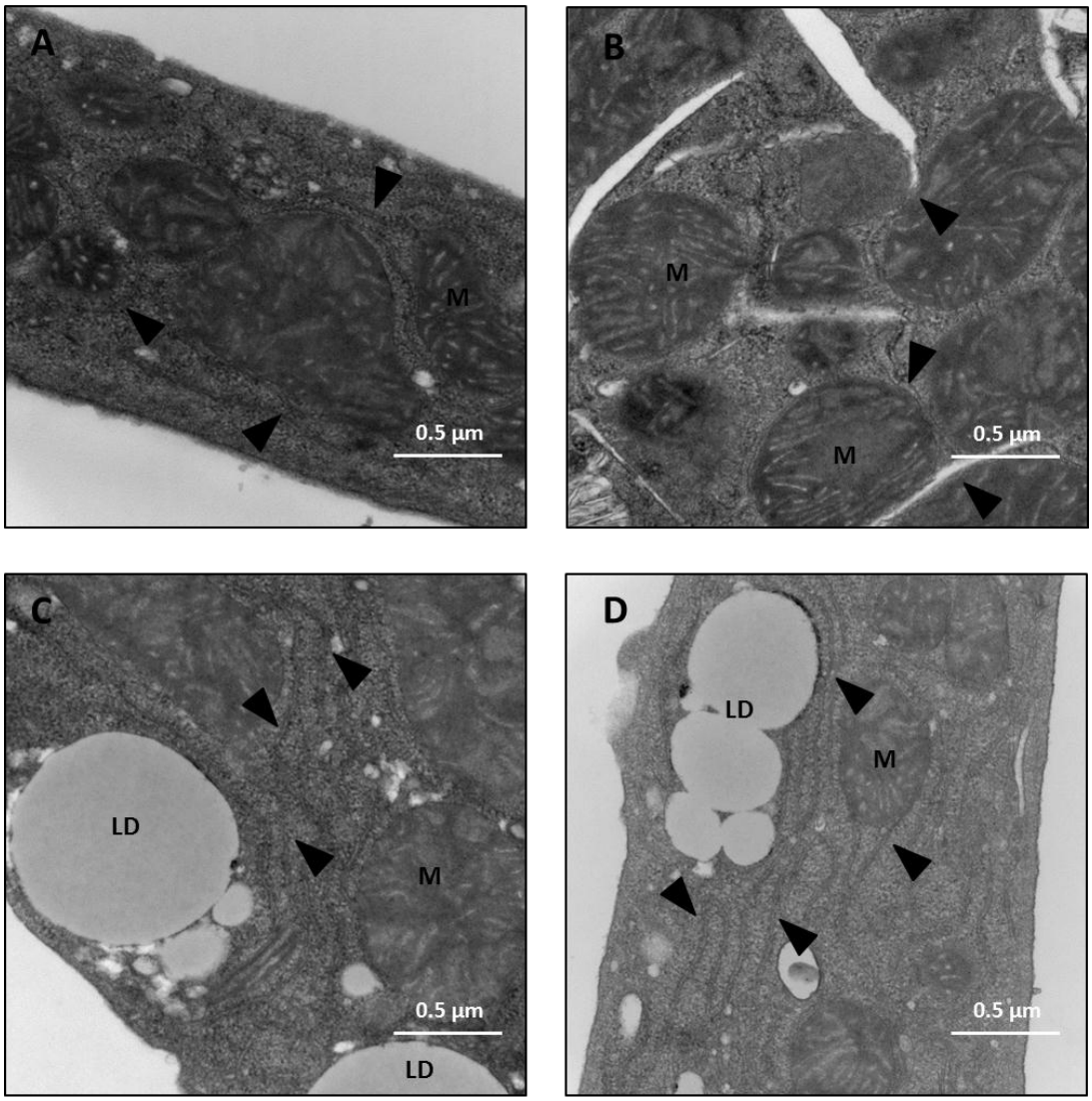

E.

Fig.	Treatment	Average ER diameter ± SE (nm)		
1A	BSA	24.59	±	1.00
1B	PA	40.22	±	2.86[b]
1C	OA	23.60	±	0.64
1D	PA+OA	22.87	±	0.65

Figure 3-1. **Incubation of freshly isolated primary hepatocytes with PA results in expansion of the ER membrane while co-treatment with OA blocks PA-induced dilation**. Primary hepatocytes were incubated for 12 h with **(A)** BSA vehicle, **(B)** 400 µM PA, **(C)** 400 µM OA or **(D)** 400 µM PA + 400 µM OA. Changes in ER morphology were observed by high-resolution imaging with transmission electron microscopy. Arrowheads point towards ER cisternae. **M**, mitochondria; **LD**, lipid droplets. Average ER diameter was quantified using ImageJ length analysis and results are displayed in **(E)**. Scale bars = 500 nm; [b],$p < 0.01$ versus cells treated with BSA.

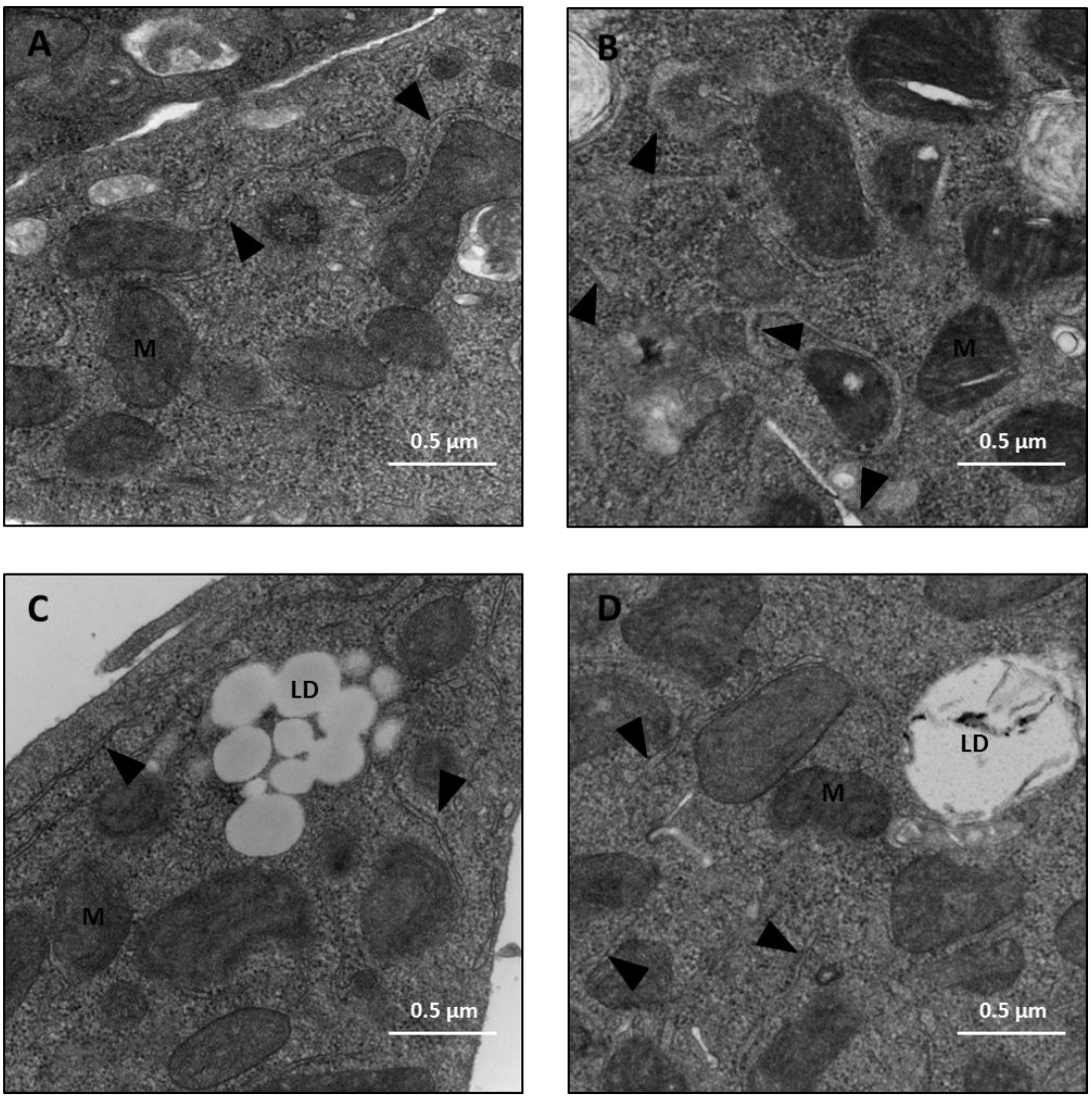

E.

Fig.	Treatment	Average ER diameter ± SE (nm)		
2A	BSA	25.79	±	0.90
2B	PA	64.08	±	2.93[b]
2C	OA	25.63	±	0.77
2D	PA+OA	26.08	±	0.84

Figure 3-2. Incubation of H4IIEC3 cells with PA results in expansion of the ER membrane while co-treatment with OA blocks PA-induced dilation. H4IIEC3 were incubated for 4 h with **(A)** BSA vehicle, **(B)** 400 µM PA, **(C)** 400 µM OA or **(D)** 400 µM PA + 400 µM OA. Changes in ER morphology were observed by high-resolution imaging with transmission electron microscopy. Arrowheads point towards ER cisternae. M, mitochondria; LD, lipid droplets. Average ER diameter was quantified using ImageJ length analysis and results are displayed in **(E)**. Scale bars = 500 nm; [b],$p < 0.01$ versus cells treated with BSA.

Neither primary hepatocytes nor H4IIEC3 cells treated with 400 μM OA experienced any significant changes in ER morphology compared to vehicle-treated cells, despite carrying the same fatty acid load as those treated with PA alone (Fig. 3-1C and -32C). Quantification of ER thickness revealed no significant differences between OA- and vehicle-treated primary hepatocytes (23.6 ± 0.64 nm vs. 24.59 ± 1.00 nm, Fig. 3-1E) or H4IIEC3 cells (25.63±0.77 nm vs. 25.79 ± 0.90 nm, Fig. 3-2E). OA-treated cells, conversely, did demonstrate significant increases in lipid droplet accumulation, composed primarily of TAGs, compared to those treated solely with PA, as indicated by the white, spherical droplets appearing on the electron micrographs (labeled "LD"). Co-incubation of PA-treated cells with 400 μM OA reversed the distended ER morphology observed in cells exposed to PA alone; the ER structure of these co-treated cells closely resembled that of control cells both in terms of visual morphology (Fig. 1D and 2D) and quantified thickness (Fig. 3-1E and 3-2E) in both primary hepatocytes and H4IIEC3 cells, respectively. All other subcellular structures appear normal and similar at this time point amongst all treatment groups. Taken together, there is clearly a substantial difference in ER morphology between hepatic cells treated with saturated versus monounsaturated fatty acids. Additionally, the structural changes in the ER associated with PA exposure can be completely reversed by co-treatment with OA.

Changes in levels of ER stress markers associated with PA, but not PA+OA co-supplementation, closely followed trends in ER morphological alterations corresponding to the same treatments in H4IICE3 cells. We used CHOP/GADD153 as a marker of ER stress due to its known function as a pro-apoptotic protein up-regulated during the ER stress response. Based on a time course of CHOP protein levels (Supplementary Fig. 3-8S A), 8h was determined as an optimal point for assessing differences in CHOP expression in response to PA treatment. The intensity of CHOP expression increased in a concentration-dependent manner at 8h (Supplementary Fig. 3-8S B), similar to the increases in cell death (Supplementary Figure 3-6S A). At this time point, H4IIEC3 cells treated with PA demonstrated significantly increased levels of CHOP, indicating substantial upregulation of UPR and confirming that ER stress is associated with PA-induced lipotoxicity (Fig. 3-3). This response was completely reversed by the addition of OA, a representative western blot of which is shown in Fig. 3-3.

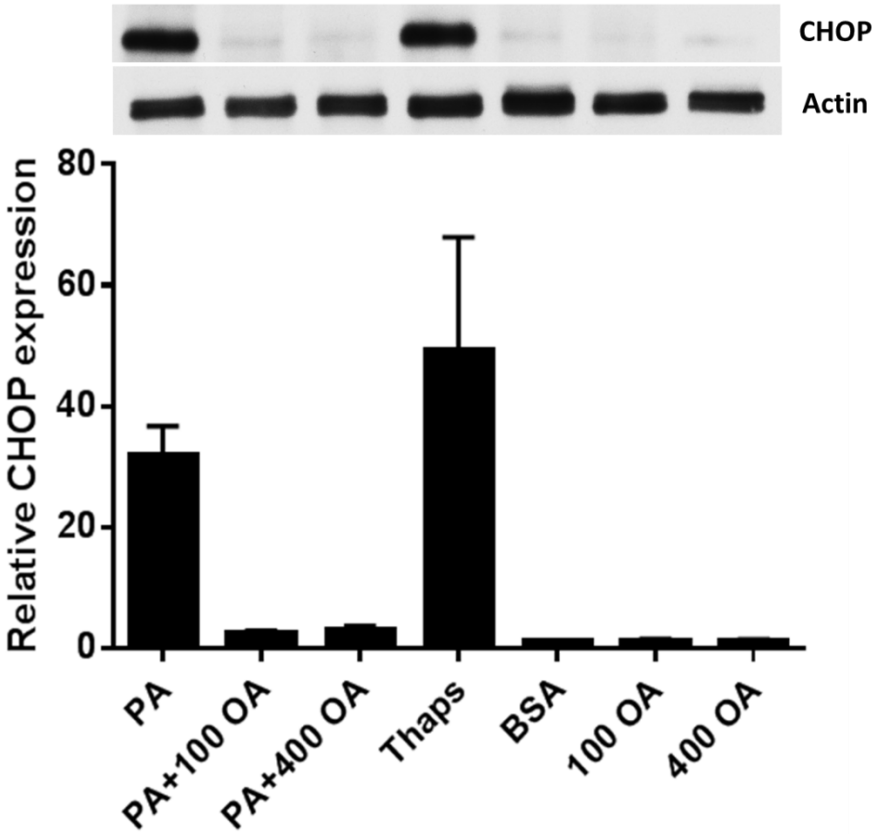

Figure 3-3. PA-induced increases in CHOP expression was completely reversed by co-treatment with OA. H4IIEC3 were treated with 400 μM PA with or without OA supplementation for 8 h. Levels of CHOP expression were assessed using Western blotting techniques and quantified with ImageJ densiometric analysis. *Upper panel,* Representative blot; *Lower panel,* Quantification of CHOP/Actin. Thapsigargin (Thaps) was used as a positive control. Data represent mean ± SE of n=3. [a], $P<0.05$, vs cells treated with PA.

Oleic acid (OA) co-supplementation modifies PA partitioning into intracellular lipid pools

Due to the dramatic and differential effects that PA and OA had on ER structure and function, we sought to assess the consequences of PA treatment on intracellular lipid flux. There are two possible mechanisms by which OA could restore normal PL saturation: (i) by sequestering PA flux away from PL synthesis and into alternate lipid pathways or (ii) by competing with PA for esterification into the PL pool. We first examined the partitioning of ^{3}H-PA into the five main classes of cellular lipids: phospholipids, diacylglycerols, free fatty acids, triacylglycerols, and cholesterol esters. These data confirm that PL and TAG are the two major fates of exogenous PA, with diacylglycerols (DAGs) also prominent in primary hepatocytes. Primary hepatocytes treated with only PA incorporated ~22% of the exogenous PA into the phospholipid fraction (Fig 4A). The addition of 100 μM and 400 μM OA significantly reduced the PA incorporation into PLs after 24h by approximately 50% and 64%, respectively (~11.6% total PA in PL with the addition of 100 μM OA and ~7.9% with 400 μM OA, versus 21.9% with PA treatment alone).

The redistribution of PA appeared to mainly be channeled towards incorporation into the TAG fraction. In H4IIEC3 cells treated for 12h with PA alone, ~36% of intracellular PA was partitioned into PLs, with nearly all of the remainder incorporated into TAGs (Fig. 3-4B). Additionally, since primary hepatocytes and H4IIEC3 cells achieved similar degrees of gross phenotype and cellular dysfunction based on analysis of TEM images at differing times (Figs. 3-1 vs 3-2, respectively), it is not surprising that molecular partitioning processes achieve similar scales of change at different times shown in Fig. 3-4A vs 3-4B.

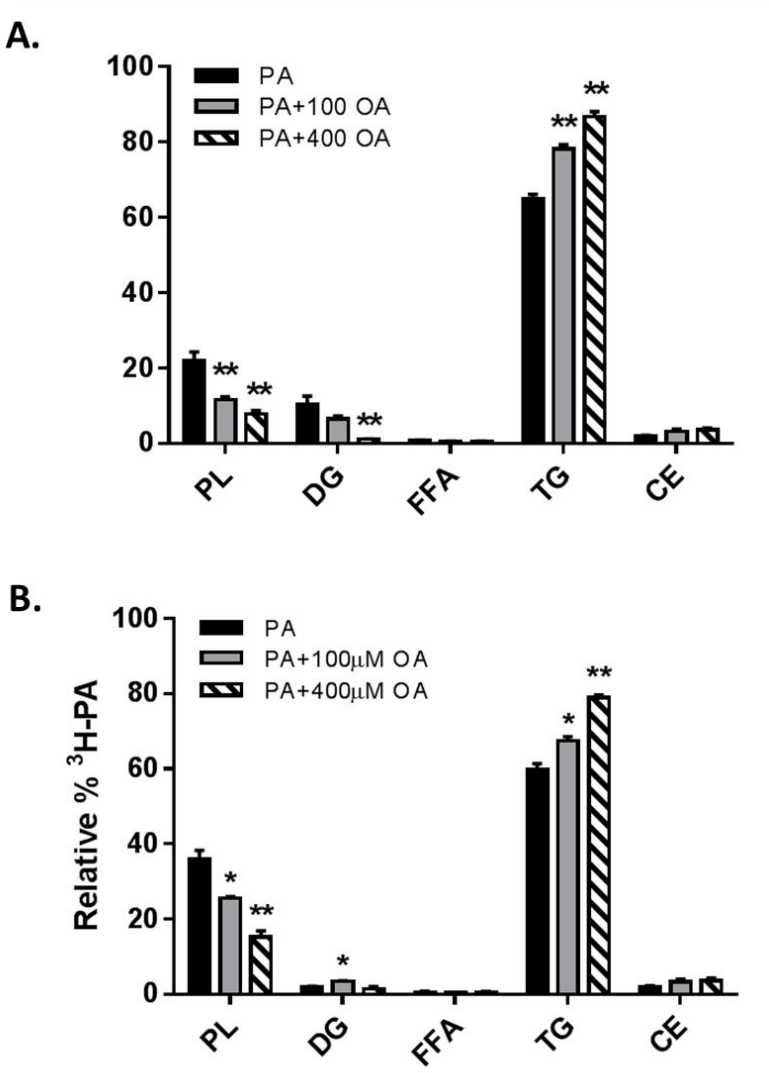

Figure 3-4. OA supplementation reduces PA incorporation into phospholipids while increasing TAG synthesis and PA incorporation in the TAG fraction. Cells were treated with 400 μM ^{3}H-PA with or without OA supplementation for 24h in primary hepatocytes **(A)** or 12h in H4IIEC3 cells **(B)**. Lipid class incorporation was determined using TLC separation and scintillation counting of each lipid spot. PL, phospholipid; DG; diacylglyceride; FFA, free fatty acid; TG, triglyceride; CE, cholesterol ester. Data represent mean ± SE of n=3. *, $p < 0.05$; **, $p < 0.01$ vs. cells treated with PA.

As we hypothesized, co-supplementation with OA resulted in a concentration-dependent reduction in PA incorporation into PLs and a corresponding increase in its TAG esterification in both primary hepatocytes and H4IIEC3 hepatic cells. Thus, in the presence of PA alone, hepatic cells incorporated a higher percentage of exogenous PA into structural and signaling phospholipids than cells co-supplemented with OA. The addition of OA partially redirected the fate of exogenous PA away from PLs and toward incorporation into the more biologically inert TAGs.

Palmitic acid is rapidly incorporated into cellular phospholipids and alters the composition of the phospholipid pool

Due to the effects of OA treatment in modifying the intracellular partitioning of PA into different lipid pools and reversing PA-induced lipotoxicity, we evaluated the consequences of PA treatment on total cellular PL composition. The relative percentage of saturated acyl chain substituents on cellular PLs was found to increase significantly within 1 h of exogenous PA treatment in H4IIEC3 cells. The increase in PA incorporation was especially striking; in PA-only treated cells, there was more than a 50% increase in percent total composition PA in the PLs of the PA- versus vehicle-treated hepatomas within the first hour (Table 3-1). This increase in PA incorporation came mainly at the expense of monounsaturated 18:1 moieties, which were significantly reduced under PA treatment. These data indicate that treatment with 400 μM PA leads to rapid incorporation of exogenous PA into cellular PLs, resulting in increased PL saturation. After 6 h (Table 3-2) and 12 h (Supplementary Table 3-1S), the percentage of PA-containing phospholipids continued to steadily climb in PA-treated cells. By 12 hours, PA comprised approximately 43% of all phospholipid fatty acids in PA-treated cells (Supplementary Table 3-1S) compared to only approximately 13% in those treated with vehicle (BSA). These changes in cellular phospholipid composition were closely associated with the onset of PA-induced decreases in mitochondrial membrane potential, apoptotic caspase activation, and cell death (Supplementary Fig. 3-6S and 3-7S).

Fatty Acid	PA	PA+100OA	PA+400 OA	BSA	100 OA	400 OA
14:0	0.65 ± 0.02	0.57 ± 0.01	0.50 ± 0.09	0.72 ± 0.05	0.60 ± 0.05	0.66 ± 0.06
16:0	17.66 ± 0.15	16.33 ± 0.07[a]	15.54 ± 0.63[a]	11.52 ± 0.25[a]	9.75 ± 0.17[a]	10.25 ± 0.08[a]
16:1	5.93 ± 0.11	5.36 ± 0.09[a]	4.99 ± 0.22[a]	5.39 ± 0.18	4.29 ± 0.13[a]	4.45 ± 0.08[a]
18:0	17.24 ± 0.19	16.61 ± 0.12	17.95 ± 0.62	18.33 ± 0.30	16.76 ± 0.14	16.55 ± 0.04
18:1w9	29.88 ± 0.07	32.80 ± 0.09[a]	35.80 ± 0.07[a]	33.11 ± 0.14[a]	39.42 ± 0.34[a]	42.36 ± 0.29[a]
18:1w7	7.56 ± 0.02	7.30 ± 0.01[a]	7.24 ± 0.06[a]	8.44 ± 0.04	7.68 ± 0.02[a]	7.23 ± 0.03[a]
18:2	2.92 ± 0.01	2.80 ± 0.01[a]	2.76 ± 0.03[a]	3.14 ± 0.04[a]	2.83 ± 0.02[a]	2.75 ± 0.01[a]
18:3 w3	0.46 ± 0.01	0.49 ± 0.01[a]	0.00 ± 0.00[a]	0.53 ± 0.02[a]	0.50 ± 0.00[a]	0.20 ± 0.17[a]
20:3w6	0.94 ± 0.01	0.92 ± 0.01	0.85 ± 0.03	0.95 ± 0.02	0.89 ± 0.01	0.79 ± 0.00
20:4	11.75 ± 0.03	11.63 ± 0.10	9.21 ± 0.42[a]	12.48 ± 0.14[a]	11.94 ± 0.10	10.64 ± 0.01[a]
22:5w3	2.06 ± 0.03	2.15 ± 0.04	1.88 ± 0.09	2.21 ± 0.09	2.21 ± 0.03	1.69 ± 0.01
22:6	2.96 ± 0.03	3.04 ± 0.05	2.72 ± 0.14	3.16 ± 0.12	3.14 ± 0.04	2.42 ± 0.02
%SFA	35.54 ± 0.05	33.51 ± 0.14[a]	33.99 ± 0.15[a]	30.58 ± 0.19[a]	27.11 ± 0.19[a]	27.46 ± 0.12[a]
%UFA	64.46 ± 0.05	66.49 ± 0.14[a]	66.01 ± 0.15[a]	69.42 ± 0.19[a]	72.89 ± 0.19[a]	72.54 ± 0.12[a]

Table 3-1. Phospholipid fatty acid composition of H4IIEC3 cells treated with PA and OA for 1 h (% of total composition). H4IIEC3 cells were incubated with 400 μM PA and/or 100μM or 400μM OA for 1 h. Phospholipids were separated by thin layer chromatography and analyzed by gas chromatography-flame ionization detection (GC-FID). Data represent mean fatty acid %± SE of n=4. [a], $P<0.05$ vs cells treated with PA alone. SFA, saturated fatty acids; UFA, unsaturated fatty acids. SFA, saturated fatty acids; UFA, unsaturated fatty acids.

Fatty Acid	PA	PA+100 OA	PA+400 OA	BSA	100 OA	400 OA
14:0	0.75 ± 0.02	0.66 ± 0.03	0.56 ± 0.07	1.36 ± 0.07[a]	1.13 ± 0.11	0.72 ± 0.05[a]
16:0	35.14 ± 0.42	26.20 ± 0.08[a]	23.32 ± 0.85[a]	13.67 ± 0.16[a]	11.43 ± 0.07[a]	10.29 ± 0.25[a]
16:1	6.83 ± 0.09	6.37 ± 0.06[a]	4.43 ± 0.09[a]	6.09 ± 0.19[a]	4.57 ± 0.08[a]	3.32 ± 0.14[a]
18:0	15.59 ± 0.12	16.63 ± 0.14[a]	14.87 ± 0.47	19.52 ± 0.29[a]	17.26 ± 0.33[a]	16.96 ± 0.24[a]
18:1w9	20.48 ± 0.21	28.82 ± 0.15	37.72 ± 1.06	31.71 ± 0.20	40.80 ± 0.17	48.38 ± 0.16
18:1w7	4.46 ± 0.01	4.44 ± 0.01[a]	3.79 ± 0.07[a]	7.20 ± 0.06[a]	5.85 ± 0.01[a]	4.93 ± 0.01[a]
18:2	1.96 ± 0.00	2.12 ± 0.01[a]	1.95 ± 0.04	2.84 ± 0.08[a]	2.37 ± 0.04[a]	1.87 ± 0.02[a]
20:3w6	0.39 ± 0.23	0.56 ± 0.19	0.23 ± 0.23	0.42 ± 0.24	0.51 ± 0.17	0.54 ± 0.01
20:4	9.72 ± 0.09	9.67 ± 0.07	9.24 ± 0.22	11.85 ± 0.23[a]	11.31 ± 0.24[a]	9.30 ± 0.28
22:4w6	1.16 ± 0.02	1.14 ± 0.03	0.90 ± 0.04[a]	1.26 ± 0.02[a]	0.96 ± 0.03[a]	0.90 ± 0.04[a]
22:5w3	1.49 ± 0.03	1.49 ± 0.03	1.30 ± 0.04[a]	1.78 ± 0.03[a]	1.58 ± 0.05	1.14 ± 0.05[a]
22:6	2.02 ± 0.05	1.91 ± 0.03	1.70 ± 0.07[a]	2.29 ± 0.04[a]	2.24 ± 0.07	1.64 ± 0.08
%SFA	51.48 ± 0.56	43.49 ± 0.26[a]	38.76 ± 1.39[a]	34.55 ± 0.53[a]	29.82 ± 0.51[a]	27.97 ± 0.54[a]
%UFA	48.52 ± 0.72	56.51 ± 0.56[a]	61.24 ± 1.74[a]	65.45 ± 1.09[a]	70.18 ± 0.84[a]	72.03 ± 0.77[a]

Table 3-2. Phospholipid fatty acid composition of H4IIEC3 cells treated with PA and OA for 6 h (% total composition). H4IIEC3 cells were incubated with 400 μM PA and/or 100μM or 400μM OA for 6 h. Phospholipids were separated by thin layer chromatography and analyzed by gas chromatography-flame ionization detection (GC-FID). Data represent mean ± SE of n=4. [a], P<0.05 vs cells treated with PA alone. SFA, saturated fatty acids; UFA, unsaturated fatty acids.

Oleic acid co-supplementation partially restores normal phospholipid composition

We further conjectured that OA co-treatment would reverse PA-induced lipoapotosis by alleviating the oversaturation of PL membrane species. Therefore, we examined the effects of co-supplementing PA with OA at various ratios. We found that H4IIEC3 cells co-supplemented with OA incorporated significantly less PA into phospholipids after 1h of treatment (Table 3-1) and demonstrated substantial reductions in relative PA abundance after both 6 and 12 h (Table 3-2, Supplementary Table 3-1S), which was accompanied by recovery of relative OA abundance back to levels approaching the vehicle-treated controls by 12 h. In particular, co-treatment with 100 μM or 400 μM OA for only 6 h reduced PA abundance by ~25% and 33%, respectively, while overall PL saturation was reduced similarly by ~16% and 25%, respectively (Table 3-2). This significant drop in total saturation was mainly attributable to differences in the percentage of palmitic (16:0), palmitoleic (16:1), and oleic (18:1w9) fatty acyl components. Restoration of cellular phospholipid composition was closely associated with a reversal of PA-induced lipotoxicity markers (Supplementary Fig. 3-6S and 3-7S).

Palmitic acid treatment increases de novo lipid biosynthesis resulting in changes in DAGs and PLs while OA-supplementation ameliorates these changes by increased esterification into TAGs

Additionally, we analyzed hepatic cells treated with defined fatty acid supplements in order to quantify the distribution of both neutral and phospho- lipids at 12h. H4IIEC3 hepatic cells treated with PA show significantly increased levels of 16:0 LPA (Fig. 3-5A) and both total and 16:0-containing phosphatidic acid (Fig. 3-5B), specifically 32:0 PtdOH (Supplementary Fig. 3-9S B), suggesting augmented *de novo* lipid biosynthesis though the canonical Kennedy pathway in response to SFA supplementation. PA treated cells accumulated increased quantities of total and 16:0-containing DAG (Fig. 3-5D), particularly 32:0 DAG (Supplementary Fig. 3-10S B) and had significantly higher levels of total phospholipid content, including an almost two-fold increase in the amount of PA moieties contained within the phospholipid pool (Fig. 3-5C). Additionally, the PA treated cells were not able to as effectively synthesize TAGs in comparison to cells supplemented with equimolar concentrations of the unsaturated fatty acid OA (Fig. 3-5E). Alternatively, co-treatment with OA drastically shifted the incorporation of PA in glycero- and phospholipids. The presence of OA led to a dramatic reversal of PA-induced increases in 16:0 LPA, PtdOH and DAGs (Fig. 3-5A, 3-5B and 3-5D, respectively), particularly PA-containing 32:0 species within these classes (Supplementary Fig. 3-9S B and 3-10S A). Furthermore, OA supplementation significantly reduced both total and 16:0-containing PLs while simultaneously shifting incorporation of the PA toward TAG synthesis (Fig. 3-5C and 3-5E, respectively).

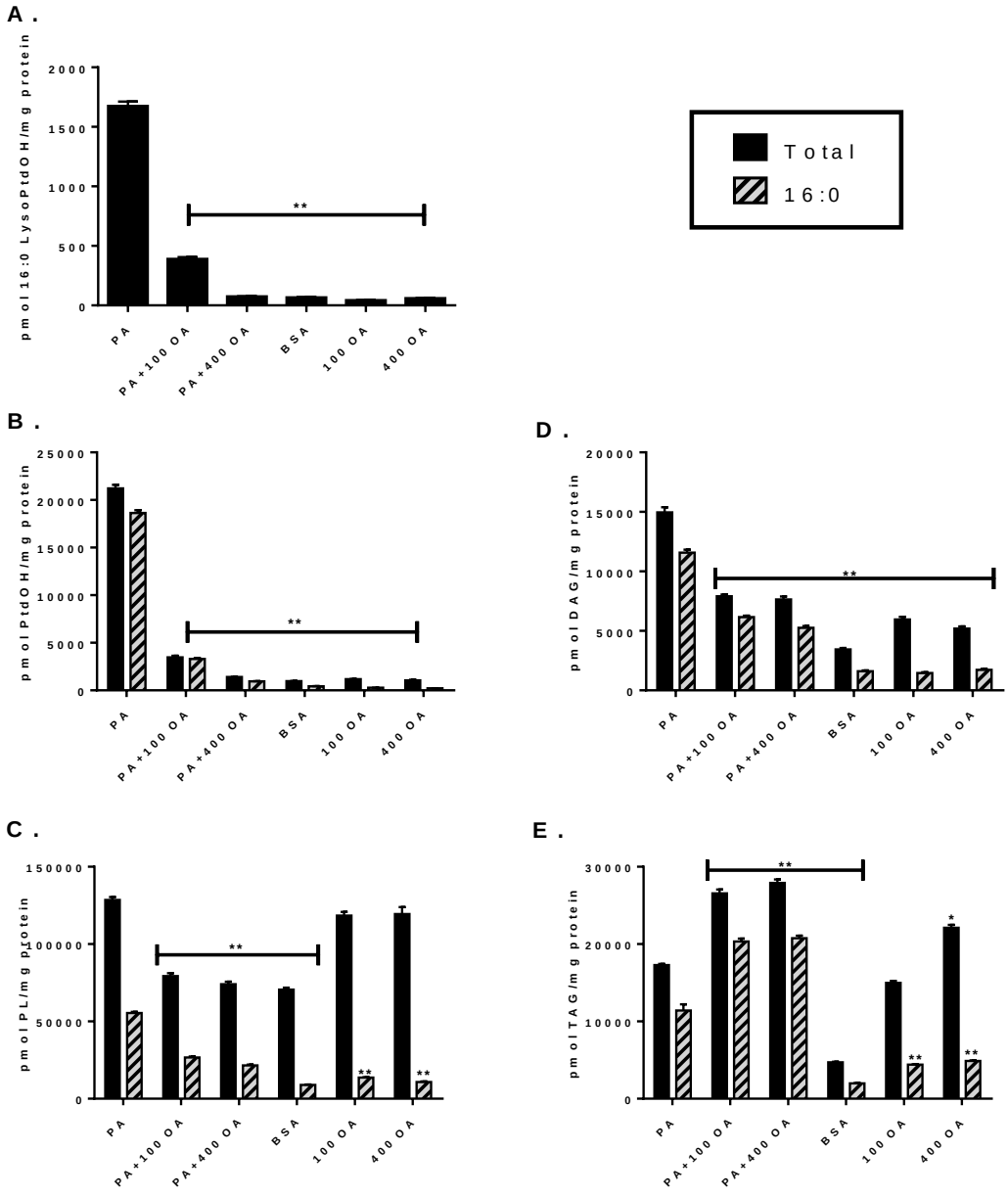

Figure 3-5. PA treatment increases 16:0 lysophosphatidic acid, phosphatidic acid, PL and DAG, but not TAG, accumulation. In contrast, co-treatment with OA substantially decreases PL while increasing TAG accumulation. H4IIEC3 cells were treated with 400 μM PA with or without OA supplementation for 12h. Lipids were determined and quantified using a LC-MS method. Both total and 16:0 containing lysophosphatidic acid (**A**), phosphatidic acid (**B**), phospholipid (**C**) and DAG (**D**) abundance was significantly increased in the presence of PA but was reversed by the addition of OA. Conversely, OA was much more readily incorporated into TAGs than the saturated PA, and co-supplementation with the two fatty acids synergistically increased overall triglyceride accumulation and 16:0 containing TAGs (**E**). Data represent mean ± SE of n=9; *, $p < 0.05$; **,$p < 0.01$ vs. cells treated with PA.

Discussion

ER stress has been previously identified as a key mediator in the lipoapoptosis of CHO and hepatic cells (8, 13, 21). Other studies have demonstrated that ER stress precedes apoptosis in HeLa cells (34) and hepatic models of lipotoxicity (41). Borradaile *et al.* found a connection between ER stress and the degree of fatty acid saturation in membrane lipids of CHO cells supplemented with PA (13). Since the disruption of ER function appears to play an early and critical role in the response to SFA overload, we sought to better understand how lipid metabolism and partitioning of PA into specific lipid classes is affected by OA availability in hepatic cells. We examined the effect that supplementing hepatic cells with PA and OA, alone or in combination, has on lipid metabolism, fatty acid composition of membrane phospholipids, and particularly on ER function.

Species level analysis of the PL pool provides insight into mechanistic aspects of lipid synthesis in response to supplementation with differing fatty acids. Treatment of the H4IIEC3 hepatic cell line with PA resulted in dramatic increases in production of both 16:0 LPA and 32:0 PtdOH, strongly suggestive of *de novo* lipid biosynthesis characteristic of the canonical Kennedy pathway. This was not present in cells co-treated with both PA and OA or those grown in the absence of PA (Fig. 3-5A and Supplementary Fig. 3-9S B, respectively). Specifically, there was a dramatic increase in total PA esterified into PLs and DAGs that was significantly reduced by approximately 50% with the co-addition of only 100 μM OA (Fig. 3-5C and 3-5D, respectively). In contrast, the co-supplementation with OA resulted in significant increases in PA incorporation into TAGs.

Palmitate treatment has been previously shown to increase DAG species in skeletal muscle models of FFA-induced insulin resistance (42-43). However, DAG accumulation in our hepatic cell model is secondary to even larger increases in overall PL synthesis, as evidenced by a strong and highly significant increase in both total and PA-containing phospholipids in cells treated with palmitate alone. This represents a significant finding that provides further context for a potential mechanism in which disordered PL metabolism is the initiator of palmitate-induced ER stress and downstream lipoapoptosis. In addition, observed differences in the molecular species distribution within distinct glycerophospholipid classes, particularly phosphatidylcholine (PC), phosphatidylinostitol (PI) and phosphatidylserine (PS), are in good agreement with results from a preclinical study of human liver samples from steatotic, cirrhotic and normal patients (Supplementary Fig. 3-9S C, G and H, respectively) (42). Such agreement provides evidentiary support for utilizing hepatocyte lipotoxicity experiments as models to explore remediation of human NAFLD progression.

High-resolution TEM images of cells visually demonstrate the substantial divergence in cellular response to feeding hepatocytes saturated versus monounsaturated fatty acids. Supplementing cells with PA had a deleterious effect on the structural integrity of the ER membrane of both H4IIEC3 cells and primary hepatocytes after 4h and 12h of incubation, respectively, as indicated

by obvious dilation of the ER cisternae. This phenomenon has been previously observed in other cell types, specifically CHO (13) and C2C12 muscle cells (43) under similar PA-induced lipotoxic conditions. An identical fatty acid load of OA, however, had no such effect on the ER, and the supplementation of PA-treated cells with OA reversed ER membrane distention and normalized ER morphology. Changes in ER morphology due to fatty acid treatment correlated with augmentation of the ER stress marker CHOP in the presence of exogenous PA (Fig. 3-3). As with ER dilation and distention, increases in markers of ER stress due to PA treatment were completely reversed by supplementing with OA (Fig. 3-3).

Changes in ER morphology and function correlated with changes in PA partitioning among lipid classes. PA supplementation resulted in dramatic increases in PA incorporation into PL fatty acyl chains and overall PL saturation (Table 3-1, 3-2 and Supplementary Table 3-3S). OA co-supplementation reduced PA incorporation into PLs at all examined time points in H4IIEC3 cells (1, 6, and 12 h). This finding is supported by the differential changes in PA partitioning in response to supplementation alone or in combination with OA. We found that under PA/OA co-treatment there was reduced partitioning into the PLs and increased incorporation into the TAG class. These data suggest that the ability of OA to reverse the lipotoxic effects of PA may be tied to its roles in altering the fate of PA away from PL incorporation and toward TAG synthesis and/or in restoring the saturation index of membrane phospholipids in compositionally sensitive organelles such as the ER.

Overall, our data demonstrate that PA treatment caused increased *de novo* PL synthesis though the Kennedy pathway, which was not found in hepatocytes co-treated with PA and OA and, to our knowledge, has not been shown previously in models of hepatic lipotoxicity. Furthermore, we observed parallel trends in reversal of apoptotic cell death, Kennedy pathway flux and overall PL saturation, markers of ER stress, and physical ER dilation upon co-incubation of PA-treated cells with OA, indicating a strong association between these phenotypic responses. Notably, OA co-supplementation reduced levels of PA in the overall phospholipid composition, which in parallel diminished CHOP expression and ER distention, and reversed PA-induced markers of lipotoxicity in two hepatocyte models. Furthermore, the observed changes in PL composition and ER morphology preceded the onset of mitochondrial dysfunction, as assessed by changes in mitochondrial potential (JC1) and TEM images, as well as caspase activation, suggesting that ER stress may be a critical upstream mediator of the lipotoxic phenotype. This study demonstrates that increased phospholipid saturation is a hallmark and committed step of SFA lipotoxicity in *in vitro* hepatic models and that reversing saturation of membrane phospholipids may have a beneficial effect on hepatic cells exposed to a toxic SFA load. Treatments designed to limit the phospholipid saturation index may point towards novel strategies for improving hepatocyte function under these conditions.

Acknowledgments

This work was supported by NSF CAREER award CBET-0955251 (to JDY). Robert A. Egnatchik was supported by the NSF Graduate Research Fellowship Program. Masakazu Shiota was supported by NIH DK060667. Partial support for the work was also provided by National Institutes of Health Grant U54 GM69338 (to HAB). Fatty acyl lipid analysis was performed by the Vanderbilt Diabetes Research and Training Center's Hormone Assay Core, which is supported by NIH DK020593. Electron Microscopy was performed in part through the use of the VUMC Cell Imaging Shared Resource (supported by NIH grants CA68485, DK20593, DK58404, HD15052, DK59637 and EY08126).

References

1. Ibrahim, S. H., R. Kohli, and G. J. Gores. 2011. Mechanisms of Lipotoxicity in NAFLD and Clinical Implications. *Journal of Pediatric Gastroenterology and Nutrition* **53**.
2. Cazanave, S. C., and G. J. Gores. 2010. Mechanisms and clinical implications of hepatocyte lipoapoptosis. *Clinical Lipidology* **5**.
3. Feldstein, A. E., A. Canbay, P. Angulo, M. Taniai, L. J. Burgart, K. D. Lindor, and G. J. Gores. 2003. Hepatocyte apoptosis and Fas expression are prominent features of human nonalcoholic steatohepatitis. *Gastroenterology* **125**.
4. Cusi, K. 2012. Role of Obesity and Lipotoxicity in the Development of Nonalcoholic Steatohepatitis: Pathophysiology and Clinical Implications. *Gastroenterology* **142**.
5. Leamy, A. K., R. A. Egnatchik, and J. D. Young. 2012. Molecular mechanisms and the role of saturated fatty acids in the progression of non-alcoholic fatty liver disease. *Prog Lipid Res.*
6. Noguchi, Y., J. D. Young, J. O. Aleman, M. E. Hansen, J. K. Kelleher, and G. Stephanopoulos. 2009. Effect of Anaplerotic Fluxes and Amino Acid Availability on Hepatic Lipoapoptosis. *J. Biol. Chem.* **284**: 33425-33436.
7. Li, Z. Z., M. Berk, T. M. McIntyre, and A. E. Feldstein. 2009. Hepatic Lipid Partitioning and Liver Damage in Nonalcoholic Fatty Liver Disease - Role of stearoyl-CoA desaturase. *J. Biol. Chem.* **284**: 5637-5644.
8. Wei, Y., D. Wang, C. L. Gentile, and M. J. Pagliassotti. 2009. Reduced endoplasmic reticulum luminal calcium links saturated fatty acid-mediated endoplasmic reticulum stress and cell death in liver cells. *Molecular and Cellular Biochemistry* **331**: 31-40.
9. Pagliassotti, M., Y. R. Wei, and D. Wang. 2005. Saturated fatty acids induce cytotoxicity in hepatocytes via effects on the endoplasmic reticulum. *Obesity Research* **13**: A31-A31.
10. Listenberger, L. L., X. L. Han, S. E. Lewis, S. Cases, R. V. Farese, D. S. Ory, and J. E. Schaffer. 2003. Triglyceride accumulation protects against fatty acid-induced lipotoxicity. *Proceedings of the National Academy of Sciences of the United States of America* **100**: 3077-3082.
11. Charlton, M., A. Krishnan, K. Viker, S. Sanderson, S. Cazanave, A. McConico, H. Masuoko, and G. Gores. 2011. Fast food diet mouse: novel small animal model of NASH with ballooning, progressive fibrosis, and high physiological fidelity to the human condition. *Am. J. Physiol.-Gastroint. Liver Physiol.* **301**: G825-G834.
12. Listenberger, L. L., D. S. Ory, and J. E. Schaffer. 2001. Palmitate-induced apoptosis can occur through a ceramide-independent pathway. *J. Biol. Chem.* **276**: 14890-14895.
13. Borradaile, N. M., X. Han, J. D. Harp, S. E. Gale, D. S. Ory, and J. E. Schaffer. 2006. Disruption of endoplasmic reticulum structure and integrity in lipotoxic cell death. *J. Lipid Res.* **47**: 2726-2737.
14. Choi, S.-E., I.-R. Jung, Y.-J. Lee, S.-J. Lee, J.-H. Lee, Y. Kim, H.-S. Jun, K.-W. Lee, C. B. Park, and Y. Kang. 2011. Stimulation of Lipogenesis as Well as Fatty Acid Oxidation Protects against Palmitate-Induced INS-1 beta-Cell Death. *Endocrinology* **152**: 816-827.

15. Busch, A. K., E. Gurisik, D. V. Cordery, M. Sudlow, G. S. Denyer, D. R. Laybutt, W. E. Hughes, and T. J. Biden. 2005. Increased fatty acid desaturation and enhanced expression of stearoyl coenzyme A desaturase protects pancreatic beta-cells from lipoapoptosis. *Diabetes* **54**: 2917-2924.

16. Hardy, S., W. El-Assaad, E. Przybytkowski, E. Joly, M. Prentki, and Y. Langelier. 2003. Saturated fatty acid-induced apoptosis in MDA-MB-231 breast cancer cells - A role for cardiolipin. *J. Biol. Chem.* **278**: 31861-31870.

17. Wei, Y., D. Wang, F. Topczewski, and M. J. Pagliassotti. 2006. Saturated fatty acids induce endoplasmic reticulum stress and apoptosis independently of ceramide in liver cells. *Am. J. Physiol.-Endocrinol. Metab.* **291**: E275-E281.

18. Srivastava, S., and C. Chan. 2008. Application of metabolic flux analysis to identify the mechanisms of free fatty acid toxicity to human hepatoma cell line. *Biotechnology and Bioengineering* **99**: 399-410.

19. Egnatchik, R. A., A. K. Leamy, Y. Noguchi, M. Shiota, and J. D. Young. 2014. Palmitate-induced Activation of Mitochondrial Metabolism Promotes Oxidative Stress and Apoptosis in H4IIEC3 Rat Hepatocytes. *Metabolism-Clinical and Experimental* **63**: 283-295.

20. Turpin, S. M., G. I. Lancaster, I. Darby, M. A. Febbraio, and M. J. Watt. 2006. Apoptosis in skeletal muscle myotubes is induced by ceramides and is positively related to insulin resistance. *Am. J. Physiol.-Endocrinol. Metab.* **291**: E1341-E1350.

21. Pfaffenbach, K. T., C. L. Gentile, A. M. Nivala, D. Wang, Y. R. Wei, and M. J. Pagliassotti. 2010. Linking endoplasmic reticulum stress to cell death in hepatocytes: roles of C/EBP homologous protein and chemical chaperones in palmitate-mediated cell death. *Am. J. Physiol.-Endocrinol. Metab.* **298**: E1027-E1035.

22. Fu, S., L. Yang, P. Li, O. Hofmann, L. Dicker, W. Hide, X. Lin, S. M. Watkins, A. R. Ivanov, and G. S. Hotamisligil. 2011. Aberrant lipid metabolism disrupts calcium homeostasis causing liver endoplasmic reticulum stress in obesity. *Nature* **473**: 528-531.

23. Van der Sanden, M. H. M., M. Houweling, L. M. G. Van Golde, and A. B. Vaandrager. 2003. Inhibition of phosphatidylcholine synthesis induces expression of the endoplasmic reticulum stress and apoptosis-related protein CCAAT/enhancer-binding protein-homologous protein (CHOP/GADD153). *Biochemical Journal* **369**: 643-650.

24. Spector, A. A., and M. A. Yorek. 1985. Membrane lipid-Composition and cellular function. *J. Lipid Res.* **26**: 1015-1035.

25. Ron, D., and P. Walter. 2007. Signal integration in the endoplasmic reticulum unfolded protein response. *Nature Reviews Molecular Cell Biology* **8**: 519-529.

26. Deguil, J., L. Pineau, E. C. R. Snyder, S. Dupont, L. Beney, A. Gil, G. Frapper, and T. Ferreira. 2011. Modulation of Lipid-Induced ER Stress by Fatty Acid Shape. *Traffic* **12**: 349-362.

27. Kennedy, E. P. 1987. Metabolism and function of membrane lipids. *J. Mol. Med.* **65**: 205-212.

28. Arndt-Jovin, D. J., and T. M. Jovin. 1989. Fluorescence Labeling and Microscopy of DNA. *Methods in Cell Biology* **30**.

29. Bligh, E. G., and W. J. Dyer. 1959. A rapid method for total lipid extraction and purification. *Can. J. Biochem. Physiol.* **37**: 911-917.

30. Ivanova, P. T., S. B. Milne, M. O. Byrne, Y. Xiang, and H. A. Brown. 2007. Glycerophospholipid identification and quantitation by electrospray ionization mass spectrometry. *Lipidomics and Bioactive Lipids: Mass-Spectrometry-Based Lipid Analysis* **432**: 21-57.

31. Myers, D. S., P. T. Ivanova, S. B. Milne, and H. A. Brown. 2011. Quantitative analysis of glycerophospholipids by LC-MS: Acquisition, data handling, and interpretation. *Biochimica Et Biophysica Acta-Molecular and Cell Biology of Lipids* **1811**: 748-757.

32. Lord, C. C., J. L. Betters, P. T. Ivanova, S. B. Milne, D. S. Myers, J. Madenspacher, G. Thomas, S. Chung, M. Liu, M. A. Davis, R. G. Lee, R. M. Crooke, M. J. Graham, J. S. Parks, D. L. Brasaemle, M. B. Fessler, H. A. Brown, and J. M. Brown. 2012. CGI-58/ABHD5-Derived Signaling Lipids Regulate Systemic Inflammation and Insulin Action. *Diabetes* **61**: 355-363.

33. Schroeder, F., and E. H. Goh. 1980. Effect of fatty acids on physical properties of microsomes from isolated perfused rat liver. *Chemistry and Physics of Lipids* **26**: 207-224.

34. Ariyama, H., N. Kono, S. Matsuda, T. Inoue, and H. Arai. 2010. Decrease in Membrane Phospholipid Unsaturation Induces Unfolded Protein Response. *J. Biol. Chem.* **285**: 22027-22035.

35. Alberts, B., A. Johnson, J. Lewis, M. Raff, K. Roberts, and P. Walter. 2002. The Endoplasmic Reticulum. *In* Molecular Biology of the Cell. Garland Science, New York City.

36. Seth, G., P. Hossler, J. C. Yee, and W.-S. Hu. 2006. Engineering cells for cell culture bioprocessing - Physiological fundamentals. *Cell Culture Engineering* **101**.

37. Ozcan, U., Q. Cao, E. Yilmaz, A. H. Lee, N. N. Iwakoshi, E. Ozdelen, G. Tuncman, C. Gorgun, L. H. Glimcher, and G. S. Hotamisligil. 2004. Endoplasmic reticulum stress links obesity, insulin action, and type 2 diabetes. *Science* **306**: 457-461.

38. Puri, P., F. Mirshahi, O. Cheung, R. Natarajan, J. W. Maher, J. M. Kellum, and A. J. Sanyal. 2008. Activation and dysregulation of the unfolded protein response in nonalcoholic fatty liver disease. *Gastroenterology* **134**: 568-576.

39. Oezcan, U., E. Yilmaz, L. Oezcan, M. Furuhashi, E. Vaillancourt, R. O. Smith, C. Z. Goerguen, and G. S. Hotamisligil. 2006. Chemical chaperones reduce ER stress and restore glucose homeostasis in a mouse model of type 2 diabetes. *Science* **313**: 1137-1140.

40. Xue, X., J. H. Piao, A. Nakajima, S. Sakon-Komazawa, Y. Kojima, K. Mori, H. Yagita, K. Okumura, H. Harding, and H. Nakano. 2005. Tumor necrosis factor alpha (TNF alpha) induces the unfolded protein response (UPR) in a reactive oxygen species (ROS)-

dependent fashion, and the UPR counteracts ROS accumulation by TNF alpha. *J. Biol. Chem.* **280**: 33917-33925.

41. Wang, D., Y. R. Wei, and M. J. Pagliassotti. 2006. Saturated fatty acids promote endoplasmic reticulum stress and liver injury in rats with hepatic steatosis. *Endocrinology* **147**: 943-951.

42. Gorden, D. L., P. T. Ivanova, D. S. Myers, J. O. McIntyre, M. N. VanSaun, J. K. Wright, L. M. Matrisian, and H. A. Brown. 2011. Increased Diacylglycerols Characterize Hepatic Lipid Changes in Progression of Human Nonalcoholic Fatty Liver Disease; Comparison to a Murine Model. *Plos One* **6**.

43. Peng, G., L. Li, Y. Liu, J. Pu, S. Zhang, J. Yu, J. Zhao, and P. Liu. 2011. Oleate Blocks Palmitate-Induced Abnormal Lipid Distribution, Endoplasmic Reticulum Expansion and Stress, and Insulin Resistance in Skeletal Muscle. *Endocrinology* **152**: 2206-2218.

Appendix: Supplementary Data

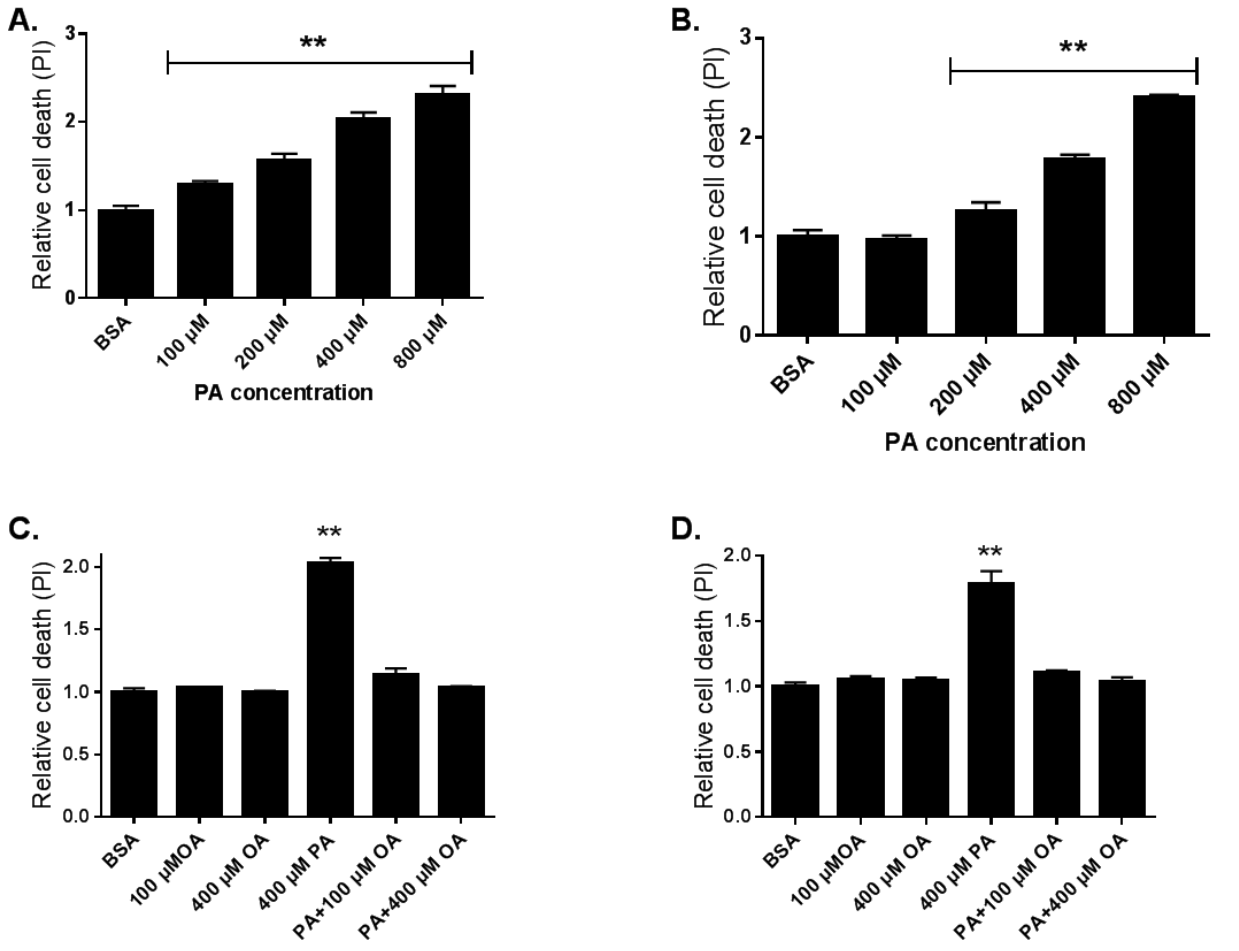

Figure 3-6S. PA treatment induces cell death in a concentration dependent manner and co-supplementation with OA reverses PA-mediated increases in cell death. Cells were treated with increasing concentrations of PA for 12 h in H4IIEC3 cells (A) and 24h in primary hepatocytes (B). Cell toxicity was assessed using the fluorescent dye propidium iodide (PI) relative to control cells treated with BSA vehicle. Treatment with different concentrations of OA (100 µM OA and 400 µM OA) demonstrated no evidence of increased cell death while co-supplementing H4IIEC3 cells (C) and primary hepatocytes (D) with either concentration of OA reversed PA-induced cell death after 12h and 24h, respectively. Data represent mean ± SE of n=4. *, $p < 0.05$; **, $p < 0.01$ versus cells treated with BSA.

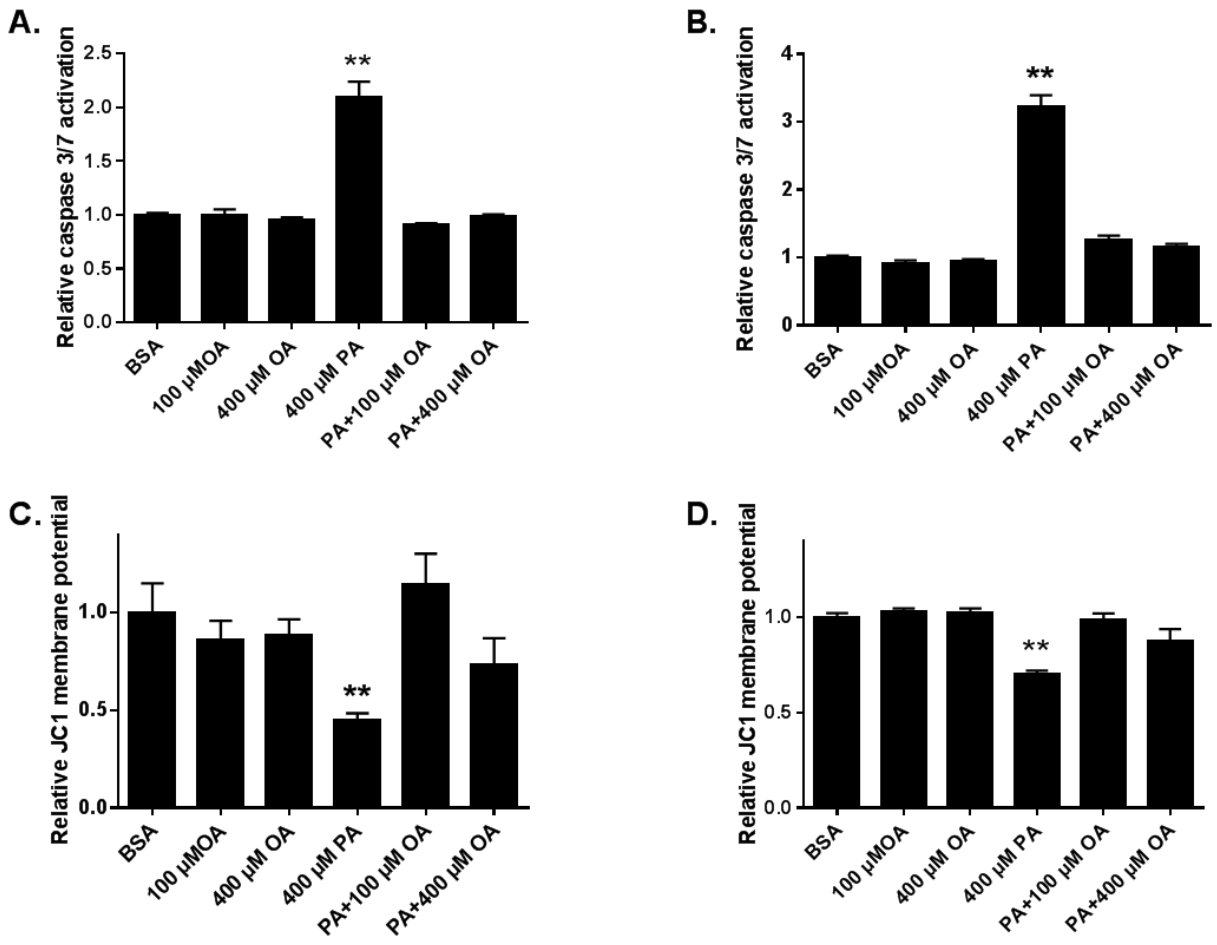

Figure 3-7S. Treatment of hepatic cells increases markers of apoptotic caspase activation and indicators of mitochondrial dysfunction though loss of membrane potential, all of which is reversed by co-treatment with OA. . Hepatic cells were treated with 400 µM PA for 6 h in H4IIEC3 cells (A) and 12 h in primary hepatocytes (B) at which time caspase 3/7 activation was assessed by the ApoONE assay. Treatment with OA alone caused no significant increase in caspase 3/7 activation and co-treatment with OA completely reversed activation in PA treated cells. Indicators of mitochondrial dysfunction were determined by measuring loss of mitochondrial membrane potential using the JC-1 fluorescent dye and is depicted as the relative ratio between red and green fluorescent signals. PA treatment resulted in loss of mitochondrial potential in H4IIEC3 cells at 6h (C) and in primary hepatocytes at 12h (D). The addition of similar concentrations of OA demonstrated no deleterious effect on mitochondrial potential and its co-supplementation significantly reversed losses induced by PA treatment in both cell types. Data represent mean ± SE of n=4. *, $p < 0.05$; **, $p < 0.01$ versus cells treated with BSA.

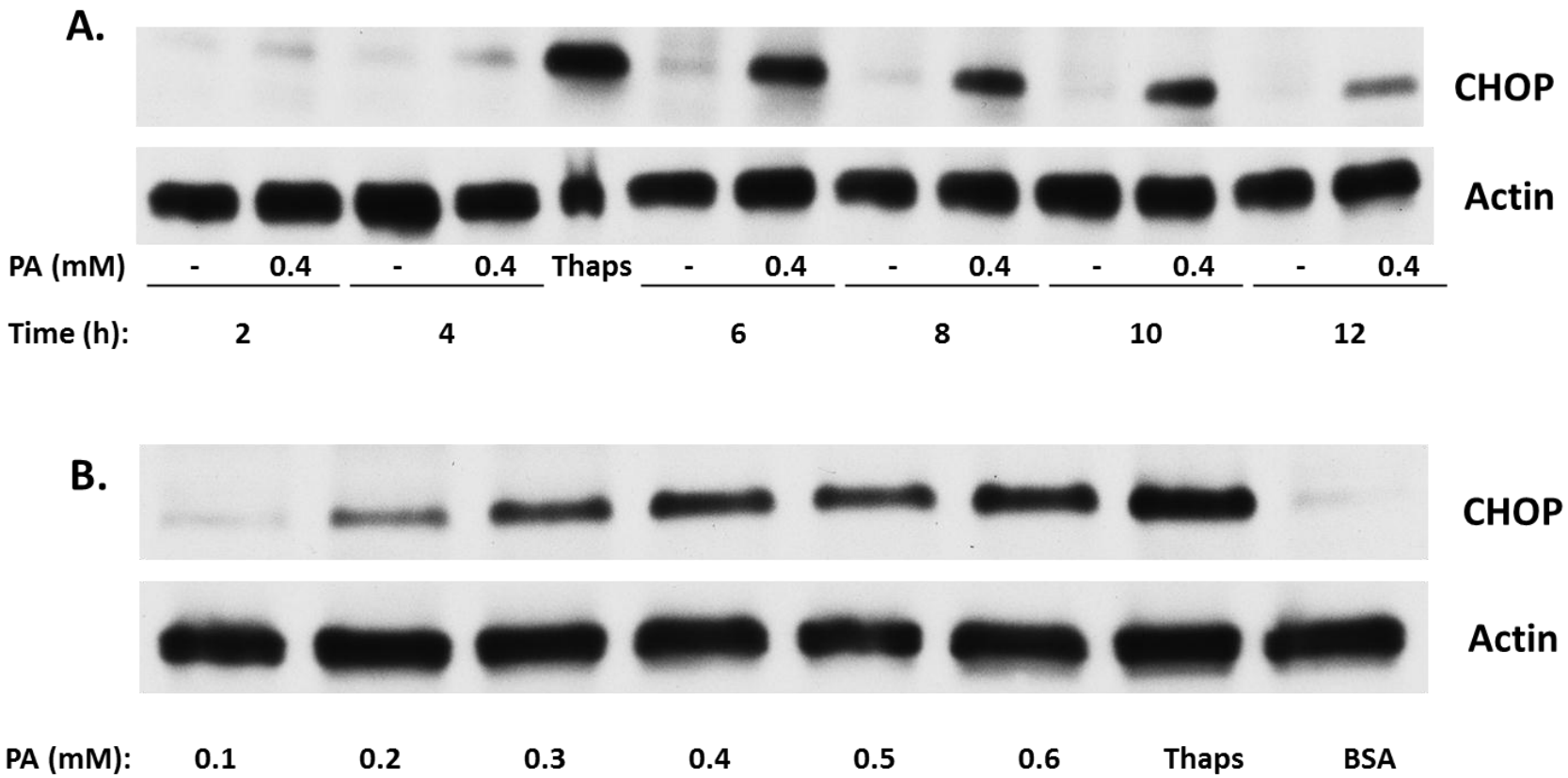

Figure 3-8S. PA treatment results in concentration- and time-dependent increases in CHOP expression. (A) Western blot of PA-induced increases in CHOP expression over time in response to 400 μM PA. (B) PA concentration-dependent increases in CHOP expression at 8 h assessed by Western blot. Thapsigargin (Thaps) was used as a positive control. Data shown are a representative blot of n=3 western blots.

Fatty Acid	PA	PA+100 OA	PA+400 OA	BSA	100 OA	400 OA
14:0	0.00± 0.00	0.25± 0.12	0.00± 0.00	0.81± 0.02[a]	0.73± 0.03[a]	0.53± 0.01[a]
16:0	43.12± 0.21	33.58± 0.31[a]	29.17± 0.28[a]	12.71± 0.22[a]	11.51± 0.10[a]	9.01± 0.10[a]
16:1	8.44± 0.13	8.23± 0.14	4.72± 0.09[a]	4.88± 0.15[a]	2.94± 0.02[a]	1.75± 0.01[a]
18:0	13.92± 0.22	13.96± 0.52[a]	13.68± 0.30	19.75± 0.34[a]	15.65± 0.09[a]	13.49± 0.16
18:1w9	12.77± 0.06	22.57± 0.15[a]	32.24± 0.27[a]	28.80± 0.68[a]	44.25± 0.12[a]	54.31± 0.43[a]
18:1w7	3.65± 0.02	3.38± 0.01[a]	3.01± 0.01[a]	7.43± 0.17[a]	6.03± 0.05[a]	4.29± 0.04[a]
18:2	1.96± 0.03	2.17± 0.01[a]	2.06± 0.03	5.38± 1.93	2.16± 0.01[a]	2.18± 0.58
20:3w6	0.88± 0.01	0.83± 0.02	0.71± 0.00[a]	1.15± 0.02[a]	0.35± 0.18	0.14± 0.14[a]
20:4	7.87± 0.06	7.67± 0.21	7.75± 0.17	10.40± 0.18[a]	8.52± 0.08[a]	7.11± 0.04[a]
20:5	0.15± 0.15	0.46± 0.01	0.45± 0.01	0.00± 0.00[a]	0.00± 0.00	0.00± 0.00
22:4w6	0.74± 0.01	0.65± 0.03	0.53± 0.01[a]	1.18± 0.03[a]	0.94± 0.43	1.70± 0.07[a]
22:5w6	0.98± 0.01	1.02± 0.01[a]	1.01± 0.02	1.66± 0.04[a]	1.30± 0.02[a]	1.27± 0.02[a]
22:5w3	2.50± 0.03	2.35± 0.06	2.11± 0.03[a]	2.84± 0.07[a]	2.46± 0.03	1.81± 0.02[a]
22:6	3.02± 0.03	2.86± 0.03[a]	2.56± 0.04[a]	3.01± 0.07	3.15± 0.04	2.41± 0.02[a]
% SFA	57.03± 0.10	47.79± 0.20[a]	42.85± 0.14[a]	33.27± 0.13[a]	27.89± 0.05[a]	23.03± 0.06[a]
% UFA	42.97± 0.13	52.21± 0.13[a]	57.15± 0.13[a]	66.73± 0.23[a]	72.11± 0.14[a]	76.97± 0.15[a]

Table 3-3S. Phospholipid fatty acid composition of H4IIEC3 cells treated with PA and OA for 12 h (% of total composition). H4IIEC3 cells were incubated with 400 μM PA and/or 100μM or 400μM OA for 12 h. Phospholipids were separated by thin layer chromatography (TLC) and analyzed by gas chromatography-flame ionization detection (GC-FID). Data represent mean fatty acid % ± SE of n=4. [a], $P<0.05$ vs cells treated with PA alone. SFA, saturated fatty acids; UFA, unsaturated fatty acids.

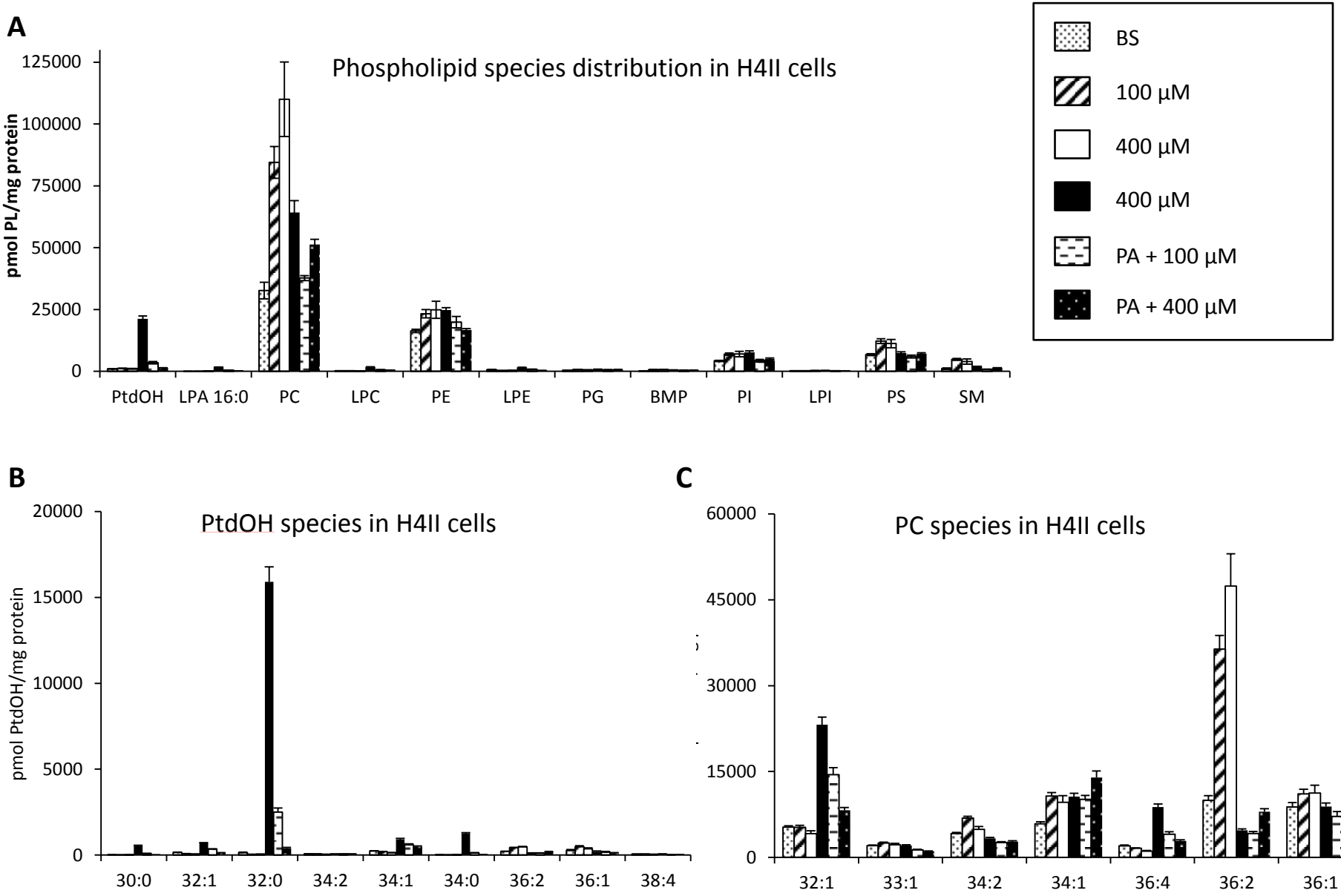
A
Phospholipid species distribution in H4II cells
pmol PL/mg protein
125000
100000
75000
50000
25000
0
PtdOH
LPA 16:0
PC
LPC
PE
LPE
PG
BMP
PI
LPI
PS
SM
BS
100 µM
400 µM
400 µM
PA + 100 µM
PA + 400 µM
B
PtdOH species in H4II cells
pmol PtdOH/mg protein
20000
15000
10000
5000
0
30:0
32:1
32:0
34:2
34:1
34:0
36:2
36:1
38:4
C
PC species in H4II cells
60000
45000
30000
15000
0
32:1
33:1
34:2
34:1
36:4
36:2
36:1

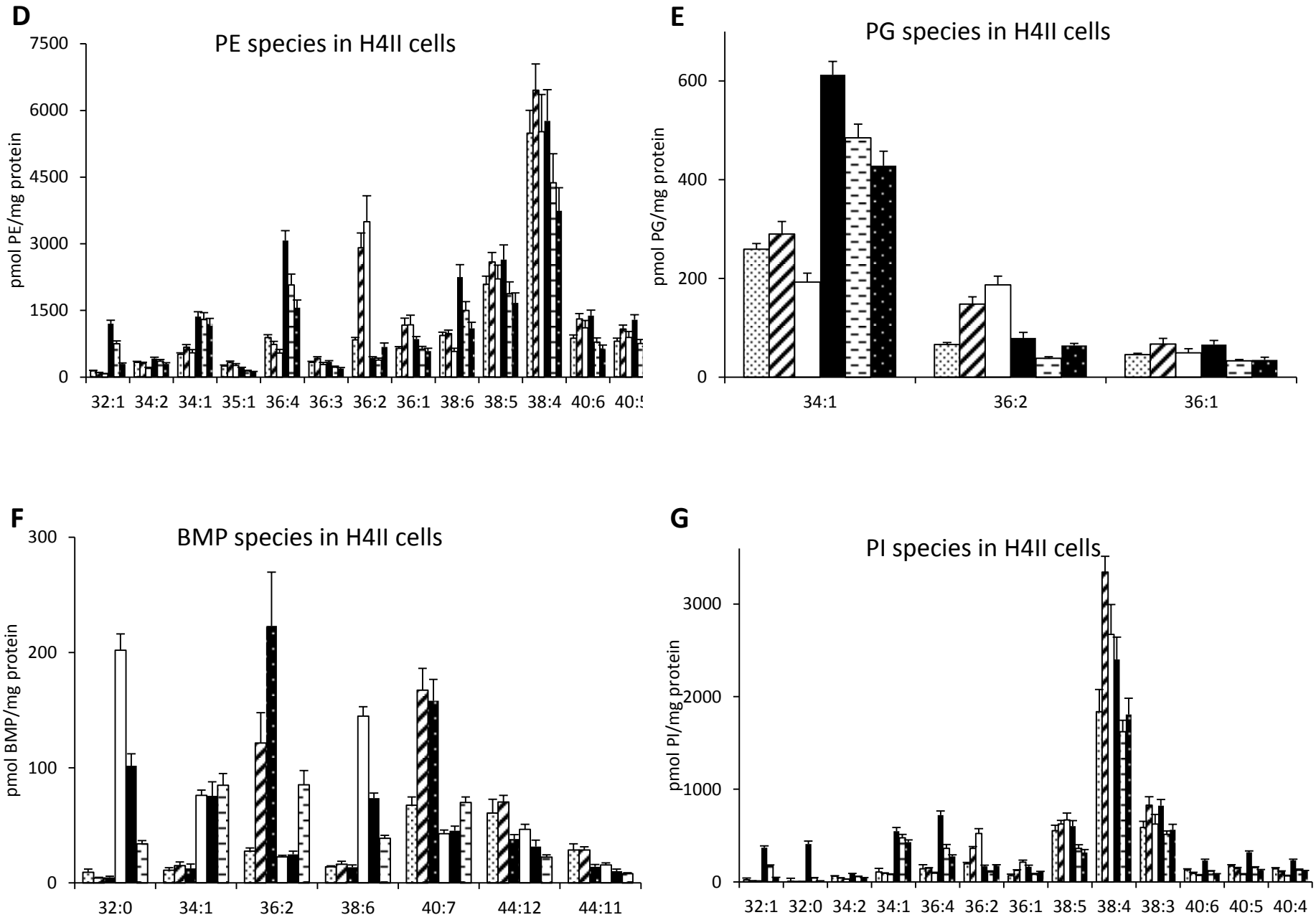
D
PE species in H4II cells
pmol PE/mg protein
7500
6000
4500
3000
1500
0
32:1 34:2 34:1 35:1 36:4 36:3 36:2 36:1 38:6 38:5 38:4 40:6
E
PG species in H4II cells
pmol PG/mg protein
600
400
200
0
34:1 36:2 36:1
F
BMP species in H4II cells
pmol BMP/mg protein
300
200
100
0
32:0 34:1 36:2 38:6 40:7 44:12 44:11
G
PI species in H4II cells
pmol PI/mg protein
3000
2000
1000
0
32:1 32:0 34:2 34:1 36:4 36:2 36:1 38:5 38:4 38:3 40:6 40:5 40:4

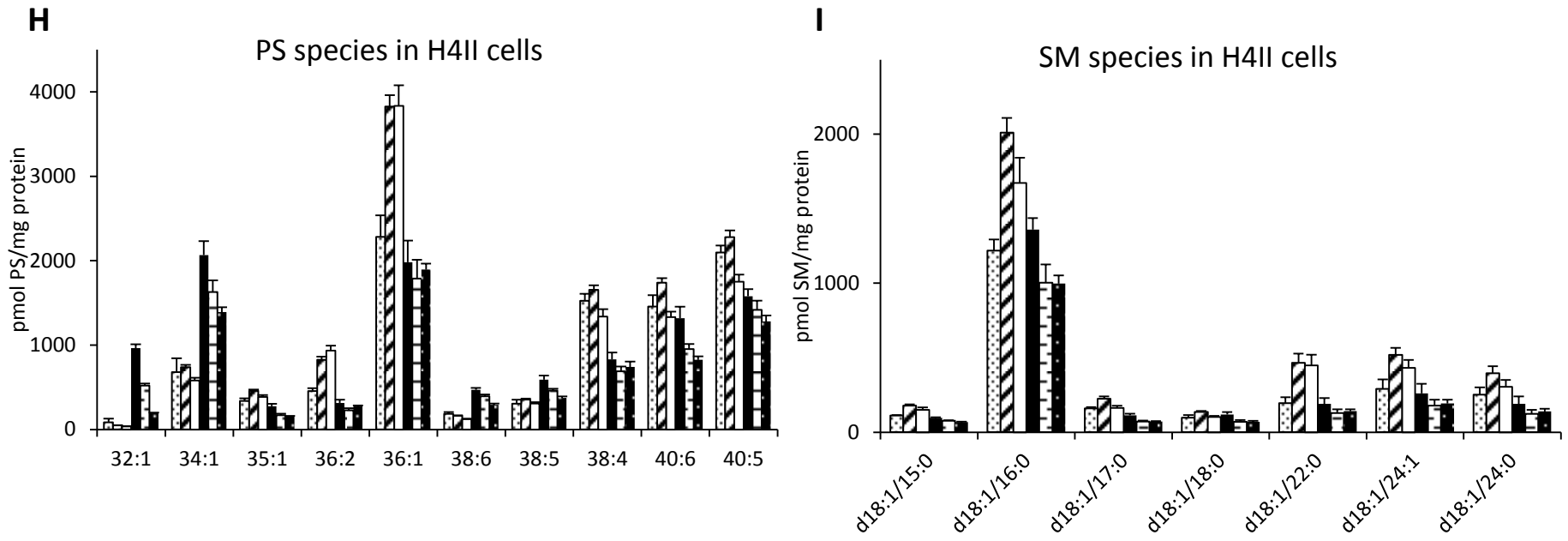

Figure 3-9S. Selected glycerophospholipid species distribution from H4IIEC3 hepatic cells treated for 12h. H4IIEC3 cells were treated with 400 μM PA with or without OA supplementation for 12h in H4IIEC3. Lipids were determined and quantified using a previously published LC-MS method. Selected species distributions of total glycerophospholipids, phosphatidic acid (PtdOH), phosphatidylcholine (PC), phosphatidylethanolamine (PE), phosphatidylglycerol (PG), Bis(monoacylglycerol)phosphate (BMP), phosphatidylinostitol (PI), phosphatidylserine (PS) and sphingomyelin (SM) are represented (A, B, C, D, E, F, G, H, and I respectively). Data represent mean ± SE of n=9.

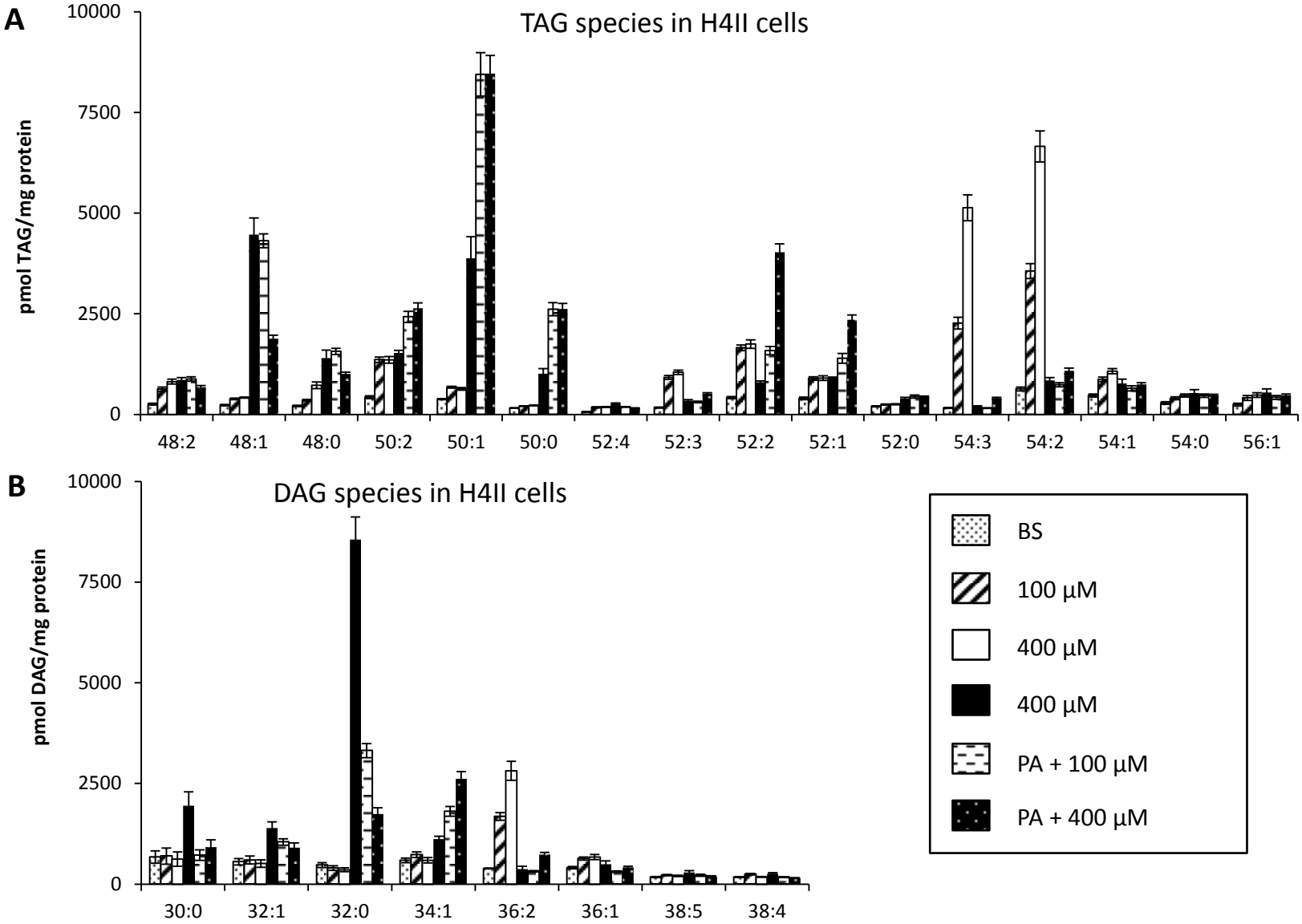

Figure 3-10S. Selected glycerolipid species distribution from H4IIEC3 hepatic cells treated for 12h. . H4IIEC3 cells were treated with 400 µM PA with or without OA supplementation for 12h in H4IIEC3. Lipids were determined and quantified using a LC-MS method. Selected species distributions of triacylglycerols (TAG) and diacylglycerols (DAG) are shown (A and B, respectively). Data represent mean ± SE of n=9.

CHAPTER 4

INHIBITION OF TRIGLYCERIDE SYNTHESIS DOES NOT SENSITIZE HEPATIC CELLS TO LIPTOXICITY OR INTERFERE WITH OLEATE-MEDIATED RESCUE OF PALMITATE-TREATED CELLS

Introduction

Obesity has reached epidemic proportions both in the U.S. and abroad, creating ballooning healthcare costs. Metabolic diseases associated with obesity, including type 2 diabetes, non-alcoholic fatty liver disease (NAFLD) and cardiovascular disease, have also seen concomitant increases in population incidence rates. NAFLD, the hepatic manifestation of metabolic syndrome, is characterized by chonic ectopic lipid accumulation in the liver and is estimated to affect over one-third of the U.S. general population and up to 80% of obese and diabetic individuals (1, 2). An estimated 10-25% of NAFLD patients progress to a more severe condition known as non-alcoholic steatohepatitis (NASH), characterized by chonic inflammation and hepatic cell death that can eventually lead to cirrhosis (3). Despite its high prevalence, the molecular mechanisms underlying the progression from NAFLD to NASH are not well understood and represent a critical area of investigation in order to develop more targeted and effective therapeutics for fatty liver disease.

Unger *et al.* introduced the concept of lipoapotosis (4-6), which involves cellular dysfunction and death due to the overaccumulation of lipids in non-adipose tissues (7). Hepatocyte lipoapoptosis due to liver fat accumulation is one of the hallmark features of NASH in humans (2, 8). The large body of literature published since the introduction of this concept indicates that lipid-induced hepatocyte toxicity is most acute when cells are exposed to elevated saturated fatty acids (SFAs) such as palmitate (PA) (9-12). Clinical studies indicate that diets high in saturated fat may be linked to NASH progression while, conversely, unsaturated fat can impart a protective effect (7, 13). *In vivo* studies using rodent diets high in saturated fat have shown increased hepatic inflammation, cell death, and markers of liver injury compared to normal high fat and chow diets (14-16).

In vitro experiments in a wide variety of cell types including Chinese hamster ovary (CHO) cells (17-19), pancreatic beta cells (20-22), breast cancer cells (23), HeLa cells (24) and hepatic cells (9, 10, 12, 25-28) have consistently demonstrated the acute lipotoxic effects of saturated fatty acids, such as PA, but not unsaturated fatty acids. Palmitate-mediated lipotoxicity is characterized by endoplasmic reticulum (ER) stress, ER calcium release, reactive oxygen species (ROS) accumulation, caspase activation and cell death (11, 29). Cells treated with monunsaturated fatty acids (MUFAs), such as oleate (OA), exhibit none of these features but instead demonstrate significant increases in triglyceride (TG) synthesis and accumulation (9, 12, 17).

Adding OA to PA-treated cells can fully reverse PA lipotoxicity though mechanisms that are not well defined but which have been previously attributed to increased TG accumulation and sequestration of PA into neutral lipid stores (17, 20, 21). However, this hypothesis has never been directly tested by experimentally modulating the relative partitioning of PA/OA between TGs and other lipid fates in hepatocytes. In this study, we test the alternative hypothesis that the rescue effect of PA/OA co-treatment (relative to treatment with PA alone) is due to its ability to normalize the composition of phospholipid membranes, rather than its ability to divert PA into neutral TG species. This hypothesis was suggested by our prior lipidomic profiling study that showed dramatic accumulation of saturated phospholipid species in response to PA treatment of liver hepatocytes, which was completely reversed by PA/OA co-treatment (9).

The fatty acyl chain composition and degree of unsaturation in phospholipids determines the biophysical characteristics of cellular membranes, including fluidity and assembly, which in turn influence their function (30). The ER membrane typically contains unsaturated phosphatidylcholine (PC) as its major phospholipid component (31), and its composition is tightly regulated; even small changes in fatty acyl composition and saturation may induce ER stress. Recent literature suggests that not only do obese individuals have chonic underlying levels of ER stress (32-35), but that ER stress pathways, known collectively as the unfolded protein response (UPR), are activated in NAFLD and may play an important role in the development and progression of this disease (36, 37). Markers of ER stress, including CCAAT/enhancer-binding protein homologous protein (CHOP) downstream of PERK activation, appear rapidly after treatment with PA but not OA (9, 38). Aberrant phospholipid metabolism and composition has been previously postulated as the link between ER stress and lipotoxicity (9, 11, 24, 25, 32).Abnormal incorporation of SFAs and subsequent oversaturation of the ER membrane can result in detrimental stiffening and loss of function leading to ER stress (30, 39). Increased phospholipid saturation may also impair the function of important membrane-bound proteins such as sarco-endoplasmic reticulum calcium ATPase (SERCA), which is critical for intracellular calcium homeostatsis (32, 40). Interestingly, we have shown that increased Ca^{2+} efflux from the ER can promote overactivation of mitochondrial metabolism leading to ROS accumulation and apoptosis in response to PA treatments (28).

In this study we show that addition of OA to PA-treated hepatocytes decreases overall phospholipid saturation while rescuing PA-induced apoptotic cell death. As shown previously, this rescue effect is accompanied by enhanced TG synthesis and, specifically, increased incorporation of PA into TG stores. However, simultaneous knockdown of both liver isoforms of diacylglycerol acyltransferase (DGAT), the rate-limiting step in TG synthesis, significantly reduced TG accumulation but without altering the ability of OA to prevent PA lipotoxicity. In both wild-type and DGAT knockdown cells, co-treatment with OA significantly reduced overall phospholipid saturation in comparison to cells treated with PA alone. These data indicate that OA's protective effects are mainly due to its ability to normalize the composition of cellular phospholipids in the presence of a PA load, rather than to divert toxic PA into inert TG stores.

Methods

Materials and Reagents

Oleic and palmitic acids, bovine serum albumin (BSA), and Dulbecco's modified Eagle's medium (DMEM) were all purchased from Sigma-Aldrich (St. Louis, MO). CHOP primary (mouse) and goat anti-mouse secondary antibodies were purchased from Abcam (Cambridge, MA). β-Actin primary (goat) and donkey anti-goat secondary antibodies were procured from Santa Cruz Biotechnology. Cleaved PARP primary (rabbit) and mouse anti-rabbit secondary antibodies were purchased from Cell Signaling (Danvers, MA). All other chemicals were purchased from standard commercial sources.

Preparation of Fatty Acid Solutions

Fatty acid treatment solutions were prepared by coupling free fatty acids BSA. Specifically, palmitate or oleate was fully dissolved in 200-proof ethanol for a concentration of 195 mM. This FFA stock solution was added to a pre-warmed BSA solution (10% w/w, 37°C) for a final FFA concentration of 3 mM, ensuring that the concentration of ethanol in the FFA solution did not exceed 0.5% by volume. The solution was fully dissolved by warming at 37°C for an additional 10 minutes. The final ratio of FFA:BSA was 2:1. Vehicle control treatments were prepared using stocks of 10% w/w BSA with an equivalent volume of ethanol added to match that contained in the final FFA stock. The final concentration of ethanol was less than 1% in all experiments.

Cell Culture and siRNA Transfections

Rat hepatoma cells, H4IIEC3 (ATCC), were cultured in low-glucose Dulbecco's modified Eagle's medium (DMEM) supplemented with 10% fetal bovine serum and 1% penicillin/streptomycin/glutamine (2mM). Measurements were obtained at 70-80% confluency. Hepatic cells were transfected with siRNA using Lipofectamine RNAiMAX (Invitrogen) according to the manufacturer's protocol. The final concentration of siRNA was 25 nM.

Cell Toxicity

Toxicity was assessed using the dead cell dye propidium iodide as described previously (41). Propidium iodide is an intercalating dye that can only permeate dead cells. It becomes highly fluorescent when embedded in the double-stranded DNA exposed after cell death. After culturing cells in 96-well plates with experimental treatments, the medium was removed and replaced with a solution of the dye and serum-free DMEM. Cells were incubated at 37°C for 1 h in the dark prior to fluorescence measurement at ex/em wavelengths of 530/645 nm.

Caspase Activation

The Apo-ONE Homogenous Caspase 3/7 Assay kit was used to measure apoptotic caspase activation. Cells were cultured in 96-well plates and incubated with desired treatments for 6

hours. The Apo-ONE kit uses a lysis buffer combined with a caspase 3/7 specific substrate (Z-DEVD-R110), which becomes fluorescent once these caspases remove its DEVD peptide. Fluorescence was measured at ex/em wavelengths of 485/535 nm.

Western Blotting

Cells were lysed with ice-cold RIPA lysis buffer (sc-24948, Santa Cruz Biotechnology, Inc., Santa Cruz, CA) supplemented with Na-orthovanadate, protease inhibitor cocktail, and PMSF for 30 min on ice. Samples were centrifuged at 16,100 rcf and 4°C for 20 min, and the resulting supernatants constituted the total protein extracts. Protein concentrations were determined by BCA assay (Thermo Fisher Scientific, Rockford, IL). Samples were added in concentrations of 30 μg/lane for SDS-PAGE western blotting. Dilutions of the primary antibodies were Anti-CHOP (1:1000), anti-β-actin (1:1000) and anti-cleaved parp (1:1000) all dissolved in 5% BSA. Secondary anti-bodies (anti-mouse, anti-goat and anti-rabbit, respectively) were all dissolved in a 1:1 mix of TBST : 5% BSA at a dilution of 1:10,000.

Total RNA Isolation and Quantitative Real-Time PCR

Total RNA was isolated from cells using RNeasy Mini Kit (Qiagen, Germantown, MD) according to the manufacturer's protocol and then reverse transcribed using a cDNA reverse transcriptase kit (BioRad, Hercules, CA). Quantitative real-time PCR was done using iQ SYBR Green Supermix (BioRad, Hercules, CA) and BioRad CFX96 Cycler (BioRad, Hercules, CA). The sequences of the primers were as follows: C/EBP homologous protein (CHOP) forward (5'-CTCAGCTGCCATGACTGTA-3') and reverse (5'-CGTCGATCATACCATGTTGAAGA-3'), ATF3 forward (5'-CGCCTCCTTTTTCTCTCATCT-3') and reverse (5'-CCATCCAGAACAAGCACCT-3'), ribosomal 18s forward (5'-CGGACAGGATTGACAGAT-3') and reverse (5'-CGCTCCACCAACTAAGAA-3'), diacylglycerol acyltransferase 1 (DGAT1) forward (5'-TTACCGTGGTATCCTGAA-3') and reverse (5'-GCCATACTTGATAAGATTCTC-3'), diacylglycerol acyltransferase 2 (DGAT2) forward (5'-AGACACCATAGACTACTT-3') and reverse (5'-ATACCTCATTCTCTCCAA-3'). Target gene expression was normalized on the basis of 18s content.

Phospholipid Fatty Acid Profiles

Cells seeded in 10-cm Petri dishes at an initial density of 4×10^6 cells per plate were incubated in standard medium until reaching ~70-80% confluency, at which time experimental treatments were administered. Cells were then trypsinized for 3 min and scraped using cold PBS. Cell suspensions were pelleted by centrifugation and resuspended in fresh PBS. Fatty acyl lipid analysis was performed by the Vanderbilt Hormone Assay and Analytical Services Core using thin-layer chromatography (TLC) and gas chromatography-flame ionization detection (GC-FID) techniques. Briefly, lipids were extracted from the aforementioned cell pellets using a modified Folch separation. An internal standard (1,2-dipentadecanoyl-*sn*-glycero-3-phosphocholine) for phospholipids was added to the lipid-containing chloroform phase. Total lipids were then

extracted and separated by TLC using petroleum ether/ethyl ether/acetic acid (80/20/1, v/v/v) on silica plates. Spots corresponding to different lipid pools were visualized with rhodamine 6G in 95% ethanol and scraped individually into glass tubes for transmethylation. Transmethylation was performed using a boron trifluoride-methanol 10% (w/w) solution. Derivatized lipids were then analyzed using GC-FID, where standardized calibration curves were used to analyze fatty acid composition and quantify total content.

^{3}H-Palmitate Lipid Class Incorporation

Cells seeded in 6-well dishes at 1.5×10^{6} cells per well were incubated in standard medium until reaching ~70-80% confluency. Next, the cells were incubated for the indicated duration at 37°C in 400 μM [9,10-^{3}H] palmitic acid (1 μCi ^{3}H/μmol PA), either in the presence or absence of oleic acid. Lipids were extracted using a modified Folch procedure; twice, 0.75 mL chilled methanol was added to each well and cells were scraped into 1:1 chloroform:water. Once vortexed and centrifuged, the lipid-containing chloroform phase was vacuum dried without heat. Lipid classes were separated by TLC, as described above. Each TLC spot was added to an individual vial and radioactivity was assessed by scintillation counting.

Statistical Analysis

All data are represented as mean ± standard error. Type I ANOVA (Student's t test) was used to assess statistical differences involving multiple (two) treatments. ANOVA was followed with Tukey-Kramer post-hoc testing for ^{3}H-labeled PA experiments and lipid fatty acyl chain composition .

Results

DGAT knockdown effectively reduces triglyceride synthesis in hepatic cells

DGAT plays an important role in determining the rate of cellular TG synthesis. Therefore, we sought to examine how inhibiting the expression of DGAT affects PA-induced lipoapoptosis and cellular lipid composition. We chose to simultaneously inhibit both DGAT1 and DGAT2, since both isoforms have demonstrated activity in hepatocytes (42, 43). Simultaneous transfection of siRNAs targeted against rat DGAT1 and DGAT2 (siDGAT1/2) in H4IIEC3 cells efficiently reduced mRNA expression levels of both DGAT1 and DGAT2 by approximately 70% and 85%, respectively (Fig. 4-1A). Oleate is a potent activator of TG synthesis in hepatocytes though its binding and inactivation of the constitutive DGAT-inhibitory protein Ubxd8 (44). OA administration was used to demonstrate the functional inhibition of cellular TG synthesis in response to siDGAT1/2 transfection. siDGAT1/2 cells treated with 400 μM OA showed significantly less TG accumulation than cells transfected with a non-targeted siRNA control (NTC) vector (Fig. 4-1B). Despite these differences in TG synthesis, there was no difference in

cell death between siDGAT1/2 and NTC cells after treatment with OA (Fig. 4-1C). These data indicate that reduced TG synthesis capabilities do not sensitize hepatocytes to lipotoxicity in response to MUFA treatment.

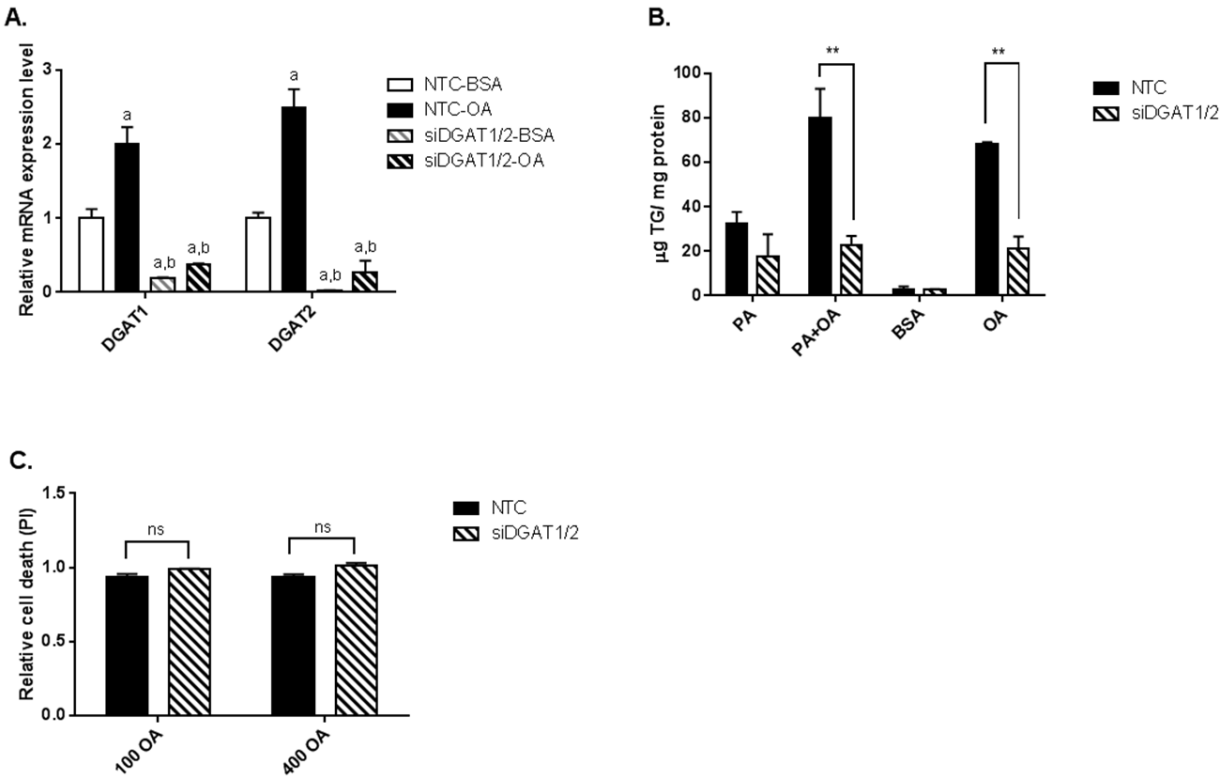

Figure 4-1. siRNA mediated knockdown of DGAT1/2 significantly reduced TG accumulation in H4IIEC3 cells but did not sensitize them to fatty acid lipotoxicity. Simultaneous siRNA mediated knockdown of DGAT1 and DGAT2 expression (siDGAT1/2) reduced mRNA transcript levels of both proteins (A). siDGAT1/2 cells demonstrated significantly reduced TG accumulation in comparison to non-targeted control (NTC) cells when supplemented with identical fatty acid loads (B). TGs were separated by thin layer chromatography and analyzed by gas chromatography-flame ionization detection (GC-FID). Amounts were normalized to mg protein for absolute quantification. Inhibition of TG synthesis did not sensitize siDGAT1/2 cells to OA lipotoxicity (C). Data represent mean ± SE of n=4. **, P<0.05, vs. cells supplemented with the same treatment; ^{a}, P<0.05, vs BSA-control cells with same genetic manipulation (NTC or siDGAT1/2); ^{b}, P<0.05, vs cells with same treatment; *ns*, not significant.

Inhibition of TG synthesis does not sensitize hepatic cells to FFA-induced apoptosis

Previous work has shown that PA is toxic to a wide variety of cell types, including hepatocytes, while OA is not acutely toxic (6, 9, 11). In fact, co-supplementing PA-treated cells with OA effectively reverses all lipotoxic phenotypes associated with PA overload. Prior literature

suggests that this rescue is due to the ability of OA to induce TG synthesis and thereby sequester PA away from metabolic fates that promote cellular stress and dysfunction. Therefore, we sought to investigate how inhibition of TG synthesis affects the ability of OA to rescue PA-treated hepatic cells.

Similar to prior studies, PA treatment of H4IIEC3 cells transfected with NTC siRNA resulted in significant increases in cell death while OA treatment did not initiate cell death (Fig. 4-2A). PA toxicity was associated with increased activity of caspases 3 and 7 (Fig. 4-2B) and accumulation of cleaved PARP (Fig. 4-2C), indicative of apoptosis-mediated cell death in PA-treated cells. Co-supplementation of OA to PA-treated NTC cells completely abolished PA toxicity. Interestingly, knockdown of DGAT1/2 in H4IIEC3 cells did not alter the apoptotic response to PA and/or OA treatments. Palmitate was toxic to siDGAT1/2 cells while OA was not, and most surprisingly, cells supplemented with PA were still rescued by the addition of OA even in the absence of appreciable TG synthesis (Figure 4-2A). Furthermore, OA co-supplementation was still able to protect against caspase 3/7 activation and accumulation of cleaved PARP in siDGAT1/2 cells, indicating a rescue from PA-mediated cell apoptosis.

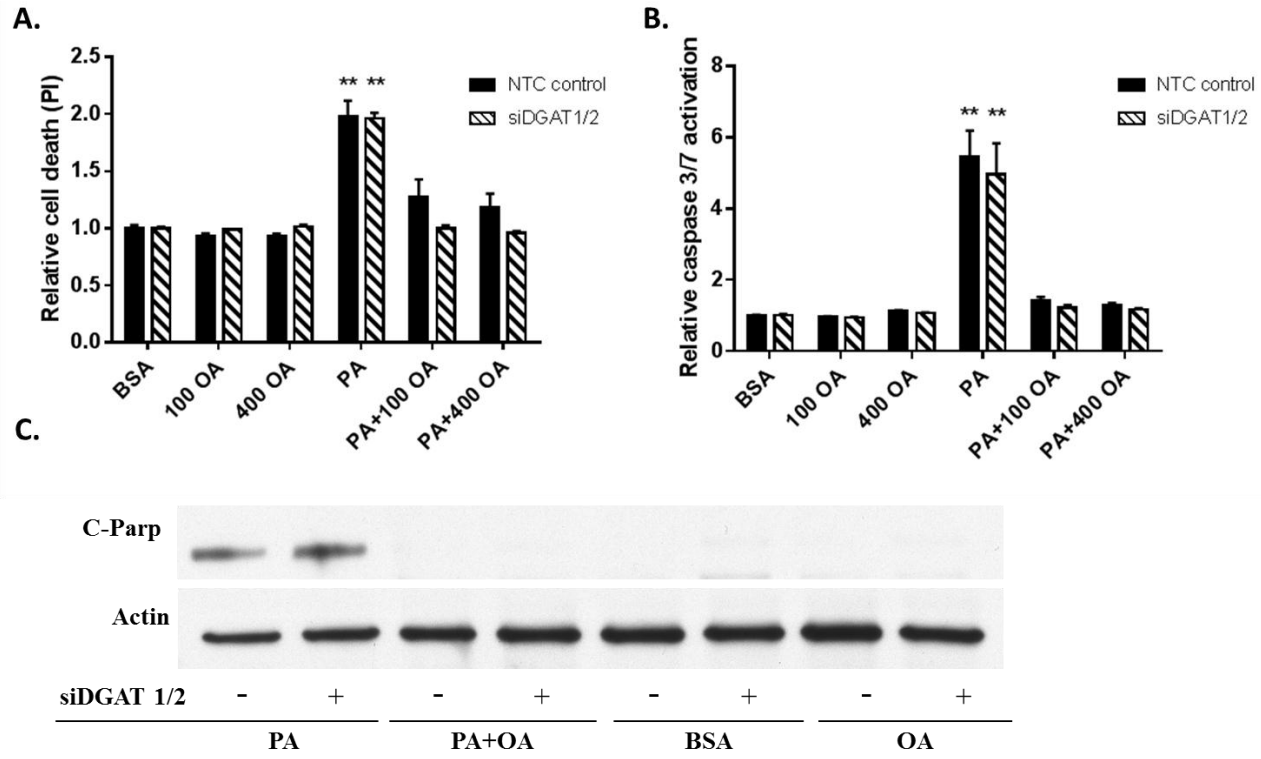

Figure 4-2. OA-mediated rescue of PA-induced lipoapoptosis was not inhibited by siDGAT1/2 knockdown. siDGAT1/2 cells demonstrated statistically identical responses to treatment with PA and/or OA (A) as assessed by propidium iodide (PI) staining of dead cells expressed relative to BSA-treated controls. Consistent trends were observed in cell apoptosis assessed by caspase 3/7 activity (B) and expression level of cleaved PARP (C). Data represent mean ± SE of n=4. **, $P<0.05$, vs cells supplemented with the same treatment.

DGAT1/2 knockdown does not affect palmitate- and oleate-induced markers of ER stress

Next, we sought to examine whether DGAT1/2 knockdown affected other aspects of PA-induced lipotoxicity aside from cell death and apoptosis. Previous studies show that PA exposure induces acute ER stress, also known as unfolded protein response (UPR), as part of the lipotoxicity cascade (9, 38). The purpose of UPR is to respond to deleterious changes in ER function, which can result from accumulation of misfolded proteins (45) or changes in ER membrane composition (24, 25, 39). Thee transmembrane ER proteins, inositol-requiring 1 (IRE1), PERK and activating transcription factor 6 (ATF6), are upregulated during UPR. We measured expression of several genes associated with downstream and prolonged UPR, specifically CHOP and ATF3, as surrogate markers of ER stress during lipotoxic treatments.

Quantitative real-time PCR analysis showed a marked increase in CHOP and ATF3 expression levels in response to PA but not OA treatment in both NTC vector and siDGAT1/2 transformed cells (Figure 4-3A). Co-treatment with OA in both control and knockdown cells restored these markers of ER stress to basal levels. The same trend was observed in measurements of CHOP protein expression (Figure 4-3B). These results indicate that elevated TG synthesis is not required for OA to inhibit PA-induced ER stress in hepatocytes.

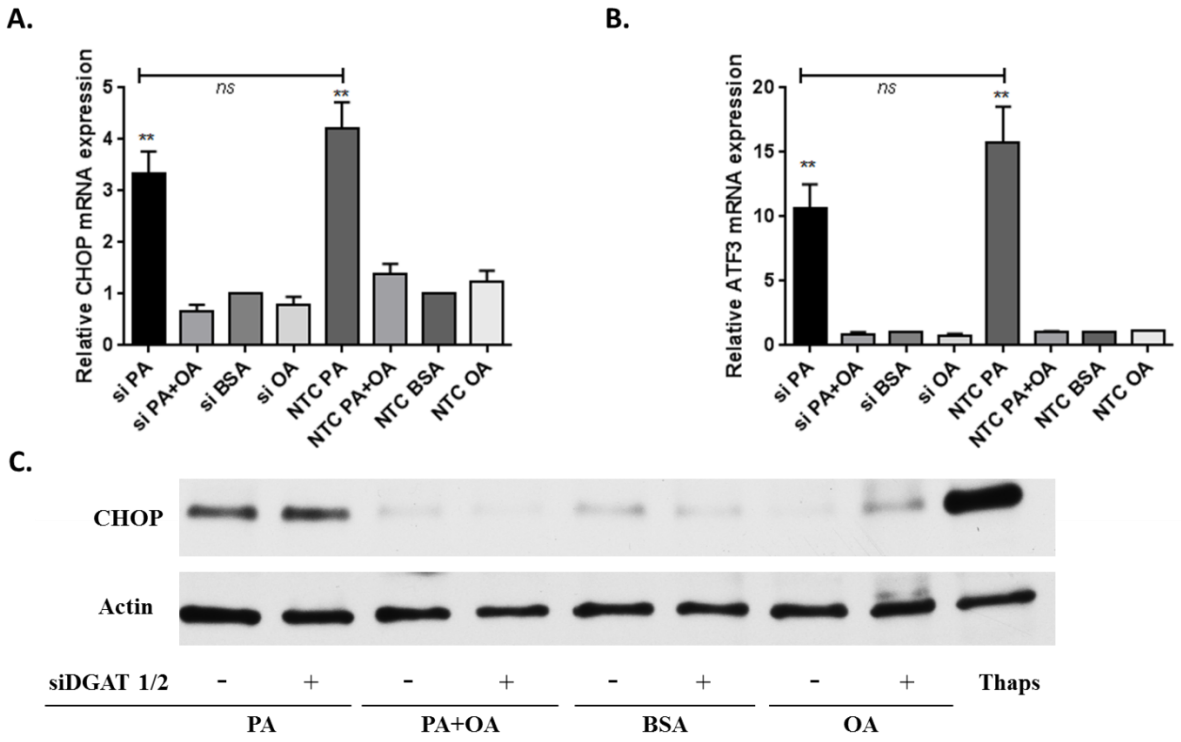

Figure 4-3. PA-induced increases in markers of ER stress were completely reversed by co-treatment with OA regardless of DGAT expression level. Both NTC and siDGAT1/2 H4IIEC3 cells were treated with 400 μM PA with or without 400 μM OA supplementation to assess markers of ER stress. Relative mRNA transcript levels of CHOP (A) and ATF3 (B) were assessed at 6h. Levels of CHOP protein expression were assessed by Western blot at 8h, with one representative blot shown (C). Thapsigargin (Thaps) is a positive control. Data represent mean ± SE of n=3. **, P<0.05, vs cells treated w PA.

DGAT1/2 knockdown alters palmitate distribution amongst lipid pools and modulates phospholipid composition

We next examined the effects of siDGAT1/2 knockdown on PA incorporation into the main cellular lipid pools. As expected, DGAT knockdown significantly reduced partitioning of radiolabeled ^{3}H-PA into the TG pool, both alone and in the presence of OA (Figure 4-4).There was a small, but significant, increase in accumulation of ^{3}H-PA into the diacylglycerol pool in the siDGAT1/2 cells. However, the majority of the radiolabeled PA was alternatively channeled into the phospholipid pool in these knockdown cells. These results indicate that knockdown of DGAT1/2 alters the intracellular fate of exogenous fatty acids away from TG synthesis and into other lipid end-products. The vast majority of ^{3}H-PA was alternatively incorporated into phospholipids. Interestingly, a higher percentage of total cellular ^{3}H-PA was partitioned into the phospholipid fraction of siDGAT1/2 cells co-treated with PA+400μM OA than NTC cells treated with PA alone, and yet these cells were protected from lipotoxicity while the PA-treated NTC cells were not. This finding is inconsistent with the notion that oleate's capacity to prevent PA lipotoxicity is simply a consequence of its ability to divert PA into TG synthesis.

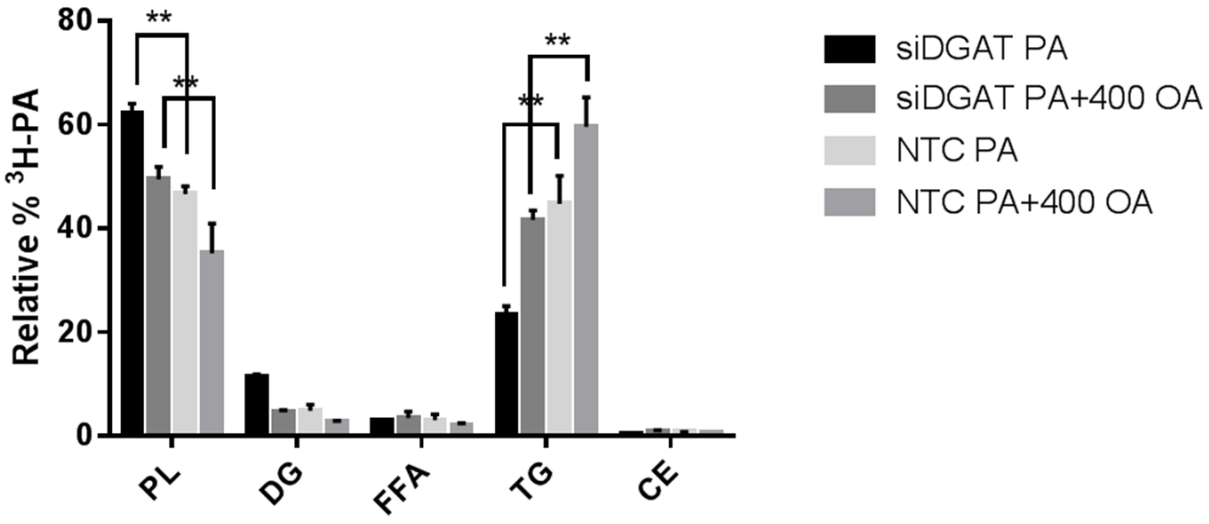

Figure 4-4. Knockdown of DGAT1/2 repartitions PA into phospholipids and away from TGs. H4IIEC3 cells were treated with 400 μM ^{3}H-PA with or without OA supplementation for 12h in both NTC and siDGAT1/2 knockdown cells . Lipid class incorporation was determined using TLC separation and scintillation counting of each lipid spot. PL, phospholipid; DG; diacylglyceride; FFA, free fatty acid; TG, triglyceride; CE, cholesterol ester. Data represent mean ± SE of n=3. **,$p < 0.01$ NTC vs siDGAT1/2 cells with same treatment.

Next, we measured the phospholipid composition in DGAT1/2 knockdown cells to see if the increased partitioning of PA into the phospholipid fraction was reflected in compositional changes (Table 4-1). Administration of PA resulted in significant increases in the abundance of palmitic acid (16:0) in phospholipids compared to BSA treatment in both NTC cells (48.73 ± 0.62% versus 12.87 ± 0.14%) and DGAT1/2 knockdown cells (53.06 ± 2.66% versus 13.58 ± 0.18%). This correlated with a significant increase in total phospholipid saturation in PA-treated cells versus BSA control cells. Similar to previous reports (9), PA/OA co-treatment of NTC cells significantly reduced both the abundance of PA in phospholipids (30.05 ± 0.24% versus 48.73 ± 0.62%) and overall phospholipid saturation (40.80 ± 0.27% versus 61.55 ± 0.85%) compared to those treated with PA alone. Most interestingly, siDGAT1/2 cells exhibited similar shifts in PA abundance (30.77 ± 0.22% versus 53.06 ± 2.66%) as well as total saturation level of phospholipids (40.62 ± 0.24% versus 64.94 ± 2.77%) when PA/OA co-treated cells were compared to cells treated with PA alone. In fact, there were no statistical differences in 16:0 abundance or phospholipid saturation level between the NTC and siDGAT1/2 cells administered the same fatty acid treatments. These data suggest that inhibition of TG synthesis does not alter oleate's ability to normalize the composition of membrane phospholipids in PA-treated cells.

Fatty Acid	NTC PA	NTC PA+OA	NTC BSA	NTC OA	siDGAT PA	siDGAT PA+OA	siDGAT BSA	siDGAT OA
14:0	0.00 ± 0.00	0.00 ± 0.00	0.89 ± 0.02	0.48 ± 0.03	0.00 ± 0.00	0.00 ± 0.00	0.69 ± 0.35	0.00 ± 0.00
16:0	48.73 ± 0.62	30.05 ± 0.23[a]	12.87 ± 0.14[a]	8.29 ± 0.10[a]	53.06 ± 2.66[b]	30.77 ± 0.22[a]	13.58 ± 0.18[a]	7.18 ± 0.11[a]
16:1	8.82 ± 0.24	6.50 ± 0.06[a]	6.71 ± 0.10[a]	2.40 ± 0.08[a]	9.70 ± 0.72	5.37 ± 0.09[a]	5.88 ± 0.05[a]	1.47 ± 0.02[a]
18:0	12.82 ± 0.58	10.75 ± 0.12[a]	18.75 ± 0.55[a]	12.64 ± 0.42	11.88 ± 0.77	9.84 ± 0.10[a]	18.92 ± 0.31[a]	10.77 ± 0.20
18:1w9	11.06 ± 0.07	34.34 ± 0.40[a]	28.19 ± 0.74[a]	58.03 ± 0.05[a]	12.28 ± 0.30	37.68 ± 0.14[a,b]	30.22 ± 0.66[a,b]	66.40 ± 0.22[a,b]
18:1w7	3.22 ± 0.02	2.83 ± 0.02	8.01 ± 0.42[a]	4.17 ± 0.08	2.92 ± 0.09	2.97 ± 0.02	7.36 ± 0.20[a]	4.00 ± 0.05
18:2	1.80 ± 0.08	2.08 ± 0.01	4.08 ± 0.14[a]	1.75 ± 0.05	1.10 ± 0.55	1.76 ± 0.04[a]	3.82 ± 0.14[a]	1.42 ± 0.01[a]
20:3w6	0.66 ± 0.33	0.96 ± 0.01	1.51 ± 0.03	0.60 ± 0.01	0.00 ± 0.00	0.00 ± 0.00	0.85 ± 0.42	0.00 ± 0.00
20:4	8.52 ± 0.07	7.73 ± 0.14	10.56 ± 0.03[a]	6.64 ± 0.07	6.72 ± 0.29	7.30 ± 0.02	10.51 ± 0.15[a]	5.77 ± 0.11
20:5	0.00 ± 0.00	0.12 ± 0.12	0.34 ± 0.17	0.00 ± 0.00	0.00 ± 0.00	0.00 ± 0.00	0.00 ± 0.00	0.00 ± 0.00
22:4w6	0.00 ± 0.00	0.87 ± 0.05	1.38 ± 0.01	0.59 ± 0.01	0.00 ± 0.00	1.03 ± 0.09	1.84 ± 0.05	0.00 ± 0.00
22:5w6	0.00 ± 0.00	0.00 ± 0.00	0.65 ± 0.42	1.05 ± 0.01	0.00 ± 0.00	0.00 ± 0.00	0.81 ± 0.40	0.51 ± 0.26
22:5w3	2.34 ± 0.09	1.75 ± 0.05	2.83 ± 0.03	1.43 ± 0.01	1.17 ± 0.59	1.73 ± 0.01	2.76 ± 0.04	1.22 ± 0.03
22:6	2.02 ± 0.01	2.01 ± 0.04	3.23 ± 0.01	1.91 ± 0.01	1.74 ± 0.06	1.56 ± 0.03	2.78 ± 0.02	1.25 ± 0.01
% SFA	61.55 ± 0.85	40.80 ± 0.26[a]	32.52 ± 0.57[a]	21.42 ± 0.44[a]	64.94 ± 2.77[b]	40.62 ± 0.24[a]	33.18 ± 0.50[a]	17.96 ± 0.22[a,b]
% UFA	38.45 ± 0.44	59.20 ± 0.45[a]	67.48 ± 0.98[a]	78.58 ± 0.15[a]	35.06 ± 1.16[b]	59.38 ± 0.20[a]	66.82 ± 0.93[a]	82.04 ± 0.36[a,b]

Table 4-1. Phospholipid fatty acid composition of NTC and siDGAT1/2 H4IIEC3 cells treated with PA and/or OA for 12 h (% of total abundance). H4IIEC3 cells were incubated with 400 μM PA and/or 400 μM OA for 12 h. Phospholipids were separated by thin layer chromatography and analyzed by gas chromatography-flame ionization detection (GC-FID). Data represent mean fatty acid % ± SE of n=4. a, $p<0.05$ vs cells treated with PA alone and same genetic manipulation (NTC or siDGAT1/2); b, $p<0.05$ NTC vs siDGAT1/2 cells with same treatment. SFA, saturated fatty acids; UFA, unsaturated fatty acids.

Discussion

Currently, it is a widely held assumption that increases in TG accumulation are responsible for oleate's ability to rescue cells from PA-induced lipotoxicity (17, 38, 44, 46, 47). This assumption is supported by the finding that Dgat1$^{-/-}$ primary mouse embryonic fibroblasts (MEFs) showed increased sensitivity to OA toxicity (17). We therefore sought to examine the effects of OA supplementation on PA-treated H4IIEC3 cells with partial DGAT knockdown to assess whether corresponding decreases in cell viability would be observed in liver hepatocytes. Surprisingly, while DGAT knockdown effectively prevented TG accumulation (Fig. 4-1), it did not modify the differential effects of fatty acid treatments on cell viability or apoptosis (Fig. 4-2). In contrast to prior reports, these data suggest that increased TG synthesis is not necessary for OA-mediated rescue of PA lipotoxicity.

We have shown previously (9) that addition of PA rapidly induces ER stress, which is correlated with increases in apoptosis and cell death. Addition of OA to PA-treated cells prevented ER stress and correlated with a change in PA distribution within cellular lipid pools: specifically, PA incorporation into the phospholipid fraction was reduced. We therefore examined the impact that inhibition of TG synthesis would have on PA partitioning and overall phospholipid composition in hepatic cells. DGAT knockdown cells incorporated a higher percentage of exogenous PA into the phospholipid fraction and less into TGs, even in the presence of OA, than vector control cells (Fig. 4-4). However, this change in relative PA partitioning had no impact on ER stress markers (Fig. 4-3). This is likely explained by the lack of any meaningful differences in phospholipid saturation between DGAT knockdown and vector control cells (Table 4-1). Most interestingly, there were no differences in relative PA abundance or overall saturation of phospholipid species between DGAT knockdown and vector control cells co-treated with equimolar concentrations of OA and PA. Although DGAT knockdown changed the relative partitioning of exogenous PA into cellular lipid pools, OA partitioning apparently adjusted in a proportional manner to maintain constant phospholipid composition. This ability of OA to counteract PA's effects on phospholipid saturation correlated with a reduction in markers of ER stress and lipoapoptosis, irrespective of DGAT expression levels.

The ER membrane is estimated to contain up to 50% of total cellular phospholipids and is characterized by a "disordered" composition; low concentrations of "ordering" cholesterol moieties and high concentrations of unsaturated fatty acids that increase membrane fluidity (30). Small changes in ER membrane fluidity can result in impaired ER function and initiation of UPR. Exogenous saturated fatty acids have been shown to rapidly incorporate into phospholipids of the ER membrane and alter its structure though increased order and reduced fluidity (9, 38, 39, 48). The precise nature of the link between reduced membrane fluidity and ER stress has not been fully elucidated, but recent literature suggests that changes in lipid composition substantially affect ER membrane proteins (40). For example, the sarcoendoplasmic reticulum calcium ATPase (SERCA) pump is an ER-resident, membrane-bound protein that functions to maintain proper cellular calcium concentrations by sequestering excess cytosolic calcium into the ER lumen. Increased saturation of the ER membrane effectively inhibits the activity of the SERCA pump both *in vivo* (32) and *in vitro* (40), resulting in ER calcium depletion and initiation of the UPR. This dysfunctional ER calcium buffering may play a role in downstream events characteristic of PA-mediated lipotoxicity including mitochondrial dysfunction and apoptotic cell death (10, 28). Additionally, Volmer *et al.* have recently demonstrated that increased lipid acyl-chain saturation of the ER membrane can directly activate ER transmembrane proteins IREα and PERK, whose stimulation initiates two of the three main arms of the UPR (48). This is consistent with our results in PA-treated hepatic cells showing upregulation of ER stress markers CHOP and ATF3, both of which are activated though the PERK pathway in the UPR.

The composition of fatty acyl chains of membrane phospholipids is determined though both *de novo* and remodeling pathways (49-51). *De novo* phospholipid synthesis though the canonical

Kennedy pathway begins with a glycerol-3-phosphate that is sequentially acylated to form phosphatidic acid, which serves as a precursor for downstream lipid products including diacylglycerol, phospholipids and TGs. In general, phospholipids produced though *de novo* synthesis contain a saturated fatty acid at the *sn-1* position, typically 16:0 (PA), and an unsaturated fatty acid at the *sn*-2 position (52). Glycerophospholipid remodeling, known as the Lands' cycle, involves tandem removal and re-acylation of fatty acyl chains to generate phospholipid diversity and to maintain homeostatic membrane composition and fluidity (51, 53-56). In the presence of PA overload, hepatic cells readily incorporate the exogenous PA into phospholipids leading to increased saturation (Table 4-1) and initiation of ER stress (Fig. 4-3). When OA is supplemented to PA-treated cells, remodeling enzymes are able to efficiently balance PA and OA incorporation to achieve a more normal phospholipid composition (Table 4-1).

Our study demonstrates that any increased capacity for PA disposal via esterification into TGs is not necessary for OA to exert its protective effects. However, the results of this study seem to contradict the previous results, such as the Listenberger et al. study which demonstrated increased cellular sensitivity to all free fatty acids, including MUFAs, in response to triglyceride synthesis knockdown in MEFs (17). Additional studies in yeast screens for fatty acid sensitive strains seem to support those results (57, 58). There are several possible explanations for these seemingly contradictory findings. All of these studies were done in different cell types other than hepatocytes and thus have difference metabolic profiles. Additionally, the lipotoxicity experiments in these studies utilized complete knockdown models. Complete ablation of triglyceride synthesis may lead to toxic accumulation of lipid intermediates or death by a mechanism that is different from palmitate lipotoxicity. Another complication to point out is that some of the knockdowns, such as ARV1 in the yeast mutants (58), that lead to depressed triglyceride synthesis and FFA sensitivity actually demonstrate high levels of basal ER stress without fatty acid stress (59), a fact that complicates interpretation of these results in comparison to our own. Further studies are needed to fully elucidate the mechanism by which OA incorporation into phospholipids in enhanced in our model that leads to rescue from palmitate-induced lipotoxicity.

Saturated fatty acids induce lipotoxicity in a variety of cell types and are postulated to be a contributing factor to pathological disorders including metabolic syndrome, insulin resistance and type 2 diabetes (60, 61). Both *in vitro* and *in vivo* models (16, 19, 37) have been used to study the mechanisms of lipotoxicity and demonstrate the apoptotic inducing effects of saturated fatty acids. PA mediated lipotoxicity is typically characterized by increases in mitochondrial dysfunction, ROS accumulation and caspase activation that culminates in apoptotic cell death. Increasing evidence points toward ER stress as an integral player in both acute lipotoxicity and more chronic metabolic disease and that PA may act directly at the ER membrane to mediate this response. Specifically, PA rapidly incorporates in ER membrane phospholipids, increasing the saturation ratios and impairing ER integrity (9, 38). Measures intended to reverse palmitate-

mediated saturation, such as overexpressing the LPCAT3 enzyme to increase unsaturated fatty acid incorporation in the phospholipids (25), have shown beneficial results for reducing ER stress. Our study demonstrates that co-supplementation with OA in PA treated cells may act in a similar manner, integrating into the membrane phospholipids, reversing oversaturation and preventing PA mediated ER stress and lipotoxicity. Although OA-mediated rescue has been traditionally attributed to its capacity to increase PA storage in TGs, our data shows its effect on phospholipid composition is sufficient to attenuate lipotoxicity. These findings suggest that more research directed toward understanding phospholipid composition and metabolism may represent a promising direction for developing therapeutic interventions for chronic metabolic diseases.

References

1. Barshop, N. J., C. B. Sirlin, J. B. Schwimmer, and J. E. Lavine. 2008. Review article: epidemiology, pathogenesis and potential treatments of paediatric non-alcoholic fatty liver disease. *Aliment. Pharmacol. Ther.* **28**: 13-24.

2. Wieckowska, A., A. J. McCullough, and A. E. Feldstein. 2007. Noninvasive diagnosis and monitoring of nonalcoholic steatohepatitis: Present and future. *Hepatology* **46**: 582-589.

3. Michelotti, G. A., M. V. Machado, and A. M. Diehl. 2013. NAFLD, NASH and liver cancer. *Nature Reviews Gastroenterology & Hepatology* **10**: 656-665.

4. Shimabukuro, M., Y. T. Zhou, M. Levi, and R. H. Unger. 1998. Fatty acid-induced beta cell apoptosis: A link between obesity and diabetes. *Proceedings of the National Academy of Sciences of the United States of America* **95**: 2498-2502.

5. Unger, R. H. 2002. Lipotoxic diseases. *Annual Review of Medicine* **53**: 319-336.

6. Unger, R. H., and L. Orci. 2002. Lipoapoptosis: its mechanism and its diseases. *Biochimica Et Biophysica Acta-Molecular and Cell Biology of Lipids* **1585**: 202-212.

7. Gentile, C. L., and M. J. Pagliassotti. 2008. The role of fatty acids in the development and progression of nonalcoholic fatty liver disease. *Journal of Nutritional Biochemistry* **19**: 567-576.

8. Feldstein, A. E., A. Canbay, P. Angulo, M. Taniai, L. J. Burgart, K. D. Lindor, and G. J. Gores. 2003. Hepatocyte apoptosis and Fas expression are prominent features of human nonalcoholic steatohepatitis. *Gastroenterology* **125**: 437-443.

9. Leamy, A. K., R. A. Egnatchik, M. Shiota, P. T. Ivanova, D. S. Myers, H. A. Brown, and J. D. Young. 2014. Enhanced synthesis of saturated phospholipids is associated with ER stress and lipotoxicity in palmitate-treated hepatic cells. *J. Lipid Res.* **55**: 1478-1488.

10. Egnatchik, R. A., A. K. Leamy, Y. Noguchi, M. Shiota, and J. D. Young. 2014. Palmitate-induced Activation of Mitochondrial Metabolism Promotes Oxidative Stress and Apoptosis in H4IIEC3 Rat Hepatocytes. *Metabolism-Clinical and Experimental* **63**: 283-295.

11. Leamy, A. K., R. A. Egnatchik, and J. D. Young. 2013. Molecular mechanisms and the role of saturated fatty acids in the progression of non-alcoholic fatty liver disease. *Prog. Lipid Res.* **52**: 165-174.

12. Noguchi, Y., J. D. Young, J. O. Aleman, M. E. Hansen, J. K. Kelleher, and G. Stephanopoulos. 2009. Effect of Anaplerotic Fluxes and Amino Acid Availability on Hepatic Lipoapoptosis. *J. Biol. Chem.* **284**: 33425-33436.

13. de Wit, N. J. W., L. A. Afman, M. Mensink, and M. Muller. 2012. Phenotyping the effect of diet on non-alcoholic fatty liver disease. *Journal of Hepatology* **57**: 1370-1373.

14. Pagliassotti, M. J., P. A. Prach, T. A. Koppenhafer, and D. A. Pan. 1996. Changes in insulin action, triglycerides, and lipid composition during sucrose feeding in rats. *American Journal of Physiology-Regulatory Integrative and Comparative Physiology* **271**: R1319-R1326.

15. Commerford, S. R., J. B. Ferniza, M. E. Bizeau, J. S. Thresher, W. T. Willis, and M. J. Pagliassotti. 2002. Diets enriched in sucrose or fat increase gluconeogenesis and G-6-Pase but not basal glucose production in rats. *Am. J. Physiol.-Endocrinol. Metab.* **283**: E545-E555.

16. Nivala, A. M., L. Reese, M. Frye, C. L. Gentile, and M. J. Pagliassotti. 2013. Fatty acid-mediated endoplasmic reticulum stress in vivo: Differential response to the infusion of Soybean and Lard Oil in rats. *Metabolism-Clinical and Experimental* **62**: 753-760.

17. Listenberger, L. L., X. L. Han, S. E. Lewis, S. Cases, R. V. Farese, D. S. Ory, and J. E. Schaffer. 2003. Triglyceride accumulation protects against fatty acid-induced lipotoxicity. *Proceedings of the National Academy of Sciences of the United States of America* **100**: 3077-3082.

18. Listenberger, L. L., D. S. Ory, and J. E. Schaffer. 2001. Palmitate-induced apoptosis can occur through a ceramide-independent pathway. *J. Biol. Chem.* **276**: 14890-14895.

19. Charlton, M., A. Krishnan, K. Viker, S. Sanderson, S. Cazanave, A. McConico, H. Masuoko, and G. Gores. 2011. Fast food diet mouse: novel small animal model of NASH with ballooning, progressive fibrosis, and high physiological fidelity to the human condition. *Am. J. Physiol.-Gastroint. Liver Physiol.* **301**: G825-G834.

20. Choi, S.-E., I.-R. Jung, Y.-J. Lee, S.-J. Lee, J.-H. Lee, Y. Kim, H.-S. Jun, K.-W. Lee, C. B. Park, and Y. Kang. 2011. Stimulation of Lipogenesis as Well as Fatty Acid Oxidation Protects against Palmitate-Induced INS-1 beta-Cell Death. *Endocrinology* **152**: 816-827.

21. Busch, A. K., E. Gurisik, D. V. Cordery, M. Sudlow, G. S. Denyer, D. R. Laybutt, W. E. Hughes, and T. J. Biden. 2005. Increased fatty acid desaturation and enhanced expression of stearoyl coenzyme A desaturase protects pancreatic beta-cells from lipoapoptosis. *Diabetes* **54**: 2917-2924.

22. Cunha, D. A., P. Hekerman, L. Ladriere, A. Bazarra-Castro, F. Ortis, M. C. Wakeham, F. Moore, J. Rasschaert, A. K. Cardozo, E. Bellomo, L. Overbergh, C. Mathieu, R. Lupi, T. Hai, A. Herchuelz, P. Marchetti, G. A. Rutter, D. L. Eizirik, and M. Cnop. 2008. Initiation and execution of lipotoxic ER stress in pancreatic beta-cells. *Journal of Cell Science* **121**: 2308-2318.

23. Hardy, S., W. El-Assaad, E. Przybytkowski, E. Joly, M. Prentki, and Y. Langelier. 2003. Saturated fatty acid-induced apoptosis in MDA-MB-231 breast cancer cells - A role for cardiolipin. *J. Biol. Chem.* **278**: 31861-31870.

24. Ariyama, H., N. Kono, S. Matsuda, T. Inoue, and H. Arai. 2010. Decrease in Membrane Phospholipid Unsaturation Induces Unfolded Protein Response. *J. Biol. Chem.* **285**: 22027-22035.

25. Rong, X., C. J. Albert, C. Hong, M. A. Duerr, B. T. Chamberlain, E. J. Tarling, A. Ito, J. Gao, B. Wang, P. A. Edwards, M. E. Jung, D. A. Ford, and P. Tontonoz. 2013. LXRs Regulate ER Stress and Inflammation through Dynamic Modulation of Membrane Phospholipid Composition. *Cell Metabolism* **18**: 685-697.

26. Pagliassotti, M., Y. R. Wei, and D. Wang. 2005. Saturated fatty acids induce cytotoxicity in hepatocytes via effects on the endoplasmic reticulum. *Obesity Research* **13**: A31-A31.

27. Wei, Y., D. Wang, F. Topczewski, and M. J. Pagliassotti. 2006. Saturated fatty acids induce endoplasmic reticulum stress and apoptosis independently of ceramide in liver cells. *Am. J. Physiol.-Endocrinol. Metab.* **291**: E275-E281.

28. Egnatchik, R., A. Leamy, D. Jacobson, M. Shiota, and J. Young. 2014. ER calcium release promotes mitochondrial dysfunction and hepatic cell lipotoxicity in response to palmitate overload. *Molecular Metabolism* **3**: 544-553.

29. Brookheart, R. T., C. I. Michel, and J. E. Schaffer. 2009. As a Matter of Fat. *Cell Metabolism* **10**: 9-12.

30. Spector, A. A., and M. A. Yorek. 1985. Membrane lipid-Composition and cellular function. *J. Lipid Res.* **26**: 1015-1035.

31. Van der Sanden, M. H. M., M. Houweling, L. M. G. Van Golde, and A. B. Vaandrager. 2003. Inhibition of phosphatidylcholine synthesis induces expression of the endoplasmic reticulum stress and apoptosis-related protein CCAAT/enhancer-binding protein-homologous protein (CHOP/GADD153). *Biochemical Journal* **369**: 643-650.

32. Fu, S., L. Yang, P. Li, O. Hofmann, L. Dicker, W. Hide, X. Lin, S. M. Watkins, A. R. Ivanov, and G. S. Hotamisligil. 2011. Aberrant lipid metabolism disrupts calcium homeostasis causing liver endoplasmic reticulum stress in obesity. *Nature* **473**: 528-531.

33. Wek, R. C., and T. G. Anthony. 2010. Obesity: stressing about unfolded proteins. *Nature Medicine* **16**: 374-376.

34. Sharma, N. K., S. K. Das, A. K. Mondal, O. G. Hackney, W. S. Chu, P. A. Kern, N. Rasouli, H. J. Spencer, A. Yao-Borengasser, and S. C. Elbein. 2008. Endoplasmic Reticulum Stress Markers Are Associated with Obesity in Nondiabetic Subjects. *Journal of Clinical Endocrinology & Metabolism* **93**: 4532-4541.

35. Gregor, M. F., L. Yang, E. Fabbrini, B. S. Mohammed, J. C. Eagon, G. S. Hotamisligil, and S. Klein. 2009. Endoplasmic Reticulum Stress Is Reduced in Tissues of Obese Subjects After Weight Loss. *Diabetes* **58**: 693-700.

36. Puri, P., F. Mirshahi, O. Cheung, R. Natarajan, J. W. Maher, J. M. Kellum, and A. J. Sanyal. 2008. Activation and dysregulation of the unfolded protein response in nonalcoholic fatty liver disease. *Gastroenterology* **134**: 568-576.

37. Wang, D., Y. R. Wei, and M. J. Pagliassotti. 2006. Saturated fatty acids promote endoplasmic reticulum stress and liver injury in rats with hepatic steatosis. *Endocrinology* **147**: 943-951.

38. Borradaile, N. M., X. Han, J. D. Harp, S. E. Gale, D. S. Ory, and J. E. Schaffer. 2006. Disruption of endoplasmic reticulum structure and integrity in lipotoxic cell death. *J. Lipid Res.* **47**: 2726-2737.

39. Pineau, L., J. Colas, S. Dupont, L. Beney, P. Fleurat-Lessard, J.-M. Berjeaud, T. Berges, and T. Ferreira. 2009. Lipid-Induced ER Stress: Synergistic Effects of Sterols and Saturated Fatty Acids. *Traffic* **10**: 673-690.

40. Li, Y. K., M. T. Ge, L. Ciani, G. Kuriakose, E. J. Westover, M. Dura, D. F. Covey, J. H. Freed, F. R. Maxfield, J. Lytton, and I. Tabas. 2004. Enrichment of endoplasmic reticulum with cholesterol inhibits sarcoplasmic-endoplasmic reticulum calcium ATPase-

2b activity in parallel with increased order of membrane lipids - Implications for depletion of endoplasmic reticulum calcium stores and apoptosis in cholesterol-loaded macrophages. *J. Biol. Chem.* **279**: 37030-37039.

41. Arndt-Jovin, D. J., and T. M. Jovin. 1989. Fluorescence Labeling and Microscopy of DNA. *Methods in Cell Biology* **30**.

42. Yen, C.-L. E., S. J. Stone, S. Koliwad, C. Harris, and R. V. Farese, Jr. 2008. DGAT enzymes and triacylglycerol biosynthesis. *J. Lipid Res.* **49**: 2283-2301.

43. Cases, S., S. J. Stone, P. Zhou, E. Yen, B. Tow, K. D. Lardizabal, T. Voelker, and R. V. Farese. 2001. Cloning of DGAT2, a second mammalian diacylglycerol acyltransferase, and related family members. *J. Biol. Chem.* **276**: 38870-38876.

44. Lee, J. N., H. Kim, H. Yao, Y. Chen, K. Weng, and J. Ye. 2010. Identification of Ubxd8 protein as a sensor for unsaturated fatty acids and regulator of triglyceride synthesis. *Proceedings of the National Academy of Sciences of the United States of America* **107**: 21424-21429.

45. Henkel, A., and R. M. Green. 2013. The Unfolded Protein Response in Fatty Liver Disease. *Semin. Liver Dis.* **33**: 321-329.

46. Thorn, K., and P. Bergsten. 2010. Fatty Acid-Induced Oxidation and Triglyceride Formation Is Higher in Insulin-Producing MIN6 Cells Exposed to Oleate Compared to Palmitate. *Journal of Cellular Biochemistry* **111**: 497-507.

47. Mantzaris, M. D., E. V. Tsianos, and D. Galaris. 2011. Interruption of triacylglycerol synthesis in the endoplasmic reticulum is the initiating event for saturated fatty acid-induced lipotoxicity in liver cells. *Febs Journal* **278**: 519-530.

48. Volmer, R., K. van der Ploeg, and D. Ron. 2013. Membrane lipid saturation activates endoplasmic reticulum unfolded protein response transducers through their transmembrane domains. *Proceedings of the National Academy of Sciences of the United States of America* **110**: 4628-4633.

49. Lands, W. E. M. 2000. Stories about acyl chains. *Biochimica Et Biophysica Acta-Molecular and Cell Biology of Lipids* **1483**: 1-14.

50. Kennedy, E. P., and S. B. Weiss. 1956. The function of cytidine coenzymes in the biosynthesis of phospholipids. *J. Biol. Chem.* **222**: 193-214.

51. Lands, W. E. M. 1958. Metabolism of glycerolipids: A comparison of lecithin and triglyceride synthesis. *J. Biol. Chem.* **231**: 883-888.

52. Hanahan, D. J. 1954. The site of action of lecinthinase on lecinthin. *J. Biol. Chem.* **207**: 879-884.

53. Yamashita, A., Y. Hayashi, Y. Nemoto-Sasaki, M. Ito, S. Oka, T. Tanikawa, K. Waku, and T. Sugiura. 2014. Acyltransferases and transacylases that determine the fatty acid composition of glycerolipids and the metabolism of bioactive lipid mediators in mammalian cells and model organisms. *Prog. Lipid Res.* **53**: 18-81.

54. Kita, Y., T. Ohto, N. Uozumi, and T. Shimizu. 2006. Biochemical properties and pathophysiological roles of cytosolic phospholipase A(2)s. *Biochimica Et Biophysica Acta-Molecular and Cell Biology of Lipids* **1761**: 1317-1322.

55. Shindou, H., D. Hishikawa, T. Harayama, K. Yuki, and T. Shimizu. 2009. Recent progress on acyl CoA: lysophospholipid acyltransferase research. *J. Lipid Res.* **50**: S46-S51.

56. Hishikawa, D., T. Hashidate, T. Shimizu, and H. Shindou. 2014. Diversity and function of membrane glycerophospholipids generated by the remodeling pathway in mammalian cells. *J. Lipid Res.* **55**: 799-807.

57. Garbarino, J., M. Padamsee, L. Wilcox, P. M. Oelkers, D. D'Ambrosio, K. V. Ruggles, N. Ramsey, O. Jabado, A. Turkish, and S. L. Sturley. 2009. Sterol and Diacylglycerol Acyltransferase Deficiency Triggers Fatty Acid-mediated Cell Death. *J. Biol. Chem.* **284**: 30994-31005.

58. Ruggles, K. V., J. Garbarino, Y. Liu, J. Moon, K. Schneider, A. Henneberry, J. Billheimer, J. S. Millar, D. Marchadier, M. A. Valasek, A. Joblin-Mills, S. Gulati, A. B. Munkacsi, J. J. Repa, D. Rader, and S. L. Sturley. 2014. A Functional, Genome-wide Evaluation of Liposensitive Yeast Identifies the "ARE2 Required for Viability" (ARV1) Gene Product as a Major Component of Eukaryotic Fatty Acid Resistance. *J. Biol. Chem.* **289**: 4417-4431.

59. Shechtman, C. F., A. L. Henneberry, T. A. Seimon, A. H. Tinkelenberg, L. J. Wilcox, E. Lee, M. Fazlollahi, A. B. Munkacsi, H. J. Bussemaker, I. Tabas, and S. L. Sturley. 2011. Loss of Subcellular Lipid Transport Due to ARV1 Deficiency Disrupts Organelle Homeostasis and Activates the Unfolded Protein Response. *J. Biol. Chem.* **286**.

60. Unger, R. H., and P. E. Scherer. 2010. Gluttony, sloth and the metabolic syndrome: a roadmap to lipotoxicity. *Trends in Endocrinology and Metabolism* **21**: 345-352.

61. McGarry, J. D., and R. L. Dobbins. 1999. Fatty acids, lipotoxicity and insulin secretion. *Diabetologia* **42**: 128-138.

CHAPTER 5

PHARMACOLOGICAL STIMULATION OF BETA OXIDATION EXERTS PROTECTIVE EFFECTS AGAINST, BUT DOES NOT FULLY REVERSE, PALMITATE-INDUCED LIPTOXOCITY

Introduction

Free fatty acid induced toxicity is used in *in vitro* hepatic models to recapitulate the lipotoxicity characteristic of obesity, type 2 diabetes and other diseases associated with metabolic syndrome (1-4). Under normal conditions, free fatty acids provide substrate for critical functions in hepatocytes including esterification into triglycerides and phospholipids, oxidation in β-oxidation and as part of signaling pathways and other biochemical pathways. However, during chonic exposure or high-concentration acute exposure, certain free fatty acids can induce hepatocyte dysfunction and death. Specifically, long-chain saturated fatty acids (SFAs) such as palmitate (16:0) and sterate (18:0) are known to induce a pro-apoptotic effect (5-7), while monounsaturated fatty acids (MUFAs) such as oleate (18:1) do not cause apoptosis and actually provide a protective mechanism to detoxify harmful concentrations of SFAs.

The mechanism by which SFAs, but not MUFAs, induce lipoapoptosis is not fully understood. *In vitro* experiments in a variety of cell types, including Chinese hamster ovary (CHO) (8-10), pancreatic beta cells (11, 12) and hepatic cells (6, 13-17), among others, have demonstrated that acute exposure to high concentrations of SFAs is characterized by endoplasmic reticulum (ER) impairment, elevated ROS and eventual apoptosis. In contrast, mono- and poly-unsaturated fatty acids (MUFAs and PUFAs, respectively) induce significant triglyceride (TG) formation but do not initiate apoptosis (6, 9).

Under stress, the ER induces a cascade known as the unfolded protein response (UPR) to mitigate the stress and restore ER homeostasis. SFA overexposure has been shown to rapidly induce this ER stress cascade, including depletion of Ca^{2+} stores from the ER lumen (10, 18) and increased expression levels of CCAAT/enhancer-binding protein homologous protein (CHOP), but evidence of UPR has not been found in cells treated with MUFAs alone (19).

Although there is no definitive mechanism for how SFAs induce ER stress, increasing evidence points to disordered phospholipid metabolism as a key initiating factor. Unsaturated fatty acids are readily incorporated into inert TGs, but excess SFAs remain largely unesterified (6). Recent literature suggests that these free SFAs are rapidly assembled into saturated phospholipid species that are subsequently integrated into ER membrane bilayers (10). The degree of saturation in membrane phospholipids plays an important role in many membrane-associated functions and homeostasis. Atypical accumulations of saturated fatty acids or other species known to have a membrane ordering effect, such as cholesterol (20), can result in deleterious stiffening of organelle membranes and subsequent loss of function (21). Under normal physiological

conditions, the ER membrane is composed mainly of unsaturated phosphatidylcholine (PC) (10, 22) as its major phospholipid component (23). ER membrane composition is tightly monitored such that even seemingly small changes in membrane fluidity can trigger ER stress response mechanisms (i.e., UPR) and dysregulated calcium sequestration (22, 24). Therefore, even limited incorporation of saturated phospholipid species into the membrane lipid bilayer could impair ER function and lead to the ER stress response and signaling that is observed in SFA lipotoxicity.

Alternative pathways of lipid metabolism, such as β-oxidation and TG esterification, may play significant roles in mitigating this response. Long-chain fatty acids, such as palmitate (PA), enter the cell and are immediately transformed into their activated form, long-chain fatty acyl coenzyme-As, by fatty acyl-CoA synthetase. For use as substrates in cellular energy production, long chain fatty acyl-CoAs must be transported into the mitochondria by carnitine palmitoyl transferase 1 (CPT1) and then undergo subsequent β-oxidation. It would seem that overexposure of hepatic cells to SFAs provides a large increase in substrate availability for β-oxidation and stimulation of this cycle may lead to increased downstream ROS production. However, literature reports on the role of β-oxidation in lipotoxicity have been inconclusive, with some studies indicating that it is a major source of ROS (25) while others indicate that ROS overproduction is due to mitochondrial dysfunction resulting from an upstream target of SFA-induced impairment (6). Understanding whether β-oxidation plays a protective or inflammatory role in PA-induced lipotoxicity is important as it may open up a novel method for redirecting PA flux toward an oxidative use and away from other toxic pathways.

In the present study, we sought to examine the effects of modulating the initial steps of lipid metabolism on PA-induced hepatic cell lipoapoptosis in H4IIEC3 rat hepatomas. β-oxidation was stimulated with the AMP-activated protein kinase (AMPK) activator AICAR and inhibited by treatment with the CPT-1 inhibitor etomoxir. The effects of these metabolic modulations on PA-induced cell death were characterized by examining key lipotoxic responses including ROS accumulation, 3/7 caspase activation and cell death. Because we expect that disordered phospholipid metabolism and altered membrane composition plays a critical role in triggering ER stress and the lipoapoptosis cascade, we also measured markers of ER stress and phospholipid composition. Total membrane phospholipid data were used as a proxy for ER phospholipid composition as it is known that the ER constitutes more than half of total membrane in hepatocytes (26, 27). In this study, we demonstrate in our H4IIEC3 hepatic model that PA is rapidly and preferentially incorporated into membrane phospholipids in the absence of alternative pathways of fatty acid metabolism and that this is associated with an increase in markers of ER stress and lipotoxicity. Furthermore, redirecting the fate of PA to an alternative route of lipid metabolism, specifically the β-oxidation pathway, can reduce SFA incorporation into phospholipids and partially reduce markers of ER stress and lipotoxicity, suggesting that modulating lipid metabolism can have a beneficial effect on hepatocytes during SFA overexposure.

Methods

Materials and Reagents

AICAR, etomoxir, palmitic acid, albumin from bovine serum (BSA) and Dulbecco's modified Eagle's medium (DMEM) were all purchased from Sigma-Aldrich (St. Louis, MO). CHOP primary and goat anti-mouse secondary antibodies were purchased from Abcam (Cambridge, MA). β-Actin primary and donkey anti-goat secondary antibodies were procured from Santa Cruz Biotechnology. All other chemicals were purchased from standard commercial sources.

Cell Culture

Rat hepatoma cells, H4IIEC3 (ATCC), were cultured in low glucose DMEM supplemented with 10% fetal bovine serum and 1% penicillin/streptomycin/glutamine (2mM). Measurements were obtained at 70-80% confluency.

ROS Measurement

Intracellular ROS production was measured using 2',7'-dichlorodihydrofluoresceindiacate (H_2DCFDA, Invitrogen) as described previously (28). H_2DCFDA is a non-polar compound that readily passes though the cell membrane where intracellular esterases remove the acetate groups resulting in a non-fluorescent dichlorodihydrofluorescein dye that is strongly retained by the cell. In the presence of ROS production, dichlorodihydrofluorescein is oxidized and becomes highly fluorescent. After indicated treatments were applied to cells cultured in 96-well plates, the medium was removed and cells were washed twice with Hanks' balanced salt solution (HBSS). Cells were then incubated at 37°C for 1 h in the dark in a 10 μM solution of H_2DCFDA in HBSS. The fluorescence intensity was measured at an excitation/emission wavelength of 485/530 nm using a Biotek FL600 microplate analyzer.

Cell viability and toxicity

Toxicity was assessed using the dead cell dye propidium iodide (PI) as described previously (29). PI is an intercalating dye that can only permeate dead cells and becomes highly fluorescent when it is embedded in the double-stranded DNA exposed after cell death. After indicated treatments were applied to cells cultured in 96-well plates, the medium was removed and replaced with a solution of PI and serum-free DMEM. Cells were incubated at 37°C for 4 h in the dark before fluorescence measurement with the microplate analyzer at an excitation/emission wavelength of 530/645.

Caspase Activation

The Apo-ONE Homogenous Caspase 3/7 Assay kit was used to measure markers of apoptotic activation. H4IIEC3 hepatoma cells were cultured in 96-well plates and then incubated with indicated treatments for 6 hours. The Apo-ONE kit uses a lysis buffer combined with a caspase

3/7 specific substrate (Z-DEVD-R110), which becomes fluorescent once these caspases remove its DEVD peptide. Fluorescence was then measured at ex/em of 485/535.

Western Blotting

H4IIEC3 cells were lysed with ice-cold RIPA lysis buffer (sc-24948, Santa Cruz Biotechnology, Inc., Santa Cruz, CA) supplemented with DTT (15 µl/ml) for 30 min on ice. Samples were centrifuged at 13,200 rpm/4°C for 20 min and the resulting supernatants constituted the total protein extracts. Protein concentrations were determined by BCA assay (Thermo Fisher Scientific, Rockford, IL). Samples were added in concentrations of 30 µg/lane for SDS-PAGE Western blotting. Dilutions of the primary antibodies were anti-CHOP (1:1000) and anti-β-actin (1:1000).

Lipid Profiles

Cells seeded in 100-mm Petri dishes at 4×10^6 cells per dish were incubated in standard medium until reaching ~70-80% confluency. Upon reaching this point, they were incubated for the specified duration of time at 37°C in standard medium with or without BSA-bound palmitate and/or oleate (400 µM or 100 µM, respectively) in the presence of indicated chemical modulators. Cells were trypsinized for 3 min then quenched and scraped using cold PBS. Cell solutions were pelleted by centrifugation and resuspended in fresh PBS. Lipid analysis was then provided by the Vanderbilt DRTC Lipid Lab (DK20593) using TLC and GC-FID techniques. Briefly, lipids were extracted from the aforementioned cell pellets using a modified Folch separation. An internal standard (1,2-dipentadecanoyl-sn-glycero-3-phosphocholine) for phospholipids was added to the lipid-containing chloroform phase. Total lipids were then extracted and separated by thin layer chromatography using petroleum ether/ethyl ether/acetic acid (80/20/1, v/v/v) on silica TLC plates. Spots corresponding to PLs, TGs and FFAs were visualized with rhodamine 6G in 95% ethanol and scraped individually into glass tubes for methylation. Methylation was completed using a boron trifluoride-methanol 10% (w/w) solution. Transmethylated lipids were then analyzed using GC-FID, where standardized calibration curves were used to assess the lipid content.

β-Oxidation Measurements

Cell cultures fed tritiated fatty acid produce ^3H_2O at a rate proportional to that of mitochondrial beta oxidation (30). Albumin-bound [9,10-^{3}H(N)] palmitic acid (4 µCi ^{3}H/µmol palmitate) was added to cells grown to confluency in 6-well dishes at 400 µM. The final volume of media solution, including inhibitors/activators and palmitate, was adjusted to exactly 2 mL per well. After 6 hours of incubation, 1.5 mL of media was removed directly from each well and collected in individual round-bottom snap-top tubes. Then 75 µL of 60% perchloric acid was added to each sample for deproteinization to remove albumin-bound un-oxidized PA from the sample media. The deproteinization reaction continued overnight at 4°C.

Following deproteinization, samples were centrifuged for 30 min. Then 1.2 mL of sample was collected into a new centrifuge tube and 5 μL of pH indicator dye and 36 μL of 5M K_2CO_3 were added for neutralization. This reaction was allowed to continue overnight at 4°C. After neutralization, samples were centrifuged for 30 min. To remove remaining PA, 0.8 ml of neutralized sample was applied to an individual AG 1-X8 Resin (BioRad, Hercules, CA) column and the column was allowed to empty under gravity flow. Each column was flushed twice with 0.6 mL of distilled water. The initial charge (0.8 ml) and all subsequent washes (1.2 ml) were collected in a scintillation vial (PerkinElmer, Waltham, MA). 10 mL of EcoLite scintillation cocktail fluid (MP Biomedical, Santa Ana, CA) was added to each sample vial, shaken vigorously and read in a scintillation counter.

Statistical Analysis

Data from fluorescence plate readers were converted to mean ± S. E. Student's t-test was used to determine statistical differences between two samples ($p < 0.05$). Statistical differences between multiple treatments were assessed using Type I ANOVA with Tukey-Kramer *post hoc* testing.

Results

ROS accumulation and apoptotic cell death characterize H4IIEC3 liver cell exposure to PA treatment

We examined the lipotoxic effects of varying PA concentrations on H4IIEC3 hepatomas using the fluorescent stain propidium iodide to quantify cell death at 24 hours. Cell death increased in a concentration-dependent manner (Fig. 5-1A), and a concentration of 400 μM PA was found to significantly increase cell death while remaining within a physiologically acceptable range (31). PA-induced cell death was primarily due to apoptosis as indicated by increased caspase 3/7 activity as early as 6 h (Fig. 5-1B), which also varied with PA in a concentration-dependent manner (Fig. 5-1C). ROS accumulation peaked at 6 hours, after which time it began to decrease presumably due to increases in cell death (Fig. 5-1D).

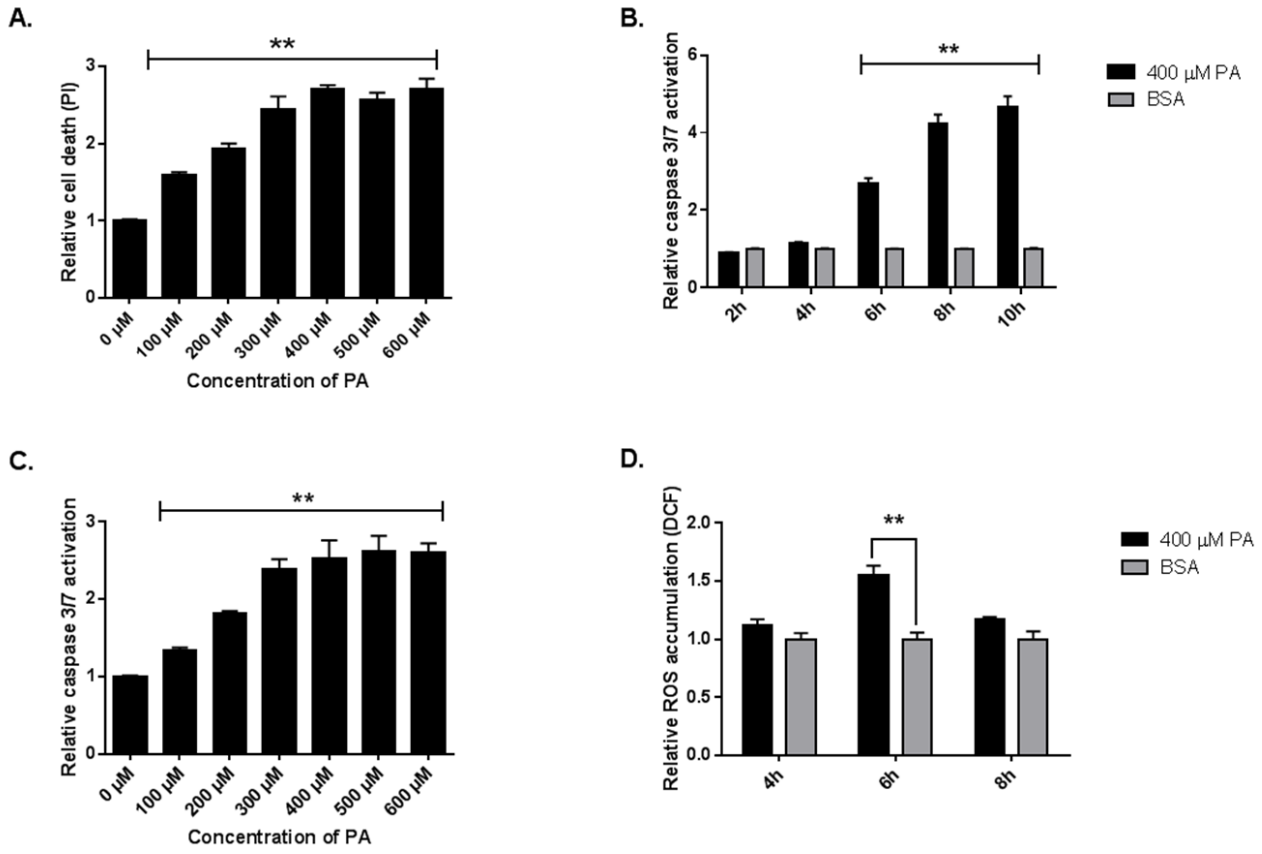

Figure 5-1. PA-induced cell death, caspase activation and ROS accumulation in H4IIEC3 cells. A, H4IIEC3 cells were treated with increasing concentrations of PA for 24 h. Cell toxicity was assessed using the fluorescent dye propidium iodide (PI). **B**, Caspase 3/7 was activated in a time-dependent manner starting at 6 h as measured by the Apo-ONE kit. **C**, At 6 h, caspase 3/7 demonstrated a PA concentration-dependent activation as measured by the Apo-ONE kit. **D**, ROS accumulation also displayed time dependency, peaking at 6 h and falling off quickly thereafter. ROS was measured using the fluorescent probe H_2DCFDA. All data represent mean ± SE of n=4. *, P<0.05; **, P<0.01 vs. cells treated with BSA alone.

Enhanced fatty acid oxidation prevents PA-induced cell death and ROS accumulation in liver cells.

The impact of β-oxidation in hepatic oxidative stress and lipotoxicity remains disputed (6, 25), and the molecular mechanism defining its role has yet to be fully elucidated. However, data from studies in β-cells indicate that increased fatty acid oxidation (FAO) may serve a protective role in PA-induced lipotoxicity. Pharmacological inhibition of FAO with etomoxir (32) or siRNA-mediated knockdown of CPT-1 (12) augmented PA-induced cell death, while genetic CPT-1 overexpression reduced the lipotoxic effects of PA (33). Therefore, we sought to investigate the

effects of modulating FAO on PA-induced cell death. Etomoxir (Eto) is a specific inhibitor of CPT-1 and, consequently, of mitochondrial fatty acid β-oxidation (34). The AMP kinase activator 5-aminoimidazole-4-carboxamide-1-β-D-ribofuranoside (AICAR) has been used previously as a stimulant of FAO (10, 35). The pharmacologic modulation of FAO with Eto and AICAR was directly determined by measuring H^3-labeled water produced from H^3-labeled PA. FAO stimulation with 500 μM AICAR doubled the oxidation rate of PA while 250 μM Eto significantly decreased the rate of FAO (Fig. 5-2A). Eto treatment was also able to effectively block the FAO stimulation provided by AICAR, reducing the oxidative rate of the combined AICAR+Eto+PA treatment down to the level Eto+PA alone (Fig. 5-2A). These data demonstrated that AICAR and Eto were able to positively and negatively modulate the rate of PA oxidation, respectively.

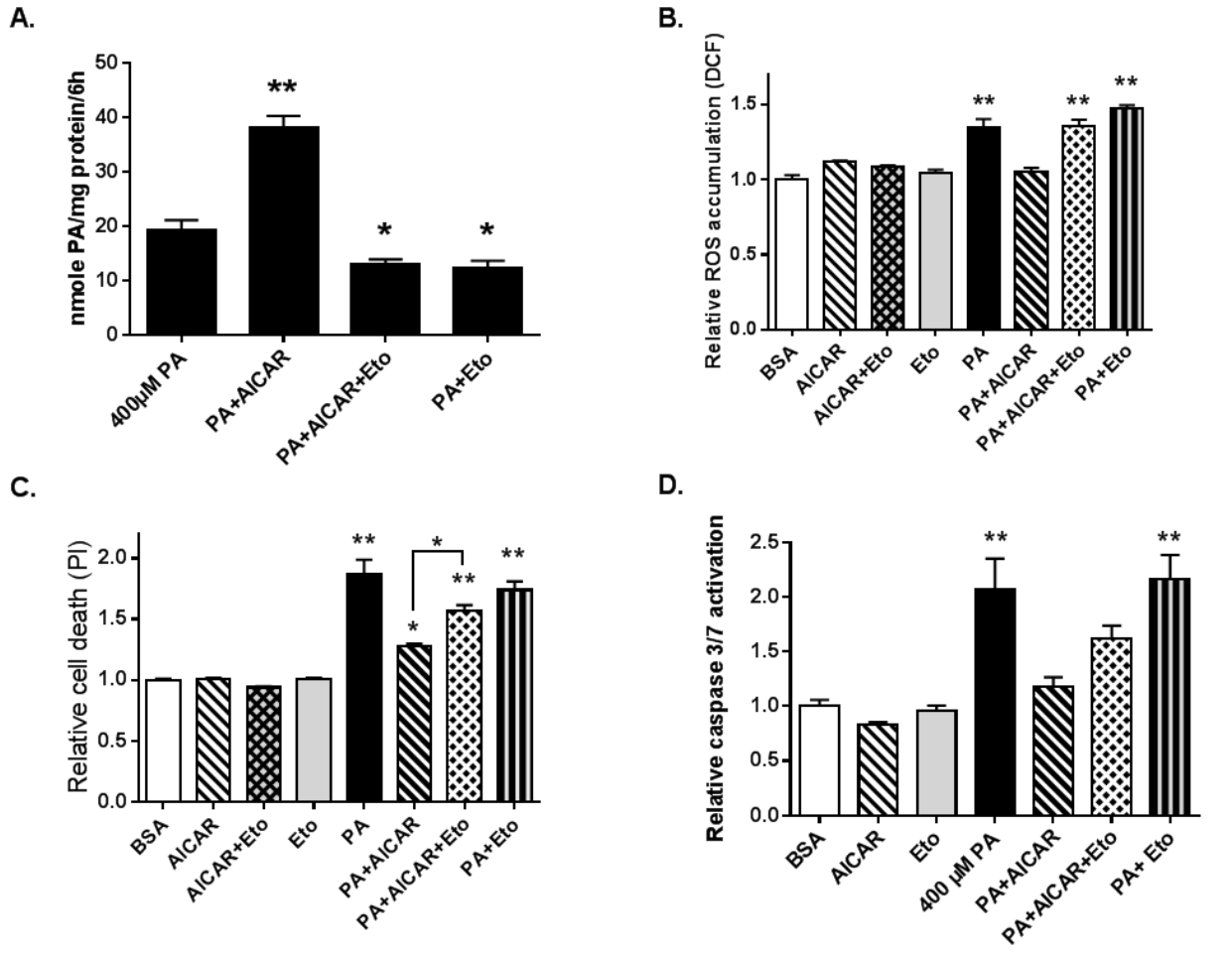

Figure 5-2. Enhancing mitochondrial β-oxidation reduces lipotoxicity while inhibiting β-oxidation has no positive effects on the PA-induced phenotype. **A**, H4IIEC3 were treated with 400 μM ^{3}H-PA with or without 500 μM AICAR and/or 250 μM etomoxir (Eto) for 6 h. PA oxidation rate was determined by the measurement of $^{3}H_2O$ produced. Data represent mean ± SE from thee independent experiments. *, P<0.05, **, P<0.01 vs cells treated with PA; **B**, PA-induced ROS accumulation at 6 h with AICAR and/or Eto co-treatment as measured by H_2DCFDA. **C**, After 24 h, the effect of modulating β-oxidation on cell toxicity with AICAR and/or Eto was assessed by PI. **D**, Caspase 3/7 activation after 6 h of treatment was measured with the Apo-ONE kit. B-D data represent mean ± SE of n=4. *, P<0.05 vs BSA; **, P<0.01 vs BSA.

We then examined the question of whether modulating FAO could affect PA-induced lipotoxic responses including ROS accumulation, caspase activation and cell death. Treatment with AICAR significantly reduced all three of these markers of lipoapoptosis; ROS accumulation and caspase 3/7 returned to vehicle-treated levels (Fig. 5-2B and D, respectively) and, correspondingly, there was a significant reduction in cell death at 24 hs (Fig. 5-2C). On the other

hand, Eto co-treatment had no effect on ROS accumulation (Fig. 5-3B), caspase activation (Fig. 5-2D) or cell death (Fig. 5-2C). These data suggest that FAO inhibition may play a role in PA-induced lipotoxicity and stimulation of this pathway could provide a protective effect in this setting. Surprisingly, however, Eto only partially reversed AICAR-induced protective effects on PA-mediated caspase activation (Fig. 5-2D) and cell death (Fig. 5-2C), in constrast to its ability to completely inhibit PA oxidation rate as described in Fig. 5-2A. This indicates that although AICAR significantly increases FAO in the presence of PA, its protective effects on PA-induced lipoapoptosis may be partially mediated by other off-target effects.

PA treatment results in increased phospholipid saturation and ER stress

ER stress has been implicated as a critical moderator in the PA-induced lipoapoptotic cascade (10, 18, 19). Increased saturation of the ER membrane has also been postulated as a possible cause of PA-mediated ER stress (10, 36). Therefore, we sought to investigate the effect of PA treatment on the cellular phospholipid composition and changes in levels of CHOP, a proapoptotic protein up-regulated during the ER stress response. Previous work has shown that the intensity of CHOP expression increased in a concentration dependent manner (16), similar to the increases in cell death associated with changes in PA concentration described in Fig. 5-1. Based on a time course of increases in CHOP protein level (16), 8 h was determined as an optimal point for assessing the differences in ER stress due to PA-induced lipotoxicity. At this time point, H4IIEC3 cells treated with PA demonstrated significantly increased levels of CHOP indicating that cells were experiencing significant up-regulation of UPR in response to PA treatment alone and confirming that ER stress is involved in the PA-induced lipotoxic cascade.

We then sought to assess the consequences of PA treatment on phospholipid composition, as this has been hypothesized to be an important contributing factor to PA-induced ER stress (37) and subsequent lipotoxicity (10, 36). The relative percentage of saturated acyl chain substituents on phospholipids was found to increase significantly within 1 h of exogenous PA treatment. The increase in total percent PA (16:0) chains on cellular phospholipids was especially striking; there was over 50% increase in PA incorporation into phospholipids in the PA- versus control-treated cells within the first hour (Fig. 5-3A). This trend was further exaggerated after a 24-h incubation with PA. Cells supplemented with 400 μM PA contained ~75% more saturated fatty acid motieties than BSA control-treated cells; the proportion of PA contained in phospholipids was more than 3-fold higher in PA- versus control- treated cells (Fig. 5-3B). These data indicate that exogenous PA was rapidly incorporated into cellular phospholipids resulting in increased saturation of these species in H4IIEC3 cells treated with 400μM PA.

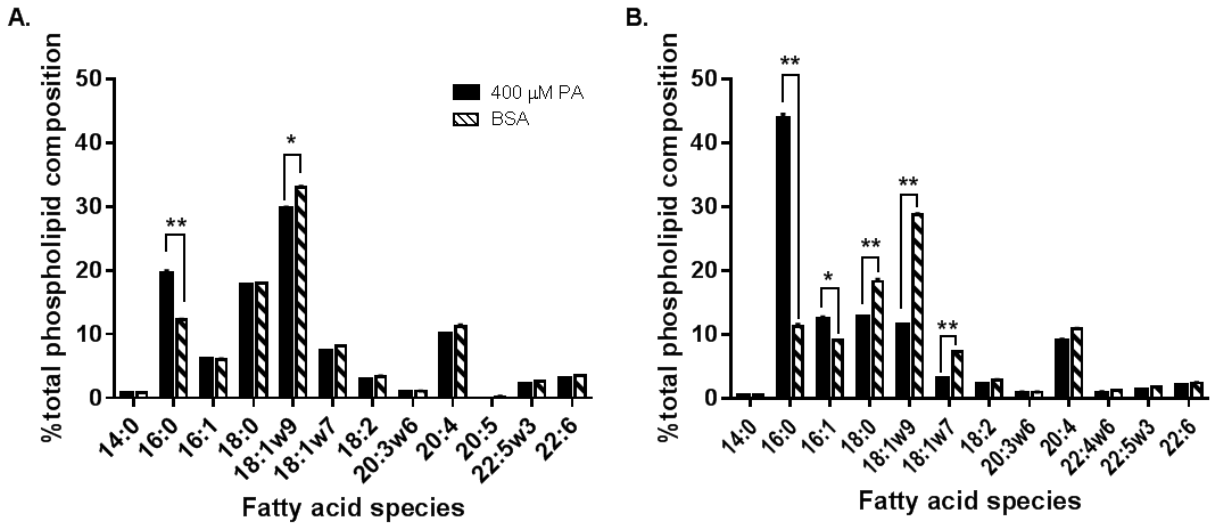

Figure 5-3. PA treatment rapidly alters phospholipid composition after 1 h and continues to increase after 24h. H4IIEC3 were treated with 400 μM PA or BSA for 1 h (A) and 24h (B) and phospholipid composition was subsequently determined using thin layer chromatography, FAME esterification and GC-FID. Data represent mean ± SE from n=4. *, P<0.05; **, P<0.01 vs cells treated with BSA.

Increased fatty acid oxidation significantly reduces PA-induced ER stress and incorporation of SFAs into phospholipids

We sought to determine if modulating catabolism of fatty acids though β-oxidation would result in changes in phospholipid composition. As described above, AICAR and etomoxir were used to stimulate and suppress, respectively, rates of mitochondrial β-oxidation. Phospholipid composition was subsequently determined at 1 and 24h, and CHOP expression levels were analyzed at 8h post-treatment. As shown in Table 5-1, PA was rapidly incorporated into phospholipids resulting in an over 1.5-fold increase in PA-containing species compared to vehicle-treated controls after just 1 h of PA treatment. The overall saturation of phospholipids was also increased after only 1 h of incubation time. In this time frame, AICAR significantly reduced PA-induced increases in both %PA composition (~20%) and total saturation of phospholipids (~35%) with respect to control BSA levels (Table 5-1). Etomoxir treatment alone had no effect on fatty acid composition of phospholipids but partially reversed the effectiveness of AICAR administration. A similar trend held after 24h of incubation: PA treatment resulted in large increases in both PA incorporation and overall phospholipid saturation while supplementing cells with AICAR significantly reduced both markers of lipotoxicity. Etomoxir alone had no statistically significant effect on either of these factors (Table 5-2), but co-

administration of AICAR and etomoxir with PA treatment partially reversed the rescue effects imparted by AICAR. Similarly, ER stress at 8h was significantly reduced by AICAR treatment, as assessed by western blotting of CHOP expression levels (Fig. 5-4). As with phospholipid composition, etomoxir alone had no significant effect on CHOP expression levels, but co-treatment of AICAR+Eto served to partially reverse the rescuing effect of AICAR on PA-induced ER stress.

Fatty Acid	PA	PA+AICAR	PA+AICAR+ Eto	PA+Eto	BSA
14:0	0.71 ± 0.06	0.74 ± 0.05	0.74 ± 0.05	0.61 ± 0.03	0.81 ± 0.02[a]
16:0	19.52 ± 0.42	17.94 ± 0.32[a]	19.08 ± 0.28[b]	19.23 ± 0.15	12.25 ± 0.12[a]
16:1	6.09 ± 0.15	8.00 ± 0.32[a]	7.36 ± 0.27[a]	6.63 ± 0.25	6.02 ± 0.13
18:0	17.63 ± 0.16	16.65 ± 0.28[a]	16.74 ± 0.26[a]	17.26 ± 0.19	17.94 ± 0.09
18:1w9	29.75 ± 0.17	30.85 ± 0.44	31.10 ± 0.27[a]	31.07 ± 0.48	33.01 ± 0.16[a]
18:1w7	7.30 ± 0.08	7.20 ± 0.05	7.26 ± 0.09	7.34 ± 0.10	8.10 ± 0.01[a]
18:2	2.87 ± 0.09	2.71 ± 0.10	2.55 ± 0.02	2.59 ± 0.17	3.39 ± 0.06[a]
20:3w6	0.98 ± 0.02	1.07 ± 0.01[a]	1.01 ± 0.01[b]	0.95 ± 0.01	1.09 ± 0.01[a]
20:4	9.92 ± 0.19	9.97 ± 0.25	9.63 ± 0.06	9.46 ± 0.15	11.21 ± 0.21[a]
20:5	0.00 ± 0.00	0.00 ± 0.00	0.00 ± 0.00	0.23 ± 0.13	0.14 ± 0.14[a]
22:5w3	2.20 ± 0.03	2.02 ± 0.13	1.84 ± 0.03[a]	1.89 ± 0.10[a]	2.57 ± 0.06
22:6	3.01 ± 0.04	2.84 ± 0.12	2.68 ± 0.06[a]	2.74 ± 0.10	3.47 ± 0.07[a]
% SFA	37.87 ± 0.64	35.33 ± 0.65[a]	36.56 ± 0.03[a,b]	37.10 ± 0.36	31.01 ± 0.23[a]
% UFA	62.13 ± 0.78	64.67 ± 1.42[a]	63.44 ± 0.03[a,b]	62.90 ± 1.35	68.99 ± 0.71[a]

Table 5-1. Phospholipid composition of cells treated with PA with or without AICAR and/or etomoxir after 1 h. H4IIEC3 cells were incubated with 400 μM PA with or without 500 μM AICAR and/or 250 μM etomoxir (Eto) for 1 h. Phospholipids were separated by thin layer chromatography and analyzed by gas chromatography-flame ionization detection (GC-FID). Data represent mean ± SE of n=4. [a], $p<0.05$ vs cells treated with PA alone; [b], $p<0.05$ vs cells treated with PA+AICAR.

Fatty Acid	PA	PA+AICAR	PA+AICAR+ Eto	PA+Eto	BSA
14:0	0.63± 0.04	0.42± 0.02[a]	0.16± 0.16	0.21± 0.21	0.34± 0.03[a]
16:0	46.10± 1.76	38.78± 0.37[a]	40.07± 0.72[a]	41.13± 0.29	9.01± 0.24[a]
16:1	12.40± 1.33	17.09± 0.42[a]	9.69± 0.80[b]	7.30± 0.60[a]	5.76± 0.19[a]
18:0	14.81± 0.19	11.87± 0.28[a]	16.08± 0.44[b]	18.53± 0.38[a]	20.94± 0.14[a]
18:1w9	11.17± 0.23	13.64± 0.16[a]	13.78± 0.39[a]	12.84± 0.26[a]	36.68± 0.09[a]
18:1w7	3.17± 0.06	3.06± 0.04	3.68± 0.05[a,b]	3.79± 0.08[a]	8.46± 0.07[a]
18:2	1.86± 0.05	2.31± 0.03[a]	2.08± 0.02[a,b]	1.94± 0.03	2.79± 0.03[a]
20:3w6	0.77± 0.02	0.90± 0.01[a]	0.29± 0.29	0.33± 0.33	1.05± 0.02[a]
20:4	6.34± 0.06	7.75± 0.08[a]	9.84± 0.67[a]	9.39± 0.47[a]	9.34± 0.19[a]
20:5	0.00± 0.00	0.00± 0.00[a]	0.00± 0.00	0.00± 0.00	0.49± 0.01[a]
22:4w6	0.00± 0.00	0.57± 0.01[a]	0.00± 0.00[b]	0.00± 0.00	0.68± 0.02[a]
22:5w3	1.02± 0.05	1.50± 0.02[a]	1.63± 0.11[a]	1.78± 0.10[a]	1.69± 0.05[a]
22:6	1.72± 0.05	2.30± 0.05[a]	2.68± 0.16[a]	2.76± 0.14[a]	2.76± 0.09[a]
% SFA	61.55± 1.64	51.07± 0.32[a]	56.32± 0.16[a,b]	59.87± 0.18	30.29± 0.16[a]
% UFA	38.45± 1.64	48.93± 0.32[a]	43.68± 0.16[a,b]	40.13± 0.18	69.71± 0.16[a]

Table 5-2. Phospholipid composition of cells treated with PA with or without AICAR and/or etomoxir for 24 h. H4IIEC3 cells were incubated with 400 μM PA with or without 500 μM AICAR and/or 250 μM etomoxir (Eto) for 24 h. Phospholipids were separated by thin layer chromatography and analyzed by gas chromatography-flame ionization detection (GC-FID). Data represent mean ± SE of n=4. [a], $p<0.05$ vs cells treated with PA alone; [b], $p<0.05$ vs cells treated with PA+AICAR.

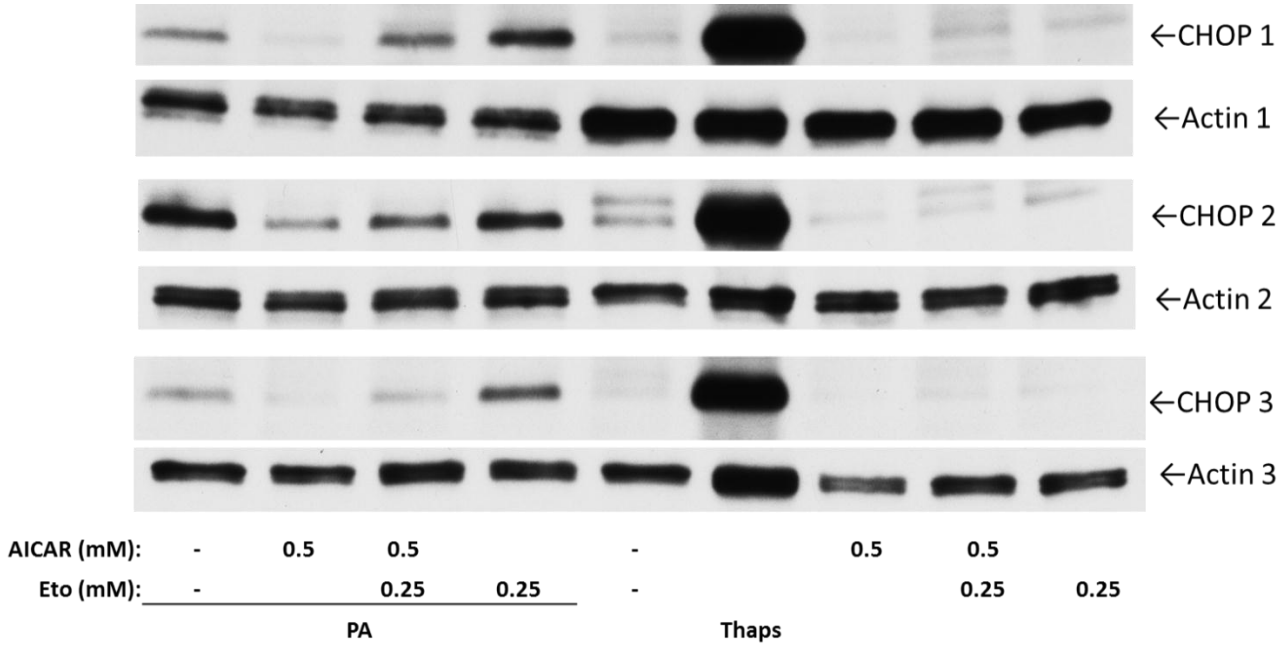

Figure 5-4. Stimulation of β-oxidation in PA-treated H4IIEC3 cells reduces CHOP expression, a marker of ER stress. PA-induced increases in CHOP abundance were reversed by increasing β-oxidation with AICAR but inhibiting PA oxidation with Eto had no positive effect on CHOP expression. H4IIEC3 hepatocytes were treated with 400 μM PA alone or in the presence of 500 μM AICAR and/or 250 μM Eto for 8 h in three independent experiments. Levels of CHOP abundance were assessed using Western blotting techniques. Thapsigargin (Thaps) was used as a positive control.

Discussion

This study was designed to examine the effect that modulating β-oxidation has on PA-induced hepatic lipoapoptosis. Stimulation of the fatty acid β-oxidation pathway by the AMPK agonist AICAR served to significantly reduce PA-induced H4IIEC3 ROS accumulation and apoptotic cell death. Inhibition of β-oxidation by the CPT-1 specific inhibitor etomoxir had no effect on PA-promoted ROS accumulation and cell apoptosis. These data suggest that PA-induced lipotoxicity can be regulated by modulating rates of FFA disposal though alternative routes of lipid metabolism such as β-oxidation.

We investigated how modifications in lipid metabolism affect PA-induced UPR activation because ER stress has been shown to be a key mediator in the lipoapoptosis cascade (10, 18, 19). Borradaile et al. postulated a connection between ER stress and degree of fatty acid saturation in the membrane of CHO cells, implicating this connection as a potentially critical mediator of SFA-induced lipotoxicity (10). In their experimental model, PA was rapidly incorporated into saturated phospholipids and TGs resulting in drastic dilatation and disruption of the ER structure and loss of functional integrity. Markers of ER impairment have been shown as early as 30 minutes post-PA treatment (10) while our data indicates that significant increases in ROS

accumulation does not occur until at least 6 h after PA supplementation. Additionally, previous TEM images from our lab (16) show changes in ER structure at 4 h in response to PA while there are no significant changes in mitochondrial structure. These data suggest that SFA incorporation into the ER membrane is a key event initiating ER impairment and stress connected to the subsequent lipotoxic cascade and was not just a by-product of downstream events such as oxidative stress (e.g., ROS production). Other studies have also indicated that ER stress in hepatic models of lipotoxicity precedes apoptosis, indicating that disruption of ER function plays an early and key role in SFA overload (38), and this ER response is mediated by changes in membrane phospholipid saturation (10, 36). Therefore, understanding the partitioning of PA into specific lipid classes may better elucidate the mechanism by which SFAs induce ER stress and subsequent lipoapoptosis. Therefore, we examined the effect of lipid metabolism on both ER stress and fatty acid composition of cellular phospholipids. PA treatment alone progressively augmented expression levels of the ER stress marker CHOP and total phospholipid saturation as incubation time increased (Fig 5-4 and Tables 5-1 and 5-2).

Our study indicates that stimulation of mitochondrial β-oxidation can significantly prevent increases in phospholipid saturation and reduce CHOP expression levels in response to PA treatment. Consistent with previous studies, AICAR-mediated stimulation of β-oxidation prevented PA-induced lipoapoptosis (10, 32, 35, 39) and ER stress (10) (Fig. 5-2). We expanded upon these observations by demonstrating that increasing the partitioning of PA towards β-oxidation resulted in a significant reduction in PA content in membrane phospholipids (Tables 5-1 and 5-2). In contrast, inhibition of β-oxidation with etomoxir had no effect on PA-mediated increases in CHOP expression or overall membrane phospholipid saturation. Curiously, although etomoxir completely repressed AICAR-mediated stimulation of β-oxidation, etomoxir did not fully block AICAR's ability to suppress phospholipid alterations or CHOP expression. This may be the result of AMPK's effects on other pathways besides beta-oxidation and/or non-AMPK-dependent effects of AICAR. Previous research has demonstrated that either AICAR-stimulated or constitutively activated AMPK can alleviate lipid-induced ER stress and lipoapoptosis though AMPK-induced expression of the ER-associated chaperone, 150-kDA oxygen regulated protein (ORP150) (40). Other groups have also found that AICAR mediates inhibition of phospholipid synthesis which is independent of AMPK activation (41, 42). Therefore, these off-target effects may be partially responsible for AICAR's ability to rescue palmitate lipotoxicity.

In summary, this study indicates that alterations in lipid metabolism can modulate PA-induced markers of lipotoxicity as well as ER stress response and phospholipid composition/saturation. We also found that these changes appear to be positively correlated. For example, reduced PA incorporation into phospholipids was accompanied by diminished CHOP expression and reversal of PA-induced ROS accumulation, caspase activation and cell death. While it is not possible from these data to eliminate a concomitant effect of PA directly on the mitochondria, another key organelle implicated in lipotoxicity, our data indicate that the impact of initial SFA metabolism

on the ER is a critical mediator in this phenotype. Our results, combined with consistent data from other studies, suggest that perturbations in lipid metabolism resulting from SFA overexposure initiate a potent cellular death signal that originates at the ER and involves functional impairments of this important organelle. This study demonstrates that modulating specific pathways of lipid metabolism can have beneficial effects on the response of hepatic cells to SFA overexposure and may point towards therapeutic strategies for improving hepatocyte function under these conditions. In particular, interventions designed to increase oxidative metabolism of free fatty acids through β-oxidation in clinical applications may represent an important treatment option for patients.

References

1. Schaffer, J. E. 2003. Lipotoxicity: when tissues overeat. *Current Opinion in Lipidology* **14**: 281-287.

2. Unger, R. H. 2002. Lipotoxic diseases. *Annual Review of Medicine* **53**: 319-336.

3. Cazanave, S. C., and G. J. Gores. 2010. Mechanisms and clinical implications of hepatocyte lipoapoptosis. *Clinical Lipidology* **5**: 71-85.

4. Feldstein, A. E., A. Canbay, P. Angulo, M. Taniai, L. J. Burgart, K. D. Lindor, and G. J. Gores. 2003. Hepatocyte apoptosis and Fas expression are prominent features of human nonalcoholic steatohepatitis. *Gastroenterology* **125**: 437-443.

5. Cazanave, S. C., and G. J. Gores. 2010. Mechanisms and clinical implications of hepatocyte lipoapoptosis. *Clinical Lipidology* **5**.

6. Noguchi, Y., J. D. Young, J. O. Aleman, M. E. Hansen, J. K. Kelleher, and G. Stephanopoulos. 2009. Effect of Anaplerotic Fluxes and Amino Acid Availability on Hepatic Lipoapoptosis. *J. Biol. Chem.* **284**: 33425-33436.

7. Li, Z. Z., M. Berk, T. M. McIntyre, and A. E. Feldstein. 2009. Hepatic Lipid Partitioning and Liver Damage in Nonalcoholic Fatty Liver Disease - Role of stearoyl-CoA desaturase. *J. Biol. Chem.* **284**: 5637-5644.

8. Listenberger, L. L., D. S. Ory, and J. E. Schaffer. 2001. Palmitate-induced apoptosis can occur through a ceramide-independent pathway. *J. Biol. Chem.* **276**: 14890-14895.

9. Listenberger, L. L., X. L. Han, S. E. Lewis, S. Cases, R. V. Farese, D. S. Ory, and J. E. Schaffer. 2003. Triglyceride accumulation protects against fatty acid-induced lipotoxicity. *Proceedings of the National Academy of Sciences of the United States of America* **100**: 3077-3082.

10. Borradaile, N. M., X. Han, J. D. Harp, S. E. Gale, D. S. Ory, and J. E. Schaffer. 2006. Disruption of endoplasmic reticulum structure and integrity in lipotoxic cell death. *J. Lipid Res.* **47**: 2726-2737.

11. Busch, A. K., E. Gurisik, D. V. Cordery, M. Sudlow, G. S. Denyer, D. R. Laybutt, W. E. Hughes, and T. J. Biden. 2005. Increased fatty acid desaturation and enhanced expression of stearoyl coenzyme A desaturase protects pancreatic beta-cells from lipoapoptosis. *Diabetes* **54**: 2917-2924.

12. Choi, S.-E., I.-R. Jung, Y.-J. Lee, S.-J. Lee, J.-H. Lee, Y. Kim, H.-S. Jun, K.-W. Lee, C. B. Park, and Y. Kang. 2011. Stimulation of Lipogenesis as Well as Fatty Acid Oxidation Protects against Palmitate-Induced INS-1 beta-Cell Death. *Endocrinology* **152**: 816-827.

13. Wei, Y., D. Wang, F. Topczewski, and M. J. Pagliassotti. 2006. Saturated fatty acids induce endoplasmic reticulum stress and apoptosis independently of ceramide in liver cells. *Am. J. Physiol.-Endocrinol. Metab.* **291**: E275-E281.

14. Srivastava, S., and C. Chan. 2008. Application of metabolic flux analysis to identify the mechanisms of free fatty acid toxicity to human hepatoma cell line. *Biotechnology and Bioengineering* **99**: 399-410.

15. Pagliassotti, M., Y. R. Wei, and D. Wang. 2005. Saturated fatty acids induce cytotoxicity in hepatocytes via effects on the endoplasmic reticulum. *Obesity Research* **13**: A31-A31.

16. Leamy, A. K., R. A. Egnatchik, M. Shiota, P. T. Ivanova, D. S. Myers, H. A. Brown, and J. D. Young. 2014. Enhanced synthesis of saturated phospholipids is associated with ER stress and lipotoxicity in palmitate-treated hepatic cells. *J. Lipid Res.* **55**: 1478-1488.

17. Egnatchik, R. A., A. K. Leamy, Y. Noguchi, M. Shiota, and J. D. Young. 2014. Palmitate-induced Activation of Mitochondrial Metabolism Promotes Oxidative Stress and Apoptosis in H4IIEC3 Rat Hepatocytes. *Metabolism-Clinical and Experimental* **63**: 283-295.

18. Wei, Y., D. Wang, C. L. Gentile, and M. J. Pagliassotti. 2009. Reduced endoplasmic reticulum luminal calcium links saturated fatty acid-mediated endoplasmic reticulum stress and cell death in liver cells. *Molecular and Cellular Biochemistry* **331**: 31-40.

19. Pfaffenbach, K. T., C. L. Gentile, A. M. Nivala, D. Wang, Y. R. Wei, and M. J. Pagliassotti. 2010. Linking endoplasmic reticulum stress to cell death in hepatocytes: roles of C/EBP homologous protein and chemical chaperones in palmitate-mediated cell death. *Am. J. Physiol.-Endocrinol. Metab.* **298**: E1027-E1035.

20. Li, Y. K., M. T. Ge, L. Ciani, G. Kuriakose, E. J. Westover, M. Dura, D. F. Covey, J. H. Freed, F. R. Maxfield, J. Lytton, and I. Tabas. 2004. Enrichment of endoplasmic reticulum with cholesterol inhibits sarcoplasmic-endoplasmic reticulum calcium ATPase-2b activity in parallel with increased order of membrane lipids - Implications for depletion of endoplasmic reticulum calcium stores and apoptosis in cholesterol-loaded macrophages. *J. Biol. Chem.* **279**: 37030-37039.

21. Spector, A. A., and M. A. Yorek. 1985. Membrane lipid-Composition and cellular function. *J. Lipid Res.* **26**: 1015-1035.

22. Deguil, J., L. Pineau, E. C. R. Snyder, S. Dupont, L. Beney, A. Gil, G. Frapper, and T. Ferreira. 2011. Modulation of Lipid-Induced ER Stress by Fatty Acid Shape. *Traffic* **12**: 349-362.

23. Van der Sanden, M. H. M., M. Houweling, L. M. G. Van Golde, and A. B. Vaandrager. 2003. Inhibition of phosphatidylcholine synthesis induces expression of the endoplasmic reticulum stress and apoptosis-related protein CCAAT/enhancer-binding protein-homologous protein (CHOP/GADD153). *Biochemical Journal* **369**: 643-650.

24. Ron, D., and P. Walter. 2007. Signal integration in the endoplasmic reticulum unfolded protein response. *Nature Reviews Molecular Cell Biology* **8**: 519-529.

25. Nakamura, S., T. Takamura, N. Matsuzawa-Nagata, H. Takayama, H. Misu, H. Noda, S. Nabemoto, S. Kurita, T. Ota, H. Ando, K.-i. Miyamoto, and S. Kaneko. 2009. Palmitate Induces Insulin Resistance in H4IIEC3 Hepatocytes through Reactive Oxygen Species Produced by Mitochondria. *J. Biol. Chem.* **284**: 14809-14818.

26. Alberts, B., A. Johnson, J. Lewis, M. Raff, K. Roberts, and P. Walter. 2002. The Endoplasmic Reticulum. *In* Molecular Biology of the Cell. Garland Science, New York City.

27. Seth, G., P. Hossler, J. C. Yee, and W.-S. Hu. 2006. Engineering cells for cell culture bioprocessing - Physiological fundamentals. *Cell Culture Engineering* **101**.

28. Eruslanov, E., and S. Kusmartsev. 2010. Identification of ROS Using Oxidized DCFDA and Flow-Cytometry. *Advanced Protocols in Oxidative Stress II* **594**.

29. Arndt-Jovin, D. J., and T. M. Jovin. 1989. Fluorescence Labeling and Microscopy of DNA. *Methods in Cell Biology* **30**.

30. Egnatchik, R., A. Leamy, D. Jacobson, M. Shiota, and J. Young. 2014. ER calcium release promotes mitochondrial dysfunction and hepatic cell lipotoxicity in response to palmitate overload. *Molecular Metabolism* **3**: 544-553.

31. Donnelly, K. L., C. I. Smith, S. J. Schwarzenberg, J. Jessurun, M. D. Boldt, and E. J. Parks. 2005. Sources of fatty acids stored in liver and secreted via lipoproteins in patients with nonalcoholic fatty liver disease. *J. Clin. Invest.* **115**.

32. El-Assaad, W., J. Buteau, M. L. Peyot, C. Nolan, R. Roduit, S. Hardy, E. Joly, G. Dbaibo, L. Rosenberg, and M. Prentki. 2003. Saturated fatty acids synergize with elevated glucose to cause pancreatic beta-cell death. *Endocrinology* **144**.

33. Sol, E. r. M., E. Sargsyan, G. Akusjaervi, and P. Bergsten. 2008. Glucolipotoxicity in INS-1E cells is counteracted by carnitine palmitoyltransferase 1 over-expression. *Biochem. Biophys. Res. Commun.* **375**.

34. Weis, B. C., A. T. Cowan, N. Brown, D. W. Foster, and J. D. McGarry. 1994. Use of a selective inhibitor of liver carnitine palmitoyltransferase-I (CPT-I) allows quantification if its contribution to total CPT-1 activity in rat-heat - Evidence that the dominant cardiac CPT-1 isoform is identical to the skeletal muscle enzyme. *J. Biol. Chem.* **269**: 26443-26448.

35. Hardy, S., W. El-Assaad, E. Przybytkowski, E. Joly, M. Prentki, and Y. Langelier. 2003. Saturated fatty acid-induced apoptosis in MDA-MB-231 breast cancer cells - A role for cardiolipin. *J. Biol. Chem.* **278**: 31861-31870.

36. Ariyama, H., N. Kono, S. Matsuda, T. Inoue, and H. Arai. 2010. Decrease in Membrane Phospholipid Unsaturation Induces Unfolded Protein Response. *J. Biol. Chem.* **285**: 22027-22035.

37. Fagone, P., and S. Jackowski. 2009. Membrane phospholipid synthesis and endoplasmic reticulum function. *J. Lipid Res.* **50**.

38. Wang, D., Y. R. Wei, and M. J. Pagliassotti. 2006. Saturated fatty acids promote endoplasmic reticulum stress and liver injury in rats with hepatic steatosis. *Endocrinology* **147**: 943-951.

39. Miller, T. A., N. K. LeBrasseur, G. M. Cote, M. P. Trucillo, D. R. Pimentel, Y. Ido, N. B. Ruderman, and D. B. Sawyer. 2005. Oleate prevents palmitate-induced cytotoxic stress in cardiac myocytes. *Biochem. Biophys. Res. Commun.* **336**.

40. Wang, Y., Z. Wu, D. Li, D. Wang, X. Wang, X. Feng, and M. Xia. 2011. Involvement of Oxygen-regulated Protein 150 in AMP-activated Protein Kinase-mediated Alleviation of Lipid-induced Endoplasmic Reticulum Stress. *J. Biol. Chem.* **286**.

41. Houweling, M., W. Klein, and M. J. H. Geelen. 2002. Regulation of phosphatidylcholine and phosphatidylethanolamine synthesis in rat hepatocytes by 5-aminoimidazole-4-carboxamide ribonucleoside (AICAR). *Biochemical Journal* **362**: 97-104.

42. Jacobs, R. L., S. Lingrell, J. R. B. Dyck, and D. E. Vance. 2007. Inhibition of hepatic phosphatidylcholine synthesis by 5-aminoimidazole-4-carboxamide-1-beta-4-ribofuranoside is independent of AMP-activated protein kinase activation. *J. Biol. Chem.* **282**: 4516-4523.

CHAPTER 6

INHIBITION OF PHOSPHOLIPID SYNTHESIS AND REMODELING SHOWS LIMITED PROTECTION AGAINST PALMITATE LIPOTOXICITY IN HEPATIC CELLS

Introduction

Phospholipids are arguably the most important component of biological membranes as they are integral for both extracellular and intracellular compartmentalization in living cells (1). They facilitate a wide array of essential physiological processes including signal transduction, vesicular trafficking, molecular transport, and biosynthesis. Phospholipids can themselves be used as substrates in reactions for generation of active signaling molecules including diacylglycerol and lysophosphatidic acid (2).

Phospholipids display a vast diversity in both structure and fatty acyl composition. The head group moiety determines species shape while both chain length and degree of saturation of the fatty acid chains determine the biophysical properties of the membrane (3, 4). The relative degree of fluidity in the membrane associated with the ratio of unsaturated and saturated fatty acids is crucial for many membrane associated proteins including ion channels such as the sacro-endoplasmic reticulum calcium ATPase (SERCA) (5, 6). Alterations in the degree of membrane saturation and structure can have detrimental effects on membrane functionality, and in particular, are thought to contribute to ER dysfunction and induction of a stress response (5, 7-10). Deguil *et al*. demonstrated that the capacity of particular fatty acids to induce or relieve ER stress in yeast is dependent on their ability to directly incorporate into phospholipid species and to destroy or restore, respectively, optimal membrane organization (11). This ER stress response has been implicated in a wide variety of diseased states including obesity, diabetes, fatty liver and heart disease, among others (6, 12-15).

Phospholipids, along with other biologically relevant lipids, are synthesized *de novo* though the Kennedy pathway (16) (Fig. 6-1). Newly synthesized phospholipids undergo significant remodeling via fatty acyl deacylation (via phospholipases) and reacylation (via lysophospholipid acyltransferases, LPLATs) though a pathway known as Lands' cycle (17) (Fig. 6-1). Phosphatidylcholine (PC) is the most abundant phospholipid in cellular membranes, accounting for approximately 50% of total cellular phospholipid mass (1, 18, 19), and is known to play a significant role in ER structure and function (19). The CDP-choline pathway produces the choline headgroup that is esterified with diacylglycerol (DAG) from the Kennedy pathway to form PC. The rate limiting step in PC production is generally accepted to be the transfer of cytidine monophosphate (CMP) from cytidine triphosphate (CTP) to phosphocholine to form CDP-choline, which is catalyzed by the enzyme CTP:phosphocholine cytidylyltransferase (CCT) and encoded by the gene *Pcyt1* (Fig. 6-1). CCT is activated though phosphorylation and

binding events and is translocated to the ER membrane in response to changes in lipid composition to regulate PC synthesis flux (19).

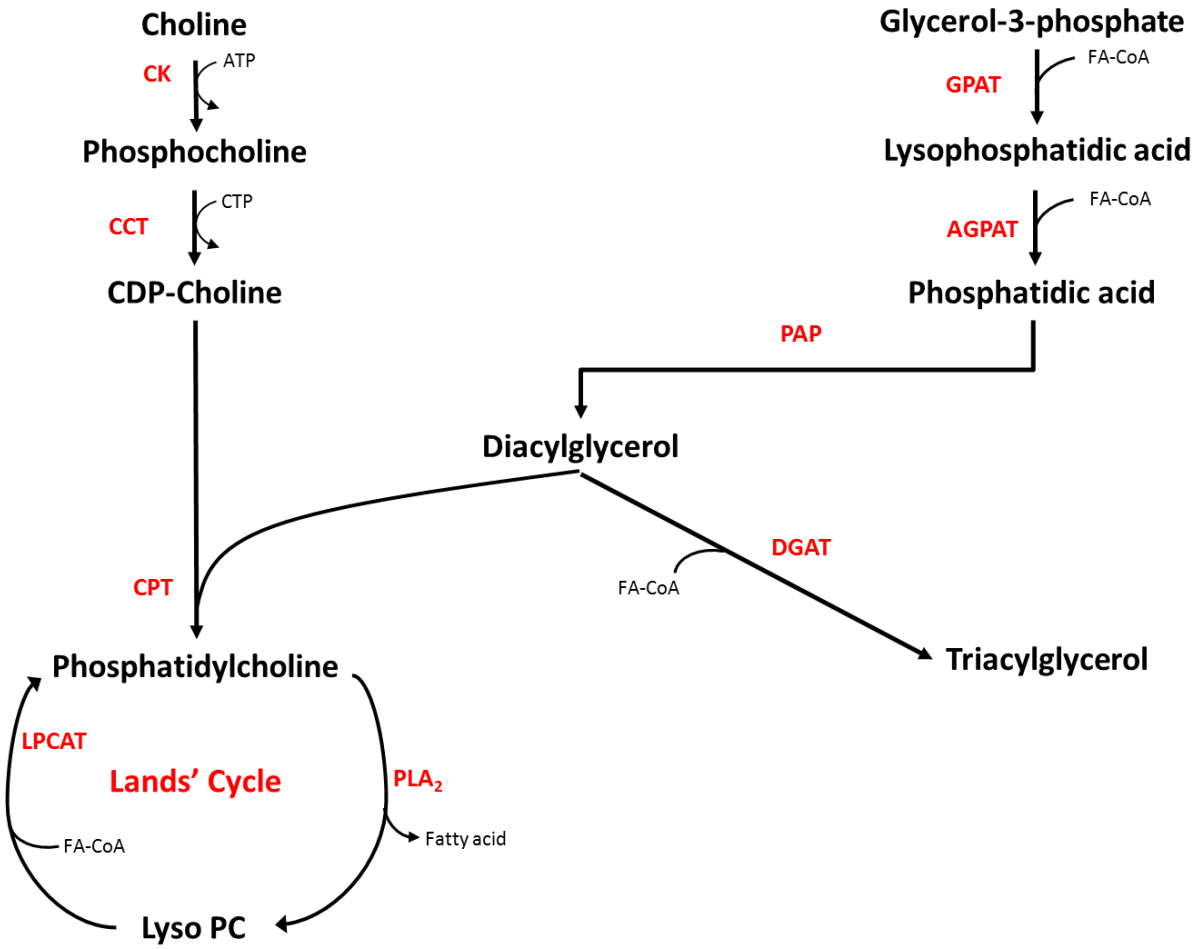

Figure 6-1. Kennedy pathway lipid synthesis and Lands' cycle phosphatidylcholine recycling. Abbreviations are as follows: GPAT, glycerol-3-acyltransferase; AGPAT, acylglycerophosphate acyltransferase; PAP, phosphatidic acid phosphatase; DGAT, diacylglycerol acyltransferase; CK, choline kinase; CCT, CTP:phosphocholine cytidylyltransferase; CPT, choline phosphotransferase; PLA_2, phospholipase A_2; LPCAT, lysophosphatidylcholine acyltransferase; FA-CoA, fatty acyl CoA.

The deacylation enzyme thought to play a major role in membrane phospholipid remodeling is calcium-independent phospholipase A_2 ($iPLA_2$), which cleaves at the *sn-2* position of phospholipids releasing a lysophospholipid and a fatty acid as products (19-21). Remodeling though the Lands' cycle is responsible for the creation of significant diversity in fatty acyl chain composition as acylation enzymes in the *de novo* synthesis pathway have little substrate

specificity with regard to saturation or chain length (22). LPLATs demonstrate considerably higher substrate specificity in regards to fatty acyl donors and lysophospholipid acceptors (23). For example, lysophosphotidylcholine acyltransferase 1 (LPCAT1) almost exclusively incorporates saturated fatty acids, such as palmitate (16:0), into PC (24, 25) while LPCAT3 has broader specificity for incorporating polyunsaturated fatty acids (PUFAs) and some monounsaturated fatty acids in membrane PC (7, 23, 26).

Several groups (7-9, 11, 22, 27) have been in interested in the impact of incorporation of specific fatty acids and overall remodeling of PLs in relation to lipotoxicity. Most of the investigations have focused on the changes that result due to fatty acid supplementation (8, 9, 27) (us, borr, yeast ER) or changes in LPCAT3 expression (LXR and PL unsaturation). Others have looked at the effect inhibiting $iPLA_2$ has lysophospholipid levels (28, 29). Focusing on preventing PA incorporation into PLs by inhibiting specific pathways in PL metabolism specifically has not been fully explored and represents an important gap in knowledge that must be more fully understood in order to accurately describe the connection between PA-induced apoptosis and phospholipid saturation, ER stress and the lipotoxic cascade.

Increased ER stress and lipotoxicity have shown strong association with elevated phospholipid saturation in models of palmitate (PA) mediated lipotoxicity (7-9, 22, 30). In this study, we investigate methods for modulating phospholipid synthesis and remodeling in order to inhibit PA incorporation into phospholipid species that results in oversaturation of membrane bilayers. Our aim was to prevent PA-induced lipotoxity by targeting both phospholipid synthesis and remodeling pathways in attempt to reduce ER stress and subsequent lipoapotosis. Our results show that impeding deacylation of existing phospholipids (remodeling) using a pharmacological inhibitor of $iPLA_2$, palmityl trifluoromethyl ketone ($PACOCF_3$), did impart some positive benefits for PA-treated hepatic cells. We demonstrate small reductions in membrane saturation and ER stress that led to depressed markers of lipoapoptosis. Similarly, genetic knockdown of *Pcyt1a*, the regulatory step in PC synthesis, also resulted in decreases in membrane saturation and other downstream markers of lipotoxicity, though the effect was small. Overall, manipulations designed to more effectively reduce saturated fatty acid incorporation into membrane phospholipids presents an interesting target for preventing lipotoxicity and its physiological consequences.

Methods

Materials and Reagents

Oleic and palmitic acids, bovine serum albumin (BSA), Dulbecco's modified Eagle's medium (DMEM), and palmityl trifluoromethyl ketone (PACOCF3) were all purchased from Sigma-Aldrich (St. Louis, MO). CHOP primary (mouse) and goat anti-mouse secondary antibodies were purchased from Abcam (Cambridge, MA). β-Actin primary (goat) and donkey anti-goat

secondary antibodies were procured from Santa Cruz Biotechnology. siRNA was purchased in the TriFECTA kit from Integrated DNA Technologies (Coralville, IA). All other chemicals were purchased from standard commercial sources.

Preparation of fatty acid solutions

Fatty acid solutions were prepared by coupling free fatty acids to bovine serum albumin (BSA). Specifically, palmitate or oleate was fully dissolved in 200-proof ethanol for a concentration of 195 mM. This FFA stock solution was added to a pre-warmed BSA solution (10% w/w, 37°C) for a final FFA concentration of 3 mM, ensuring that the concentration of ethanol in the FFA solution did not exceed 0.5% by volume. The solution was fully dissolved by warming at 37°C for an additional 10 minutes. The final ratio of FFA:BSA was 2:1. Vehicle control treatments were prepared using stocks of 10% w/w BSA with an equivalent volume of ethanol added to match that contained in the final FFA stock. The final concentration of ethanol was less than 0.2% in all experiments.

Cell Culture and siRNA transfections

Rat hepatoma cells, H4IIEC3 (ATCC), were cultured in low-glucose Dulbecco's modified Eagle's medium (DMEM) supplemented with 10% fetal bovine serum and 1% penicillin/streptomycin/glutamine (2mM). Measurements were obtained at 70-80% confluency. Hepatic cells were transfected with siRNA using Lipofectamine RNAiMAX (Invitrogen) according to the manufacturer's protocol with a final volume of 10 μL of Lipofectamine RNAiMAX per 2 mL media solution. The final concentration of siRNA was 25 nM.

Total RNA Isolation and Quantitative Real-Time PCR

Total RNA was isolated from cells using RNeasy Mini Kit (Qiagen, Germantown, MD) according to manufacturer's protocol and then reverse transcribed using cDNA reverse transcriptase kit (BioRad, Hercules, CA). Quantitative real-time PCR was performed using iQ SYBR Green Supermix (BioRad, Hercules, CA) and BioRad CFX96 Real-Time PCR Detection System (BioRad, Hercules, CA). The sequence of the primers were as follows: C/EBP homologous protein (CHOP) forward (5'-CTCAGCTGCCATGACTGTA-3') and reverse (5'-CGTCGATCATACCATGTTGAAGA-3'), ATF3 forward (5'-CGCCTCCTTTTTCTCTCATCT-3') and reverse (5'-CCATCCAGAACAAGCACCT-3'), ribosomal 18s forward (5'-CGGACAGGATTGACAGAT-3') and reverse (5'-CGCTCCACCAACTAAGAA-3'), CTP: phosphocholine cytidylyltransferase 1, alpha (Pcyt1a) forward (5'-CTTTACCTTATCAACTCGTTCTTGC-3') and reverse (5'-TCCGTGACTATGATGTGTATGC-3'). Target gene expression was normalized on the basis of 18s content.

ROS

Intracellular ROS production was measured using 2',7'-dichlorodihydrofluoresceindiacate (H_2DCFDA, Invitrogen) as described previously (31). H_2DCFDA is a non-polar compound that easily passes though the cell membrane where intracellular esterases remove the acetate groups resulting in a non-fluorescent dichlorodihydrofluorescein dye that is strongly retained by the cell. In the presence of ROS production, dichlorodihydrofluorescein is oxidized and becomes highly fluorescent. After indicated treatments for cells cultured in 96-well plates, the medium was removed and cells were washed twice with Hanks' balanced salt solution (HBSS). Cells were then incubated at 37°C for 1 h in the dark in a 10 μM solution of H_2DCFDA in HBSS. The fluorescence intensity was measured at an excitation/emission wavelength of 485/530 nm using a Biotek FL600 microplate analyzer.

Cell Toxicity

Toxicity was assessed using the dead cell dye propidium iodide as described previously (32). Propidium iodide is an intercalating dye that can only permeate dead cells. It becomes highly fluorescent when embedded in the double-stranded DNA exposed after cell death. After culturing cells in 96-well plates with experimental treatments, the medium was removed and replaced with a solution of the dye and serum-free DMEM. Cells were incubated at 37°C for 1 h in the dark prior to the fluorescence measurement at ex/em wavelengths of 530/645 nm.

Caspase Activation

The Apo-ONE Homogenous Caspase 3/7 Assay kit was used to measure apoptotic caspase activation. Cells were cultured in 96-well plates and incubated with desired treatments for 6 hours. The Apo-ONE kit uses a lysis buffer combined with a caspase 3/7 specific substrate (Z-DEVD-R110), which becomes fluorescent once these caspases remove its DEVD peptide. Fluorescence was measured at ex/em wavelengths of 485/535 nm.

Western Blotting

Cells were lysed with ice-cold RIPA lysis buffer (sc-24948, Santa Cruz Biotechnology, Inc., Santa Cruz, CA) supplemented with Na-orthovanadate, protease inhibitor cocktail, and PMSF for 30 min on ice. Samples were centrifuged at 16,100 rcf and 4°C for 20 min, and the resulting supernatants constituted the total protein extracts. Protein concentrations were determined by BCA assay (Thermo Fisher Scientific, Rockford, IL). Samples were added in concentrations of 30 μg/lane for SDS-PAGE western blotting. Dilutions of the primary antibodies were anti-CHOP (1:1000) and anti-β-actin (1:1000).

Phospholipid Fatty Acid Profiles

Cells seeded in 10-cm Petri dishes at an initial density of 4×10^6 cells per plate were incubated in standard medium until reaching ~70-80% confluency, at which time experimental treatments

were administered. Cells were then trypsinized for 3 min and scraped using cold PBS. Cell suspensions were pelleted by centrifugation and resuspended in fresh PBS. Fatty acyl lipid analysis was performed by the Vanderbilt Hormone Assay and Analytical Services Core using thin-layer chromatography (TLC) and gas chromatography-flame ionization detection (GC-FID) techniques. Briefly, lipids were extracted from the aforementioned cell pellets using a modified Folch separation. An internal standard (1,2-dipentadecanoyl-sn-glycero-3-phosphocholine) for phospholipids was added to the lipid-containing chloroform phase. Total lipids were then extracted and separated by TLC using petroleum ether/ethyl ether/acetic acid (80/20/1, v/v/v) on silica plates. Spots corresponding to phospholipids (PLs), triglycerides (TAGs), and free fatty acids (FFAs) were visualized with rhodamine 6G in 95% ethanol and scraped individually into glass tubes for transmethylation. Transmethylation was performed using a boron trifluoride-methanol 10% (w/w) solution. Derivatized lipids were then analyzed using a GC-FID, where standardized calibration curves were used to analyze fatty acid content.

Transmission electron microscopy

Cells were seeded in 10-cm dishes at 4×10^6 cells per dish and incubated in standard medium until reaching ~70-80% confluency. Cells were then incubated with desired treatments at 37°C for the indicated time period and then washed thoroughly with 0.1M sodium cacodylate buffer (with 1% calcium chloride), pH 7.4. After washing, cells were fixed with a 2.5% glutaraldehyde solution in 0.1 M sodium cacodylate buffer for 1 h at room temperature followed by 23 h at 4°C. Samples were postfixed in 1.25% osmium tetroxide and subsequently stained with 2% aqueous uranyl acetate. Embedded cells were then thin-sectioned and viewed on a Philips/FEI T-12 high-resolution transmission electron microscope.

Results

Palmitate-induced ER stress is accompanied by formation of large phospholipid accumulations, known as myelin figures

Results from prior work demonstrate that the lipotoxic effect of PA in various cell types, including hepatocytes, occurs by inducing cellular dysfunction and apoptosis-mediated cell death (8, 9, 33-39). We have shown previously that this PA-induced liptoxicity is characterized by increased saturation and disordered metabolism of phospholipids and induction of ER stress (9). TEM images of PA-treated hepatic cells, both H4IIEC3 rat hepatomas (Fig. 6-2) and freshly isolated primary rat hepatocytes (Fig. 6-3), revealed striking evidence of disordered phospholipid metabolism *in vitro* though the formation of lamellar structures known as myelin figures (Fig. 6-2B, Fig. 6-3B). Myelin figures (MFs) are essentially concentric layers of phospholipid aggregates that are thought to indicate dysregulated phospholipid synthesis and metabolism in cells. Compared to hepatic cells treated with BSA-vehicle control (Fig 6-2A, Fig. 6-3A), cells treated with PA *in vitro* exhibited repeatable formation of MFs (Fig 6-2B, Fig. 6-3B). In contrast,

hepatocytes supplemented with equimolar concentrations of OA alone (Fig 6-2C, Fig. 6-3C) presented normal lipid droplet accumulations without any indication of myelin figure formation.

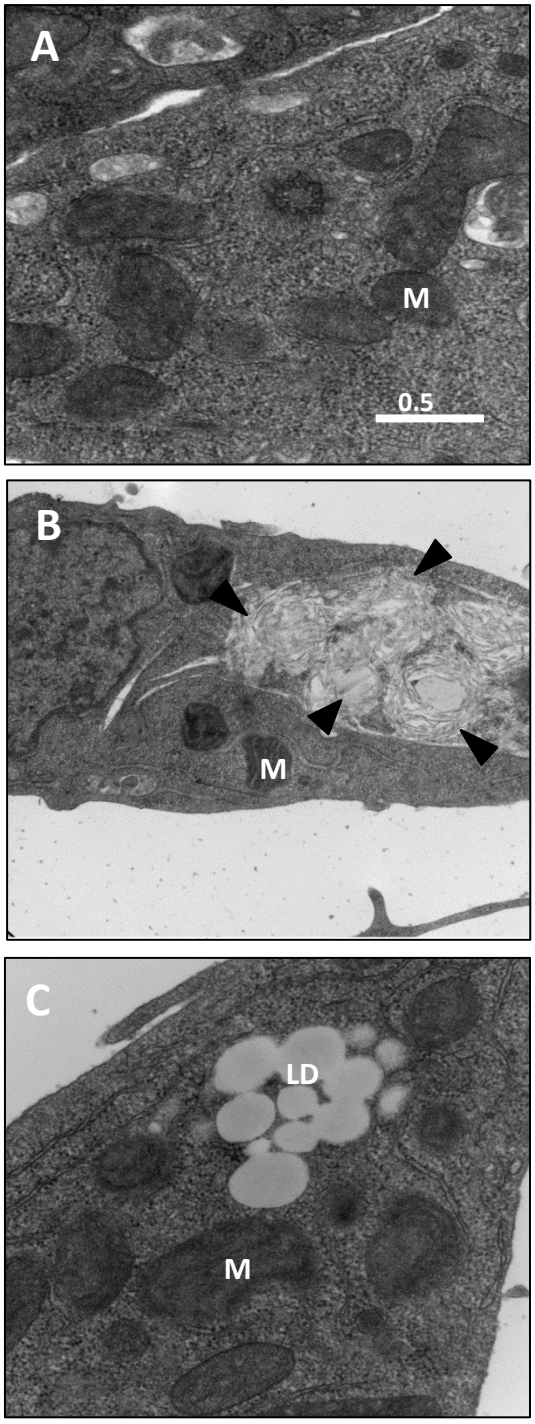

Figure 6-2. Incubation of H4IIEC3 cells with PA results in formation of myelin figures, which are absent from cells treated with BSA or OA. H4IIEC3 cells were incubated for 4 h with (A) BSA vehicle, (B) 400 μM PA, or (C) 400 μM OA. Changes in cellular morphology were observed by high-resolution imaging with transmission electron microscopy. Arrowheads point towards myelin figures. M, mitochondria; LD, lipid droplets

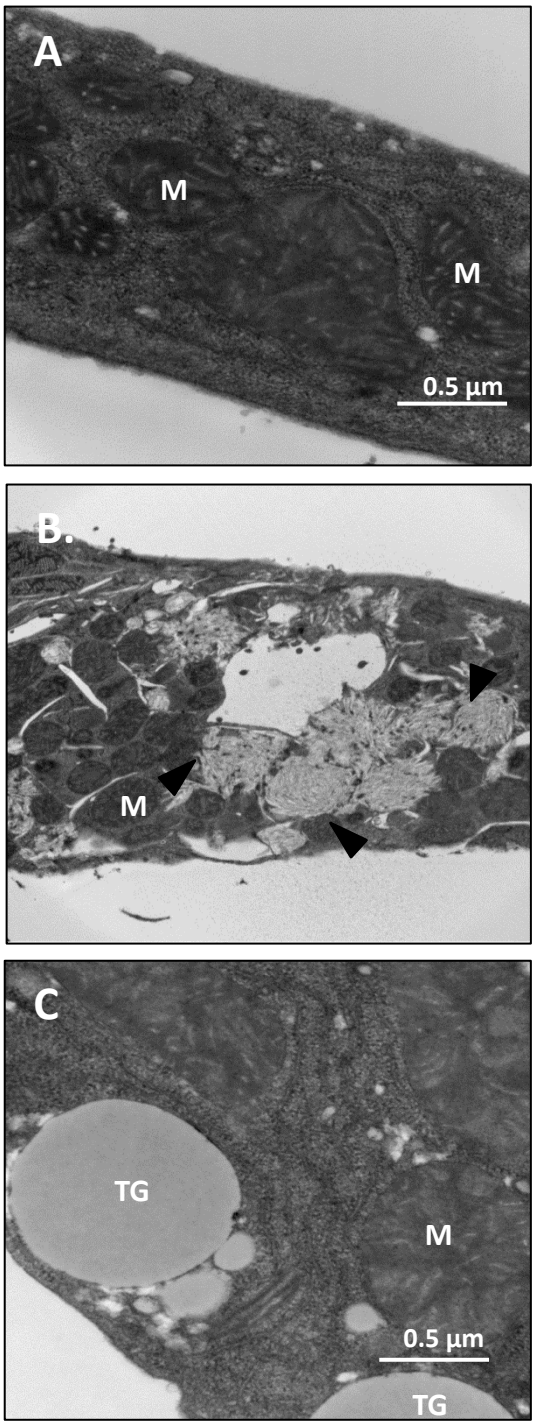

Figure 6-3. Incubation of freshly isolated rat hepatocytes with PA results in formation of myelin figures, which are absent from cells treated with BSA or OA. Hepacotyes were incubated for 12 h with (A) BSA vehicle, (B) 400 µM PA, or (C) 400 µM OA. Changes in cellular morphology were observed by high-resolution imaging with transmission electron microscopy. Arrowheads point towards myelin figures. M, mitochondria; LD, lipid droplets

Pharmacological inhibition of iPLA$_2$ activity results in small reductions in markers of palmitate-induced lipotoxicity

Our observations that disordered phospholipid metabolism plays a role in PA-induced lipotoxicity, particularly oversaturation of membrane phospholipids, led us to experiment with methods designed to alter PA incorporation into these integral cellular components. First, we aimed to prevent PA incorporation into phospholipids by targeting the Lands' remodeling cycle. New phospholipids are primarily produced though the Kennedy lipid synthesis pathway, but extensive post-synthesis remodeling is thought to provide much of the diversity in acyl-chain composition and positional distribution on the glycerol backbone. In Lands' cycle, phospholipases hydrolyze a fatty acid bonded to the phospholipid and acyltransferases re-esterify the specific moiety. Since we were interested in fatty acid composition, we examined enzymes involved in this remodeling cycle. Different phospholipases hydrolyze the *sn*-1 or sn-*2* position of the phospholipid bond, releasing a lysophospholipid and a fatty acid. Lysophospholipid acyltransferases utilize the emancipated lysophospholipid as a substrate and reacylate the same position with a new fatty acid moiety thereby providing significant species diversity (2, 23). Calcium-independent phospholipase A_2 (iPLA$_2$) is an abundant enzyme in all tissues that hydrolyzes the fatty acid *sn-2* position of phospholipids (40). We chose to inhibit this enzyme using the commercially available small molecule palmityl trifluoromethyl ketone (PACOCF$_3$). This molecule has been previously shown to significantly inhibit iPLA$_2$ activity (41) in other studies on different hepatic models (29).

Pre-treating H4IIEC3 cells with PACOCF$_3$ reduced PA-mediated markers of lipotoxicity including ROS, caspase 3/7 activation and cell death compared to cells treated with PA alone. After 6 hours, PA supplementation increased total cellular ROS levels by almost two-fold while pre-treatment with PACOCF$_3$ reduced this accumulation by approximately 40% (Fig. 6-4A). Similarly, PA induced caspase 3/7 activity almost thee-fold after 8h and increased cell death two-fold after 12h over BSA-control treatments (Fig 6-4 B and C, respectively). Supplementation with the iPLA$_2$ inhibitor PACOCF$_3$ reduced these levels by approximately 35% in comparison to PA-only treated cells. Although PACOCF$_3$ did not completely reverse PA-mediated lipoapoptosis, the observed reductions were statistically significant and closely correlated with the observed reductions in ROS.

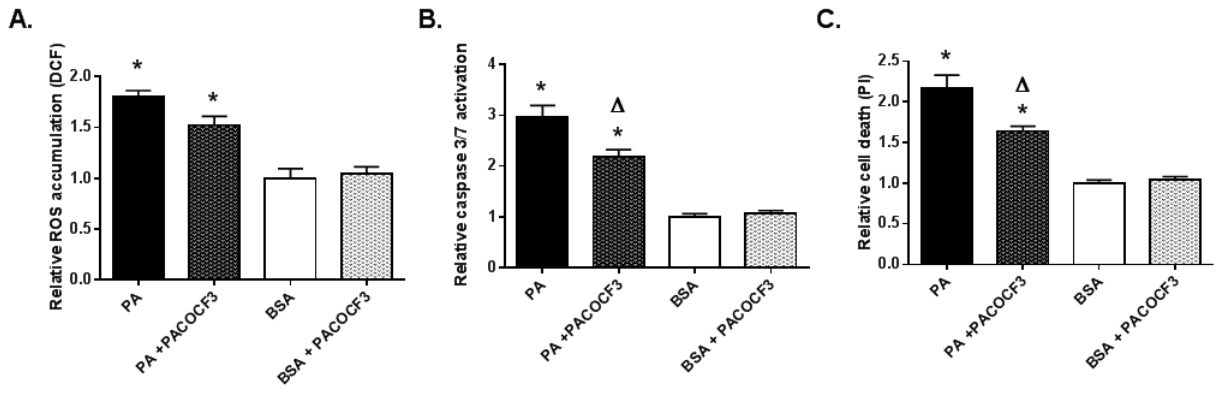

Figure 6-4. Induction of ROS accumulation, caspase 3/7 activation and cell death by palmitate treatment is partially reversed by co-treatment with the iPLA$_2$ inhibitor PACOCF$_3$. H4IIEC3 cells were incubated with indicated treatments (PA = 400 μM PA, PACOCF3 = 100 μM PACOCF$_3$) and assayed for ROS accumulation at 6 h (A), activation of caspase 3/7 at 9 h (B) and cell death at 12 h (C). ROS was assessed using the fluorescent dye H$_2$DCFDA, caspase 3/7 activation with Apo-ONE and cell toxicity via propidium iodide, all of which were normalized to control cells treated with BSA vehicle. Data represent mean ± SE of n=4. *, $p < 0.05$ vs. cells treated with BSA; Δ, $p < 0.05$ cells treated with PA+PACOCF3 vs. cells treated with PA alone.

Next, we were interested to investigate if pre-treatment with PACOCF$_3$ reduced PA incorporation into phospholipids and markers of ER stress. Examining the fatty acid composition of the phospholipid fraction after 6h and 24h of incubation revealed that, in comparison to PA-only treated cells, co-treatment with PACOCF$_3$ led to small, but significant, decreases in PA incorporation (~44% vs 34%, 24h) and total phospholipid saturation (~57.5% vs ~49.5%, 24h) (Table 6-1 and 6-2, respectively). This correlated to a small reduction in ER stress after 8 h, as assessed by reduction in CHOP levels (Fig. 6-5). These data indicate that while inhibition of iPLA$_2$ did provide some positive benefits to PA-treated hepatic cells, it was unable to completely reverse the lipotoxic effects of PA treatment.

Fatty Acid	PA	PA+PACOCF$_3$	BSA	BSA+PACOCF$_3$
14:0	0.56 ± 0.14	0.61 ± 0.02	0.69 ± 0.15	0.63 ± 0.09
16:0	32.13 ± 0.68	27.56 ± 0.74[a]	12.72 ± 0.43[a]	13.14 ± 0.05[a]
16:1	11.14 ± 0.28	10.78 ± 0.44	6.93 ± 0.39[a]	5.78 ± 0.23[a]
18:0	13.84 ± 0.18	15.30 ± 0.17[a]	18.54 ± 0.54[a]	19.86 ± 0.42[a]
18:1w9	20.11 ± 0.16	22.43 ± 0.45[a]	33.38 ± 0.32[a]	30.39 ± 0.27[a]
18:1w7	4.94 ± 0.05	5.10 ± 0.05	7.95 ± 0.08[a]	8.08 ± 0.04[a]
18:2	2.34 ± 0.03	2.57 ± 0.06	2.88 ± 0.00	3.03 ± 0.08
20:3w6	0.77 ± 0.24	0.76 ± 0.01	0.80 ± 0.03	0.78 ± 0.01
20:4	8.93 ± 0.21	9.43 ± 0.17	10.45 ± 0.05[a]	11.91 ± 0.32[a]
20:5	0.22 ± 0.21	0.28 ± 0.01	0.00 ± 0.00	0.16 ± 0.09
22:4w6	0.96 ± 0.26	0.95 ± 0.01	1.11 ± 0.01	1.07 ± 0.01
22:5w6	0.38 ± 0.00	0.39 ± 0.01	0.29 ± 0.13	0.33 ± 0.11
22:5w3	1.61 ± 0.04	1.61 ± 0.02	1.79 ± 0.05	2.00 ± 0.05
22:6	2.05 ± 0.04	2.25 ± 0.06	2.49 ± 0.04	2.84 ± 0.10
% SFA	46.53 ± 1.01	43.46 ± 0.76[a]	31.95 ± 0.71[a]	33.63 ± 0.43[a]
% UFA	53.47 ± 0.72	56.54 ± 0.66[a]	68.05 ± 0.53[a]	66.37 ± 0.52[a]

Table 6-1. Phospholipid composition of cells treated with PA with or without PACOCF$_3$ for 6 h. H4IIEC3 cells were incubated with 400 μM PA with or without 100 μM PACOCF$_3$ for 6 h. Phospholipids were separated by thin layer chromatography and analyzed by gas chromatography-flame ionization detection (GC-FID). Data represent mean fatty acid %± SE of n=3. a, $p<0.05$ vs cells treated with PA alone. SFA, saturated fatty acids; UFA, unsaturated fatty acids.

Fatty Acid	PA	PA+PACOCF$_3$	BSA	BSA+PACOCF$_3$
14:0	0.41 ± 0.14	0.52 ± 0.02	0.55 ± 0.04	0.82 ± 0.02
16:0	43.86 ± 0.68	33.99 ± 0.37[a]	11.29 ± 0.26[a]	12.00 ± 0.12[a]
16:1	12.44 ± 0.28	15.99 ± 0.18[a]	6.87 ± 0.07[a]	6.20 ± 0.05[a]
18:0	12.71 ± 0.18	14.56 ± 0.29[a]	19.98 ± 0.38[a]	20.50 ± 0.06[a]
18:1w9	11.42 ± 0.16	14.89 ± 0.22[a]	32.79 ± 0.11[a]	31.75 ± 0.11[a]
18:1w7	3.13 ± 0.05	3.64 ± 0.05	8.25 ± 0.07[a]	8.66 ± 0.05[a]
18:2	2.17 ± 0.03	2.31 ± 0.03	3.02 ± 0.04[a]	3.16 ± 0.03
20:3w6	0.72 ± 0.24	0.84 ± 0.00	0.92 ± 0.02	0.85 ± 0.01
20:4	9.06 ± 0.21	8.87 ± 0.12	10.77 ± 0.18[a]	10.47 ± 0.06[a]
22:4w6	0.77 ± 0.26	0.90 ± 0.02	1.26 ± 0.03	1.11 ± 0.01
22:5w6	0.00 ± 0.00	0.09 ± 0.09	0.12 ± 0.12	0.45 ± 0.00
22:5w3	1.36 ± 0.04	1.36 ± 0.05	1.73 ± 0.04	1.62 ± 0.02
22:6	1.94 ± 0.04	1.96 ± 0.06	2.46 ± 0.05	2.25 ± 0.02
% SFA	56.99 ± 0.72	49.07 ± 0.47[a]	31.82 ± 0.46[a]	33.33 ± 0.14[a]
% UFA	43.01 ± 0.84	50.93 ± 0.35[a]	68.18 ± 0.34[a]	66.67 ± 0.19[a]

Table 6-2. Phospholipid composition of cells treated with PA with or without PACOCF$_3$ for 24 h. H4IIEC3 cells were incubated with 400 μM PA with or without 100 μM PACOCF$_3$ for 24 h. Phospholipids were separated by thin layer chromatography and analyzed by gas chromatography-flame ionization detection (GC-FID). Data represent mean fatty acid % ± SE of n=3. a, $p<0.05$ vs cells treated with PA alone. SFA, saturated fatty acids; UFA, unsaturated fatty acids.

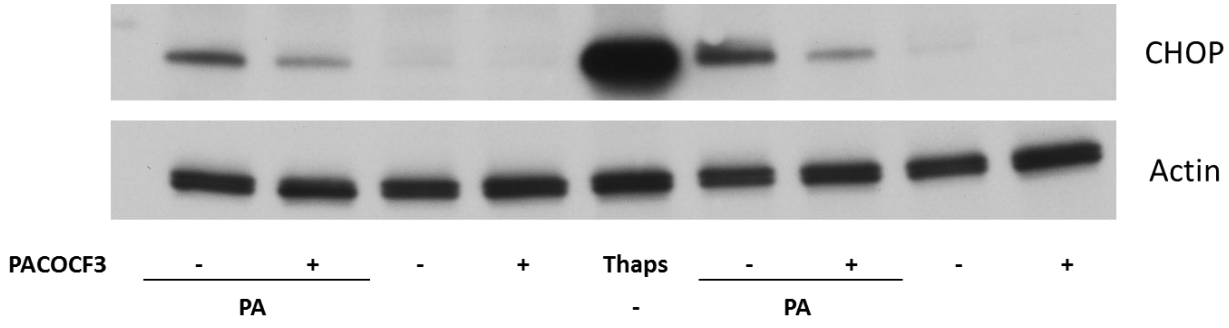

Figure 6-5. Inhibition of iPLA$_2$ in PA-treated H4IIEC3 cells reduces CHOP expression, a marker of ER stress. PA-induced increases in CHOP abundance were reduced by inhibiting iPLA$_2$ with the small molecule specific inhibitor PACOCF$_3$. H4IIEC3 hepatocytes were treated with 400 μM PA alone or in the

presence of 100 μM $PACOCF_3$ for 8 h in independent experiments. Levels of CHOP abundance were assessed using Western blotting techniques. Actin was the loading control and thapsigargin (Thaps) was used as a positive control.

Inhibition of phospholipid synthesis via siRNA knockdown of Pcyt1α results in a small reversal in ER saturation and markers of lipoapoptosis.

Based on our previous data that showed increased phospholipid synthesis though the Kennedy pathway in the presence of PA (9), we were interested in investigating the effect of reducing phosphatidylcholine (PC) synthesis. PC constitutes the most abundant phospholipid in membrane bilayers (1), and therefore presents the best single phospholipid species to target. PC is synthesized *de novo* though the CDP-choline pathway (Fig. 1) in which the rate limiting step, conversion from phosphocholine to CDP-choline, is regulated by the enzyme CCT encoded by the gene *Pcyt1* (16, 42) . Two isoforms are known to exist (*Pcyt1a* and *Pcyt1b*). *Pcyt1a* is thought to be the predominant form in the liver (43) and has been shown previously to be stimulated via translocation of the enzyme from the cytosol to the microsomal membrane by fatty acid treatment (44). Using siRNA, we knocked down *Pcyt1a* expression in H4IIEC3 hepatic cells to determine if this genetic manipulation imparted any effect on lipotoxic phenotypes in PA-treated cells (Fig. 6-6A).

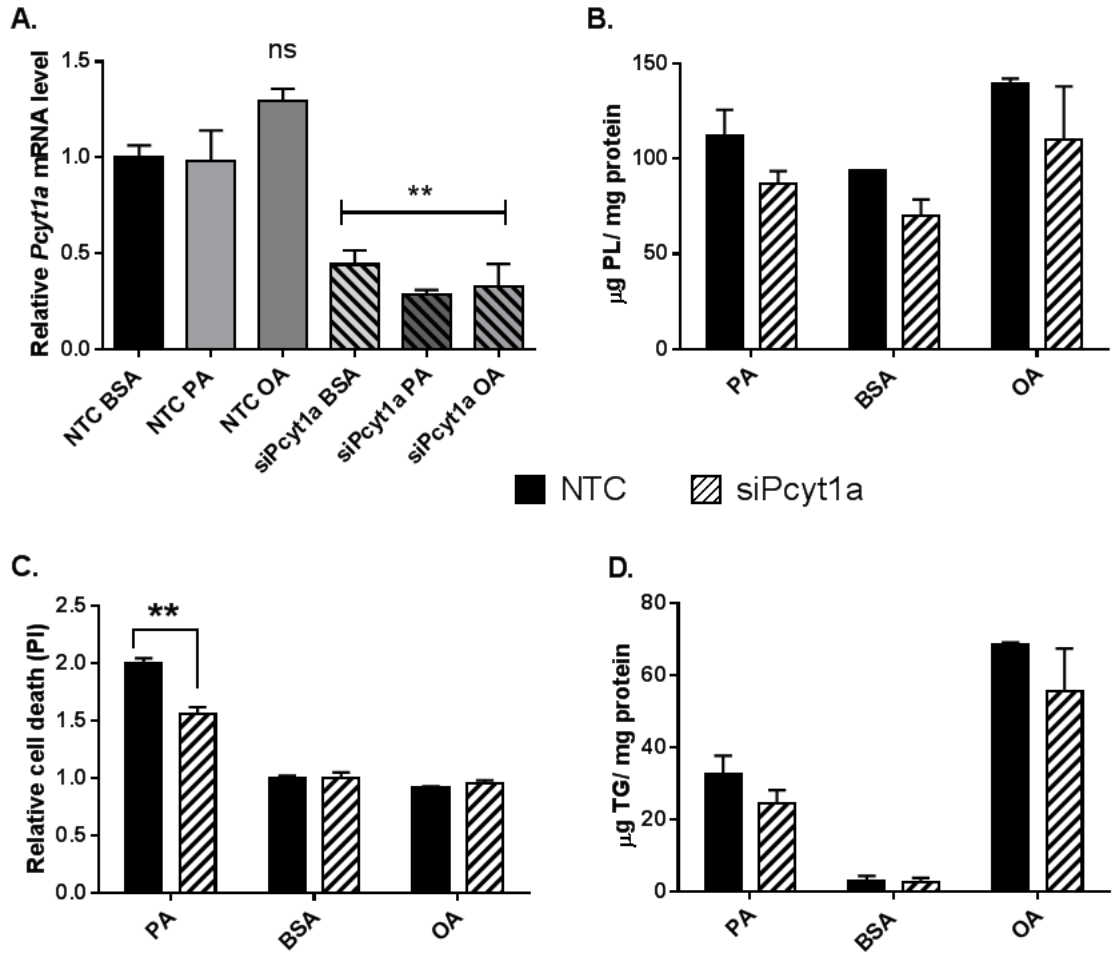

Figure 6-6. siRNA mediated knockdown of *Pcyt1a* expression trended towards reduced phospholipid synthesis without reductions in triglyceride synthesis in H4IIEC3 cells and partially reduced palmitate lipotoxicity. Knockdown of *Pcyt1a* (siPcyt1a), the rate limiting step in de novo PC synthesis, reduced mRNA transcript levels of the gene regardless of treatment (A). H4IIEC3 cells transfected with siRNA targeted to *Pcyt1a* demonstrated a downward trend in phospholipid synthesis in comparison to non-targeting control siRNA treated cells (NTC), but the effect was not statistically significant (B). siPcyt1a partially reduced toxicity when combined with PA treatment (C). There were no statistically significant changes in TG accumulation between siPcyt1a and NTC groups (D). Data represent mean ± SE of n=4. **, P<0.05, vs. cells supplemented with the same treatment; ns, not significant.

Knocking down *Pcyt1a* (siPcyt1a) resulted in a trend toward reduced phospholipid synthesis after 12h, but the differences between NTC and siPcyt1a cells were not statistically significant (Fig. 6-6B). However, *Pcyt1a* knockdown did reduce PA associated cell death in H4IIEC3 cells by approximately 40% (Fig. 6-6C). Manipulation of this gene had no effect on OA treated cells. Due to the known function of PC as a coating phospholipid for lipid droplets, we tested whether inhibition of *Pcyt1a* had any effect on triglyceride synthesis. Although there was a slight

downward trend, there were no statistical differences in triglyceride accumulation between NTC and siPcyt1a cells with the same fatty acid treatments (Fig. 6-6D).

Because inhibiting *Pcyt1a* resulted in significant reduction in PA-induced cell death, we were interested to see if it also reduced other facets of lipotoxicity including ER stress and phospholipid saturation that we had observed in prior studies. Changes in CHOP protein expression levels were inconclusive (Fig. 6-7B). Additionally, siPcyt1a cells demonstrated a decrement in the percentage of PA incorporated into phospholipids correlating to a small but significant decrease in overall percent saturation after 12h (Table 6-3). The PA (16:0) abundance in cellular phospholipids was reduced by ~18% in siPcyt1a cells compared to NTC cells treated with PA (42.56% ± 0.42 vs 48.73% ±0.62). Total phospholipid saturation was reduced by ~25%. Overall, these data point toward knockdown of *Pcyt1a* expression as an interesting and novel target for prevention of lipoapoptosis, with some significant effects on PA-induced lipotoxicity. However, *Pcyt1a* knockdown of PA-treated cells did not completely restore cell viability or other lipotoxic markers to their basal levels.

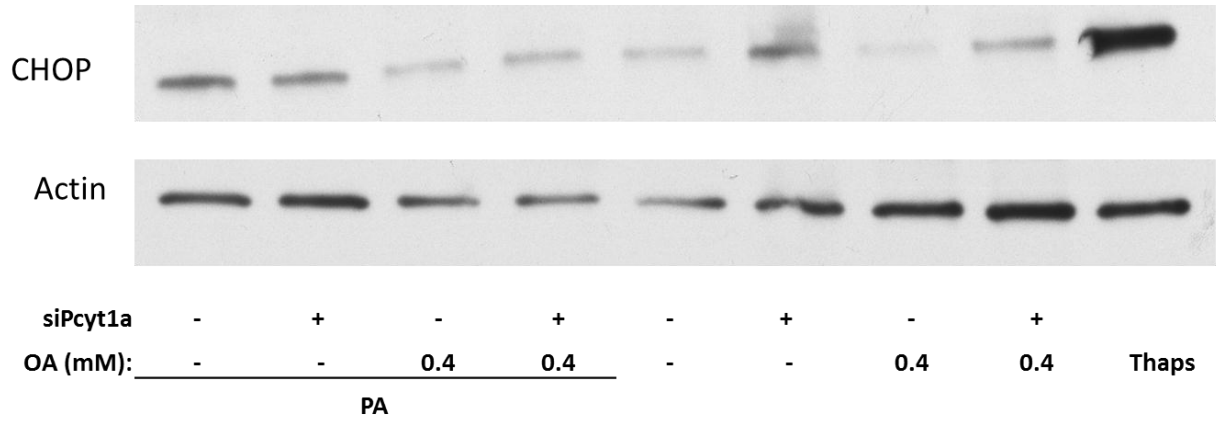

Figure 6-7. Knockdown of *Pcyt1a* expression in H4IIEC3 cells has no significant effect on PA-induced CHOP expression. Knocking down *Pcyt1a* in H4IIEC3 had only slight effects on PA-mediated increases in CHOP abundance. H4IIEC3 hepatocytes were transfected with either non-targeted control siRNA (NTC), indicated as (-), or siPcyt1a, indicated by (+), and treated with 400 μM PA either alone or in combination with 400 μM OA for 8 h in independent experiments (representative blot shown). Levels of CHOP abundance were assessed using Western blotting techniques. Actin was the loading control and thapsigargin (Thaps) was used as a positive control.

Fatty Acid	NTC PA	NTC BSA	NTC OA	siPcyt1a PA	siPcyt1a BSA	siPcyt1a OA
14:0	0.00 ± 0.00	0.89 ± 0.02	0.48 ± 0.03	0.00 ± 0.00	0.00 ± 0.00	0.00 ± 0.00
16:0	48.73 ± 0.62	12.87 ± 0.14	8.29 ± 0.10	42.56 ± 0.41[a]	14.19 ± 0.15[a]	8.83 ± 0.14
16:1	8.82 ± 0.24	6.71 ± 0.10	2.40 ± 0.08	13.02 ± 0.17[a]	6.21 ± 0.07	1.85 ± 0.04
18:0	12.82 ± 0.58	18.75 ± 0.55	12.64 ± 0.42	11.63 ± 0.12[a]	20.34 ± 0.43[a]	13.10 ± 0.25
18:1w9	11.06 ± 0.07	28.19 ± 0.74	58.03 ± 0.05	12.88 ± 0.15[a]	28.82 ± 0.29	58.81 ± 0.20
18:1w7	3.22 ± 0.02	8.01 ± 0.42	4.17 ± 0.08	3.26 ± 0.04	6.95 ± 0.02[a]	4.28 ± 0.02
18:2	1.80 ± 0.08	4.08 ± 0.14	1.75 ± 0.05	2.14 ± 0.02	3.84 ± 0.02	1.75 ± 0.01
20:3w6	0.66 ± 0.33	1.51 ± 0.03	0.60 ± 0.01	1.10 ± 0.01	1.42 ± 0.02	0.00 ± 0.00
20:4	8.52 ± 0.07	10.56 ± 0.03	6.64 ± 0.07	7.54 ± 0.11	11.20 ± 0.02	7.44 ± 0.08
20:5	0.00 ± 0.00	0.34 ± 0.17	0.00 ± 0.00	0.00 ± 0.00	0.00 ± 0.00	0.00 ± 0.00
22:4w6	0.00 ± 0.00	1.38 ± 0.01	0.59 ± 0.01	0.96 ± 0.03	1.58 ± 0.06	0.00 ± 0.00
22:5w6	0.00 ± 0.00	0.65 ± 0.42	1.05 ± 0.01	0.81 ± 0.01	0.00 ± 0.00	0.63 ± 0.31
22:5w3	2.34 ± 0.09	2.83 ± 0.03	1.43 ± 0.01	1.87 ± 0.03	2.71 ± 0.01	1.53 ± 0.01
22:6	2.02 ± 0.01	3.23 ± 0.01	1.91 ± 0.04	2.23 ± 0.04	2.75 ± 0.04	1.77 ± 0.02
% SFA	61.55 ± 0.85	32.52 ± 0.57	21.42 ± 0.44	54.19 ± 0.42[a]	34.52 ± 0.46[a]	21.93 ± 0.29
% UFA	38.45 ± 0.44	67.48 ± 0.98	78.58 ± 0.15	45.81 ± 0.26[a]	65.48 ± 0.32[a]	78.07 ± 0.38

Table 6-3. Knockdown of *Pcyt1a* results in a small reduction in PA incorporation and overall phospholipid saturation in PA-treated hepatic cells (%composition). Phospholipid composition of either NTC control or siPcyt1a H4IIEC3 cells was measured following incubation with 400 μM PA, 400 μM OA or corresponding amounts of BSA for 12 h. Phospholipids were separated by thin layer chromatography and analyzed by gas chromatography-flame ionization detection (GC-FID). Data represent mean fatty acid % ± SE of n=3. [a], $p<0.05$, NTC vs siPcyt1a cells with same treatment. SFA, saturated fatty acids; UFA, unsaturated fatty acids.

Discussion

Hepatic lipotoxicity in H4IIEC3 cells is characterized by disordered phospholipid metabolism resulting in increased saturation of membrane bilayers. Manipulating fatty acyl composition of phospholipids directly in intact living cells is currently a challenge that has not been resolved fully in a laboratory setting to date. Therefore, in this study we sought to determine if limiting PC synthesis or reducing phospholipid remodeling via inhibition of $iPLA_2$ would suppress PA-induced lipotoxic phenotypes, including ER stress and cell death, via reduction in phospholipid saturation.

Newly synthesized phospholipid species have been previously shown to undergo significant remodeling within 1h (40, 45) and existing phospholipids are continuously recycled in this

manner. As such, remodeling may present an important avenue though which PA is incorporated into phospholipids in PA-mediated lipotoxicity. By inhibiting $iPLA_2$, the major deacylation enzyme in the Lands' cycle, we sought to prevent remodeling of synthesized phospholipids and subsequent reacylation of saturated fatty acids onto phospholipid backbones. We used $PACOCF_3$, a pharmacological agent that has been demonstrated to specifically inhibit $iPLA_2$ activity (29, 41). Our data indicate that this approach did have small, but significant, effects on phospholipid composition and lipotoxic markers. Pre-treatment of H4IIEC3 hepatic cells with $PACOCF_3$ resulted in a significant decrease in the percent incorporation of PA into the phospholipid fraction after 6h and almost one third reduction after 24h. This correlated to decreases in other hallmark indicators of lipotoxicity including markers of ER stress (CHOP protein levels), ROS accumulation, caspase 3/7 activation and cell death (Fig. 6-4 and 6-5).

Though our results suggest that inhibiting $iPLA_2$ had significant effects on lipoapoptosis, other factors must also be considered when interpreting the response to $PACOCF_3$ treatment. LysoPC has been previously implicated as a death effector in hepatic cells (28, 29), and inhibition of $iPLA_2$ would also be expected to limit accumulation of this lipid intermediate. Kakisaka et al. demonstrated that intracellular LysoPC (16:0) accumulated with PA treatment and that cells supplemented with LysoPC alone underwent apoptosis in a concentration-dependent manner (28). LysoPC-mediated apoptosis was accompanied by increases in ER stress, p53 upregulated modulator of apoptosis (PUMA) and CHOP expression, and JNK phosphorylation, similar to PA treatment alone. They showed that inhibition of CHOP or JNK reversed LysoPC-induced lipoapotosis (28). However, this is in contrast to previous data that shows inhibition of CHOP or JNK can delay the onset of apoptosis but does not rescue hepatic cells from PA-mediated lipoapoptosis (36), indicating that PA and LysoPC may differ in their mechanisms of lipotoxic cell death.

We also examined knockdown of de novo phospholipid synthesis though siRNA-mediated inhibition of Pcyt1a gene expression, the enzyme product (CCT) of which is responsible for activating the choline head group during the rate-limiting step of PC synthesis. Previous studies have demonstrated upregulated expression of this ER resident gene in human metabolic syndrome and obesity (6, 46); thus it presents a physiologically relevant target. As PC is the major constituent of membranes (1, 18, 19), reducing its synthesis should have a substantial impact on total phospholipid composition. Several studies have targeted the reacylation step in Lands' cycle remodeling pathway as a means of modulating phospholipid composition. In particular, LPCAT3 has generated significant interest as it is more specific for incorporation of unsaturated as opposed to saturated fatty acids. One study demonstrated that activation of the liver X receptor (LXR) enzyme induced expression of LPCAT3 and ameliorates PA induced ER stress (22). Conversely, knockdown of LPCAT3 in this model, even in the presence of activated LXR, exacerbated PA-mediated ER stress and inflammation (22). Another group investigated the effect of sterol CoA desaturase 1 (SCD1), an enzyme responsible for desaturating saturated long chain fatty acids such as palmitate and sterate, and LPCAT3 in the context of PA-induced

lipotoxicity in HeLa cells (7). Reducing the ability of cells to desaturate toxic SFAs through SCD1 knockdown resulted in increased expression of LPCAT3 but also increased PA-mediated ER stress and lipotoxicity compared to untransfected cells only treated with PA. Knockdown of LPCAT3 in SCD1 deficient cells synergistically enhanced ER stress and lipoapoptosis (7). Both of these studies focus on increasing incorporation of unsaturated fatty acids in phospholipids via LPCAT3 as a means of reducing PA apoptosis. To our knowledge, no previous studies have focused on reducing PC synthesis as a means for reducing PA-induced lipotoxicity. However, complete and prolonged inhibition of PC synthesis can itself result in ER stress (47) and therefore this line of investigation must be targeted with caution. Our data demonstrate that siRNA targeted Pcyt1a knockdown (siPcyt1a) resulted in small, but statistically significant, improvements in several key markers of lipotoxicity including reductions in PA incorporation and overall phospholipid saturation (Table 6-3), markers of ER stress (Fig. 6-7), and cell death (Fig. 6-6).

These results are encouraging, but do not reflect a full reversal of lipotoxic phenotypes. Although the knockdown efficiency was high (greater than approximately 90%, Fig. 6-5A), the ability to reduce lipotoxic markers was not correspondingly high. As Fig. 6-5B shows, siPcyt1a knockdown cells demonstrated a trend of reduced phospholipid levels, but the reduction was not significant. This could be the result of a number of potential limitations of the study design. First, while PC is the major component of membrane phospholipids, there is still a large constituent of other species that also comprise the phospholipid measurements shown in Fig. 6-5B and are not directly impacted by *Pcyt1a* knockdown. Additionally, the significant reduction in mRNA transcript levels may not necessarily correlate to as significant a drop in activity of the CCT enzyme. Increased fatty acid levels are known to promote translocation and activation of this enzyme (44, 48-50), and this may provide a compensatory mechanism to partially recover PC synthesis in these conditions.

Additional compensatory pathways may also play a role in limiting the reversal of lipotoxic phenotypes by *Pcyt1a* knockdown. In most tissues, the CDP-choline pathway accounts for the vast majority of PC synthesis. In the liver, however, there is a pathway to convert phosphatidylenthanolamine (PE) into PC though a series of thee methylation reactions catalyzed by the enzyme phosphatidylenthanolamine N-methyltransferase (PEMT), which can account for up to 30% of hepatic PC synthesis under normal conditions (51, 52). In rodent models fed a choline-deficient (CD) diet, which is designed to prevent normal PC synthesis, PEMT levels were significantly increased (53). Elevation of PEMT expression was also observed in liver-specific CCT knockout mice fed a standard chow diet (54). An increased ratio of PC/PE has also been implicated as a contributing factor to ER stress in obesity (6) and to perturbations in ER calcium due to inhibition of the SERCA transporter (5, 6). Alternatively, decreases in PC/PE ratio have been linked to enhanced membrane permeability, organelle leakage, and increased plasma content of alanine aminotransferase (ALT, a clinical biomarker of hepatotoxicity) (55,

56). Therefore, increased flux though PEMT may mitigate the effects of *Pcyt1a* knockdown on phospholipid composition and explain the mixed results of this study.

Abnormal phospholipid composition and fluidity has been observed in several diseased states and has been connected to dysfunction of the ER membrane. Our previous work (9) led to the hypothesis that inhibiting incorporation of PA into phospholipids by targeting pathways for phospholipid remodeling or PC synthesis would reduce PA-mediated lipotoxicity in an in vitro hepatic model. The results of this study indicate that methods designed to impede PA incorporation into phospholipids can provide some protective effects in conditions of acute PA oversupply. Either inhibition of remodeling by $iPLA_2$ or inhibition of de novo PC biosynthesis via CCT provided modest protection against markers of lipotoxicity in our hepatic model. Neither intervention could by itself fully block PA incorporation into PL, most likely due to functional redundancy of PL synthesis and remodeling pathways. One interesting suggestion for a future study might be to combine inhibition of multiple PL metabolic pathways (e.g., $PACOCF_3$ with *Pcyt1a* knockdown), although cell toxicity may become a concern with such combinations as phospholipids are necessary for cell survival. These findings suggest that modulating these or other phospholipid synthesis and remodeling pathways may represent an effective target for intervention in NASH and related liver diseases.

References

1. Fagone, P., and S. Jackowski. 2009. Membrane phospholipid synthesis and endoplasmic reticulum function. *J. Lipid Res.* **50**.

2. Zhao, Y., Y. Q. Chen, T. M. Bonacci, D. S. Bredt, S. Y. Li, W. R. Bensch, D. E. Moller, M. Kowala, R. J. Konrad, and G. Q. Cao. 2008. Identification and characterization of a major liver lysophosphatidylcholine acyltransferase. *J. Biol. Chem.* **283**: 8258-8265.

3. Spector, A. A., and M. A. Yorek. 1985. Membrane lipid-Composition and cellular function. *J. Lipid Res.* **26**: 1015-1035.

4. Holzer, R. G., E.-J. Park, N. Li, H. Tran, M. Chen, C. Choi, G. Solinas, and M. Karin. 2011. Saturated Fatty Acids Induce c-Src Clustering within Membrane Subdomains, Leading to JNK Activation. *Cell* **147**: 173-184.

5. Li, Y. K., M. T. Ge, L. Ciani, G. Kuriakose, E. J. Westover, M. Dura, D. F. Covey, J. H. Freed, F. R. Maxfield, J. Lytton, and I. Tabas. 2004. Enrichment of endoplasmic reticulum with cholesterol inhibits sarcoplasmic-endoplasmic reticulum calcium ATPase-2b activity in parallel with increased order of membrane lipids - Implications for depletion of endoplasmic reticulum calcium stores and apoptosis in cholesterol-loaded macrophages. *J. Biol. Chem.* **279**: 37030-37039.

6. Fu, S., L. Yang, P. Li, O. Hofmann, L. Dicker, W. Hide, X. Lin, S. M. Watkins, A. R. Ivanov, and G. S. Hotamisligil. 2011. Aberrant lipid metabolism disrupts calcium homeostasis causing liver endoplasmic reticulum stress in obesity. *Nature* **473**: 528-531.

7. Ariyama, H., N. Kono, S. Matsuda, T. Inoue, and H. Arai. 2010. Decrease in Membrane Phospholipid Unsaturation Induces Unfolded Protein Response. *J. Biol. Chem.* **285**: 22027-22035.

8. Borradaile, N. M., X. Han, J. D. Harp, S. E. Gale, D. S. Ory, and J. E. Schaffer. 2006. Disruption of endoplasmic reticulum structure and integrity in lipotoxic cell death. *J. Lipid Res.* **47**: 2726-2737.

9. Leamy, A. K., R. A. Egnatchik, M. Shiota, P. T. Ivanova, D. S. Myers, H. A. Brown, and J. D. Young. 2014. Enhanced synthesis of saturated phospholipids is associated with ER stress and lipotoxicity in palmitate-treated hepatic cells. *J. Lipid Res.* **55**: 1478-1488.

10. Volmer, R., K. van der Ploeg, and D. Ron. 2013. Membrane lipid saturation activates endoplasmic reticulum unfolded protein response transducers through their transmembrane domains. *Proceedings of the National Academy of Sciences of the United States of America* **110**: 4628-4633.

11. Deguil, J., L. Pineau, E. C. R. Snyder, S. Dupont, L. Beney, A. Gil, G. Frapper, and T. Ferreira. 2011. Modulation of Lipid-Induced ER Stress by Fatty Acid Shape. *Traffic* **12**: 349-362.

12. Pagliassotti, M. J. 2012. Endoplasmic Reticulum Stress in Nonalcoholic Fatty Liver Disease. *Annual Review of Nutrition, Vol 32* **32**: 17-+.

13. Ozcan, U., Q. Cao, E. Yilmaz, A. H. Lee, N. N. Iwakoshi, E. Ozdelen, G. Tuncman, C. Gorgun, L. H. Glimcher, and G. S. Hotamisligil. 2004. Endoplasmic reticulum stress links obesity, insulin action, and type 2 diabetes. *Science* **306**: 457-461.

14. Leamy, A. K., R. A. Egnatchik, and J. D. Young. 2013. Molecular mechanisms and the role of saturated fatty acids in the progression of non-alcoholic fatty liver disease. *Prog. Lipid Res.* **52**: 165-174.

15. Gregor, M. F., L. Yang, E. Fabbrini, B. S. Mohammed, J. C. Eagon, G. S. Hotamisligil, and S. Klein. 2009. Endoplasmic Reticulum Stress Is Reduced in Tissues of Obese Subjects After Weight Loss. *Diabetes* **58**: 693-700.

16. Kennedy, E. P., and S. B. Weiss. 1956. The function of cytidine coenzymes in the biosynthesis of phospholipids. *J. Biol. Chem.* **222**: 193-214.

17. Lands, W. E. M. 1958. Metabolism of glycerolipids: A comparison of lecithin and triglyceride synthesis. *J. Biol. Chem.* **231**: 883-888.

18. Testerink, N., M. H. M. van der Sanden, M. Houweling, J. B. Helms, and A. B. Vaandrager. 2009. Depletion of phosphatidylcholine affects endoplasmic reticulum morphology and protein traffic at the Golgi complex. *J. Lipid Res.* **50**: 2182-2192.

19. Lagace, T. A., and N. D. Ridgway. 2013. The role of phospholipids in the biological activity and structure of the endoplasmic reticulum. *Biochimica Et Biophysica Acta-Molecular Cell Research* **1833**: 2499-2510.

20. Murakami, M., and I. Kudo. 2002. Phospholipase A(2). *Journal of Biochemistry* **131**: 285-292.

21. Murakami, M. M. M., Y. Taketomi, Y. Miki, H. Sato, T. Hirabayashi, and K. Yamamoto. 2011. Recent progress in phospholipase A(2) research: From cells to animals to humans. *Prog. Lipid Res.* **50**: 152-192.

22. Rong, X., C. J. Albert, C. Hong, M. A. Duerr, B. T. Chamberlain, E. J. Tarling, A. Ito, J. Gao, B. Wang, P. A. Edwards, M. E. Jung, D. A. Ford, and P. Tontonoz. 2013. LXRs Regulate ER Stress and Inflammation through Dynamic Modulation of Membrane Phospholipid Composition. *Cell Metabolism* **18**: 685-697.

23. Shindou, H., D. Hishikawa, T. Harayama, K. Yuki, and T. Shimizu. 2009. Recent progress on acyl CoA: lysophospholipid acyltransferase research. *J. Lipid Res.* **50**: S46-S51.

24. Chen, X., B. A. Hyatt, M. L. Mucenski, R. J. Mason, and J. M. Shannon. 2006. Identification and characterization of a lysophosphatidylcholine acyltransferase in alveolar type II cells. *Proceedings of the National Academy of Sciences of the United States of America* **103**: 11724-11729.

25. Nakanishi, H., H. Shindou, D. Hishikawa, T. Harayama, R. Ogasawara, A. Suwabe, R. Taguchi, and T. Shimizu. 2006. Cloning and characterization of mouse lung-type acyl-CoA: Lysophosphatidylcholine acyltransferase 1 (LPCAT1) - Expression in alveolar type II cells and possible involvement in surfactant production. *J. Biol. Chem.* **281**: 20140-20147.

26. Hishikawa, D., T. Hashidate, T. Shimizu, and H. Shindou. 2014. Diversity and function of membrane glycerophospholipids generated by the remodeling pathway in mammalian cells. *J. Lipid Res.* **55**: 799-807.

27. Pineau, L., J. Colas, S. Dupont, L. Beney, P. Fleurat-Lessard, J.-M. Berjeaud, T. Berges, and T. Ferreira. 2009. Lipid-Induced ER Stress: Synergistic Effects of Sterols and Saturated Fatty Acids. *Traffic* **10**: 673-690.

28. Kakisaka, K., S. C. Cazanave, C. D. Fingas, M. E. Guicciardi, S. F. Bronk, N. W. Werneburg, J. L. Mott, and G. J. Gores. 2012. Mechanisms of lysophosphatidylcholine-induced hepatocyte lipoapoptosis. *Am. J. Physiol.-Gastroint. Liver Physiol.* **302**: G77-G84.

29. Han, M. S., S. Y. Park, K. Shinzawa, S. Kim, K. W. Chung, J.-H. Lee, C. H. Kwon, K.-W. Lee, J.-H. Lee, C. K. Park, W. J. Chung, J. S. Hwang, J.-J. Yan, D.-K. Song, Y. Tsujimoto, and M.-S. Lee. 2008. Lysophosphatidylcholine as a death effector in the lipoapoptosis of hepatocytes. *J. Lipid Res.* **49**: 84-97.

30. Cnop, M., L. Ladriere, M. Igoillo-Esteve, R. F. Moura, and D. A. Cunha. 2010. Causes and cures for endoplasmic reticulum stress in lipotoxic beta-cell dysfunction. *Diabetes Obesity & Metabolism* **12**: 76-82.

31. Eruslanov, E., and S. Kusmartsev. 2010. Identification of ROS Using Oxidized DCFDA and Flow-Cytometry. *Advanced Protocols in Oxidative Stress II* **594**.

32. Arndt-Jovin, D. J., and T. M. Jovin. 1989. Fluorescence Labeling and Microscopy of DNA. *Methods in Cell Biology* **30**.

33. Egnatchik, R. A., A. K. Leamy, Y. Noguchi, M. Shiota, and J. D. Young. 2014. Palmitate-induced Activation of Mitochondrial Metabolism Promotes Oxidative Stress and Apoptosis in H4IIEC3 Rat Hepatocytes. *Metabolism-Clinical and Experimental* **63**: 283-295.

34. Egnatchik, R., A. Leamy, D. Jacobson, M. Shiota, and J. Young. 2014. ER calcium release promotes mitochondrial dysfunction and hepatic cell lipotoxicity in response to palmitate overload. *Molecular Metabolism* **3**: 544-553.

35. Wei, Y., D. Wang, C. L. Gentile, and M. J. Pagliassotti. 2009. Reduced endoplasmic reticulum luminal calcium links saturated fatty acid-mediated endoplasmic reticulum stress and cell death in liver cells. *Molecular and Cellular Biochemistry* **331**: 31-40.

36. Pfaffenbach, K. T., C. L. Gentile, A. M. Nivala, D. Wang, Y. R. Wei, and M. J. Pagliassotti. 2010. Linking endoplasmic reticulum stress to cell death in hepatocytes: roles of C/EBP homologous protein and chemical chaperones in palmitate-mediated cell death. *Am. J. Physiol.-Endocrinol. Metab.* **298**: E1027-E1035.

37. Hardy, S., W. El-Assaad, E. Przybytkowski, E. Joly, M. Prentki, and Y. Langelier. 2003. Saturated fatty acid-induced apoptosis in MDA-MB-231 breast cancer cells - A role for cardiolipin. *J. Biol. Chem.* **278**: 31861-31870.

38. Listenberger, L. L., D. S. Ory, and J. E. Schaffer. 2001. Palmitate-induced apoptosis can occur through a ceramide-independent pathway. *J. Biol. Chem.* **276**: 14890-14895.

39. Noguchi, Y., J. D. Young, J. O. Aleman, M. E. Hansen, J. K. Kelleher, and G. Stephanopoulos. 2009. Effect of Anaplerotic Fluxes and Amino Acid Availability on Hepatic Lipoapoptosis. *J. Biol. Chem.* **284**: 33425-33436.

40. Schmid, P. C., E. Deli, and H. H. O. Schmid. 1995. GENERATION AND REMODELING OF PHOSPHOLIPID MOLECULAR-SPECIES IN RAT HEPATOCYTES. *Archives of Biochemistry and Biophysics* **319**: 168-176.

41. Shinzawa, K., and Y. Tsujimoto. 2003. PLA(2) activity is required for nuclear shrinkage in caspase-independent cell death. *Journal of Cell Biology* **163**: 1219-1230.

42. Kent, C. 1990. REGULATION OF PHOSPHATIDYLCHOLINE BIOSYNTHESIS. *Prog. Lipid Res.* **29**: 87-105.

43. Karim, M., P. Jackson, and S. Jackowski. 2003. Gene structure, expression and identification of a new CTP : phosphocholine cytidylyltransferase isoform. *Biochimica Et Biophysica Acta-Molecular and Cell Biology of Lipids* **1633**: 1-12.

44. Pelech, S. L., P. H. Pritchard, D. N. Brindley, and D. E. Vance. 1983. FATTY-ACIDS PROMOTE TRANSLOCATION OF CTP-PHOSPHOCHOLINE CYTIDYLYLTRANSFERASE TO THE ENDOPLASMIC-RETICULUM AND STIMULATE RAT HEPATIC PHOSPHATIDYLCHOLINE SYNTHESIS. *J. Biol. Chem.* **258**: 6782-6788.

45. Schmid, P. C., I. Spimrova, and H. H. O. Schmid. 1995. INCORPORATION OF EXOGENOUS FATTY-ACIDS INTO MOLECULAR-SPECIES OF RAT HEPATOCYTE PHOSPHATIDYLCHOLINE. *Archives of Biochemistry and Biophysics* **322**: 306-312.

46. Sharma, N. K., S. K. Das, A. K. Mondal, O. G. Hackney, W. S. Chu, P. A. Kern, N. Rasouli, H. J. Spencer, A. Yao-Borengasser, and S. C. Elbein. 2008. Endoplasmic Reticulum Stress Markers Are Associated with Obesity in Nondiabetic Subjects. *Journal of Clinical Endocrinology & Metabolism* **93**: 4532-4541.

47. Van der Sanden, M. H. M., M. Houweling, L. M. G. Van Golde, and A. B. Vaandrager. 2003. Inhibition of phosphatidylcholine synthesis induces expression of the endoplasmic reticulum stress and apoptosis-related protein CCAAT/enhancer-binding protein-homologous protein (CHOP/GADD153). *Biochemical Journal* **369**: 643-650.

48. Pelech, S. L., and D. E. Vance. 1982. REGULATION OF RAT-LIVER CYTOSOLIC CTP - PHOSPHOCHOLINE CYTIDYLYLTRANSFERASE BY PHOSPHORYLATION AND DEPHOSPHORYLATION. *J. Biol. Chem.* **257**: 4198-4202.

49. Cornell, R., and D. E. Vance. 1987. TRANSLOCATION OF CTP-PHOSPHOCHOLINE CYTIDYLTRANSFERASE FROM CYTOSOL TO MEMBRANES IN HELA CELLS-STIMULATION BY FATTY-ACID, FATTY ALCOHOL, MONOACYGLYCEROL AND DIACYLGLYCEROL. *Biochimica Et Biophysica Acta* **919**: 26-36.

50. Sleight, R., and C. Kent. 1983. REGULATION OF PHOSPHATIDYLCHOLINE BIOSYNTHESIS IN MAMMALIAN-CELLS .2. EFFECTS OF PHOSPHOLIPASE-C TREATMENT ON THE ACTIVITY AND SUBCELLULAR-DISTRIBUTION OF CTP-PHOSPHOCHOLINE CYTIDYLYLTRANSFERASE IN CHINESE-HAMSTER OVARY AND LM CELL-LINES. *J. Biol. Chem.* **258**: 831-835.

51. Vance, D. E., C. J. Walkey, and Z. Cui. 1997. Phosphatidylethanolamine N-methyltransferase from liver. *Biochimica Et Biophysica Acta-Lipids and Lipid Metabolism* **1348**: 142-150.

52. Walkey, C. J., L. Q. Yu, L. B. Agellon, and D. E. Vance. 1998. Biochemical and evolutionary significance of phospholipid methylation. *J. Biol. Chem.* **273**: 27043-27046.

53. Cui, Z., and D. E. Vance. 1996. Expression of phosphatidylethanolamine N-methyltransferase-2 is markedly enhanced in long term choline-deficient rats. *J. Biol. Chem.* **271**: 2839-2843.

54. Jacobs, R. L., C. Devlin, I. Tabas, and D. E. Vance. 2004. Targeted deletion of hepatic CTP : phosphocholine cytidylyltransferase alpha in mice decreases plasma high density and very low density lipoproteins. *J. Biol. Chem.* **279**: 47402-47410.

55. Vance, D. E., Z. Li, and R. L. Jacobs. 2007. Hepatic phosphatidylethanolamine N-methyltransferase, unexpected roles in animal biochemistry and physiology. *J. Biol. Chem.* **282**: 33237-33241.

56. Li, Z. Y., L. B. Agellon, and D. E. Vance. 2005. Phosphatidylcholine homeostasis and liver failure. *J. Biol. Chem.* **280**: 37798-37802.

CHAPTER 7

INTRAVENOUS INFUSION OF ETHYL PALMITITATE CAN RECAPITULATE ACUTE LIPOTOXIC PHENOTYPES IN AN IN VIVO RODENT MODEL

Introduction

There is a burgeoning epidemic of non-alcoholic fatty liver disease (NAFLD) largely due to increases in the prevalence of obesity around the world. NAFLD is currently the leading cause of referrals to US hepatology clinics (1), and cirrhosis stemming from NAFLD progression is the third leading cause of liver transplants (2). The startling increase in NAFLD incidence rate makes it a research priority to understand the mechanisms that drive simple steatosis and its progression into more acute and deadly forms of liver disease such as non-alcoholic steatohepatitis (NASH) and/or cirrhosis.

The initial phase of NAFLD is characterized by increased accumulation of triglycerides in the liver, the fatty acid constituents of which can come from three main sources: *de novo* lipogenesis, diet, and circulating free fatty acids released from adipose tissue. Adipocytes are designed to store large amounts of excess fat, but non-adipose tissues such as the liver do not have the capacity to do so long-term. Excessive accumulation of lipids in the liver has been associated with organ dysfunction and hepatocyte cell death, known as lipotoxicity. *In vitro* experiments have demonstrated the distinctly different role that saturated versus unsaturated fatty acids play in lipotoxicity. Specifically, saturated fatty acids (SFAs) have been shown to cause widespread cellular stress and dysfunction while unsaturated fatty acids increase triglyceride accumulation but without changes in cell viability or function (3-6). These data indicate that elevations in circulating and/or hepatic SFAs may promote progressive liver damage *in vivo*.

There are two main methods for increasing physiological levels of SFAs: feeding high saturated fat diets or direct intravenous infusion of SFA. Both of these methods have been used over the years, although alterations made in diet macronutrients to favor specific fatty acids have been historically more popular due to their inherently less difficult implementation. Several groups have focused specifically on developing *in vivo* models of NAFLD/NASH by increasing the relative proportion of SFAs in rodent diets, including the so-called "cafeteria diet rat" (7) and "fast food diet mouse" (8) models. The inclusion of high levels of saturated fats in these diets appears to trigger an inflammatory stress response that results in progression of NAFLD to NASH, which is not observed in rodents fed a standard high-fat diet (5, 7, 8).

Other groups have developed methods for infusing saturated fatty acids directly into an animal's bloodstream to recapitulate the acute lipotoxic effects of SFAs observed *in vitro* and determine if elevation of SFAs alone can lead to progressive liver disease. This method is inherently more difficult due to blood solubility issues, infusion rate constraints and the intricate animal surgeries required. However, the advantage is that this approach initiates SFA lipotoxicity more rapidly

and directly than dietary interventions. As a result, there are fewer confounding factors that must be considered as contributing to alterations in liver homeostasis. One recent study demonstrated that infusion of a lard oil emulsion mainly composed of SFAs effectively induced hepatic ER stress, inflammation and cellular cytotoxicity in rats (9). A similar experiment used direct palmitate infusion (as a 1:1 ratio of ethyl palmitate) to demonstrate inflammatory and apoptotic effects in islet β-cells of mice (10).

In this preliminary study, we sought to recapitulate a progressive NASH-like liver state *in vivo* order to test the mechanistic hypotheses we generated in previously reported work regarding lipotoxicity *in vitro* (4). Our initial aim was to use a diet high in saturated fat to induce a NASH-like phenotype in Sprague-Dawley rats, a model we chose due to some inherent physiological flaws with using other NASH models such as methionine and choline deficient (MCD) diet or ApoE -/- mice, as discussed in Chapter 2. Our goal was to determine the earliest time point at which markers of liver injury begin to manifest. The pilot study was conducted over 14 weeks by feeding the same Western AIN-76 diet used by Charlton et al. (8), but without the addition of fructose to drinking water. We sacrificed one animal every two weeks, and analyzed tissue and blood samples for markers of liver injury. Although the week-14 rat was removed from the study due to an unknown illness, the rat on the diet for 12 weeks showed large increases in adiposity, elevated liver triglycerides and some indicators of cellular dysfunction. However, markers of progressive NASH were inconclusive.

In order to develop an acute model of *in vivo* lipotoxicity that would not require long-term diet interventions, we next examined the effects of direct fatty acid infusion into Sprague-Dawley rats. Though the expert assistance of the Vanderbilt Mouse Metabolic Phenotyping Center (MMPC), we were able to perform the necessary surgeries to enable continuous infusion of ethyl palmitate though a jugular vein catheter into conscious, unrestrained, and unstressed animals. Our preliminary data indicate that direct infusion of ethyl palmitate for 5 h results in changes in phospholipid composition, similar to our results *in vitro*, compared to vehicle infusions. These promising initial results will pave the way for future studies that will test hypotheses generated from our *in vitro* studies in a more physiologically relevant *in vivo* system.

Methods

Animals and surgical procedures

For the feeding study, genetically unaltered male Sprague-Dawley rats (Jackson Laboratories, Bar Harbor, ME) were maintained in common cages (3-4 rats/cage) and had free access to standard rodent chow and water one week prior to initiation of the study. The animals were labeled and maintained on a high saturated fat, fructose and cholesterol diet with ~12% saturated fat (AIN-76 Western diet, Test Diet, St. Louis, MO) for the specified duration. Mice were

weighed two times per week and euthanized by barbiturate overdose. One lobe of the liver was tied off and either snap frozen using liquid nitrogen or preserved in 10% buffered formalin.

For the lipid infusion studies, wild-type C57BL/6J mice were maintained in individual cages on a standard rodent diet with free access to food prior to catheterization surgeries. After surgeries, mice were housed individually and recovered for seven days, at minimum, to ensure they returned to within 10% of pre-surgical weight before initiating studies.

Lipid emulsions

Lipid emulsions for *in vivo* infusions were prepared using a protocol adapted and kindly provided by Dr. Kosei Eguchi of the University of Tokyo. The protocol is described briefly as follows. Mix 4.8% lecithin solution (in water), 10% glycerol (in water), and water at the ratio of 1:1:1 (Designate as 'Solution A'). To prepare the vehicle solution, mix 'Solution A' and water at the ratio of 3:1. To prepare the ethyl-palmitate solution, mix Solution A, ethyl palmitate (Sigma Aldrich), and water at the ratio of 15:4:1. Lastly, sonicate the vehicle solution and the ethyl-palmitate solution until the ethyl-palmitate solution is completely emulsified by sonicating for 5 minutes followed by 1 minute of vortex, repeated 9 times.

Euglycemic clamp and lipid infusions

Mice were fasted for five hours prior to initiation of each clamp study, and then externalized mouse catheters were attached to infusion syringes as shown in Fig. 7-1 one hour prior. Prior to the start of any infusions, an arterial blood sample was taken to evaluate arterial blood glucose concentration and hematocrit. Venous infusion of saline-washed donor erythocytes (~1 μL/min) was administered during the clamp study to prevent a decline in hematocrit due to arterial sampling.

In the first pilot study (Fig. 7-1A), ethyl palmitate was infused from t=1h until t=8h (3500 μmol/kg prime followed by 7 μmol/kg/min continuous infusion) and erythocytes were infused from t=4h until t=8h. Blood glucose was measured every hour, nonesterified fatty acids (NEFAs) were measured at t=6.7 and 8h, and insulin was measured at t=6 and 8h.

In the second pilot study (Fig. 7-1B), a euglycemic clamp with somatostatin was performed. At t=0h, somatostatin (20 μg/kg/min), glucagon (1-3 ng/kg/min) and insulin (0.8 mU/kg/min) were infused at rates based on previous methods employed in rodent studies (11). Glucose was infused at a variable rate to maintain euglycemia based on blood glucose levels measured every 10 minutes. Ethyl palmitate was continuously administered starting at t=1h until t=6h (5h total infusion) at two different levels (37.5 or 75 μmol/kg/min). Insulin, NEFAs and hematocrit were measured at the completion of the study.

In the third pilot experiment (Fig. 7-1C), ethyl palmitate or an ethanol (EtOH) emulsion vehicle control were infused for 5 hours per day over the course of 3 days at a rate of 37.5 μmol/kg/min. Arterial glucose and NEFA concentrations were measured on the third day without prior fasting.

Plasma was stored at -20°C until analysis. Mice were sacrificed via cervical dislocation and liver tissue was excised and immediately snap-frozen in liquid nitrogen. Subsequently, the frozen tissue was stored in the -80°C freezer until use.

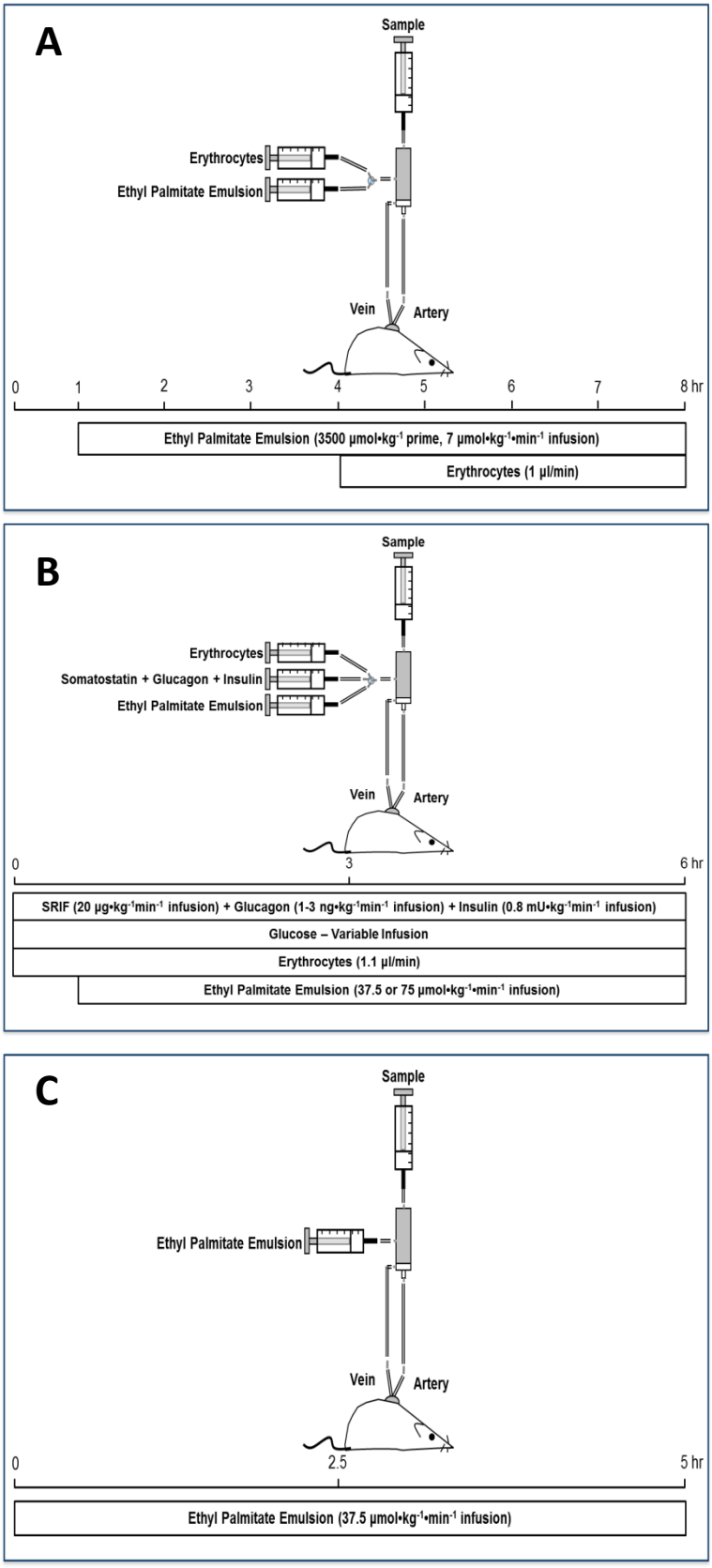

Figure 7-1. Schematic outline of experimental procedures and timeline. Arterial and jugular catheterization was performed for the sampling and infusion protocols of the ethyl palmitate (EP) infusion. Studies were performed seven days after catheterization surgeries to assess the effect of EP infusion on the liver. The first pilot study was a simple prime-continuous infusion of EP (A). The second pilot study was performed with a euglycemic clamp to control blood glucose levels requiring the infusion of somatostatin (SRIF), glucagon and insulin in addition to medium (37.5 µmol/kg/min) or high (75 µmol/kg/min) rates of continuous EP infusion (B). The third pilot study used no clamp and infused EP 5h per day over three contiguous days (C).

Histology and lipid analysis

Formalin-preserved liver tissue samples were embedded in paraffin and sectioned (5 μm thick). Deparaffinized, hydrated serial liver tissue sections were stained with hematoxylin-eosin (H&E) using standardized protocols from the Vanderbilt University Medical Center Department of Pathology. Animal pathologist Dr. Kelli Boyd analyzed H&E stained tissue sections for steatosis and markers of NASH, taking digital images with a microscope.

Fatty acyl lipid analysis was performed on snap frozen liver tissue by the Vanderbilt Hormone Assay and Analytical Services Core using thin-layer chromatography (TLC) and gas chromatography-flame ionization detection (GC-FID) techniques. Briefly, lipids were extracted from snap frozen tissue by homogenizing the sample and using a modified Folch separation. An internal standard (1,2-dipentadecanoyl-sn-glycero-3-phosphocholine) for phospholipids was added to the lipid-containing chloroform phase. Total lipids were then extracted and separated by TLC using petroleum ether/ethyl ether/acetic acid (80/20/1, v/v/v) on silica plates. Spots corresponding to PLs, TAGs, and FFAs were visualized with rhodamine 6G in 95% ethanol and scraped individually into glass tubes for transmethylation. Transmethylation was performed using a boron trifluoride-methanol 10% (w/w) solution. Derivatized lipids were then analyzed using a GC-FID, where standardized calibration curves were used to analyze fatty acid content.

TEM

After catheterizing the animal and tying off and removing one large lobe, the liver was perfused with a 2.5% glutaraldehyde fixative solution in 0.1 M sodium cacodylate. After perfusing for 10 minutes, the fixed organ was removed and tissue samples of approximately 2mm x 2mm were sectioned off and placed back into a tube containing 2.5% glutaraldehyde fixative solution in 0.1 M sodium cacodylate buffer for 1 h at room temperature followed by 23 h at 4°C. Samples were postfixed in 1.25% osmium tetroxide and subsequently stained with 2% aqueous uranyl acetate. Embedded cells were then thin-sectioned and viewed on a Philips/FEI T-12 high-resolution transmission electron microscope.

Glucose, insulin and NEFA analysis

Plasma NEFA concentrations (NEFA C kit; Wako Chemicals, Richmond, VA) and glucose were determined spectrophotometrically as previously described (12). Insulin levels were determined though a double antibody method (13).

Results

Physiological changes in the liver were limited in rats fed high saturated fat "Western diet" over the course of 12 weeks.

Animals maintained on a high saturated fat, "Western" fast-food (FF) diet continued to gain weight over the time course of 12 weeks, with no indication of plateauing (Fig. 2A). Serum alanine aminotransferase (ALT), aspartate aminotransferase (AST), cholesterol and triglycerides were highly variable across different animals and only showed a slight trend toward increased cholesterol and triglyceride levels after 10–12 weeks of FF diet feeding (Fig. 7-2).

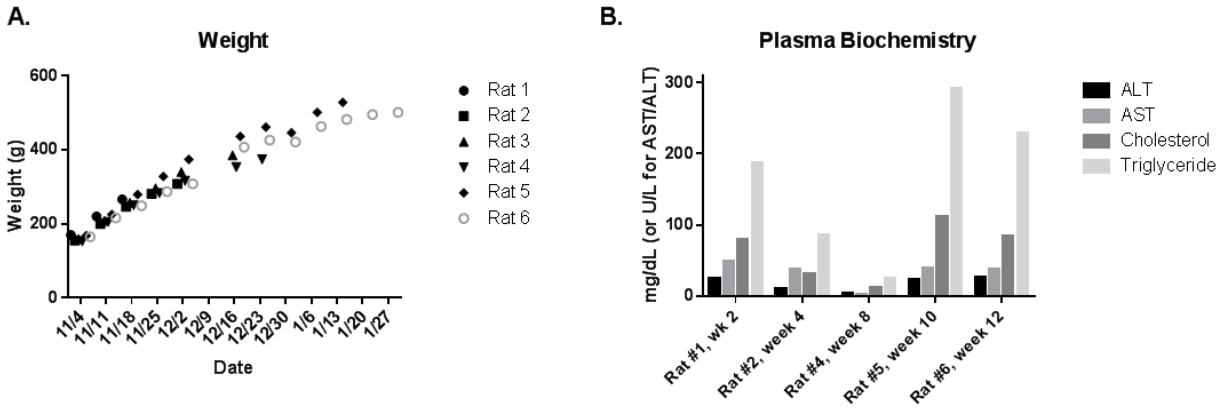

Figure 7-2. Change in weight and plasma biochemical markers over the 12-week time course. All animals on FF diet gained weight over 12 weeks. Measurements of triglycerides, cholesterol, AST and ALT were variable between rats, though it appeared that cholesterol and triglycerides increased at the end of the study while there was no clear pattern with AST and ALT. Alanine aminotransferase (ALT); Aspartate aminotransferase (AST). N=1 at each time point.

FF diet fed rats exhibit indicators of increased liver damage and ER stress but no significant changes in phospholipid composition or NASH markers

Although serum AST and ALT are used as clinical biomarkers for assessing liver damage, recent studies have found that neither is an accurate independent predictor of NASH in humans (14, 15). Therefore, we sought to examine liver tissue samples collected from FF diet fed rats for markers of NASH and liver injury. Hematoxylin-eosin stained sections of liver tissue were examined for changes in liver morphology by a pathologist. Over the 12-week timeline, there was increased lipid droplet accumulation (steatosis) in the hepatic tissue, though largely microvesicular in nature (Fig. 7-3). At week 12 (rat #6) there was evidence of inflammatory and/or immune cell infiltration in portal areas (Fig. 7-3G, H) which may indicate early signs of increased liver damage. Masson's trichome stains of the liver tissue (data not shown) did not show any indications of fibrosis associated with progressive NASH.

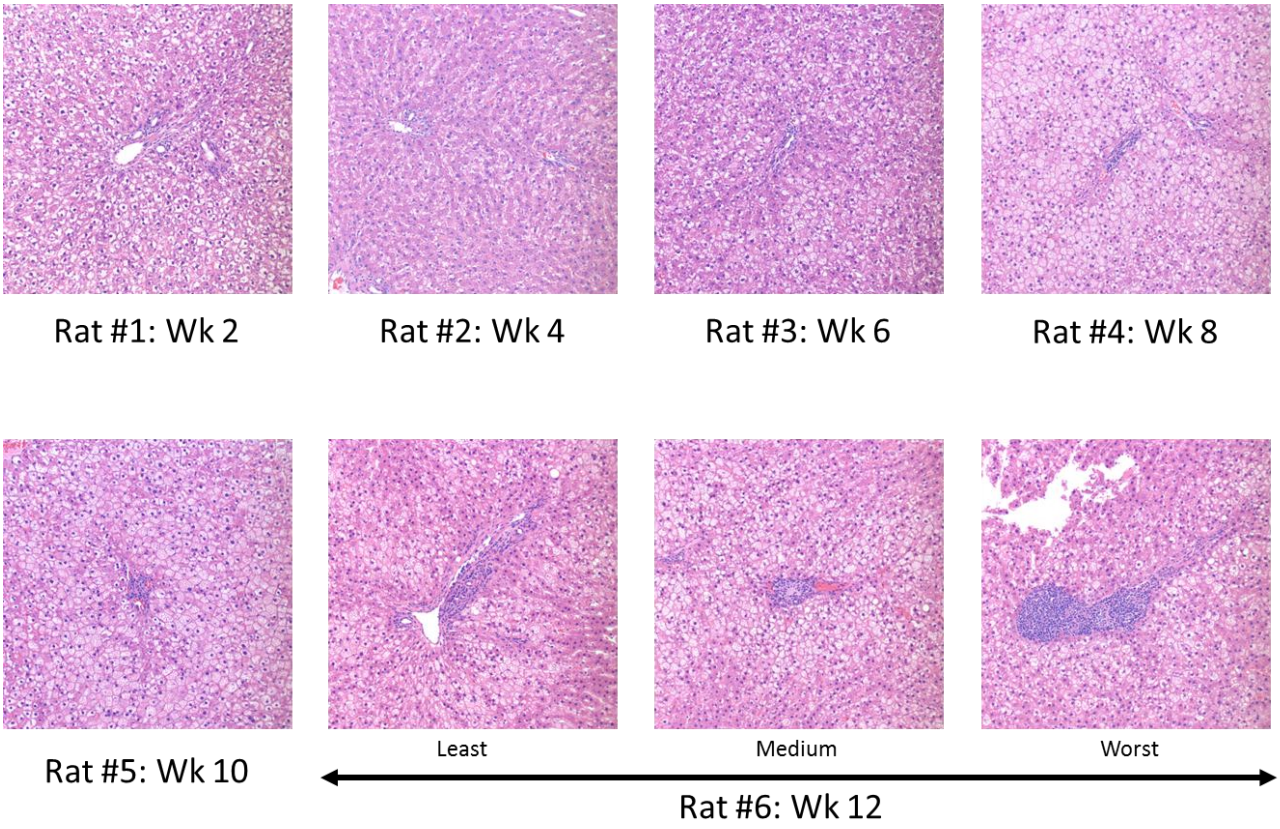

Figure 7-3. Hematoxylin-eosin (H&E) stained sections of liver tissue from FF diet fed rats. Increased lipid deposition was evident in H&E stained liver sections collected over the course of the experiment. There were no distinct markers of a NASH-like phenotype, but the Week 12 rat (#6) demonstrated various degrees of tissue injury ranging from mild ("Least") to sites of more acute indicators of disease ("Most") that had some did have some evidence of increased immune cell infiltration. N=1 at each time point.

Transmission electron microscope (TEM) images of stained liver samples show changes in hepatic morphology after long-term FF diet feeding. After 12 weeks, hepatoctyes contained lipid droplets that were both more abundant and larger in size compared those from animals on the diet for only 2 weeks (Fig. 7-4 A vs. E). In Fig. 7-4, arrowheads point toward the ER membrane and, after 12 weeks on the FF diet, it can be observed that ER cisternae show increased dilation and distention, an indicator of ER stress (4, 6).

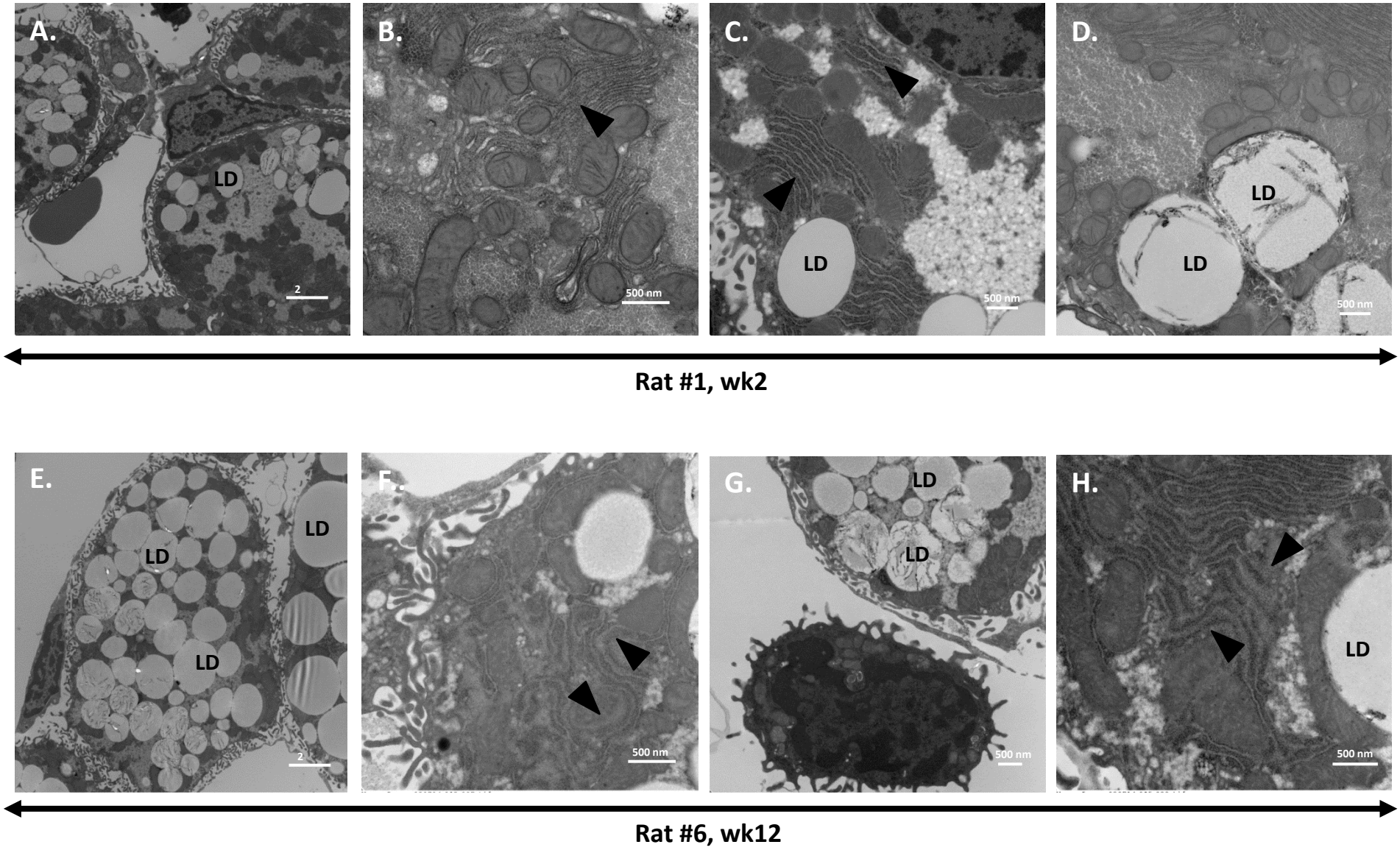

Figure 7-4. TEM images of rats on FF diet at week 2 versus week 12 showed increased triglyceride accumulation, indicators of ER membrane distention, and infiltration of immune cells. Cellular morphology in rat #1, wk 2 (A-D) and rat #6, wk12 (E-H) was observed by high-resolution imaging with transmission electron microscopy demonstrating increased triglyceride accumulation and ER dilation after longer duration on the diet (E-H). Immune cells were found in samples from rat #6, wk12 (G) but not in rat #1, wk2. Arrowheads point towards ER membrane. LD, lipid droplets.

ER stress in environments of high saturated fat, as shown here, has been previously linked to changes in phospholipid composition (4, 6, 16). However, there did not appear to be any clear trend in changes in phospholipid abundance (Fig. 7-5A) or composition (Table 7-1) over the course of the feeding study. Diacylglycerides and triacylglycerides exhibited trends of increasing accumulation for animals on the FF diet for longer periods of time (Fig. 7-5B and C), but again, there were no clear compositional changes in these lipid pools (Tables 7-2 and 7-3). Overall, the data from this study indicate that while there was progression in liver pathology over the duration of the feeding time course, there was no indication of NASH development or altered fatty acid composition in major lipid species.

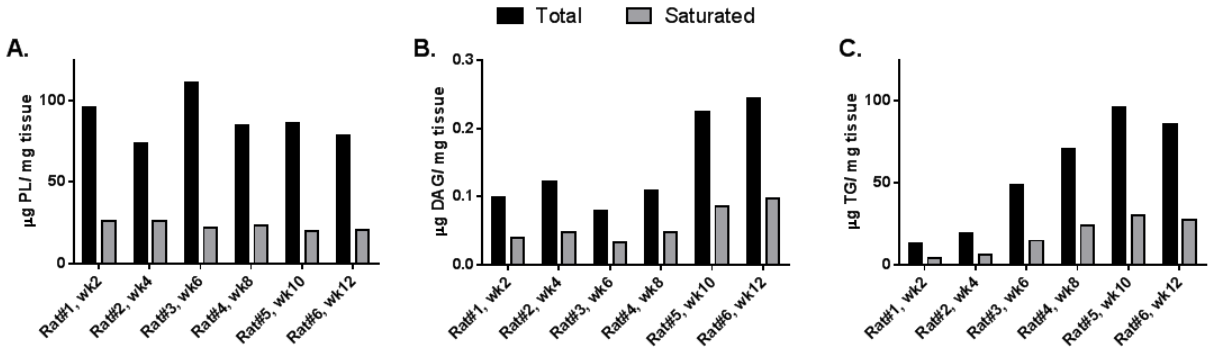

Figure 7-5. Rats on FF diet demonstrated a trend toward increased overall and saturated diacylglycerol and triglyceride accumulation, without changes in phospholipid levels. Absolute amounts of overall and saturated phospholipids (A), diacylglycerides (B) and triacylglycerides (C) were determined by thin layer chromatography (TLC) separation of lipid classes and analysis by gas chromatography flame ionization detection (GC-FID). N=1 at each time point.

Fatty Acid	Rat#1, wk2	Rat#2, wk4	Rat#3, wk6	Rat#4, wk8	Rat#5, wk10	Rat#6, wk12
14:0	0.34	0.41	0.39	0.42	0.52	0.43
16:0	18.02	17.52	17.40	16.57	16.74	15.67
16:1	0.91	1.22	1.05	1.48	2.63	1.83
18:0	20.28	18.86	19.80	20.30	16.81	19.36
18:1w9	8.13	9.51	8.20	8.73	10.01	9.20
18:1w7	2.90	4.47	2.87	2.93	3.89	3.15
18:2	12.58	11.58	12.96	13.68	13.23	11.18
20:3w6	2.19	2.85	3.49	3.98	3.15	3.20
20:4	24.45	24.80	25.60	24.55	24.01	26.80
20:5	0.47	0.44	0.44	0.60	0.68	0.55
22:4w6	0.33	0.35	0.35	0.32	0.33	0.35
22:5w3	0.90	0.62	0.97	0.81	0.83	0.73
22:6	8.48	7.36	6.50	5.64	7.19	7.54
% SFA	38.64	36.79	37.58	37.29	34.06	35.46
% UFA	61.36	63.21	62.42	62.71	65.94	64.54

Table 7-1. Phospholipid composition of liver tissue samples collected from individual rats at indicated time points. There were no observable changes in phospholipid composition over the course of the 12-week feeding study. Phospholipids were separated by thin layer chromatography and analyzed by gas chromatography-flame ionization detection (GC-FID). Data represent mean fatty acid %. N=1 at each time point. SFA, saturated fatty acids; UFA, unsaturated fatty acids.

Fatty Acid	Rat#1, wk2	Rat#2, wk4	Rat#3, wk6	Rat#4, wk8	Rat#5, wk10	Rat#6, wk12
16:0	39.32	39.25	42.03	43.67	38.43	39.53
18:0	30.41	31.58	20.84	26.57	27.93	15.03
18:1w9	16.90	25.65	29.83	25.44	28.04	32.01
18:1w7	0.00	3.52	3.64	4.32	5.60	5.24
18:2	5.68	0.00	3.66	0.00	0.00	4.71
20:4	7.69	0.00	0.00	0.00	0.00	0.00
% SFA	69.73	70.82	62.86	70.24	66.36	54.56
% UFA	30.27	29.18	37.14	29.76	33.64	45.44

Table 7-2. Diacylglycerol composition of liver tissue samples collected from individual rats at indicated time points. There was no clear pattern in changes in diacylglycerol composition over the course of the 12-week feeding study. Diacylglycerides were separated by thin layer chromatography and analyzed by gas chromatography-flame ionization detection (GC-FID). Data represent mean fatty acid %. N=1 at each time point. SFA, saturated fatty acids; UFA, unsaturated fatty acids.

Fatty Acid	Rat#1, wk2	Rat#2, wk4	Rat#3, wk6	Rat#4, wk8	Rat#5, wk10	Rat#6, wk12
14:0	3.21	4.23	4.11	4.70	3.64	3.68
16:0	31.93	31.23	30.11	33.70	31.64	32.10
16:1	4.21	6.00	4.59	8.33	8.89	7.18
18:0	2.15	1.99	1.56	1.51	1.63	1.77
18:1w9	44.41	44.74	46.10	39.63	43.52	44.44
18:1w7	4.81	5.92	3.92	4.91	5.02	4.26
18:2	8.48	5.90	7.85	6.11	5.17	5.55
18:3w6	0.00	0.00	0.12	0.00	0.00	0.10
18:3 w3	0.36	0.00	0.35	0.30	0.22	0.22
20:3w6	0.00	0.00	0.22	0.18	0.00	0.13
20:4	0.45	0.00	0.32	0.24	0.15	0.23
22:4w6	0.00	0.00	0.16	0.00	0.00	0.11
22:5w3	0.00	0.00	0.21	0.14	0.00	0.00
22:6	0.00	0.00	0.37	0.25	0.13	0.22
% SFA	37.28	37.44	35.78	39.91	36.90	37.55
% UFA	62.72	62.56	64.22	60.09	63.10	62.45

Table 7-3. Triglyceride composition of liver tissue samples collected from individual rats at indicated time points. There was no clear pattern in changes in triglyceride composition over the course of the 12 week feeding study. Triglycerides were separated by thin layer chromatography and analyzed by gas chromatography-flame ionization detection (GC-FID). Data represent mean fatty acid %. N=1 at each time point. SFA, saturated fatty acids; UFA, unsaturated fatty acids.

Pilot studies using a direct infusion of ethyl palmitate into mouse circulation yields promising initial results

Since FF diet feeding requires a great length of time to recapitulate a NASH-like liver phenotype (8) and we were unable to achieve similar results in our rat study, we chose to investigate other methods of inducing lipotoxicity *in vivo.* Prior work by Eguchi *et al.* led us to experiment with direct infusion of ethyl palmitate into the systemic circulation of mice. These experiments were performed in collaboration with the Vanderbilt MMPC.

In the first pilot experiment, ethyl palmitate (EP) was infused for 7 h at a relatively low rate (7 μmol/kg/min) and compared to mice receiving a saline infusion as a control. EP mice demonstrated reduced blood glucose levels over the duration of the infusion (Fig. 7-6A), coincident with an approximate doubling of both plasma insulin and NEFA levels (Fig. 7-6B and C, respectively).

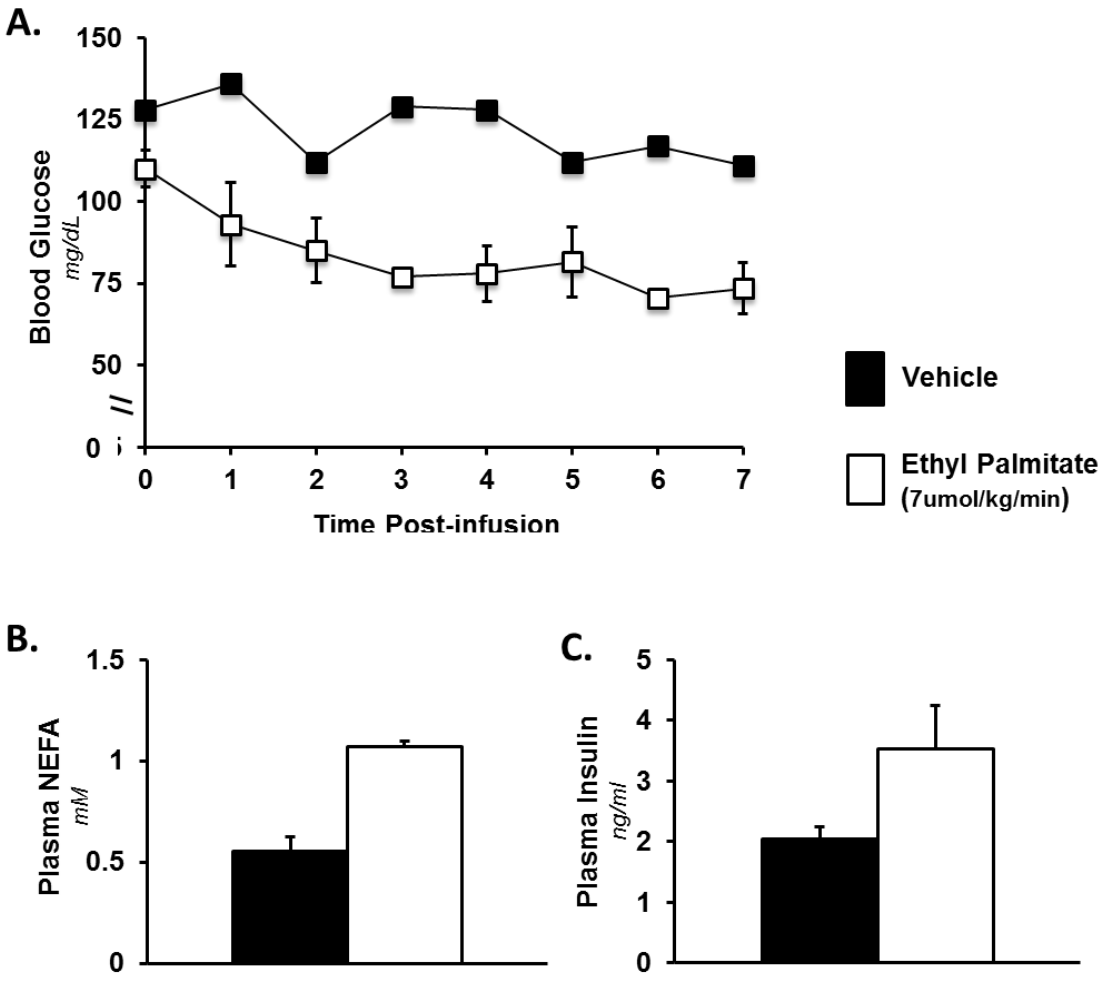

Figure 7-6. Mice infused for 7 h with ethyl palmitate (EP) in the first infusion pilot study. Mice receiving EP infusion had reduced blood glucose levels (A), but increased plasma insulin (B) and NEFA levels (C) compared to those with vehicle (saline) control infusions measured at 7h. N=1-2 at each time point.

In the second pilot experiment, we examined whether high rates of EP infusion would result in acute changes to lipid composition similar to those observed in our *in vitro* experiments with palmitate-treated hepatocytes. Due to the reduced blood glucose and increased insulin levels in response to EP observed in the first pilot study, we used a euglycemic clamp with infusion of somatostatin, glucagon, insulin, and glucose to control these variables at basal levels. EP was infused at two rates (37.5 μmol/kg/min and 75 μmol/kg/min) for 5 hours. Euglycemia (~120 mg/dL) was better maintained than in the first pilot study (data not shown). However, the insulin levels still increased sharply in a dose-dependent manner (Fig. 7-7A). There was no detectable difference in plasma NEFA levels (Fig. 7-7B). Despite the lack of change in NEFAs, there were

detectable differences in the fatty acid composition of both the phospholipid and triglyceride pools in the liver tissue of these mice (Table 7-4 and 7-5, respectively). EP infusion resulted in increased palmitate incorporation and overall saturation of phospholipids compared to saline-infused control mice. There also were slightly elevated amounts of phospholipids in those mice receiving a high EP infusion rate (~30.5 μg/mg tissue for the 75 μmol/kg/min EP infusion vs. ~27 μg/mg tissue in control infusions). These data are similar to the results we have obtained from *in vitro* models of palmitate lipotoxicity (4). Additionally, there was increased triglyceride accumulation in EP-infused mice, which was primarily composed of saturated palmitate moieties (~64% and 38% saturated in 75 and 37 μmol/kg/min EP infusions, respectively) in contrast to control mice (~27% saturated for both infusion rates). This is also reflective of the increased lipid accumulation that is usually present in steatotic and NASH livers (1).

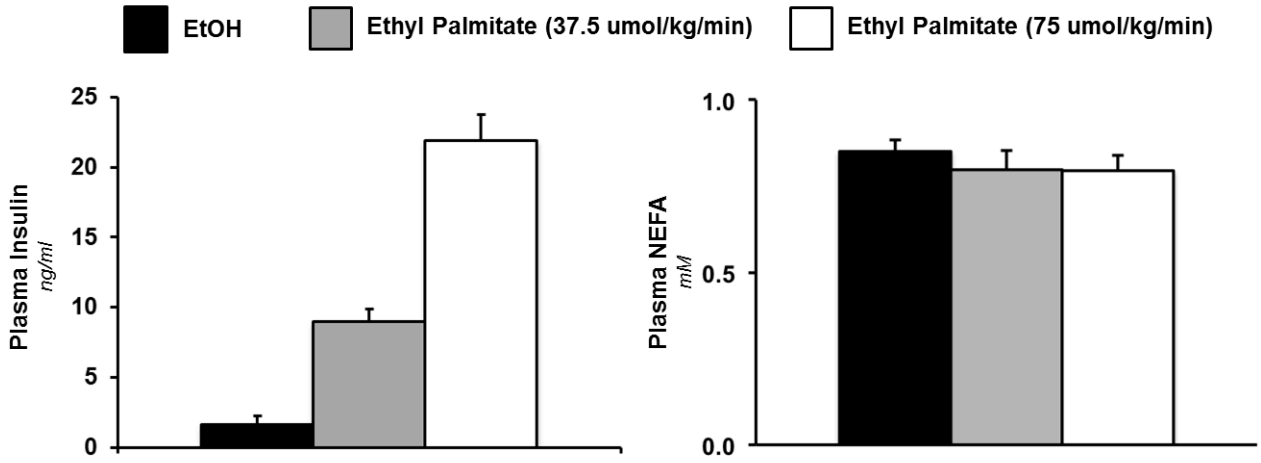

Figure 7-7. Mice were infused with EP for 5 h under a euglycemic clamp in the second pilot study. The euglycemic clamp was started by infusing somatostatin, glucagon, insulin and glucose 1 h prior to initiation of EP infusion. EP was infused at medium (37.5 μmol/kg/min) and high (75 μmol/kg/min) rates for 5 h while maintaining euglycermia. Mice receiving EP infusion had substantial increases in plasma insulin (A) but no changes in NEFA levels (B) compared to ethanol-emulsion (EtOH) vehicle controls. N=2-3.

Fatty Acid	75 umol PA	75 umol Crtl	37.5 umol PA	37.5 umol Crtl
16:0	28.77 ± 0.22	23.06	26.33 ± 0.32	21.25
16:1	0.86 ± 0.06	0.59	0.85 ± 0.08	0.64
18:0	16.39 ± 0.87	17.05	15.22 ± 0.12	18.21
18:1w9	8.65 ± 0.46	8.86	8.38 ± 0.04	7.44
18:1w7	1.21 ± 0.04	1.41	1.49 ± 0.00	1.61
18:2	15.12 ± 0.13	16.24	15.49 ± 0.11	16.07
20:3w6	1.25 ± 0.01	1.28	1.34 ± 0.09	1.27
20:4	13.11 ± 0.00	13.93	13.34 ± 0.41	16.17
20:5	0.75 ± 0.21	0.96	0.78 ± 0.03	0.95
22:5w3	0.91 ± 0.00	0.84	0.91 ± 0.11	0.84
22:6	12.98 ± 0.59	15.78	15.87 ± 0.88	15.56
% SFA	45.16 ± 0.90	40.11	41.55 ± 0.34	39.46
% UFA	54.84 ± 0.79	59.89	58.45 ± 0.99	60.54
µg PL/mg tissue	30.53 ± 0.19	27.05	28.77 ± 1.35	28.91
µg SFA PL/mg tissue	13.79 ± 0.42	10.85	11.96 ± 0.69	11.41

Table 7-4. Phospholipid composition of liver tissue samples collected from mice receiving EP infusion for 5h in the second pilot study. Infusion of EP resulted in increases in both palmitate incorporation and overall phospholipid saturation compared to controls (Crtl). Phospholipids were separated by thin layer chromatography and analyzed by gas chromatography-flame ionization detection (GC-FID). Data represent mean fatty acid %. N=1-2. SFA, saturated fatty acids; UFA, unsaturated fatty acids.

Fatty Acid	75 umol PA	75 umol Crtl	37.5 umol PA	37.5 umol Crtl
14:0	0.78± 0.17	1.51	0.51± 0.08	0.47
16:0	59.33± 5.95	22.12	34.64± 5.43	24.69
16:1	2.32± 0.41	1.32	2.98± 0.48	2.20
18:0	3.77± 0.12	3.15	2.78± 0.41	2.11
18:1w9	15.13± 2.52	33.51	27.82± 2.16	30.24
18:1w7	1.44± 0.26	2.49	2.63± 0.16	2.16
18:2	10.59± 1.68	24.90	17.87± 2.90	25.32
20:3w6	0.35± 0.03		0.57± 0.10	1.23
20:4	0.51± 0.17		0.89± 0.06	0.56
20:5	1.73± 0.45	1.91	2.02± 0.27	1.71
22:4w6	0.29± 0.00		0.42± 0.09	1.27
22:5w6	0.23± 0.23		0.64± 0.06	0.42
22:5w3	0.76± 0.15	1.73	1.54± 0.20	1.49
22:6	2.77± 0.35	7.37	4.52± 0.57	6.14
% SFA	63.88± 5.95	26.78	37.94± 5.45	27.26
% UFA	36.12± 3.13	73.22	62.06± 3.71	72.74
µg TG/mg tissue	14.54± 0.69	3.32	10.70± 0.51	8.87
µg SFA TG/mg tissue	9.33 ± 1.35	0.89	4.03 ± 0.72	2.42

Table 7-5. Triglyceride composition of liver tissue samples collected from mice receiving EP infusion for 5h in the second pilot study. Infusion of EP resulted in increases in both palmitate incorporation and overall saturation in triglycerides compared to controls (Crtl). Triglycerides were separated by thin layer chromatography and analyzed by gas chromatography-flame ionization detection (GC-FID). Data represent mean fatty acid %. N=1-2. SFA, saturated fatty acids; UFA, unsaturated fatty acids.

The third pilot experiment sought to determine the effect of acute administration of EP infused over multiple days (Fig 7-1C). In this study, we infused mice at a rate of 37.5 µmol/kg/min EP for 5 hours per day for 3 consecutive days to simulate repeated acute exposure to high levels of saturated fatty acids. We used an ethanol (EtOH)-emulsion (no palmitate) as a control in this experiment to correct for any confounding effects that might be due to ethanol present in the EP infusion. Blood glucose on the third day of the experiment remained very similar for the duration of the last infusion despite no addition of somatostatin, glucagon, insulin or exogenous glucose (Fig. 7-8A). Surprisingly, there was again no change in plasma NEFA levels (Fig. 7-8B). Lipid analysis revealed changes in phospholipid composition, specifically increases in palmitate incorporation (~24.5% vs. 18%) and overall saturation (~42.5% vs. 37.5%) in EP mice compared

to EtOH-infused controls (Table 7-6). There were also similar changes in triglyceride composition (~32.5% vs ~17.3 % for percentage of PA and 37% vs 21% for overall saturation in EP vs. control mice, Table 7-7). The EtOH-emulsion infused mouse had similar levels of triglyceride accumulation as that receiving the EP lipid infusion, but this is not altogether unexpected as alcohol is known to have a pro-lipogenic effect (17).

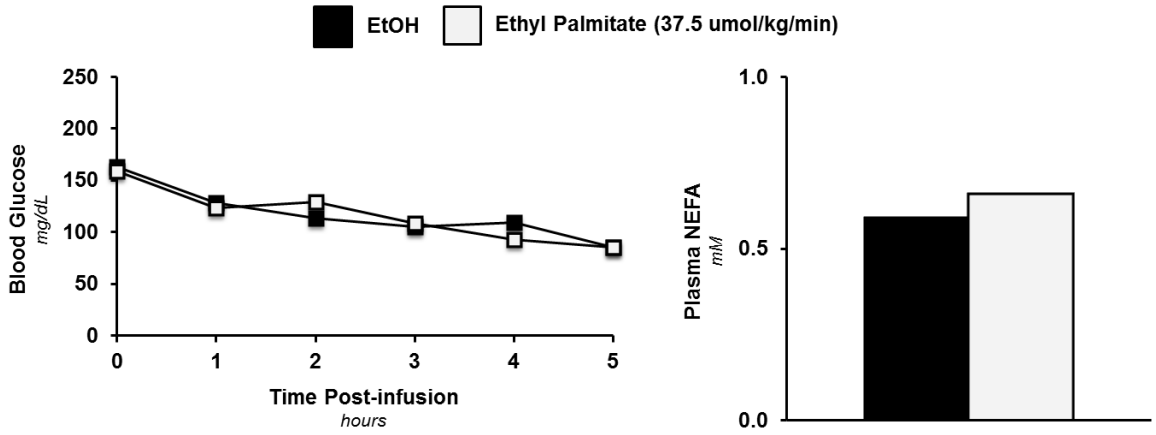

Figure 7-8. Mice infused for 5 h on 3 consecutive days with EP in the third pilot study. Measurements were taken the third day of the infusion study, and both EP-infused and control mice had similar blood glucose curves (A) and NEFA levels (B). N=1-2.

Fatty Acid	37.5 umol PA	EtOH Crtl
16:0	24.65	18.13
16:1		0.95
18:0	17.80	19.33
18:1w9	7.00	10.62
18:1w7	1.18	1.97
18:2	13.98	13.98
20:3w6	1.38	2.00
20:4	14.91	16.67
20:5	0.77	0.99
22:5w3	0.67	0.70
22:6	17.65	14.66
% SFA	42.46	37.46
% UFA	57.54	62.54
µg PL/mg tissue	30.77	33.77
µg SFA PL/mg tissue	13.06	12.65

Table 7-6. Phospholipid composition of liver tissue samples collected from mice receiving EP infusion for 5h on 3 consecutive days in the third pilot study. Infusion of EP resulted in increases in both palmitate incorporation and overall saturation in phospholipids compared to controls. Phospholipids were separated by thin layer chromatography and analyzed by gas chromatography-flame ionization detection (GC-FID). Data represent mean fatty acid %. N=1. SFA, saturated fatty acids; UFA, unsaturated fatty acids.

Fatty Acid	37.5 umol PA	EtOH Crtl
14:0	1.48	1.08
16:0	32.53	17.28
16:1	1.08	2.90
18:0	2.94	2.71
18:1w9	30.50	46.70
18:1w7	2.10	3.47
18:2	18.90	16.27
18:3 w3		0.84
20:3w6	0.69	0.87
20:4	1.38	1.40
22:4w6		0.63
22:5w3	1.39	1.15
22:6	7.02	4.70
% SFA	36.94	21.08
% UFA	63.06	78.92
µg TG/mg tissue	10.40	11.27
µg sat TG/mg tissue	3.84	2.38

Table 7-7. Triglyceride composition of liver tissue samples collected from mice receiving EP infusion for 5h on 3 consecutive days in the third pilot study. Infusion of EP resulted in increases in both palmitate incorporation and overall saturation in triglycerides compared to controls. There was no change in total amount of accumulated triglycerides most likely because ethanol (in EtOH emulsion control) is known to have a stimulatory effect on lipid synthesis in the liver. Triglycerides were separated by thin layer chromatography and analyzed by gas chromatography-flame ionization detection (GC-FID). Data represent mean fatty acid %. N=1. SFA, saturated fatty acids; UFA, unsaturated fatty acids.

Discussion

Wang *et al.* demonstrated that rats on a high SFA diet demonstrated increased liver injury and markers of endoplasmic reticulum (ER) stress, independently of obesity or changes in TNFα, insulin sensitivity and mitochondrial function, compared to rats on otherwise similar diets that were instead high in polyunsaturated fats, sucrose or starch (5). The "cafeteria diet" rat model went a step further to mimic human diet-induced obesity: male Wistar rats were fed a diet that consisted of food regularly consumed by humans in Western society including high-salt, high-

fat, low fiber, energy-dense foods such cookies, chips and processed meats (7). The livers of these animals were characterized by significant increases in inflammation, macrophage infiltration and overall clinical markers of steatohepatitis after 16 weeks, features that were notably absent in animals fed low fat, high fat or standard chow diets (7). Similarly, the "fast food" (FF) mouse model was fed a diet based on the composition of typical Western fast food: high in saturated fat, cholesterol and fructose. FF mice were compared to mice fed standard chow or the widely used high fat (HF) diet consisting mainly of unsaturated fats (8). Although HF mice developed obesity, insulin resistance and simple hepatic steatosis after six months, they did not develop the pronounced features of progressive NASH, such as hepatocyte ballooning, fibrosis, inflammation and endoplasmic reticulum stress, observed in the FF mice (8). The inclusion of high levels of saturated fat in rodent diets appears to trigger dysfunctional hepatic metabolism leading to an inflamed NASH-like state.

Overall, our results point toward high levels of hepatic steatosis and increasing inflammation and ER stress in FF diet fed rats. These animals demonstrated gradually increasing weight and a trend toward increased circulating levels of plasma triglycerides and cholesterol (Fig. 7-2). The limited data set produced only very small changes in levels of AST and ALT, two liver enzymes that have traditionally been used as surrogates to indicate liver injury. H&E histological stains of fixed liver tissue from these rodents demonstrated increased microvesicular steatosis and infiltration of inflammatory cells in certain aspects of the tissue section (Fig. 7-3). However, even at the last time point (12 weeks), histological markers of NASH were absenct. Additional staining with Masson's trichome did not reveal any indicators of fibrosis, a metric often used to gauge more progressive forms of NASH.

TEM imaging exposed wide swaths of large lipid droplet depositions that increased in density over the course of the study (Fig. 7-4). This was accompanied by indications of ER dilation and dissention, markers of ER stress that have been prominent in our studies with PA-treated hepatic cells (4), although chonic ER stress has also been linked to overnutrition in obesity (18). Additionally, we were able to identify small immune cell populations (Fig. 7-4G), which suggests progression from simple steatosis towards a more inflammatory, NASH-like state. Overall, however, the diet and timeline (12 weeks) was inadequate to promote a pathology with similarities to human NASH, so either the FF diet was not fed for a sufficient time to impart this effect or it did not have the same deleterious effects in rats as it did in the previous mouse studies by Charlton *et al.* that were conducted over a six month time course (8).

In order to develop a more rapid method for inducing a NASH-like phenotype in rodent models, we examined several direct lipid infusion protocols. After investigating the effects of high saturated fat diets in the past, Nivala *et al.* (9) recently examined the effects of intravenous lipid infusions in rats. They compared infusions of lard (enriched in saturated fats) and soybean oil (enriched in unsaturated fats) by measuring their effects on ER stress and inflammation in the liver and adipose tissue (9). Both lipid infusions increased plasma free fatty acid levels, but the lard treatment increased SFA concentrations including palmitate (16:0) by over two-fold and

stearate (18:0) by four-fold compared to control and soybean oil treatments. After only four hours of infusion, livers of the lard-infused animals were already showing significantly elevated markers of ER stress, including phosphorylated PERK, spliced-XBP1 and CHOP, as well as markers of inflammation, including Interleukin-1β (IL-1B), macrophage inflammatory protein-1α (MIP-1a) and TNFα. We expected to achieve similar results by direct infusion of palmitate in order to recapitulate the effects observed to our previous *in vitro* studies.

Typical lipid infusates are emulsified triglycerides that contain a mixture of fatty acid residues (10). Additionally, they are often infused with the anticoagulant herapin, which serves to activate lipoprotein lipases in order to release the free fatty acids from the infused triglycerides but can have the same effect on endogenous triglycerides and lipoproteins in circulation (19). These two issues are significant confounding factors that complicate the interpretation of prior studies. In contrast, infusion of unesterified fatty acids can be technically challenging due poor plasma solubility. Furthermore, protein overload and elevated oncotic pressure can result when fatty acids are complexed to albumin. Recently, Eguchi *et al.* performed an infusion of ethyl palmitate to study its effects on β-cell dysfunction. Ethyl palmitate is a 1:1 mixture of palmitate esterified to ethanol that is easily solubilized, emulsified and administered intravenously (10) and is rapidly hydrolyzed to free palmitate in the blood (20). Our lipid infusion procedures were based on this work.

The first pilot study pointed towards increased plasma NEFA levels in EP infused mice, which we postulated would recapitulate the palmitate-mediated lipotoxicity observed in our *in vitro* experiments (Fig. 7-6). Following this experiment, we decided to increase the EP infusion to both a moderate (37.5 μmol/kg/min) and high (75 μmol/kg/min) rate and to apply a euglycemic clamp to prevent the depressed blood glucose levels observed in the first pilot study (Fig. 7-6A). Interestingly, this resulted in almost 5- and 10-fold changes in plasma insulin levels but no change in NEFA concentrations despite the use of somatostatin, glucagon and a defined rate of insulin in the clamp (Fig. 7-7). Somatostatin is often used in animal research to prevent insulin secretion from the pancreas. In speculation, the EP infusion may pose a significant physiological stressor that counteracts the effects of somatostatin. Another possibility is that the insulin was ineffectively cleared from circulation as fatty acids have been reported to cause impaired insulin clearance (21). Insulin's precursor is cleaved into insulin and c-peptide. Future measurements of c-peptide could point toward whether increased secretion (higher levels of c-peptide) or reduced clearance (similar levels of c-peptide between EP infusion and control) is contributing to the elevated insulin levels. Nevertheless, the substantial increase in insulin is a likely explanation for the lack of change in NEFA levels, since insulin is a strong stimulator of fatty acid uptake by the liver and other insulin-responsive tissues (22).

Despite the fact that there was no change in plasma NEFA levels in either the 5-hour infusion (pilot 2) or 5 hours on 3 contiguous days (pilot 3), there were still interesting changes in the phospholipid composition of EP infused mice compared to controls (Table 7-5 and 7-7). There was evidence of increased palmitate incorporation into lipids and increased saturation of both

phospholipids and triglycerides. Further study is needed to assess whether these changes in lipid compositoin correlate to increased ER stress levels characteristic of *in vitro* models of palmitate lipotoxicity (4, 23, 24), as well as physiologically relevant indicators of metabolic syndrome (18, 25).

Overall, our initial results show that we can effectively modulate fatty acid composition of the *in vivo* liver using ethyl palmitate infusions. Transitioning our work from a purely *in vitro* model into more physiological relevant *in vivo* models is an important step in demonstrating the validity of our previous results and to test hypotheses generated from these studies. Further work is needed to verify these initial results and to understand the unexpected changes in insulin and NEFA levels that occursed in response to ethyl palmitate infusion. This will require a larger study size and may involve infusion of other fatty acids such as oleate that have not been shown to exert toxic effects *in vitro*.

References

1. Farrell, G. C., and C. Z. Larter. 2006. Nonalcoholic fatty liver disease: From steatosis to cirrhosis. *Hepatology* **43**: S99-S112.

2. Charlton, M. R., J. M. Burns, R. A. Pedersen, K. D. Watt, J. K. Heimbach, and R. A. Dierkhising. 2011. Frequency and Outcomes of Liver Transplantation for Nonalcoholic Steatohepatitis in the United States. *Gastroenterology* **141**: 1249-1253.

3. Listenberger, L. L., X. L. Han, S. E. Lewis, S. Cases, R. V. Farese, D. S. Ory, and J. E. Schaffer. 2003. Triglyceride accumulation protects against fatty acid-induced lipotoxicity. *Proceedings of the National Academy of Sciences of the United States of America* **100**: 3077-3082.

4. Leamy, A. K., R. A. Egnatchik, M. Shiota, P. T. Ivanova, D. S. Myers, H. A. Brown, and J. D. Young. 2014. Enhanced synthesis of saturated phospholipids is associated with ER stress and lipotoxicity in palmitate-treated hepatic cells. *J. Lipid Res.* **55**: 1478-1488.

5. Wang, D., Y. R. Wei, and M. J. Pagliassotti. 2006. Saturated fatty acids promote endoplasmic reticulum stress and liver injury in rats with hepatic steatosis. *Endocrinology* **147**: 943-951.

6. Borradaile, N. M., X. Han, J. D. Harp, S. E. Gale, D. S. Ory, and J. E. Schaffer. 2006. Disruption of endoplasmic reticulum structure and integrity in lipotoxic cell death. *J. Lipid Res.* **47**: 2726-2737.

7. Sampey, B. P., A. M. Vanhoose, H. M. Winfield, A. J. Freemerman, M. J. Muehlbauer, P. T. Fueger, C. B. Newgard, and L. Makowski. 2011. Cafeteria Diet Is a Robust Model of Human Metabolic Syndrome With Liver and Adipose Inflammation: Comparison to High-Fat Diet. *Obesity* **19**: 1109-1117.

8. Charlton, M., A. Krishnan, K. Viker, S. Sanderson, S. Cazanave, A. McConico, H. Masuoko, and G. Gores. 2011. Fast food diet mouse: novel small animal model of NASH with ballooning, progressive fibrosis, and high physiological fidelity to the human condition. *Am. J. Physiol.-Gastroint. Liver Physiol.* **301**: G825-G834.

9. Nivala, A. M., L. Reese, M. Frye, C. L. Gentile, and M. J. Pagliassotti. 2013. Fatty acid-mediated endoplasmic reticulum stress in vivo: Differential response to the infusion of Soybean and Lard Oil in rats. *Metabolism-Clinical and Experimental* **62**: 753-760.

10. Eguchi, K., I. Manabe, Y. Oishi-Tanaka, M. Ohsugi, N. Kono, F. Ogata, N. Yagi, U. Ohto, M. Kimoto, K. Miyake, K. Tobe, H. Arai, T. Kadowaki, and R. Nagai. 2012. Saturated Fatty Acid and TLR Signaling Link beta Cell Dysfunction and Islet Inflammation. *Cell Metabolism* **15**: 518-533.

11. Shiota, M. 2012. Measurement of glucose homeostasis in vivo: combination of tracers and clamp techniques. *Methods in Molecular Biology* **933**: 229-253.

12. Hughey, C. C., V. L. Johnsen, L. Ma, F. D. James, P. P. Young, D. H. Wasserman, J. N. Rottman, D. S. Hittel, and J. Shearer. 2012. Mesenchymal stem cell transplantation for

the infarcted heart: a role in minimizing abnormalities in cardiac-specific energy metabolism. *Am. J. Physiol.-Endocrinol. Metab.* **302**: E163-E172.

13. Morgan, C. R., and A. Lazarow. 1965. IMMUNOASSAY OF PANCREATIC AND PLASMA INSULIN FOLLOWING ALLOXAN INJECTION OF RATS. *Diabetes* **14**: 669-&.

14. Bacon, B. R., M. J. Farahvash, C. G. Janney, and B. A. Neuschwandertetri. 1994. NONALCOHOLIC STEATOHEPATITIS - AN EXPANDED CLINICAL ENTITY. *Gastroenterology* **107**: 1103-1109.

15. Mofrad, P., M. J. Contos, M. Haque, C. Sargeant, R. A. Fisher, V. A. Luketic, R. K. Sterling, M. L. Shiffman, R. T. Stravitz, and A. J. Sanyal. 2003. Clinical and histologic spectrum of nonalcoholic fatty liver disease associated with normal ALT values. *Hepatology* **37**: 1286-1292.

16. Ariyama, H., N. Kono, S. Matsuda, T. Inoue, and H. Arai. 2010. Decrease in Membrane Phospholipid Unsaturation Induces Unfolded Protein Response. *J. Biol. Chem.* **285**: 22027-22035.

17. You, M., M. Fischer, M. A. Deeg, and D. W. Crabb. 2002. Ethanol induces fatty acid synthesis pathways by activation of sterol regulatory element-binding protein (SREBP). *J. Biol. Chem.* **277**: 29342-29347.

18. Fu, S., L. Yang, P. Li, O. Hofmann, L. Dicker, W. Hide, X. Lin, S. M. Watkins, A. R. Ivanov, and G. S. Hotamisligil. 2011. Aberrant lipid metabolism disrupts calcium homeostasis causing liver endoplasmic reticulum stress in obesity. *Nature* **473**: 528-531.

19. Teusink, B., P. J. Voshol, V. E. H. Dahlmans, P. C. N. Rensen, H. Pijl, J. A. Romijn, and L. M. Havekes. 2003. Contribution of fatty acids released from lipolysis of plasma triglycerides to total plasma fatty acid flux and tissue-specific fatty acid uptake. *Diabetes* **52**: 614-620.

20. Hungund, B. L., Z. H. Zheng, and A. I. Barkai. 1995. TURNOVER OF ETHYL-LINOLEATE IN RAT PLASMA AND ITS DISTRIBUTION IN VARIOUS ORGANS. *Alcoholism-Clinical and Experimental Research* **19**: 374-377.

21. Wiesenthal, S. R., H. Sandhu, R. H. McCall, V. Tchipashvili, H. Yoshii, K. Polonsky, Z. Q. Shi, G. F. Lewis, A. Mari, and A. Giacca. 1999. Free fatty acids impair hepatic insulin extraction in vivo. *Diabetes* **48**: 766-774.

22. Clement, L., H. Poirier, I. Niot, V. Bocher, M. Guerre-Millo, S. Krief, B. Staels, and P. Besnard. 2002. Dietary trans-10,cis-12 conjugated linoleic acid induces hyperinsulinemia and fatty liver in the mouse. *J. Lipid Res.* **43**: 1400-1409.

23. Wei, Y., D. Wang, C. L. Gentile, and M. J. Pagliassotti. 2009. Reduced endoplasmic reticulum luminal calcium links saturated fatty acid-mediated endoplasmic reticulum stress and cell death in liver cells. *Molecular and Cellular Biochemistry* **331**: 31-40.

24. Pfaffenbach, K. T., C. L. Gentile, A. M. Nivala, D. Wang, Y. R. Wei, and M. J. Pagliassotti. 2010. Linking endoplasmic reticulum stress to cell death in hepatocytes: roles of C/EBP homologous protein and chemical chaperones in palmitate-mediated cell death. *Am. J. Physiol.-Endocrinol. Metab.* **298**: E1027-E1035.

25. Zhang, K. Z., and R. J. Kaufman. 2006. The unfolded protein response - A stress signaling pathway critical for health and disease. *Neurology* **66**: S102-S109.

CHAPTER 8

CONCLUSIONS AND FUTURE WORK

Conclusions

Saturated fatty acids, such as palmitate (PA), have long been known to induce lipotoxicity in a variety of cell types, characterized by increased ER stress, ROS accumulation and subsequent cell death, while monounsaturated fatty acids, such as oleate (OA), have been shown to exert a protective effect when co-supplemented in PA-treated cells. The mechanism though which saturated fatty acids disrupt normal cellular metabolism and function has not been fully elucidated. The purpose of this dissertation was to investigate the role that different pathways of lipid metabolism play in initiating, or preventing, the downstream cascade that culminates in hepatocellular lipoapoptosis.

In Chapter 3, we investigated the hypothesis that dysregulated phospholipid metabolism and oversaturation of lipid bilayer membranes play a contributing role in the ER stress that is characteristic of PA-treated hepatic cells. Our results demonstrate that palmitate supplementation resulted in highly significant increases in PA incorporation and overall saturation in membrane phospholipids as well as indicators of increased phospholipid synthesis though the Kennedy pathway. This was correlated to elevated expression of markers of ER stress, such ER dilation and CHOP protein levels, and increases in apoptotic cell death. Addition of OA to PA-treated hepatic cells restored the saturation of phospholipids toward basal levels, which resulted in reduced ER stress and cell death. Cells co-treated with OA were also characterized by increased triglyceride (TG) synthesis, a pathway that has been postulated to detoxify palmitate and to be responsible for the protective effect exerted by OA in PA-treated cells.

Our interest in the longstanding hypothesis that increased TG synthesis is the main mechanism of OA-mediated rescue led us to investigate the effect of inhibiting TG synthesis in Chapter 4. By knocking down the final step in the TG synthetic pathway (DGAT), we were able to significantly reduce TG accumulation in hepatic cells in response to all fatty acid combinations we tested. Most interestingly, despite severely impaired TG synthesis, OA supplementation in PA-treated cells still exerted a powerful rescue effect. Our results demonstrated that although the cells were inhibited in their ability to produce triglycerides, the phospholipid incorporation of PA and overall saturation were still restored back to basal levels. These results define a significant role of phospholipid metabolism and saturation in lipotoxicity, and shed doubt on the hypothesis that increased TG synthesis is the lone driving force responsible for OA's protective effect on PA-treated cells.

The hypothesis that re-routing PA away from phospholipid incorporation and toward less toxic lipid pathways would reduce lipotoxicity was further explored in Chapter 5. We investigated the effect that modulations of β-oxidation would have in hepatic cells. Our data demonstrated that

increased PA disposal though fatty acid oxidation by stimulating β-oxidation via AICAR did result in reduced PA incorporation into phospholipids and reduced markers of lipotoxicity. In this chapter, we again demonstrated that methods designed to reduce PA incorporation in membrane phospholipids, and therefore limit oversaturation of the bilayer, were protective against PA-mediated lipotoxicity.

Since dysregulated phospholipid metabolism and composition seems to play a significant role in PA-induced lipotoxicity, in Chapter 6 we sought to investigate direct methods for modulating PA incorporation into these species. We examined approaches for inhibiting PA incorporation by either knocking down the initial step of phosphatidylcholine synthesis or though pharmacological inhibition of phospholipid remodeling. Both methods demonstrated small, but significant, reductions in markers of PA lipotoxicity, though neither was fully protective. The limited efficacy was likely due to the inherit limitations when targeting only specific phospholipids, such as phosphatidylcholine, and only a particular pathway of phospholipid metabolism at a time. However, these results demonstrate that methods designed to target phospholipid metabolism show promise in reversing PA-mediated lipotoxicity and may play a role in preventing the progression of hepatic diseases such as NASH.

We are currently designing and testing *in vivo* rodent models to recapitulate findings and mechanisms developed in our *in vitro* models. Thus far, our initial results show interesting trends that correlate to increased saturation of phospholipids in response to PA treatment like those demonstrated in this dissertation. We will continue to pursue this line of experimentation in the hopes of better understanding the role that saturated fatty acids and phospholipid metabolism play in a more physiologically relevant model of lipotoxicity.

Overall, this dissertation provides further evidence to support the hypothesis that phospholipids play an integral part in the mechanisms of lipotoxicity. Our work is relevant in a field where other groups are exploring the role that phospholipid metabolism plays in disease (1-4). In our hepatic models, we saw that increasing saturation of membrane phospholipids though PA treatment was detrimental to cell survival, while interventions designed to prevent PA incorporation and phospholipid saturation provided beneficial effects. Oleate co-treatment rescued the lipotoxic phenotype, not simply though increased flux into triglycerides, but though its phospholipid desaturation effect. Although our experiments designed to more directly modulate PA incorporation into phospholipids demonstrated only modest success, this deserves further investigation as it may prove clinically relevant in disease states such as obesity (1) and NASH (5) where disordered phospholipids have been identified as a possible contributing factor. Interventions that modulate phospholipid saturation may relieve the characteristic ER stress and, therefore, downstream inflammation and cell death observed in these conditions.

Future work

The majority of the work presented in this dissertation demonstrates correlative data, where a treatment results in changes in specific outputs. We link the outputs together by probable mechanisms but don't have concrete evidence to fully define them. For example, our data shows significant changes in phospholipid composition in response to fatty acid treatment and we link this to changes in ER stress, a mechanism that has been demonstrated in other model systems. However, it would be more novel and interesting to develop a method to initiate direct and quantitative changes in ER phospholipid composition. Directly manipulating only ER phospholipid saturation levels and monitoring whether other markers associated with lipotoxicity, such as ER stress, Ca^{2+} efflux, ROS and cells death, also change as predicted would more definitely demonstrate the validity of our hypothetical mechanisms. We have performed some initial work in this area, as discussed in Chapter 6, but due to the modest changes imparted by these interventions, more approaches need to be investigated. Manipulating fatty acid reacylation enzymes in the Lands' cycle that demonstrate substrate specificity based on saturation and/or chain length may prove to be a very interesting avenue of research. For example, prior work in this area has focused on LPCAT3, a reacylation enzyme more specific for mono- and polyunsaturated long chain fatty acid, and has shown that modulating its activity has effects on phospholipid saturation and other markers of lipotoxicity (2, 3).

A large majority of this dissertation work was done in an immortalized rat hepatoma cell line (H4IIEC3), which has both its advantages and disadvantages. Immortalized cell lines are easier to work with and maintain in continuous culture so that many experiments can be completed in a timely fashion. They allow us to quickly optimize conditions, new treatments and assays without the large expense of both time and money that is incurred with freshly isolated primary hepatocytes. However, the disadvantages are also significant due to the fact that these cells are immortalized, cancer-derived, and grown in culture, and therefore may not recapitulate some important aspects of the *in vivo* hepatic physiology that we seek to understand. Some key experiments were done in primary hepatocytes as confirmation studies, but continued work in these and other model systems needs to be done to further solidify mechanisms that have been determined using H4IIEC3 cells.

In addition to continuing work in primary cells, moving into *in vivo* systems such as the rat or mouse would be an important next step in translating our experiments and hypothesized mechanisms into a more realistic model of NASH. There is a variety of diet-induced and genetically manipulated models of rodent NAFLD/NASH (see Chapter 2), but determining the most appropriate one to study is not always simple. Our work in Chapter 7 demonstrates our lab's first exploration into *in vivo* models of hepatic lipotoxicity. Although diet manipulation did not appear to be as successful for short-term experiments in wild-type animals, direct infusion of ethyl palmitate following the method of Eguchi *et al*. (6) has shown interesting preliminary results. Continuing to optimize and complete these studies will allow us to demonstrate the

validity of our *in vitro* results in an *in vivo* whole animal model, which represents a large step toward understanding human liver disease progression.

Other possible avenues of work that would be of interest in future studies include investigating the role and significance of myelin bodies. These interesting features found only in PA-treated cells are associated with disordered phospholipid metabolism and the significance of their biogenesis in environments of SFA supplementation may provide clues as to the phenotype and mechanism of lipotoxicity. Investigating the role that other ER proteins, such as SERCA, play in modulating ER stress in both basal conditions and under SFA stress would also be a nice extension of this work. Finally, examining the effects of treatments that have been the subject of clinical trials, such as metformin and bile acid derivatives (see Chapter 2), in both the *in vitro* and *in vivo* context of SFA toxicity, would also propel the findings of this dissertation into a better clinical understanding of lipotoxicity and hepatic disease progression.

References

1. Fu, S., L. Yang, P. Li, O. Hofmann, L. Dicker, W. Hide, X. Lin, S. M. Watkins, A. R. Ivanov, and G. S. Hotamisligil. 2011. Aberrant lipid metabolism disrupts calcium homeostasis causing liver endoplasmic reticulum stress in obesity. *Nature* **473**: 528-531.

2. Rong, X., C. J. Albert, C. Hong, M. A. Duerr, B. T. Chamberlain, E. J. Tarling, A. Ito, J. Gao, B. Wang, P. A. Edwards, M. E. Jung, D. A. Ford, and P. Tontonoz. 2013. LXRs Regulate ER Stress and Inflammation through Dynamic Modulation of Membrane Phospholipid Composition. *Cell Metabolism* **18**: 685-697.

3. Ariyama, H., N. Kono, S. Matsuda, T. Inoue, and H. Arai. 2010. Decrease in Membrane Phospholipid Unsaturation Induces Unfolded Protein Response. *J. Biol. Chem.* **285**: 22027-22035.

4. Borradaile, N. M., X. Han, J. D. Harp, S. E. Gale, D. S. Ory, and J. E. Schaffer. 2006. Disruption of endoplasmic reticulum structure and integrity in lipotoxic cell death. *J. Lipid Res.* **47**: 2726-2737.

5. Gorden, D. L., D. S. Myers, P. T. Ivanova, E. Fahy, M. R. Maurya, S. Gupta, J. Min, N. J. Spann, J. G. McDonald, S. L. Kelly, J. Duan, M. C. Sullards, T. J. Leiker, R. M. Barkley, O. Quehenberger, A. M. Armando, S. B. Milne, T. P. Mathews, M. D. Armstrong, C. Li, W. V. Melvin, R. H. Clements, M. K. Washington, A. M. Mendonsa, J. L. Witztum, Z. Guan, C. K. Glass, R. C. Murphy, E. A. Dennis, A. H. Merrill, D. W. Russell, S. Subramaniam, and H. A. Brown. 2015. Biomarkers of NAFLD progression : a lipidomics approach to an epidemic. *J. Lipid Res.*

6. Eguchi, K., I. Manabe, Y. Oishi-Tanaka, M. Ohsugi, N. Kono, F. Ogata, N. Yagi, U. Ohto, M. Kimoto, K. Miyake, K. Tobe, H. Arai, T. Kadowaki, and R. Nagai. 2012. Saturated Fatty Acid and TLR Signaling Link beta Cell Dysfunction and Islet Inflammation. *Cell Metabolism* **15**: 518-533.

APPENDIX OF DETAILED PROTOCOLS

Propidium Iodide Viability Assay

Purpose:

To measure the nonviable population of H4IIEC3 cells in response to various treatments in 96 well plates. *This protocol is specific for adherent cells.*

Mechanism

Propidium iodide (PI) is an intercalating dye and will only bind to double stranded DNA longer than 4-5 base pairs. Since PI cannot cross the cell membrane, it is useful when trying to discriminate dead from live cells in a population.

Materials:

- Propidium Iodide powder stock
- HBSS buffer
- Low glucose DMEM (Media w/out phenol red)
- 96 well plate- opaque, clear bottom.

Note: for best results seed cells at least 48 hours prior to experiment. 2x10^4 cells/well

Procedure:

- Dye preparation- dissolve PI in HBSS to make a stock solution of 1 mg/mL (1.5 mM)
- *1 hour prior to adding PI dye- add 70% ethanol solution to appropriate wells for a positive control.*
- Remove media from cells.
- Do not wash, could result in losing dead cells.
- Add 100 uL of Low glucose DMEM (or other media) that *does not* contain phenol red. This will react with the dye and result in measurement errors.
- Add .333 uL of PI stock (5 uM final concentration)*
    - *Alternatively make stock of 5 uM PI by adding 33.3 uL of PI stock to 10 mL of DMEM
- Incubate for a minimum of 1 h.
- Measure fluorescence
    - Ex 535, Em 617
    - For FL 600 use ex: 530, em: 645, bottom read, sensitivity: 100

Ordering Information

Invitrogen: http://products.invitrogen.com/ivgn/product/P1304MP?ICID=search-product

Reactive Oxygen Species (ROS) Assay

Purpose:

To measure the levels of reactive oxygen species (ROS) in H4IIEC3 cells using H_2DCFA in 96 well plates.

This protocol is specific for adherent cells.

Materials:

- H_2DCFA (Invitrogen)
- DMSO
- HBSS buffer
- 96 well plate- opaque, clear bottom.

Procedure:

- *30 minutes prior to adding H2DCFA dye- add Hydrogen Peroxide controls. Normally we use .5-1 mM concentration (final).*
- To make H_2DCFA stock solution- dissolve H_2DCFA powder in DMSO to make 10 mM solution.
- Dilute H_2DCFA in HBSS to make 10 uM working solution. H_2DCFA is light sensitive and the tube should be wrapped in tin foil to prevent any degradation due to light.
- Vortex for 30 seconds.
- Remove media from cells.
- Wash 2x with HBSS.
- Add 100 uL of H_2DCFA mixture to cells.
- Incubate for 30-45 minutes.
- To measure ROS- H_2DCFA fluorescence, set excitation wavelength to 485 nm and emission wavelength to 530 nm. Set sensitivity of reader to 150. – *specific FL-600 plate reader*

Apo-ONE Caspase 3/7 Reagent Apoptosis Detection

Purpose:

To measure apoptosis in H4IIEC3 cells by detecting the activities of caspase-3 and -7. *This protocol is specific for adherent cells.*

Mechanism

The Apo-ONE kit is used to measure apoptosis in cells by measuring caspase activity. The kit contains a lysis buffer which permeabilizes the cell population to facilitate dye introduction to caspases 3/7. When the nonfluorescent dye comes in contact with the caspases, quenching groups are removed from the dye and return it to its fluorescent rhodamine state. This protocol should be used when it is necessary to confirm apoptosis and when cell metabolism differences due to different treatments prevents use of cell titer blue dye (resazurin).

Materials:

- Apo-ONE Caspase 3/7 Kit
- 96 well plate (opaque, clear bottom)
- Low Glucose DMEM

Prior to experiment:

- 48 hs before assay, seed 2x10^4 cells per well in a 96 well plate (black, clear bottom)

Procedure:

- Dye preparation- add 100 uL Substrate into 9900 uL Buffer provided in the kit- good for 24-48 hs.
- *30 minutes prior to adding ApoONE Dye- add staurosporine positive controls.*
- Remove media from cells.
- Wash 2x with HBSS
- Add 100 uL of Low glucose DMEM (or other media) that *does not* contain phenol red. This will react with the dye and result in measurement errors.
- Add 100 uL of Apo ONE stock.
- Incubate for a minimum of 1 hours.
- Wavelengths- excitation 499, emission 521
    - For FL-600 plate reader
    - Use 485 filter for excitation and 5
    - Bottom Read
    - Set Sensitivity to 125

JC-1 Analysis of Mitochondrial Potential

Purpose:

To identify mitochondrial impairments as a function of mitochondrial potential. *This protocol is specific for adherent cells*

Mechanism:

The JC-1 dye accumulates in mitochondria in monomeric (green) form. The increase in mitochondrial potential causes the dye to form aggregates characterized by a shift from green to red fluorescence. Therefore a ratio of red to green fluorescent emissions (using the same excitation) indicates the relative mitochondrial potential.

Materials:

- JC-1 Dye (Invitrogen T-3168)
- 96 well plate, black, clear bottom
- Plate reader
- Ethanol
- Media

Prior to experiment:

- 48 hs before assay, seed 2x10^4 cells per well in a 96 well plate (black, clear bottom)
- Stock solution is 5 mg in 1 mL of ethanol (5mg/mL concentration)

Dye loading:

- Treatment final concentration is 10 ug/mL
- Make secondary stock concentration of 110 ug/mL
- Calculate total volume needed. For a 96 well plate you will need 1950 uL – 2000 uL.
- For 2000 uL add 44 uL of 5 mg/mL stock to 1956 uL DMEM in a small tube.
- VORTEX VIGOROUSLY. JC-1 is tough to dissolve. Pre-warm media ahead of time.
- Add 20 uL of 110 ug/ml of secondary stock directly on top of 200 uL media with treatments.
- Incubate for 1 hour
- Rinse 3 times with PBS
- Add 100 uL DMEM back to wells
- Excite dye at 485 nm and measure fluorescence at 530 nm (green) and 590 nm (red)

Data Analysis:

Ratio Red/Green signals, increase in this ratio indicates higher relative mitochondrial potential.

Protocol for [3H]-Palmitate Beta oxidation Measurement (Shiota Lab)

1. Plate cells on 6 well dishes
    a. ~5 x 10^4 cells/well
    b. 2-3 mL of media total
    c. Allow proliferation for 2 days until confluent
2. Cell Incubation
    a. Total of 2mL/well of buffer (media+reagents)
3. Incubate for 24 hours
4. Label 2 tubes/sample (well) for later use
5. Deprotenization
    a. Remove 1.5 mL of media separately from each well and place in appropriate tube
    b. Add 75 uL of 60% PCA
        i. Precipitates out protein from the media (i.e BSA).
        ii. This step removes ~99% of un-oxidized [3H]-PA from sample
    c. Shake and vortex thoroughly
    d. Allow samples to rest on ice for 2 hours (or overnight in 4C)
    e. Centrifuge @3000 RPM for 30 mins
6. Wash out each well with ice cold PBS x5 for protein analysis
        i. Need to remove any remaining BSA because this causes problems with protein analysis
        ii. Can put in freezer like this for later use
7. Neutralization
    a. Remove 1.2 mL of deproteinized buffer from step 6
        i. DO NOT GET ANY OF PRECIPITATE at the bottom. This is unwanted protein!
    b. Add 5 uL of S160 Universal pH indicator dye
    c. Add ~40 uL of 5M K2CO3 to each sample
        i. Want dye color in sample to turn from red (acidic) to green (neutral)
        ii. Used 36 uL/sample 9/11/12
    d. Allow neutralized samples to sit in 4C overnight
        i. Make sure they are still green in the morning
    e. Centrifuge @3000 RPM for 30 mins
8. Make Separation Columns
    a. Supplies:
        i. 2mL glass pipette for each sample
        ii. Glass wool
        iii. AG 1-X8 Resin (Bio-Rad 140-1441)
    b. Pack glass wool into narrowing of pipette
            1. Don’t want it too compact or nothing will flow though
    c. Soak in H2O

d. Pipette in Resin/water solution (~0.2g/mL)
    i. Resin should settle into ~2inches above glass wool stopper
    ii. Excess water should flow though
        1. Don't want resin leaking out (something wrong with glass wool packing)
        2. Resin will remove last remaining un-oxidized [3H]-PA
e. Allow columns to remain in water until right before using

9. Applying sample to columns
    a. Set up columns flush columns with water to ensure no resin is leaking and water is actually flowing though column
    b. Place scintillation vials (PerkinElmer) below tips to catch eluting water after flushing (1/sample)
    c. Apply 0.8 mL of each sample to column
        i. Allow sample to fully elute before next step
    d. Flush column with 0.6 mL of water x2
        i. Total volume in glass receptacle is 2 mL
    e. Add 8 mL scintillation fluid (EcoLume) that amplifies radiation from [3H] – total volume 10mL
    f. Cap tightly and shake vigorously
    g. Read in scintillation counter. Subtract nonspecificity controls as background.

Metabolite extraction from animal cells

Introduction

This protocol describes the extraction of intracellular metabolites from cultured animal cells. This is a biphasic extraction protocol, with non-polar metabolites partitioning into a chloroform phase and polar metabolites partitioning into a methanol/water phase.

Required Materials and Equipment

- Cells plated on a 100 mm dish
- Ice-cold PBS (20 mL)
- Ice-cold PIPES buffer (2 mL, contains 3 mM PIPES and 3 mM EDTA in MilliQ water at pH 7.2)
- Methanol pre-cooled to -80ºC and stored on dry ice (2 mL)
- Chloroform pre-cooled to -20ºC (4 mL)
- Cell scraper
- 15 mL centrifuge tube
- Internal standard cocktails (optional)
- Benchtop centrifuge (Forma 5678 with model 815 fixed angle rotor)
- Eppendorf tubes
- Evaporator (Pierce Reacti-Vap)
- Vortexer with attachment to hold 15 mL tubes, placed inside -20ºC freezer

Protocol

- Remove media from dish
- Wash cells twice with ice-cold PBS
- Add 1 mL pre-cooled methanol to dish
- Place dish in dry ice container for 1 min
- Scrape cells into 15 mL centrifuge tube
- Add 1 mL pre-cooled methanol to dish
- Remove remaining cells from dish into the same 15 mL tube
- Add internal standard cocktails to tube (optional)
- Add 2 mL pre-cooled chloroform
- Vortex tube for 30 min at -20ºC
- Add 2 mL of ice-cold water
- Vortex sample for 5 min at -20ºC
- Centrifuge at 3,000 rpm (~1,000g) for 20 min at lowest temperature setting
- Collect aqueous (upper) phase in two 2 mL Eppendorf tubes (label the tubes!)
- Collect organic (lower) phase in two 2 mL Eppendorf tubes (label the tubes!)
- Evaporate all extracts to dryness using aeration at room temperature
- Store samples at -80ºC

Western Blotting (Young Lab)

Lysate Buffer:

Ripa Buffer.....1mL
PMSF 20uL
Inhibitor Cocktail 10-20uL
Naorthovanadate 10uL

1. Aspirate
2. Wash 1-3xs with PBS
3. Turn on side in ice to make sure all remaining PBS drains out or accumulates in bottom
4. Aspirate out all remaining residual PBS
5. Add 75 uL Lysate buffer along whole top edge (6-cm plate)
6. Swirl around plate for ~1-2 mins to make sure lysate buffer encounters all cells on plate
7. Scrape all cells off with scrapper (THOROUGHLY)
8. Use pipette tip remove lysis/cell solution from plate
9. Aliquot into small eppendorf tube
10. Allow samples to sit 30-45 mins on ice
11. Centrifuge @13,200rpm for 20 mins @4C
12. Remove supernatant (make sure not to get the protein pellet at the bottom!) and put into fresh, prechilled tubes

Protein Assay

13. Need Reagent A &B from BioRad kit
14. Make A/B Solution: (50:1 A:B) so that there will be enough for 200uL/well
15. Add 25 uL of each BSA to 96 well plate for concentrations shown below. Only need to use 2 wells for each conc of BSA

		1	2	3	4	5	6	7	8	9
BSA	A	0 ug/uL	25 ug/uL (5uL 125 +	125 ug/uL	250 ug/uL	500 ug/uL	700 ug/uL	1000 ug/uL	1500 ug/uL	2000 ug/uL
	B									
Samples	C									
	D	Sample 1	Sample 2	Sample 3	Sample 4	Sample 5...				
	E									
Samples	F									
	G	Sample	Sample	Sample	Sample	Sample				
	H									

16. Vortex extracted sample
17. Dilute by factor of 10 (i.e at 9uL of sample to 81uL PBS)
18. Vortex each sample/PBS mixture to ensure homogeneity and then add 25uL of each sample per well. Need to use 3 wells per sample.
19. Add 200 uL A/B solution on top of each well (Do it all at the same time so the reaction happens at the same time

20. Cover with foil and put on shaker for ~5 mins
21. Incubate for ~25 so total time from reaction addition of A/B to reading is 30 mins
22. Put in plate reader

Sample Preparation

23. Use concentration information from printout to create a table for necessary dilutions, as shown below, to find appropriate QS to get required #of samples. Need ~30ug protein/sample run and the final Sample+PBS+SDS buffer solution volume needs to be divisible by #samples and <45uL (well capacity)

	Conc (ug/uL)	Conc Undiluted	uL for 30 ug	4 samples	PBS to 30uL
(6) 8 hr PA	0.89	8.92	3.36	13.45	16.55
(7) 6 hr PA	0.90	9.05	3.32	13.26	16.74
(8) 6hr BSA	0.93	9.33	3.21	12.86	17.14
(9) 4 hr PA	0.82	8.19	3.66	14.66	15.34
Control	0.85	8.49	3.53	14.13	15.87
Thaps	1.02	10.19	2.94	11.77	18.23

24. Add 10 uL of SDS PAGE buffer per 30uL of sample solution (with 1% of BME added)--- it's the blue solution sitting out (no refrigeration needed)

→Example: If have an avg conc of 5ug/uL from BCA assay, 5uL are need to get to 25 ug of total protein. If want 4 samples total for different WB then you will need 5ul X 4 samples=20uL total. If desired QS volume is 60uL, then add 40 uL PBS to the 20uL of sample. Since final PBS/sample volume is 60uL, add 20 uL of SDS-PAGE buffer to each. Overall, there is 80uL total volume for 4 samples, so 20uL of final solution will be used for each WB

25. Heat on block @95C for 10 mins
26. Store at -20C until ready to load on to gels (Best if use fresh)
    a. Reheat at 95C for 5 mins after take out of freezer

Running Gel

27. Get gel set up in electrophoresis contraption
28. Make sure to fill up inner space between 2 gels with 1XTGS (Running Buffer) and also up to the level of the base of the gel in the total container. Note: if only doing one gel, put gel sized spacer and thin smaller plastic slip (faces out) on other side of clamp to keep everything together
29. Clean out wells of gel. Use 70uL of surrounding Running buffer solution to pipette into each well and try to blow out debris. Use pipette tip to straighten out any sagging well walls.

30. Pipette Ladder (BioRad Dual Color #161-0374) and samples into wells in SPECIFIC ORDER. Write down the order that you put in samples as shown below. BE SPECIFIC.
31. Top off chamber between gels with more running buffer (until it spills over the sides)
32. Run gel @80V for 15-20 mins until ladder looks separated
    a. NOTE: Keep the electrophoresis chamber during Running VERY COLD!! Need to surround chamber with a lot of ice
33. Once ladder has separated as desired, run gel at 150-180V for ~40-45 more mins until ladder looks to be in good position (good separation for the kDa weight you'll be looking at with protein of interest). Don't let ladder run off gel! Always want protein levels to be even on running gel….Sloping=BAD!

Transferring to Membrane

34. Activate PVDF membrane by the following method:
    a. Wet in MeOH ~5-10sec each side.
        i. Make sure membrane is completely immersed and wetted
        ii. Do NOT want to overactive membrane in MeOH…it will be destroyed!
        iii. Use clean, non-perforated tweezers to hold membrane—Do NOT touch directly!
    b. Fan off excess
    c. Immediately submerge in Transfer Buffer (TB), flipping over with flathead tweezers several times (until "oil like" drops disappear). Soak in TB for >15 mins.
35. In medium sized basin filled with TB and presoaked sponges/filter paper, assemble the transfer sandwich in the following order from BOTTOM to TOP:
    BLACK SIDE OF TRANSFER BRACKET
    SPONGE
    THICK FILTER PAPER
    GEL
    MEMBRANE (DO NOT MOVE ONCE IT IS IN CONTACT WITH GEL)
    THICK FILTER PAPER
    SPONGE
    WHITE SIDE OF TRANSFER BRACKET
36. Place membrane on top of gel. CAREFULLY roll out any air bubbles. Make sure that gel and membrane do not move in relation to each other or membrane picture will be ruined.
37. Put filter paper and sponge on top of that. Roll fiber pad sandwich somewhat more vigorously.
38. Put red plastic part on top and close white clasp to complete the sandwich.
39. If only doing one gel, make an identical sandwich but with no gel or membrane
40. Place sandwich with actual membrane/gel in back of tank by black side (black part of sandwich faces black and white faces red)

41. Place sandwich with no membrane in red side, same orientation (order doesn't matter if both have gels/membranes in them)
42. Put ice pack into back of tank (but no actual ice-this would change the concentration of TB)
43. Fill up tank with pre-cooled TB to fill line
44. Place tank in 4C (fridge) surrounded by ice (NEED THIS VERY COLD!)
45. Attach leads and run at 300mA for 2.5 hours
    a. Make sure that measurement instrument reads some watts to ensure that gels are being registered as resistance
46. Remove transfer tank from 4C and take out membrane/gel and place in separate holders after cutting excess/marking membranes

Blocking

47. Place container with ~5mL Blocking buffer on rocker at RT for ~1 h
48. Remove Blocking buffer and save for later use
49. Wash with TBST for ~10 mins on shake plate

Antibodies and Imaging

50. Dissolve 5uL Primary Antibody in 5mL of new blocking buffer
    a. Label tube with type, initials, date, dilution factor, species-can use 4-5 times
    b. Make sure that 1:1000 dilution is appropriate (some require less)
51. Pour antibody solution over membrane
52. Incubate overnight on rocker at 4C
    a. Make sure this is appropriate for your antibody. Ex. Actin does not need to be incubated overnight. Incubating at RT for 1 hour is sufficient.
53. Remove antibody---put back in tube & put back in 4C for later use
54. Wash membrane with TBST @RT 2-3xs at RT for ~5-10 min each
55. Make solution of 1:1 Blocking Buffer:TBST
    a. Make secondary antibody by making 1:10,000 dilution of antibody into above solution (i.e 1uL in 10mL of solution)
    b. Use anti-species secondary of whatever the species the primary antibody came from
56. Incubate on rocker @RT for 60 mins
57. Discard Secondary antibody
58. Wash x3 TBST (~10mL) for 10 mins each on rocker. Keep in TBST for trip to imaging center.

Imaging

59. Add ~3mL of 50/50 mix of both chemiluniescence chemicals
60. Incubate 1 min

61. Remove membranes from reaction chemicals using tweezers and place inside plastic sheet protector in exposure snap case. Position as desired. Close case.
62. Go over to Light Hall 731 (Bring film!)
63. Place exposure sheet outside of plastic sheet protector and membrane. Snap lid close and exposure sheet/membrane for desired time (i.e CHOP= ~1min)
64. Remove sheet from snap case and place directly in chemical machine. Wait for developed image to emerge from back. Check to see exposure level and adjust next exposure time (+/-). Repeat until image looks satisfactory.

RNA Extraction and cDNA synthesis

- *Direct lysing (from a 96/24 well plate)*
  1. Wash with 1 vol PBS x 3
  2. Add Buffer RLT to well (75 µL for 96-well/12-well plate or 350 µL for 24 well plate or bigger)
  3. Scrap cells using lifter
  4. Collect lysate into RNA-ase free microcentrifuge tube
  5. Vortex or pipet to mix, ensuring no visible clumps

- *RNA isolation (Using RNeasy mini kit)*

  Before starting: - β-Mercaptoethanol (β -ME) must be added to Buffer RLT before use. β -ME is toxic; dispense in a fume hood and wear appropriate protective cloting. Add 10 µl of β -ME per 1 ml Buffer RLT. RLT buffer is stable for 1 month after addition of β -ME.

  1. Homogenize the sample: Pipet the lysate/Buffer RLT mixture directly onto a QIAshedder (Cat No. 79656) spin column placed in a 2 ml collection tube, and centrifuge for 2 min at full speed (13200 rpm)
  2. Add one volume 70% ethanol and mix thoroughly (one volume = same amount of Buffer RLT added)
  3. Transfer sample, including any precipitate that might have formed, to an RNeasy mini column placed in a 2 mL collection tube (no greater than 700 µL)
  4. Close the tube gently and centrifuge for 15 s at ≥ 8000xg (≥10,000 rpm). Discard flow though.
  5. Add 350 µl of Buffer RW1 to the RNeasy mini column
  6. Close the tube gently and centrifuge for 15 s at ≥ 8000xg (≥10,000 rpm). Discard flow though.
     a. Buffer RW1 is NOT compatible with Bleach so be careful discarding flow though
  7. Prepare DNAse solution (Components Cat. No. 79254)
     a. Buffer RDD → 70 µl / sample
     b. DNAse → 10 µl / sample
  8. Add the DNAse solution (80 µl / sample) to the RNeasy spin column membrane and place on the benchtop (@20-30ºC) for 15 min
  9. Add 350 µl of Buffer RW1 to the RNeasy spin column
  10. Close the tube gently and centrifuge for 15 s at ≥ 8000xg (≥10,000 rpm). Discard flow-though.
  11. Pipet 500 µl Buffer RPE onto the RNeasy column
  12. Close the tube gently and centrifuge for 15 s at ≥ 8000xg (≥10,000 rpm). Discard flow-though.
  13. Add 500 µl Buffer RPE solution to the RNeasy column
  14. Close the tube gently and centrifuge for 2 min at ≥ 8000xg (≥10,000 rpm). Discard flow-though.
  15. Place RNeasy spin column in a new 2mL collection tube.
  16. Close tube gently and centrifuge at full speed for 2 mins to dry membrane
  17. Transfer the RNeasy column to a new 1.5 ml collection tube.

18. Add 30-50 µl of RNease-free water directly onto the RNeasy column
19. Close the tube gently and let it sit for 1 min. Then centrifuge for 1 min at ≥ 8000xg (≥10,000 rpm) to elute RNA
20. Remove and discard the RNeasy column, and close the 1.5 ml collection tube
    a. RNA is not stable! Keep it in ice while working with it in downstream steps
21. Measure the RNA concentration using Nanodop
    a. Nanodrop
        i. Open Nanodrop software
            1. Make sure Nanodrop is plugged in because wavelengths will be measured when software is opened
        ii. Click on Measure DNA/RNA
        iii. Click on Measure RNA at the top right
        iv. Must run blank first (2 uL RNAse free water)
        v. Run Samples
            1. Remember to record name of sample for easy recall
            2. Use 1-2uL of sample per test
            3. Do duplicates, if not triplicates

NOTE: If the RNA needs to be stored, this should be done at -80°C. This should be avoided; the cDNA should be prepared as soon as possible.

- *cDNA synthesis (Using iScript cDNA synthesis kit)*

1. After measuring the RNA content in all the samples, determine the amount of RNA template to be used in the cDNA synthesis (it should be as close to 1µg as possible). NOTE: The initial RNA amount to use as a template should be the same for all of the samples; it will be limited by the sample with less total isolated RNA.
2. For each sample:
    a. In a nuclease-free 1ml tube add the following reagents:

Components	Volume per reaction
5x iScript reaction mix	4 µl
iScript reverse transcriptase	1 µl
Nuclease-free water	X µl
RNA template	Y µl
Total volume	20 µl

X and Y depend on the amount of RNA quantified in the sample

3. Transfer the tubes to a thermocycler and use the following protocol (40 min):
    a. 5 minutes at 25°C
    b. 30 minutes at 42°C
    c. 5 minutes at 85°C
    d. Hold at 4°C
4. Store the cDNA at -20°C

qPCR

Primer Preparation

- QuickSpin the tubes in which the dry oligos were delivered
- Add the appropriate amount of water (pH around 7 according to manufacturer's instructions) to make 100 μM solution (should be on the sheet)
- Shake and quickspin again
- To make the working primer mixture, add 2.5 μL (each) of the sense and anti-sense primers to 95 μL of water (or desired concentration)

cDNA Preparation

- Want 25 ng of cDNA/well
- Add water to appropriate cDNA so final concentration of mixture is 3.125 ng/uL
- Add 8 uL of cDNA+H20 mixture to wells

qPCR Plate Preparation

1. Calculate the number of replicates that are needed. Typically, 3 technical replicates per sample per primer are needed. Make a little bit extra to account for liquid adherence (multiply by 3.5 for 3 replicates).

2. Add to wells in the following order (per well):
   - 10 μL of 2X SYBR Green Mix
   - 8 μL of cDNA Sample
   - 2 μL of primer mixture

3. Stick film to top of plate
4. Centrifuge for 5 minutes
5. Run PCR on the instruments at the core.

Notes

1. Make sure to have some wells with just H20+SYBR Green and some with H20+primers+SYBR Green for controls

Protocol for siRNA transfection (IDT DNA)

1. Seed cells at appropriate density on plate (
    a. 0.5 million cells/ 6-cm dish
    b. ~1.00 million cells/96 well plate
2. Allow to attach for 24 hours
3. Add siRNA via transfection steps below

Transfection (make 2mL aliquots):

a. Dilute concentrated siRNA stocks (20μM) to appropriate concentrations with DNA-, RNA-, and nuclease-free water (2 μM, 0.2 μM)
b. Couple siRNA and Lipofectamine to OPTI-MEM (separately)

	μL reagent	μL Opti-MEM
25 nM siRNA	25μL of 2uM siRNA soln	175 μL
RNAiMAX	8μL Lipofectamine-RNAiMAX	192 μL

c. Couple Lipofectamine/Opti-MEM to siRNA/Opti-MEM by carefully mixing each siRNA into the respective individual lipofectamine-containing tube. Pipette up and down gently to mix.
d. Incubate at room temp for 5+ mins
e. Add lipofectamine/siRNA complex mixture to Antibiotic-Free (AF) media (contains glutamine and FBS)
    a. 1.6 mL AF media + 0.4 mL lipofectamine/siRNA complex = 2 mL total volume
f. Add to cells (150 μL media/well in 96 well plate)
g. Incubate for 24 hours
h. Remove siRNA and replace with fresh, complete media
i. Incubate 24-48 hours
j. Extract RNA using RNeasy kit (Qiagen) or add treatments using AF media

Protocol for Lipid Transmethylation (GC-MS)

1. Extract cells using protocol “metabolite extraction from mammalian cells”
2. Dry down non-polar (lipid) fraction from chloroform in glass tube
3. In glass tube, add 2 ml 5% sulfuric acid:methanol (v:v) made fresh
4. Add 0.5 ml Toluene
5. Add 30 ul (0.2 mg) C15: or C17:0 Internal Standard 6.67 ug/ul (Make internal standard from stock;weigh out a precise amount around 100 mg and dissolve in weighed out amount of heptanes, approximately 15 ml, (SG of heptane is 0.684 so 15 ml = 10.26 g) to give final concentration of 6.67 mg/ml)
6. 25ul of a 0.2% BHT in methanol soln is added (final conc’n = 0.0025%, ie.80x dilute)
7. Vortex and heat at 95°C for 2+ hours ~ occasional vortex
8. Add 3 ml H20 and shake to quench reaction
9. Extract with 2-3ml hexane 2x – spin to get good separation
10. Remove hexane and pool and dry under nitrogen, occasionally clean walls by swishing
11. Resuspend in desired amount of hexane (0.2-0.4 mL typically) and thoroughly swish to clean walls
12. Dilute to desired concentration for running on GC
13. Transfer to GC vials and run “Fatty acid Alex”

TLC Protocol:

Preparing Samples-

1. Extract cells from plates using "Metabolite Extraction for Mammalian Cells" protocol
2. Centrifuge for 15 mins at 2500 rpm
3. Aspirate off top fraction (methanol)
4. Vortex remaining chloroform fraction and transfer to 2mL sample tubes
5. Dry down using N_2 and heat (37 C) – or the vacuum dryer (Shiota lab – for radioactive samples)
6. Bring back up in 30-35uL chloroform (step 9)

Preparing Tank and Plates

7. Fill up tank with ~120 mL of tank solution:
    i. 800 mL Pet Ether
    ii. 200 mL Ethyl Ether
    iii. 10 mL Acetic Acid
    b. Make sure to saturate filter liners (Heavy Filter Paper) as tank solution is being poured in
    c. Do NOT fill up past the point where the sample will be on the plate; The samples will be ruined if directly in contact with bulk liquid
    d. Wait at least 5 mins before using tank to make sure environment is completely saturated
8. Situate plate (silica with inorganic binder) so that the edge with most glass showing is at the top.
    a. Want the greatest possible SA contact of topping with liquid in tank
9. Mark off spot ~1" from the bottom on the surface (scratch or with pencil)
10. Add 30-35 uL chloroform to dried sample & vortex
11. Using syringe, take up sample and squeeze out liquid across 2 cm on plate (2.5 cm if using only 4 samples)
    a. Leave at least 1 cm between samples so they do not bleed together
    b. Do NOT scratch plate!
12. Rinse sample vial with 30-35 mL additional chloroform and squeeze out over top of initial respective sample spot on plate
13. Place plate with silica/chalky side facing toward the center of the tank (away from respective filter paper)
14. Let run for ~20-30 mins until liquid is 1" from top of plate
15. Remove plate from liquid and spray with Rhodamine 6G spray (DO NOT SHAKE SPRAY!)
16. Allow sprayed plate to dry under hood
17. Visualize with UV if necessary

Scintillation counting and analysis for radioactive tracers

18. There will be 5 spots per sample (in order): Phospholipid (PL), Diacylglyceride (DAG), Free fatty acid (FFA), Triglyceride (TG), Cholesterol ester (CE). Scrape each spot into an individually labeled vial for scintillation counting
19. Add 10 mL of scintillation liquid to each labeled scintillation vial
20. Close tightly (dangerous substance) and shake vigorously for 30 seconds
21. Count with scintillation counter
22. Analyze sample lipid partitioning (with ^{3}H-PA) as follows:
    a. Sum up all counts for each sample (i.e. add up counts of PL+DAG+FFA+TG+CE)
    b. Divide the counts for each fraction and divide by total of all fractions summed together